ELECTROLYTIC SYNTHESIS AND CHARACTERIZATION OF BINARY ALLOY COATINGS FOR DIFFERENT APPLICATIONS

Thesis

Submitted in partial fulfillment of the requirements for the degree of

DOCTOR OF PHILOSOPHY

By

HARSHINI SAI G

(Reg. No: 197151CY010)

DEPARTMENT OF CHEMISTRY

NATIONAL INSTITUTE OF TECHNOLOGY KARNATAKA

SURATHKAL, MANGALURU-575025

OCTOBER, 2024

DECLARATION

By the Ph.D. Research Scholar

I hereby declare that the Research Thesis entitled ***'Electrolytic synthesis and characterization of binary alloy coatings for different applications'*** which is being submitted to the National Institute of Technology Karnataka, Surathkal in partial fulfillment of the requirements for the award of the degree of Doctor of Philosophy in Chemistry is a *bonafide report of the research work carried out by me*. The material contained in this Research Thesis has not been submitted to any University or Institution for the award of any degree.

G. Harshini Sai

HARSHINI SAI G

Reg. No.: 197151CY010

Department of Chemistry

Place: NITK, Surathkal

Date: 03-10-2024

CERTIFICATE

This is to certify that the Research Thesis entitled **"Electrolytic synthesis and characterization of binary alloy coatings for different applications"** submitted by **Ms. Harshini Sai G. (Register No.: 197151CY010)** as the record of research work carried out by her is *accepted as the Research Thesis submission* in partial fulfillment of the requirements for the award of the degree of Doctor of Philosophy.

Prof. A. Chitharanjan Hegde
Research Guide
Date: 03.10.2024

Chairman-DRPC 03/10/2024
Date:

डॉ. दर्शक आर त्रिवेदी (JSPS Fellow)
प्राध्यापक एवं विभागाध्यक्ष/Professor & Head
रसायन शास्त्र विभाग / Chemistry Dept.
राष्ट्रीय प्रौद्योगिकी संस्थान कर्नाटक, सुरत्कल
NITK, SURATHKAL
मंगलूरु, कर्नाटक - 575 025

ACKNOWLEDGEMENT

I would like to express my deep and respectful gratitude to my research supervisor Prof. A. Chitharanjan Hegde, Department of Chemistry, NITK, Surathkal, for his continuous motivation, encouragement and great support throughout my Ph.D. journey. His valuable suggestions, timely guidance and careful editing contributed enormously to the production of this thesis. I will forever remain indebted to him for helping me grow as a researcher.

I owe my heartfelt gratitude to my Research Progress Assessment Committee members, Prof. M.N. Satyanarayan, Department of Physics and Dr. Beneesh P.B. Department of Chemistry, NITK Surathkal for their insightful comments and valuable inputs that helped not only in making my presentations more constructive but also widened my knowledge from various perspectives.

A very special gratitude to Dr. Darshak R Trivedi., Head of the department of Chemistry and former HOD's Prof. Arun M. Isloor and Prof. Udaya Kumar D. for their great support during my research work.

Also, I would like to acknowledge all the teaching and non-teaching faculty of the Department of Chemistry, NITK Surathkal for their direct/indirect support throughout my research work. I also acknowledge the assistance given by the support staff of the Department of Chemistry, NITK Surathkal in completing the administrative tasks well in time.

I wholeheartedly thank my dear fellow lab mates Mr. Yathish Rai T, Dr. Neethu Raveendran M, Dr. Cindrella N. Gonsalves, Ms. Aishwarya S. Suvarna for their kind co-operation and constant help in various activities during my research work. I feel fortunate to have had the opportunity to share the laboratory with them. I am also thankful to the research scholars in the department, especially Ms. Madhu Sree, J.E, Ms. Shreeleka K.M, Mr. Sudhanva Prasad and Mr. Dinesh for their precious support during my doctoral studies.

I thank Central Research Facility (CRF) NITK and Central Instrumentation Facility (CIF) Manipal for their kind assistance in various characterization techniques.

I am eternally grateful to my family, Mr. P.C.L. Ramana (father), Mrs. K.R. Vijaya Lakshmi (mother), Mr. Chaithanya Sai G (brother) for their unwavering emotional support and belief that provided me strength in pursuing this work. Special thanks to my family members Mr.

Rama Kumar, Mrs. Nagamani, Mr. Kishore G, Mrs. Ashika, Vrindha Krithika Mr. Rajendra Prasad, Mrs. Geetha, Mr. Murali and Mrs. Jyothi.

I extend my special thanks to my husband Mr. Suhas Kotaki for giving invaluable love and support in completing final stages of my work. Finally, I like to thank my uncle and aunty Mr. Anil Kumar, Mrs. Suma. Without my family support, I would not have come this long. I also take this opportunity to express my due respect to all my teachers for instilling the curiosity for learning in me. Above all, I am forever grateful to God for showering His blessings in all the walks of my life.

HARSHINI SAI G.

ABSTRACT

This thesis titled ***'Electrolytic synthesis and characterization of binary alloy coatings for different applications'*** presents a comprehensive study on development and characterization of Ni/Co-based alloy coatings from newly formulated baths, namely Ni-Ti, Co-P and Co-Fe. Standard Hull cell method was used to optimize bath constituents and operating conditions for best performance of alloy coatings against corrosion, and electro-catalytic activity of water electrolysis. The corrosion protection efficacy of monolayer Ni/Co-based alloy coatings were improved further by modern methods of electroplating, namely composition modulated multilayer (CMM) and magneto-electrodeposition (MED) approaches. The attractiveness of electroplating linked to the cathode current density has been explored effectively for the development of multilayer Ni-Ti and Co-Fe alloy coatings for better corrosion resistance, compared to their monolayer counterpart. The multilayer Ni-Ti and Co-Fe alloy coatings of higher corrosion resistance were developed by proper manipulation of cyclic cathode current densities (for change of composition of layers) and duration of current pulse (for change of layers thickness). Corrosion performance of alloy coatings, were studied by electrochemical AC and DC methods in 3.5 % NaCl solution. Poorer corrosion resistance of (Ni-Ti) alloy coatings, inherited by its bath composition was successfully improved by inducing magnetic field (*B*), parallel to the process of deposition. Effect of both intensity and direction of *B* (both parallel and perpendicular) were tested. Experimental investigation revealed that corrosion protection efficacy of monolayer Ni-Ti alloy coatings can be increased seven fold better through MED technique. In addition, the electro-catalytic activity of Ni-Ti and Co-P alloy coatings have been tested for their efficacy for water splitting applications in 1.0 M KOH. The effect of addition of Ag-nanoparticles into baths of Ni-Ti and Co-P on electro-catalytic activities of their coatings were studied. The effect of composition, surface morphology and phase structure of alloy coatings on their electro-catalytic efficacies have been studied, using CV and CP methods. The process and product of electrodeposition were characterized using SEM, EDS, AFM and XRD techniques. The performance of different alloy coatings developed for same duration (10 min) through different methods (monolayer, CMM, and MED) were compared, and experimental results are discussed with Tables and Figures.

Keywords: *Electrodeposition, Ni-Ti, Co-P and Co-Fe alloys, Multilayer coating, Magneto-electrodeposition, Corrosion study, Electro-catalytic study*

CONTENTS

CHAPTER 1

INTRODUCTION……1

1.1 ALLOY COATING……..1

1.1.1 Classification of alloy plating systems……2

1.2 FACTORS INFLUENCING ALLOY DEPOSITION……3

1.2.1 Effect of bath composition ……..3

1.2.2 Current density……..4

1.2.3 Temperature……..4

1.2.4 pH of the bath…….5

1.2.5 Agitation…….5

1.2.6 Polarization…….5

1.2.7 Hydrogen Overvoltage……5

1.3 ELECTROLYTIC COATING……...6

1.4 PURPOSE OF ELECTROPLATING……....7

1.5 PRINCIPLES OF ELECTROPLATING……8

1.5.1 Chemistry and mechanism of electroplating ……..9

1.5.2 Faraday's Laws of Electrolysis ……....10

1.6 Hull cell - An invaluable analytical tool in electroplating…….11

1.7 MODERN ELECTROPLATING …..…….....…..…….....……..13

1.8 MAGNETOELECTROLYSIS……..……..14

1.8.1 Lorentz Force……14

1.9 COMPOSITION MODULATED MULTILAYER (CMM) COATING……16

1.9.1 Development Technique of CMM materials……..18

1.10 CHARACTERIZATION OF ELECTRODEPOSITED ALLOY COATINGS…….19

1.10.1 Surface Characterization…….19

1.10.2 Corrosion monitoring techniques ……..21

1.11 ELECTROCATALYSIS……...26

1.11.1 Water Splitting Reaction……26
1.11.2 Pre-requisite of electro-catalysts ……..27
1.11.3 Volcano Plot……...28
1.11.4 Kinetics of a Reaction…….29
1.11.5 Electro-catalytic study of water splitting……....30

CHAPTER 2

LITERATURE REVIEW, RESEARCH SCOPE AND OBJECTIVES.....33

2.1 Electrodeposition of Ni-Ti alloy coatings …..…….....34
2.2 Electrodeposition of Co-P alloy coatings…….……..……..34
2.3 Electrodeposition of Co-Fe alloy coatings……...35
2.4 Modern methods of electrodeposition…….37
2.4.1 Composition modulated multilayer alloy coating …….37
2.4.2 Magneto-electrodeposition ……...38
2.5 Electro-catalytic study of alloy coatings…….39
2.6 SCOPE OF THE WORK AND OBJECTIVES……..41

CHAPTER 3

EXPERIMENTAL …….....45

3.1 Hull Cell Study……46
3.2 Conventional electroplating …….....47
3.3 Development of multilayered alloy coatings……..47
3.4 Magneto-electrodeposition ……....49
3.5 Development of Ni/Co-M alloy coatings for electrocatalytic study……...50
3.6 Study of corrosion and electro catalytic behavior of Co/Ni-M alloys……50

CHAPTER 4

ELECTROCHEMICAL DEPOSITION OF MONOLAYER AND MULTILAYER Ni-Ti ALLOY COATINGS FOR IMPROVED CORROSION PROTECTION OF MILD STEEL

4.1 INTRODUCTION……53
4.2 EXPERIMENTAL……54

4.2.1 Optimization of Ni-Ti Bath…….....54
4.3 RESULTS AND DISCUSSION……..57
4.3.1 Development of monolayer Ni-Ti alloy coatings ……..…..57
4.3.2Compositional analysis…….57
4.3.3 Surface Morphology……58
4.3.4 AFM Study……...59
4.3.5 X-Ray diffraction study……60
4.3.6 Corrosion study …….....62
EIS Study……...….62
Potentiodynamic Polarization study……65
4.4 Electrodeposition of multilayer Ni-Ti alloy coatings……..67
4.4.1 Optimization of cyclic cathode current densities (CCCD's) ……...67
4.4.2 Optimization of total number of layers…….....69
i) *Electrochemical impedance study*……70
ii) *Tafel's polarization study*……...71
4.4.3 Comparison of monolayer and multilayer Ni-Ti alloy coatings……73
4.4.4 SEM analysis of multilayer coating ……..77
4.4.5 Reasons for improved corrosion resistance of multilayer (Ni-Ti) alloy coating……77
4.5 Conclusions……79

CHAPTER 5

IMPROVISATION OF CORROSION PERFORMANCE OF Ni-Ti ALLOY COATINGS THROUGH MAGNETO-ELECTRODEPOSITION ……81

5.1 INTRODUCTION……...81
5.2 EXPERIMENTAL……..83
5.2.1 Magneto-electrodeposition of Ni-Ti alloy coatings…….81
5.3 RESULTS AND DISCUSSION…….84
5.3.1 FESEM – EDS study……85
5.3.2 Effect of *B* on composition……..86
5.3.3 XRD Study…….....87

5.4 Corrosion study……..90
5.4.1 EIS study…….90
5.4.2 Potentiodynamic polarization study……93
5.5 Comparision of ED and MED Ni-Ti alloy coatings……...95
5.6 Discussion…….....97
5.7 Conclusions……100

CHAPTER 6
ELECTRO-CATALYTIC STUDY OF ELECTRODEPOSITED Ni-Ti ALLOY COATINGS AND EFFECT OF ADDITION OF Ag NANOPARTICLES……...103
6.1 INTRODUCTION…….....104
6.2 EXPERIMENTAL…….....105
6.2.1 Electrodeposition of Ni-Ti alloy coatings…….105
6.3 RESULTS AND DISCUSSION……..106
6.3.1 Characterization of Ni-Ti alloy coatings…….....106
6.3.2 Surface morphology and phase structure of alloy coatings…….....107
6.3.3 Electro-catalytic study…….....108
6.3.3.1 HYDROGEN EVOLUTION REACTION……...108
i) Cyclic Voltammetry……..108
ii) Chronopotentiometry Study…….....110
6.3.2.2 OXYGEN EVOLUTION REACTION……111
i) Cyclic Voltametry…….111
ii) Chronopotentiometry…….....112
6.4 EFFECT OF ADDITION OF SILVER NANO-PARTICLES……..114
6.4.1 Development of Ni-Ti Ag composite coating…….114
6.4.2 Characterization Ni-Ti Ag composite coating…….115
6.4.2.1 SEM-EDS Analysis……115
6.4.2.2 XRD study…….....116
6.4.2.3 AFM Study…….....117
6.5 Evaluation of HER activity of Ni-Ti Ag composite coatings……..118
Cyclic voltammetry and chronopotentiometry……118

6.6 Conclusions……..120

CHAPTER 7

ELECTROCHEMICAL DEPOSITION OF Co-P ALLOY COATINGS AND THEIR CORROSION AND ELECTRO-CATALYTIC STUDY…….123

7.1 INTRODUCTION……..……124

7.2 EXPERIMENTAL……..126

7.3 RESULTS AND DISCUSSION ……128

7.3.1 Compositional analysis…….128

7.3.2 Surface Morphology……..130

7.3.3 AFM Study…….....131

7.3.4 X-Ray diffraction study……..132

7.3.5 Corrosion study of Co-P alloy coatings……..133

i) EIS Study…….…….134

ii) Potentiodynamic polarization study…….....136

7.3.6 Cyclic polarization study……137

7.4 Development of Co-P-Ag composite coatings……..138

7.4.1 Evaluation of electro-catalytic activity of Co-P coatings…….....139

7.4.2 Electro-catalytic Study of Co-P alloy coatings…….139

7.4.3 Inverse dependency of electro-catalytic efficacy of HER and OER with composition……...145

7.4.4 Effect of addition of Ag-nanoparticles…….....147

7.4.4.1 Evaluation of HER activity of Co-P-Ag composite coatings…….147

7.4.4.2 Morphological characterization of Co-P-Ag composite coatings……..149

7.4.4.2.1 SEM-EDS Study…….....149

7.4.4.2.2 XRD Study…….….150

7.4.4.2.3 AFM Study…….151

7.5 Conclusions……152

CHAPTER 8

DEVELOPMENT OF NANOLAMINATED Co-Fe ALLOY COATINGS FOR BETTER CORROSION PROTECTION OF MILD STEEL……155

8.1 INTRODUCTION…….156

8.2 EXPERIMENTAL……157

8.2.1 Optimization of Co-Fe Bath…….....157

8.3 RESULTS AND DISCUSSION……...160

8.3.1.1 Compositional analysis……160

8.3.1.2 Surface Morphology……161

8.3.1.3 AFM Study……..161

8.3.4 X-Ray diffraction study…….163

8.3.5 Corrosion study of Co-Fe alloy coatings…….....164

8.3.5.1 EIS Study……..164

8.3.5.2 Potentiodynamic Polarization study…….165

8.3.2 Optimization of cyclic cathodic current densities (CCCD's) configuration…….167

8.3.2.1 Optimization of number of layers……...…169

8.3.2.2 Corrosion study……..170

i) EIS study……..170

ii) Potentiodynamic polarization study……173

8.4 Comparison of corrosion behavior of monolayer and multilayer Co-Fe alloy coating……..175

8.5 Conclusions…….....178

CHAPTER 9

SUMMARY AND CONCLUSIONS……181

9.1 THESIS LAYOUT…...…….....…...…….....181

9.2 EXPERIMENTAL FRAMEWORK…….182

9.2.1 Optimization of Ni-Ti, Co-P and Co-Fe .....……...182

9.2.2 Electrodeposition of conventional monolayer alloy coatings……182

9.2.3 Development of Multilayer Ni-Ti and Co-Fe coatings……..184
9.2.4 Magneto-electrodeposition of Ni-Ti alloy coatings……185
9.3 SIGNIFICANT FINDINGS……185
9.3.1 Corrosion study of electrodeposited alloy coatings……185
9.3.2 Electro-catalytic performance of alloy coatings…….187
9.4 CONCLUSIONS……191
9.5 SCOPE FOR FUTURE WORK…….193
REFERENCES…….194
RESEARCH PAPER PUBLICATIONS…….202
PAPERS PRESENTED AT CONFERENCES……202
BIODATA……....204

Figure No.	Captions	Page No.
1.1	Effect of variables on the grain size during electroplating (Adopted from (Paunovic and Schlesinger 2006)	6
1.2	Basic components of electroplating	8
1.3	Possible formation of kink sites, edge sites and adatoms during electrodeposition (adopted from (Kanani 2006))	9
1.4	Schematic diagram showing the mechanism of electrodeposition	10
1.5	Hull cell used for optimization of baths: a) 3D view, and b) top view	11
1.6	Current density distribution in Hull cell panel (Adopted from (Lima et al.2012)	12
1.7	Hull cell Ruler	13
1.8	Schematic representation of the right- hand rule governing the direction of effective force acting on charged moving particle in the direction of perpendicular B	16
1.9	Schematic representation of multilayer coating having alternate layers of two metals A and B	17
1.10	Representative Nyquist plot showing real and imaginary axes with impedance over range of frequency	24
1.11	Representative potentiodynamic polarization plots showing the extrapolation of anodic and cathodic curves to obtain and E_{corr} and i_{corr} values	25
1.12	Typical volcano plot for HER (Adopted from Bockris et. al., 2002)	29
1.13	Schematic representation of mechanisms for hydrogen evolution reaction	30
3.1	Flow chart showing the steps involved in optimization of bath using Hull cell	46

3.2	Schematic representation of set up used for conventional electrodeposition	47
3.3	Schematic diagram showing the power pattern to use for deposition composition modulated multilayer (CMM) alloy coatings of Co and Ni (lower left), and coatings developed (lower right), in comparison with that of its monolayer alloy coatings on top	48
3.4	Experimental setup to use for MED of Ni-based alloy coatings under conditions of perpendicular and parallel magnetic field B. It may be noted that current density will be kept constant throughout the process of deposition.	49
3.5	Experimental setup used for electrodeposition of alloy coatings for electro-catalytic study	50
3.6	Customized three-electrode glass cell to use for quantification of electro-catalytic activity of alloy coatings, in terms of the volume of H_2/O_2 gases liberated while using them as cathode and anode material, respectively	51
4.1	Schematic diagram showing the current patterns used for development of a) monolayer, and b) multilayer Ni-Ti alloy coatings, and the cross-sectional view of their coatings (on right)	55
4.2	Surface Morphology of Ni-Ti alloy coatings deposited at different current densities from optimal bath	58
4.3	The AFM image showing the topography of Ni-Ti alloy coatings deposited from the optimized bath at: a) 1.0 A/dm^2, b) $2.0A/dm^2$, c) $3.0A/dm^2$ and d) $4.0A/dm^2$	60
4.4	X-ray diffraction peaks of Ni-Ti alloy deposited at different current densities from optimal bath. Constancy of phase angles of coatings corresponding to different	61

4.5	current density indicate the formation of solid solution of Ni with Ti	63
4.6	Nyquist plots of Ni-Ti coatings deposited at different current densities. Highest polarization resistance (R_P) of Ni-Ti coating corresponding 4.0 A/dm^2 may be seen, compared to other coatings	64
4.7	Bode's magnitude and phase angle plots of Ni-Ti alloy coatings corresponding different current density shown respectively in (a) and (b), demonstrates that Ni-Ti $_{4.0\ A/dm^2}$ coating is the most corrosion resistant than all other coatings	65
4.8	Nyquist plot of Ni-Ti $_{4.0\ A/dm^2}$ alloy coating showing its simulation, and equivalent circuit (in the inlet	66
4.9	Potentiodynamic polarization behavior of Ni-Ti alloy coatings deposited at different current densities. Tafel plot corresponding to 4.0 A/dm^2 showing different behavior, compare to other current density may be seen	68
4.10	Corrosion response of multilayer Ni-Ti alloy coatings having 10 layers, deposited at different CCCD's using same bath, evaluated by a) Nyquist plots, and b) Tafel plots	70
4.11	Nyquist plots of multilayer Ni-Ti alloy coatings having different number of layers (from 10 to 600 layers), deposited from the same optimized bath using pulsed current	71
4.12	Tafel's plots of multilayer Ni-Ti alloy coatings having different number of layers (from 10 to 600 layers) deposited from same bath for same duration of time	74
	Impedance response of monolayer Ni-Ti $_{4.0}$ and multilayer Ni-Ti $_{2.0/4.0/120}$ alloy coatings, deposited from the same bath for same duration	

4.13	Bode's plots of monolayer Ni-Ti $_{4.0}$ and multilayer Ni-Ti $_{2.0/4.0/120}$ coatings: a) Magnitude plot showing high value of |Z|, and b) phase angle plot showing wider peaks in case of multilayer coatings, compared to its monolayer counterpart deposited from the same bath	75
4.14	Comparison of Tafel's responses of monolayer Ni-Ti $_{4.0}$ and multilayer Ni-Ti $_{2.0/4.0/120}$ coatings, deposited from same bath for same duration	76
4.15	Cross-sectional view of Ni-Ti $_{2.0/4.0/10}$ coating under SEM displaying the formation of coatings in layered pattern	77
4.16	Schematic diagram showing the mechanism for decreased corrosion rate of multilayer Ni-Ti alloy coating, compared to monolayer Ni-Ti alloy coating deposited for the same duration. It may be seen that in case of multilayer coating the corroding medium takes more time to reach substrate due to its lateral spreading across interfaces	78
5.1	The experimental set up used for magneto-electrodeposition of Ni-Ti alloy coating under two conditions magnetic field (*B*): a) parallel and b) perpendicular to the direction of electrical field. It may be noted that in a) lines of electric field and magnetic field are parallel, and in b) they are perpendicular to each other	84
5.2	The surface morphology of MED ∥ Ni-Ti alloy coatings deposited under different conditions of applied B: (a) 0.1 T, (b) 0.2 T, (c) 0.3 T and (d) 0.4 T. The surface feature of ED Ni-Ti $_{4.0}$ ($_{\text{without}}$ the effect of B) is shown in the inset for comparison purpose	85
5.3	The surface morphology of MED ⊥ Ni-Ti alloy coatings, under different conditions of applied B: (a) 0.1 T, (b) 0.2 T, (c) 0.3 T and (d) 0.4 T. The surface feature of ED Ni-Ti $_{4.0}$ (without the effect of B) is shown in the inset for comparison purpose	86

5.4	X-ray diffraction spectra of MED || Ni-Ti alloy coatings deposited under different intensities of B using optimal bath	88
5.5	X-ray diffraction spectra of MED ⊥ Ni-Ti alloy coatings deposited under different intensities of B using optimal bath	89
5.6	Nyquist responses of MED Ni-Ti alloy coatings deposited at different intensities of B under conditions of (a) parallel, and (b) perpendicular field	91
5.7	Potentiodynamic polarization behavior of MED Ni-Ti alloy coatings deposited at different conditions of applied magnetic field: (a) parallel and (b) perpendicular	94
5.8	Comparison of XRD patterns and surface morphology of MED Ni-Ti alloy coatings deposited under optimal conditions of parallel and perpendicular B, in comparison with ED Ni-Ti alloy coatings deposited from the same bath	96
5.9	Comparison of impedance responses of MED Ni-Ti alloy coatings (under parallel and perpendicular B) in relation of ED Ni-Ti coating deposited from same bath (all under optimal condition), with Tafel's responses (inset)	97
5.10	Schematic representation showing: a) Process of magneto-electrodeposition and b) decrease of diffusion layer thickness (δ) due to increase of limiting current density (i_L) on superimposition of magnetic field, B	98
5.11	Diagrammatic representation showing lines of ionic movement responsible for change in EDL thickness during electrodeposition of Ni-Ti alloy coatings: a) ED Ni-Ti natural convection b) MED Ni-Ti Parallel B, and c) MED Ni-Ti Perpendicular B	99

6.1	Schematic of the experimental setup used for: a) Electrodeposition of Ni-Ti alloy coating, and b) Electrolyser used for water splitting of HER and OER	106
6.2	X-ray diffraction peaks of Ni-Ti alloy coatings deposited at different current densities from the optimized bath. On the right are given their FESEM image showing different surface morphology responsible for their different electro-catalytic activities	107
6.3	Cyclic voltammetry curves of HER of Ni-Ti coatings deposited at different current densities from the optimized bath	109
6.4	Chronopotentiograms for Ni-Ti alloy coatings deposited at different current densities. Given in the inset are volumes of H_2 gas liberated on their surfaces	111 112
6.5	Cyclic voltammograms of OER on the surface of Ni-Ti alloy coatings deposited at different current densities	
6.6	Chronopotentiograms of Ni-Ti alloy coatings deposited at different current densities showing different responses for OER	113
6.7	SEM image of Ni-Ti-Ag composite coatings developed under different conditions: (a) Ni-Ti-Ag $_{0.5g}$, b) Ni-Ti-Ag $_{1.0g}$ and c) Ni-Ti-Ag $_{2.0g}$	116
6.8	XRD of Ni-Ti alloy coatings under different conditions: Ni-Ti, Ni-Ti-Ag $_{0.5g}$, Ni-Ti-Ag $_{1.0g}$ and Ni-Ti-Ag $_{2.0g}$	117
6.9	AFM image of Ni-Ti-Ag composite coatings developed under different conditions: Ni-Ti-$Ag_{0.5g}$, Ni-Ti - $Ag_{1.0g}$ and Ni-Ti - $Ag_{2.0g}$	118 118
6.10	CV responses for HER activity of Ni-Ti and Ni-Ti-Ag composite coatings having varied concentrations of Ag-nanoparticles, developed at 4.0 A/dm^2	

6.11	CP responses of Ni-Ti-Ag composite coatings for HER showing their electro-catalytic stability for 1800 s, and volume of H_2 gas liberated (in the inset) on the electrode surface at varied amount of Ag nanoparticles, in relation to Ni-Ti alloy coating. All coatings were deposited at 4.0 A /dm^2	119
7.1	Variation in the wt. % of Co and P in Co-P alloy coatings with change of current density. The composition reference line (CRL) corresponding to wt. % of Co and P in the bath is shown as horizontal perforated line	130
7.2	Micrograph of Co-P alloy coatings showing dependency of deposition current density on surface morphology of deposits. A characteristic cracks having specific patterns, found growing with increase of current density may be seen	131
7.3	The AFM image showing the topography of Co-P alloy coatings deposited from the optimized bath at: a) 1.0 A/dm^2 b) 4.0 A/dm^2 X-ray diffraction peaks of Co-P alloy deposited at different current densities from optimal bath.	132
7.4	Constancy of phase angles of coatings corresponding to different current density indicate the formation of solid solution of Co with P.	133
7.5	Nyquist plots of Co-P coatings deposited at different current densities. Highest polarization resistance (R_P) of Co-P coating corresponding 1.0 A/dm^2 may be seen, compared to other coatings. In the inset is given impedance spectrum of all coatings in full scale	134
7.6	Bode's magnitude and phase angle plots of Co-P alloy coatings corresponding different current density shown respectively in (a) and (b), demonstrates that Co-P $_{1.0}$ A/dm^2 coating is the most corrosion resistant than all other coatings	135

7.7	Potentiodynamic polarization behavior of Co-P alloy coatings deposited at different current densities deposited from the same bath	136
7.8	Cyclic polarization behavior of Co-P alloy coating deposited at 1.0 A/dm^2. Decreased current corresponding to corrosion product of at given potential indicates the better corrosion stability of Co-P alloy coatings is due to barrier protection of corrosion product	138 140
7.9	CV study of Co-P alloy coatings corresponding to different current densities showing their electro-catalytic efficacy for (a) HER and (b) OER	142
7.10	CP study of Co-P alloy coatings corresponding to different current densities showing their electro catalytic efficacy for (a) HER and (b) the volume of H_2 evolved for 300 s	144
7.11	CP study of Co-P alloy coatings corresponding to different current densities showing their a) electro-catalytic stability for OER and (b) volume of O_2 liberated in 300 s	146
7.12	Representational diagram showing inverse dependancy of Co-P alloy coating, deposited at different current density for HER and OER in alkaline water electrolysis	147
7.13	CV responses for HER activity of Co-P and Co-P-Ag composite coatings having varied concentrations of Ag-nanoparticles, electrodeposited	148
7.14	CP responses of Co-P-Ag composite coatings for HER showing their electro-catalytic stability, and the volume of H_2 gas liberated with varied amount of Ag nanoparticles, in relation to that of bare -Co-P alloy coatings	149
	FESEM micrographs of Co-P-Ag composite coatings having varied amount of Ag nanoparticles incorporated: a) 0.5 g L^{-1} Ag, b) 1.0 g L^{-1} Ag, c) 0.5 g L^{-1} Ag and d)	

7.15	without, deposited at 1.0 A/dm^2 from the same optimal bath	150
7.16	Comparison of XRD signals obtained for bare-Co-P and Co-P-Ag composite coatings developed at 1.0 A/dm^2	152
7.17	AFM image showing surface roughness of Co-P alloy corresponding to: a) bare - Co-P alloy, b) Co-P-Ag $_{1.0\ g,}$ and c) Co-P-Ag $_{2.0}$ deposited from the same bath	
8.1	Schematic representation of current pulses used for electrodeposition of Co-Fe alloy coatings: (A) direct current (DC) for monolayer coating, (B) pulsed DC for multilayer coating	158
8.2	Change in wt. % of Co in the deposit with current density, deposited from optimal Co-Fe bath. Horizontal line represents wt. % of Co in the bath based on bath composition	160
8.3	Surface morphology of Co-Fe alloy coatings showing dependency of deposition current density on their surface features	161
8.4	AFM images of Co-Fe alloy coating deposited at two different current densities: (a) 1.0 A/dm^2, and (b) 4.0 A/dm^2	162
8.5	X-ray diffraction peaks of Co–Fe alloy deposited at different current densities from optimal bath. Constancy of phase angles of coatings corresponding to different current density indicate the formation of solid solution of Co and Fe	162
8.6	Nyquist plots of Co-Fe coatings deposited at different current densities Highest polarization resistance (R_P) of Co-Fe coating corresponding 1.0 Adm^{-2} may be seen, compared to other coatings	164
8.7	Tafel plots of Co-Fe coatings deposited at different current densities from the optimal bath	165

8.8	Nyquist plots of multilayer Co-Fe alloy coatings having 10 layers, deposited at different CCCD's from the same optimal bath	167
8.9	Tafel's plots of multilayer Co-Fe alloy coatings having 10 layers, deposited at different CCCD's from the same optimal bath	167
8.10	Nyquist plots of multilayer Co-Fe $_{1.0/3.0}$ alloy coatings having different number of layers deposited from optimized bath. Decrease in the value of charge transfer resistance (R_{ct}) may be seen as the layering is done beyond 120 layers	170 172
8.11	Bode's plots of Co-Fe $_{1.0}$ and Co-Fe $_{1.0/3.0/120}$ alloy coatings deposited from the same bath for same duration: a) Magnitude plots, and b) phase angle plots	173
8.12	Tafel's plots of multilayer Co-Fe $_{1.0/3.0}$ alloy coatings having different number of layers deposited from optimized bath	
8.13	Comparison of anticorrosion behavior of multilayer Co-Fe $_{1.0/3.0/120}$ alloy coating with those of monolayer Co-Fe $_{1.0\ A/dm^2}$ and Co-Fe $_{3.0A/dm^2}$ alloy coating through: (a) Nyquist plots and (b) Tafel's plots	175 176
8.14	Representative diagram showing the mechanism of corrosion in Co-Fe alloy coatings, deposited under different conditions: (a) direct attract of the substrate in monolayer coating, (b) delayed corrosion due to layered structure of coating	
9.1	Flow chart of the research work presented in the thesis	181
9.2	Scheme showing different methods of electrodeposition to achieve better performances of alloy coatings for both corrosion and electro-catalytic activity using same optimal bath	183

9.3	Histogram showing the CR's of monolayer Ni-Ti, Co-P, Co-Fe, MED Ni-Ti and multilayered Co-Fe, Ni-Ti alloy coatings studied in 3.5% NaCl medium (all at optimal condition)	186
9.4	Relative electro-catalytic performance of conventionally electrodeposited Ni-Ti, Co-P, Ni-Ti-Ag and Co-P-Ag composite coatings obtained at their optimal coating configurations	189

Table No.	Captions	Page No.
4.1	The composition and operating variables of newly optimized Ni-Ti alloy bath.	55
4.2	Compositional change and corrosion rates (CR) of Ni-Ti alloy coatings with current density deposited from optimized bath.	58
4.3	The surface roughness data of Ni-Ti alloy coatings developed at different current densities, using optimized bath.	60
4.4	The electrochemical impedance parameters of Ni-Ti alloy coatings corresponding to different current density deposited from optimized bath.	63
4.5	Corrosion data of 10 layered Ni-Ti alloy coatings having different compositions, deposited at different CCCD's from the optimized bath.	69
4.6	Corrosion parameters of multilayer Ni-Ti alloy coatings of different configuration of layering, deposited using the same bath	72
5.1	Composition and corrosion data of magneto-electrodeposited Ni-Ti alloy coatings under different conditions of *B* in relation to its conventional alloy coating	87
5.2	EIS data obtained from equivalent circuit simulation of Ni-Ti alloy coatings electrodeposited under different conditions of magnetic field *(B).*	92
6.1	The electro-kinetic parameters for HER on the surface of Ni-Ti alloy coatings deposited at different current densities using same bath.	110
6.2	Electro-catalytic parameters for OER on the surface of Ni-Ti alloy coatings deposited at current densities.	113
6.3	Change in the wt.% of Ni, Ti and Ag in Ni-Ti-Ag composite coatings due to addition of varied amount of Ag nanoparticles into the bath, deposited at 4.0 A/dm^2	115

6.4	Electro-catalytic parameters of Ni-Ti-Ag composite coatings in different composition for HER alkaline water electrolysis.	120
7.1	The composition and operating variables of optimized Co-P alloy bath.	127
7.2	Change of composition and corrosion rates (CR) of Co-P alloy coatings with current density deposited from optimized bath.	129
7.3	The surface roughness data of Co-P alloy coatings developed at different current densities, using optimized bath.	132
7.4	Electro-catalytic kinetic parameters of Co-P alloy coatings corresponding to different current density for HER, with wt. % P content in the deposit.	141
7.5	Electro-catalytic kinetic parameters of Co-P alloy coatings for OER during alkaline water electrolysis, with metal contents in the deposit.	143
7.6	Electro-catalytic HER parameters obtained for bare Co-P and Co-P-Ag composite coatings developed.	150
8.1	The composition and operating variables of new optimized bath of Co-Fe alloy.	157
8.2	Change of composition and corrosion rates (CR) of Co-Fe alloy coatings with current density deposited from optimized bath.	159
8.3	Corrosion data of multilayer Co-Fe alloy coatings having 10 layers of alloys, having different compositions, deposited from the optimal bath.	168
8.4	Corrosion data of multilayer Co-Fe alloy coatings having different number of layers deposited from the optimized bath.	174
9.1	Bath compositions and deposition parameters for Ni-Ti, Co-P and Co-Fe baths arrived by standard Hull cell method	182

9.2	Comparative account of corrosion rates (CR's) of Ni-Ti, Co-P and Co-Fe alloy coatings developed from their optimal baths through different electrodeposition techniques (for duration of 10 minutes)	185
9.3	Experimental conditions employed for the electro-catalytic study of Ni-Ti, Co-P, Ni-Ti-Ag and Co-P-Ag composite coatings	187
9.4	Volume of H_2 and O_2 evolved, as a measure of their electro-catalytic activity on the surface of different alloy coatings during alkaline water electrolysis	188

NOMENCLATURE

A. LIST OF ABBREVIATIONS

AC	Alternate current
AFM	Atomic force microscopy
c.d.	Current density
CMMA	Composition modulated multilayer alloy
CMA	Composition multilayer alloy
CP	Chronopotentiometry
CR	Corrosion rate
CV	Cyclic voltammetry
CVD	Chemical vapor deposition
DBT	Dual bath technique
DC	Direct current
ED	Electrodeposition
EDL	Electrical double layer
EDX	Energy dispersive X-ray analysis
EIS	Electrochemical impedance spectroscopy
HER	Hydrogen evolution reaction
MED	Magneto electrodeposition
MHD	Magneto hydrodynamic
OCP	Open circuit potential
OER	Oxygen evolution reaction
p.d.	Power density
PVD	Physical vapor deposition
SBT	Single bath technique
SCE	Saturated calomel electrode
SED	Sono Electrodeposition
SEM	Scanning electron microscopy
wt.%	Weight percentage
XRD	X - ray diffraction

B. LIST OF SYMBOLS

A cm^{-2}	Ampere per centimeter square
A/dm^2	Ampere per decimeter square
η_a	Anodic overpotential
i_{pa}	Anodic peak current density
β_a	Anodic Tafel slope
C_{dl}	Capacitance double layer
η_c	Cathodic overpotential
i_{pc}	Cathodic peak current density
β_c	Cathodic Tafel slope
R_{ct}	Charge transfer resistance
i_{corr}	Corrosion current density
E_{corr}	Corrosion potential
δ	Diffusion layer thickness
i_o	Exchange current density
i_L	Limiting current density
C_B	Concentration of ions
F_L	Lorentz force
B	Magnetic field intensity
R_a	Mean roughness
mA	Milliampere
mV	Millivolts
R_P	Polarization resistance
R_q	Root mean square roughness
R_s	Solution resistance
E°	Standard electrode potential
E	Potential

CHAPTER- 1

INTRODUCTION

This chapter provides a brief introduction to the principles of electroplating of metals/alloys and their applications. The theory of electrodeposition with a special emphasis on their principles of alloy deposition are explained. An overview of electroplating and different factors which can influence the process and product of electrodeposition are given. Introductory aspects of corrosion and electro-catalytic activity of metals/alloys are also given. The importance of binary alloy coatings (Ni and Co) as corrosion-resistant and electro-catalytic material are briefly reviewed. An introduction to different modern methods of electroplating such as composition modulated multilayer (CMM), and magneto-electrodeposition (MED) to achieve higher performance efficiency of alloy coatings is provided.

1.1 ALLOY COATING

It is well articulated in the literature, notably by Brenner in 1963, that alloy deposits exhibit superior properties compared to single-metal electrodeposits. This implies that electrodeposited alloy coatings can possess distinct characteristics not found in individual metals. The assertion goes further to highlight that alloy deposits, within specific composition ranges, may demonstrate increased density, hardness, corrosion resistance, protective qualities for the base metal, toughness, strength, wear resistance, superior magnetic properties, suitability for conversion chemical treatments, subsequent electroplate overlays and their applications (Paunovic and Schlesinger, 2006).

Electroplating holds considerable importance in contemporary engineering practices, where individual metal coatings are increasingly replaced by their alloy counterparts, offering a broader spectrum of desirable properties. However, it is acknowledged that alloy plating is a more intricate process than depositing individual metals, necessitating stringent control of electrolyte composition, deposition conditions, and meticulous monitoring of these parameters. The technology of electrodeposited alloys finds extensive applications in electronics, surface finishing industries, and the automotive sector (Hamm et al., 2002).

1.1.1 Classification of alloy coating systems

Electrodeposition of alloys is a complex process and is ever-growing field. Based on the underlying principles, electrodeposition can be categorized into the following five types. They are: a) Regular co-deposition, b) Irregular co-deposition, c) Equilibrium co-deposition, d) Anomalous co-deposition and e) Induced co-deposition (Brenner 1963a).

a) Regular co-deposition

Regular co-deposition is characterized by the process, which is under diffusion control. The weight percentage of more noble metal in the deposit is increased by those agencies that increase the metal ion content of the cathode diffusion layer, like increase in the total content of the bath, decrease of current density, elevation of bath temperature, and increase the agitation of bath. Regular co-deposition is most likely to occur in baths containing simple metal ions, but may occur in baths containing complex ions. Sn-Ni and Ni-Co is the examples of this type of co-deposition.

b) Irregular co-deposition

In this type, the effect of plating variables on the composition of the deposit are much smaller than that of regular co-deposition. It is most likely to occur with the solution of complex ions. Brass plating is the example of this co-deposition. In this brass plating the cyanide as the complexant considerably brings the equilibrium potentials of the more metal copper to the value of zinc equilibrium potential and enables the co-deposition easily.

c) Equilibrium co-deposition

Equilibrium co-deposition occurs when deposition takes place from a solution that is in chemical equilibrium for both parent metals. Alloys like Cu-Bi and Pb-Sn fall into this category, where the ratio of metals in the deposit mirrors that in the bath.

d) Anomalous co-deposition

Anomalous co-deposition involves the preferential deposition of the less noble metal over the noble metal. For instance, in Zn-M (where M = Ni, Co, and Fe) alloy coatings, Zn is

preferentially deposited over the noble Ni. Solutions containing ions of iron-group metals (iron, cobalt, and nickel) give rise to such anomalous deposition.

e) Induced co-deposition

Induced co-deposition occurs when metals like Mo, W, V and Ti, which cannot be deposited alone from simple salt solutions, readily co-deposit with iron-group metals. Examples include Ni-Mo, Ni-Ti, and W-Co alloys. Metals that stimulate deposition are termed inducing metals, while those unable to deposit by themselves are known as reluctant metals.

1.2 FACTORS INFLUENCING ALLOY DEPOSITION

Electrodeposition provides a simple route for developing the material of specific properties. A high-quality electrodeposit is distinguished by excellent adhesion, a fine-grained structure, uniform thickness, good throwing power, and brightness. Well-formed spirals, blocks, or layers on the work piece contribute to a desirable deposit. On the other hand, a poor deposit exhibits outward (whisker dendritic) growth, along with a powdery, burnt texture, often influenced by macroscale features such as steps, ridges, and polycrystalline block growth. Given that electroplating is an atomistic deposition process, it allows for customization of materials according to specific requirements by adjusting plating conditions and bath composition. Consequently, several critical parameters need to be considered during synthesis of new coatings by electrolytic methods (electroplating) are as follows:

1.2.1 Effect of bath composition

Generally electrolytic baths, consists of metal ions or electroactive species, supporting electrolytes, complexing agents and organic additives.

a) Electroactive species:

These are the ones that can participate in electrode reactions. During electroplating, higher concentrations of metal ions increase the mass transfer leading to poor deposit. When metal salt concentration is kept high, the high current density is employed for the deposition to occur resulting in the increase in the grain size.

b) Supporting electrolytes:

These are the inorganic salts that are added to extend the conductivity of the plating bath, but they do not participate within the electrode reactions. Some of the commonly used conducting salts used in electroplating are NaCl, NH_4Cl, Na_2SO_4, etc.

c) Complexing agents:

The metal ion is converted into a complex by the inclusion of suitable complexing agent within the plating bath to induce a fine-grained and a more adherent deposit. The complexing agents imparts following effects on the process of deposition as:

1. The deposition potential will be more negative so that plating takes place at a lower potential.
2. Prevention of passivation of anodes so that anode dissolves easily and improve the current efficiency.
3. Improves the throwing power of the plating bath.
4. Inhibits the reactivity of plating ion with the cathode metal

General complexing agents are cyanides, citrates, gluconates, sulphamates etc. They are used in smooth deposition of copper, gold, zinc, cadmium in the presence of cyanide ions.

d) Organic additives:

There are the organic compounds which can bring significant structural and morphological modification in the alloy deposit. It includes *brighteners*, lik*e* thiourea, gelatin, coumarin, and *levelers*, like sodium allyl sulphonate and structure *modifiers*, like saccharin and *wetting agents, like* sodium lauryl sulfate.

1.2.2 Current density:

Increasing the current density typically results in the deposition of higher proportion of the less noble metal during electrodeposition. Additionally, the effect is more pronounced when the co-depositing metals are complexing with a common anion, a substantial change in current density may occur with little alteration in the composition of the alloy.

1.2.3 Temperature:

The process of electrodeposition is inherently an electrochemical one, its efficiency is closely linked to temperature variations. In particular, the rate of deposition exhibits a direct correlation with temperature; as temperature rises, the deposition rate tends to increase. This

phenomenon is evident in alloy deposits, where elevating the bath temperature typically results in a higher proportion of the more noble metal within the deposit. Similarly, an increase in bath agitation has a similar effect.

1.2.4 pH of the bath:

Generally, at low pH hydrogen evolution occurs at cathode resulting in a burnt deposit. At very high pH, the electrode surface gets coated with insoluble hydroxides. Therefore, an optimum pH range is recommended, depending on the chemistry of the bath. The pH of the bath is maintained by using a suitable buffer to get a sound coating.

1.2.5 Agitation:

During electrodeposition, it obvious that the concentration of metal ions around anode keep increasing, whereas around cathode it decreases. Hence, to have steady supply of metal ions near cathode, electrolyte solution should be kept under constant agitation. An increase in agitation usually increases the amount of more noble metal in the alloy plate, thus tending to the effect of an increase in ratio M_2/M_1. Agitation brings fresh noble metal ions to the cathode film and decrease the cathode layer thickness, which leads to increase in proportion of the more noble metal in the deposit.

1.2.6 Polarization:

Polarization is characterized by a variation in electrode potential caused by the slow supply of ions from the bulk solution to the electrode. When a current flow, the reduction of metal ions near the electrode surface decreases their concentration, causing a shift in equilibrium and a change in the electrode potential. This concentration gradient results in the diffusion of ions, restoring equilibrium.

1.2.7 Hydrogen Overvoltage:

Hydrogen overvoltage is the potential difference that can be found between an electrode and a reversible hydrogen electrode within a single solution. This is where hydrogen (H_2) undergoes formation from ions of hydrogen. Overvoltage or over potential (η), is defined as the excess voltage that has to be applied above the theoretical potential for continuous electrolysis. Hydrogen overvoltage is a measure of the hydrogen gas (H_2) liberated from the

electrode surface. Electrochemically, metal deposition is accompanied by hydrogen evolution. Lower overvoltage indicates quick release of hydrogen gas. The liberation of H_2 on electrode surface takes place in three steps:

$$H_3O^+ \rightarrow H^+ + H_2O \text{.....(1.1)}$$

$$H^+ + e^- \rightarrow H \text{..... (1.2)}$$

$$H + H \rightarrow H2\ (g) \text{.....(1.3)}$$

The deposition of metal takes place in one step.

$$M^{n+} + e^- \rightarrow M \text{.....(1.4)}$$

Therefore, the overvoltage for metal deposition is small compared to hydrogen overvoltage. The effect of these variables on grain size is summarized schematically as shown in Figure 1.1.

.

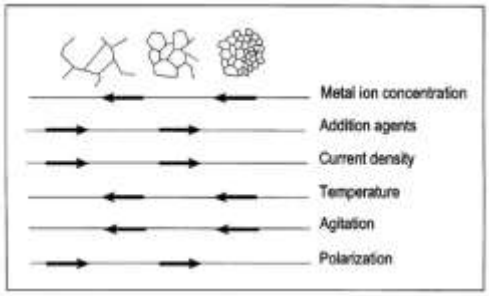

Figure 1.1 *- Effect of variables on the grain size during electroplating (Adopted from (Paunovic and Schlesinger 2006)*

1.3 ELECTROLYTIC COATING

Metals and alloys found to be the foremost critical group of engineering materials, and they are typically hard, malleable with good electrical and thermal conductivity. Alloys are made by melting two or more elements together, at least one of them being a metal. They have properties that improve better than those of the constituent elements, such as greater strength or resistance to corrosion. Owing to environmental impact and working environments, a widespread variety of metallic objects that we use in our daily lives have a short life span. Interactions involving physical contact between components are prevalent in various mechanical systems and chemical or electrochemical reactions with the environment are also common, which may sometime lead to dangerous situations. Because of its atomic structure, the surface of any substance or component is more susceptible to a variety of attacks, which may be electrochemical, mechanical, thermal, or chemical in nature. They may occur as a result

of stress, affect, or even on a regular basis. As a result, the surface can be protected from the environment. Metal finishing is the practice of surface treatment, involving the generation of a metallic coating through an electrochemical reaction within either an aqueous solution or a molten salt. Generally, deposition method and pre- and post- treatments used, determine the properties of electrodeposited coatings (Kanani 2006). The specific date of the first electroplating test is disputable, yet most agree that in 1772 Prof. G. B. Beccaria was the first to effectively store metal, by releasing a Leyden jug and utilizing the flash to deposit metal salts.

In 1796, Alessandro Volta, a student of Galvani showed that Voltaic pile scan be used as the source of energy for electrodeposition. Later, it served for a long time as a wellspring of power for electroplating on a business scale, until the electromagnetic generator replaced it. In 1805, Luigi Brugnatelli, a companion of Volta, was the first to carryout effectively gold-plating on a silver coin. Later in 1940, the Elkington cousins achieved a patent for utilizing potassium cyanide to make a possible electroplating technique for gold and silver, and this strategy turned out to be a wide spread trend across the world from Britain. (La Niece and Craddock 1993). From that point forward, electroplating technique has developed in both revolutionary and evolutionary manner, with finding its applications in all fields of applied science.

Electroplating serves for many purposes starting from its appearance till its performance. It is commonly used to improve different physico-mechanical properties of base metal (Leisner et al. 1996b), like, Appearance, corrosion resistance, wear resistance, electric and magnetic properties, temperature resistance, thermal conductivity, etc.

1.4 PURPOSE OF ELECTROPLATING

It is well known that through electroplating technique, it is possible to protect the surface of active metal from the effect of corrosion, alongside of improving its appearance. It is a process of depositing a metal/alloy coating of desired composition over a metallic or other conductive substrates by the passage of electric current through an electrolyte containing the metal ions. Electroplating serves as a versatile method for enhancing the properties of a substrate by depositing a layer of metal or alloy onto its surface. This process contributes to improved characteristics, offering a diverse range of applications in various industries. Apart from improving the aesthetics of metals, electroplating also brings about change in physical,

chemical and mechanical properties. The electroplating technique was once considered as an art, but now it is treated as pure science. Currently, this method uses eco-friendly baths and advanced power sources.

1.5 PRINCIPLES OF ELECTROPLATING

The underlying principle of electroplating is electrolysis. Electrolysis is the process of decomposition of an electrolyte in an aqueous solution when the current is passed through it and results in the discharge of electrolyte constituents at the electrodes. Electrodeposition involves electrolyzing a suitable salt solution of the metal being plated. In this process, the substrate is designated as the cathode (negative terminal). The anode (positive terminal) can be either a sacrificial anode (dissolvable anode) or a permanent anode (inert anode). Platinum and carbon are typical examples of inert anodes. The electrolyte is the electrical conductor in which ions carry current rather than free electrons (as in a metal). Electrodeposition can take place either in an aqueous electrolyte near ambient temperature (aqueous solution electroplating), or in a fused metal salt at high temperatures (fused-salt electroplating). Electrolyte completes the electrical circuit between two electrodes. When a direct current is supplied through an external DC power source, the anode undergoes dissolution into the electrolytic bath, causing positive ions within the electrolyte to migrate towards the cathode. Essentially, the metal ions present in the bath solution are deposited as metal onto the cathode, while negative ions move towards the anode. This migration of ions through the electrolyte constitutes the electric current in that part of the circuit. A schematic representation of the electroplating unit is shown in Figure 1.2

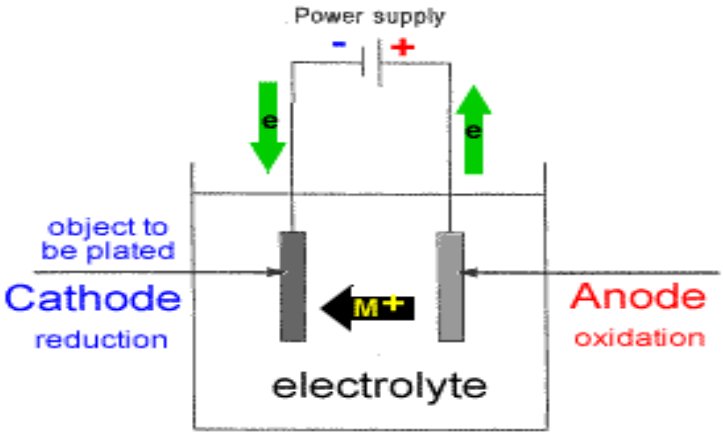

***Figure 1.2** - Basic components of electroplating*

1.5.1 Chemistry and mechanism of electroplating

During electrolysis, simultaneous oxidation and reduction occur at anode and cathode respectively in the electrolytic bath. The reactions taking place for an electrolyte *MA* is given as:

i) The ionization of electrolyte in aqueous solution

$$MA\ (aq) \rightleftharpoons M^{+}\ (aq) + A^{-}\ (aq) \ldots\ldots\ldots\ldots\ldots\ldots\ (1.5)$$

ii) Depletion of the anode to give metal ions (oxidation)

$$M^{+}(aq) \rightarrow M^{+}(aq) + e^{-} \ldots\ldots\ldots\ldots\ldots\ldots\ (1.6)$$

iii) Deposition of metal atoms by reduction of metal ions on the cathode

$$M^{+} + e^{-} \rightarrow M\ (lattice) \ldots\ldots\ldots\ldots\ldots\ldots\ (1.7)$$

But, in the case of insoluble anodes namely stainless steel and platinum, oxidation of water takes place.

$$2H_2O \rightarrow 4H^{+} + O_2 + 4e^{-} \ldots\ldots\ldots\ldots\ldots\ldots\ (1.8)$$

Since metals have well-defined crystal structures, the deposition of metal is similar to that of crystal growth. Electrodeposition occurs in two stages: i) Formation of nuclei and ii) Growth of the deposit. Formation of nuclei is the primitive stage where the substrate gets covered with a few the nuclei have attained a critical size, it undergoes fusion and grows rapidly at a relatively low overvoltage to form a metallic layer at the cathode surface. The atoms (*adatoms*) that are formed during the plating process on the crystal plane, quickly move and occupy favourable sites such as *kink site (*where an atom interacts with three neighbors) or *edge site* (two neighbors), or remain as adatoms (one neighbor).

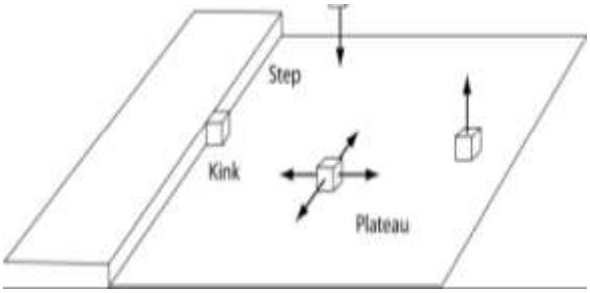

Figure 1.3 - *Possible formation of kink sites, edge sites and adatoms during electrodeposition (adopted from (Kanani 2006))*

The overall growth of the crystal on the surface of substrate takes place as follows:

a) **Ionic migration:** It involves *mass transport* of hydrated metal ion(s) in the electrolyte into the diffuse double layer on the electrode surface under the influence of applied potential.

b) **Electron transfer**: At the diffuse layer, the hydrated metal ions are loosely held by weak electric field present in this layer. Subsequently, these metal ions enter into the compact layer of the cathode surface.

c) **Surface diffusion:** Diffusion of adatoms occur across the cathode surface and is incorporated into the kink sites.

Thus, the structure of the deposit is largely determined by steps (b) and (c). Hence, during plating, the operating parameters are adjusted in such a way that these steps predominate, leading to a satisfactory coatings of high material properties.

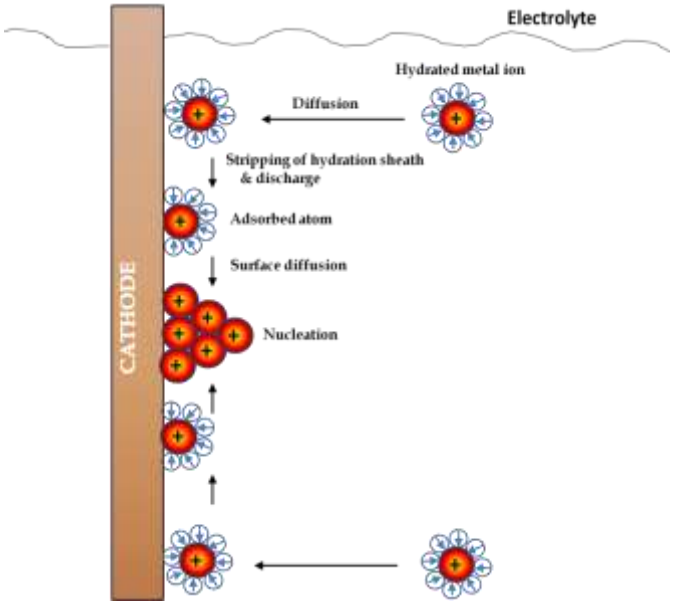

Figure 1.4 - *Schematic diagram showing the mechanism of electrodeposition*

1.5.2 Faraday's Laws of Electrolysis

The fundamental principles underlying all electrodeposition processes are governed by Faraday's laws of electrolysis. Faraday's laws provide insights into the relationship between the quantity of electricity passed and the corresponding deposition of a metal or alloy, as well as the equivalent mass of the metal to be deposited (Paunovic and Schlesinger, 2006; Kelly et al., 2002). In compliance with Faraday's first law of electrolysis, the mass of a substance (m) is directly proportional to the quantity of electricity (Q) passed during the electrodeposition process. If the mass of the substance discharged is 'm' in grams and the quantity of electricity passed is 'Q' expressed in coulombs (C), then

$$m \propto Q, \text{ or } m = MQ/zF \quad \ldots\ldots\ldots\ldots\ldots\ldots \quad \ldots\ldots (1.9)$$

Where, '*M'* is the molar mass of the substance, '*F'* is the Faraday constant = 96,485 C mol^{-1}, '*z'* is the valency of ions involved.

1.6 Hull cell – An analytical tool in electroplating

The Hull cell, named after its inventor Richard Hull, has been employed in the electroplating industry since as early as 1939 (Kanani, 2006). This miniature plating unit, devised to generate cathode deposits on a panel, serves as a practical tool for assessing the characteristics of the plating bath under evaluation (Lima et al., 2012). The Hull cell, depicted in Figure 1.5, operates as a compact electrodeposition tank. Notably, the cathode is positioned at an angle relative to the anode, resulting in a variable current density along its length, with the highest density closest to the anode, as illustrated in Figure 1.5 (b).

The current density at required point on the Hull cell panel can be determined using the given Equation.

$$I = C(5.10 - 5.24 \log L)$$

Where, *I* is the current density in A/dm^2 at any point on the cathode, *C* is the cell current used for the test, and *L* is the distance in centimeter at a point on the cathode, where the current density is desired to achieve. This method enables the assessment of the impact of varying current density within a single test run.

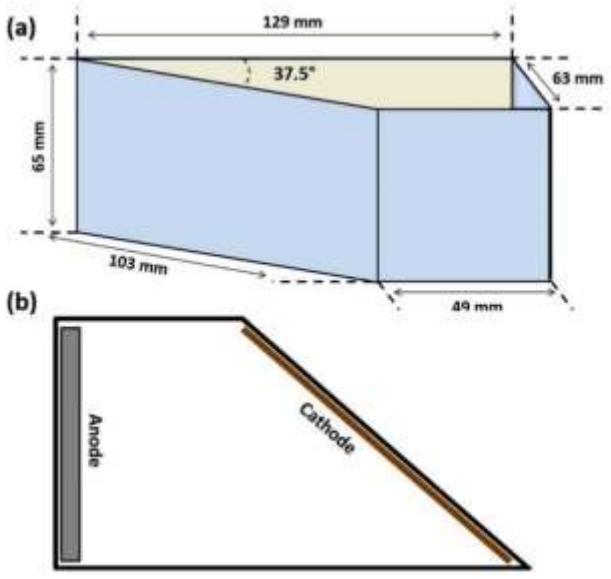

Figure 1.5 *- Hull cell used for optimization of baths: a) 3D view, and b) top view*

At the lowest levels of current density, no deposition is typically observed. The Hull cell is utilized to define the 'operating window,' representing the range of current density within which acceptable deposition takes place. A cathode, polished and pre-cleaned, is positioned at a predetermined angle opposite the anode. The desired electrolytic solution is introduced into the cell, and deposition occurs on the cathode under a specific cell current, such as 1 A, 2 A, or 3 A, with a constant duration of 10 minutes. The Hull cell ruler, as illustrated in Figure 1.4, facilitates the determination of corresponding current densities at a specific distance from the High Current Density (HCD) end.

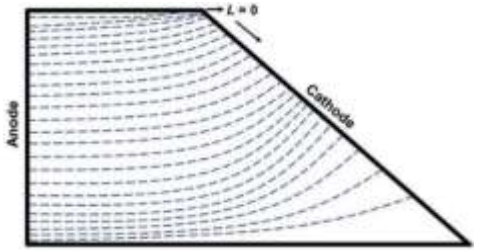

Figure 1.6 *- Current density distribution in Hull cell panel (Adapted from (Lima et al.2012)*

Based on the analysis of bath chemistry and the assessment of the panel's condition with regard to factors like brightness, hardness, uniformity, burning, etc., modifications can be introduced through controlled additions to the Hull cell plating solution. Subsequently, the procedures can be repeated to observe the effects. This allows for a systematic approach to refining the plating bath. The changes induced in the Hull cell are expected to replicate the outcomes that would be achieved by making proportionate additions to the main plating bath.

The correlation between properties, such as thickness and hardness of the coatings, at specified temperature, time and current density, provides valuable insights. These correlations aid in identifying the optimum plating range necessary to achieve the desired properties in the deposit. This systematic approach, as outlined by (Kanani 2006 and Lima et al. 2012) facilitates informed adjustments and improvements in the electroplating process.

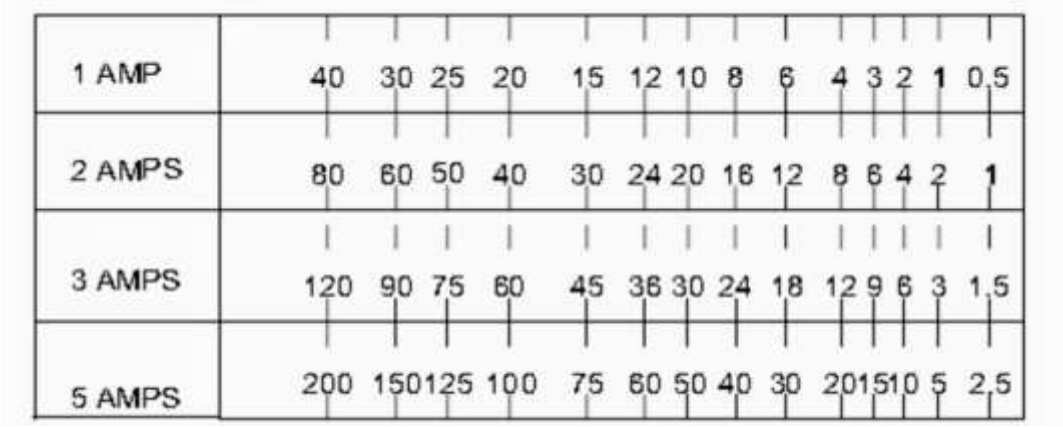

Figure 1.7- *Hull cell ruler to know the desired current density, based cell current used (Lima et al. 2012)*

1.7 MODERN ELECTROPLATING

Conventional metal plating is not able to cater to many of the recent technological demands. Therefore, the deposits with new properties are to be tailored to cater to the needs of advanced applications. A widely used technique to impact the formation of crystal structures is to utilize a growth medium that includes additives capable of selectively adsorbing onto particular crystallographic planes.

1.8 MAGNETOELECTROLYSIS

An electrodeposition process under the effect of magnetic field, or magnetoelectrodeposition (MED) cause the increment of limiting current and the change of electrodeposits become more compact. The problem of obtaining a uniform, dense and compact deposition has plagued researchers ever since the discovery of the electrodeposition process in the early 1800s. One of the methods for tackling this problem is through MED. MED or magnetolysis is a process of depositing the metal/alloy under the influence of induced magnetic field (*B*). MED has been particularly studied for various applications, and is one of the most actively studied sub-areas of magneto-electrochemistry. The MED brings change in the properties of coatings to large extent. Such deposition produces a uniform and compact alloy deposit. The effect of magnetic field on process of electrodeposition was established since 1881, when Remsen observed the effect of a magnetic field in copper electrodeposition. Since then, MED is observed to possess

several noticeable advantages when compared to the conventional deposition process. They are listed as below (Fernanda and Paulo 2006).

1. MED does not require vacuum technology and consequently is less expensive.
2. It can be easily scaled up for use in large size areas.
3. The experimental systems are simple.
4. It can be a room temperature technology.

Thus the above benefits of MED play a vital role in the electrodeposition process to synthesize metals/alloys as thin films, multilayers, nanowires, multilayer nanowires, dot arrays and nano-contacts which are the technologies of the future to build the next generation microelectronic devices. Magnetolysis encompasses four key dimensions of interactions between electric or magnetic fields: i) the impact of magnetic fields on electrolyte properties, known as the magneto hydrodynamic effect; ii) the study of electrolytic mass transport; iii) considerations of electrode kinetics, albeit to a lesser extent; and iv) the examination of how these fields influence the nature and quality of the deposited material. In essence, magnetolysis delves into the diverse ways in which electric or magnetic fields interact with electrolyte solutions, influencing processes ranging from mass transport to the characteristics of the final deposited materials. (Fahidy 2001).

1.8.1 Lorentz Force

In the electrodeposition process, the limiting current (i_L) is referred as the maximum current that can be achieved for an electrode reaction at a given concentration of the reactant in the presence of a large excess of supporting electrolytes. It can affect the optimum mass transport achieved in the electrodeposition process. When magnetic fields are superimposed on the electrodeposition process, there is an increase in the limiting current and a drastic change in the growth pattern of the deposit. This effect, known as the magneto hydrodynamic effect (*MHD*), and is generally explained by the appearance of the Lorentz force (F_L) (Fahidy 1983b).

$$FL = qE + qvB \ldots\ldots\ldots\ldots\ldots\ldots\ldots \quad (1.1)$$

The initial segment of the equation pertains to the electric force, straightforwardly contingent on the applied current density. In the context of common electrochemical processes, the current density is predominantly determined by the Faradaic current. The second segment pertains to the magnetic force, with its magnitude hinging on the angle between the magnetic

field (B) and the velocity vector (v), or equivalently, the applied current (i) since ions move in the direction of the applied current. Mathematically, the magnitude of the magnetic force is expressed as $F = q \times v \times B \times \sin(\theta)$. Notably, when the angle (θ) between the magnetic field and current density is 90˚ (i.e., B and v are perpendicular), the magnetic force is at its maximum, resulting in the highest impact of the Lorentz force. Conversely, when $\theta = 0$ and B and i are parallel, the magnetic force is minimized. The Lorentz force, being capable of mobilizing charged particles like ions, induces convection of the electrolyte when a magnetic field is applied during electrolysis. Therefore, the Lorentz force, or the electromagnetic body force, emerges from the vector product of the current density (i) and magnetic induction (B).

$$F_L = i \times B \quad \ldots\ldots\ldots\ldots\ldots\ldots\ldots\ldots\ldots\ldots (1.2)$$

Hence, when the orientation of the magnetic field (B) is perpendicular to the line of the electric force, the Lorentz force induces a change in the direction of charged particles as they traverse the magnetic field lines (Fahidy 1983). The effect of an additional convection occurrence may be a change of the alloy composition, structure and morphology. The differences may affect the electro-catalytic properties of such alloys (Mohanta and Fahidy, 1978). All magnetic fields exert a strong influence on electrode processes. They can modify deposit structure, increase the rate of deposition of the reaction product(s), change flow patterns, and increase the intensity of mixing. The presence of a magnetic field has a pronounced impact on the motion of charged particles, mass transport, and the corrosion behavior and deposit characteristics etc. In fact, the applied magnetic field brings change in the properties of electrodeposited coatings by decreasing the thickness of electrical double layer (EDL), between substrate and electrolyte solution. This change is effected due to swirling action of electrolyte solution near EDL. The resultant force is consequently directed outward from the palm, as illustrated in Figure 1.8 (a). For a precise determination of the effective force's direction, curl the fingers and rotate them into the plane of B; the thumb then indicates the exact direction of the effective force, as depicted in Figure 1.8 (b).

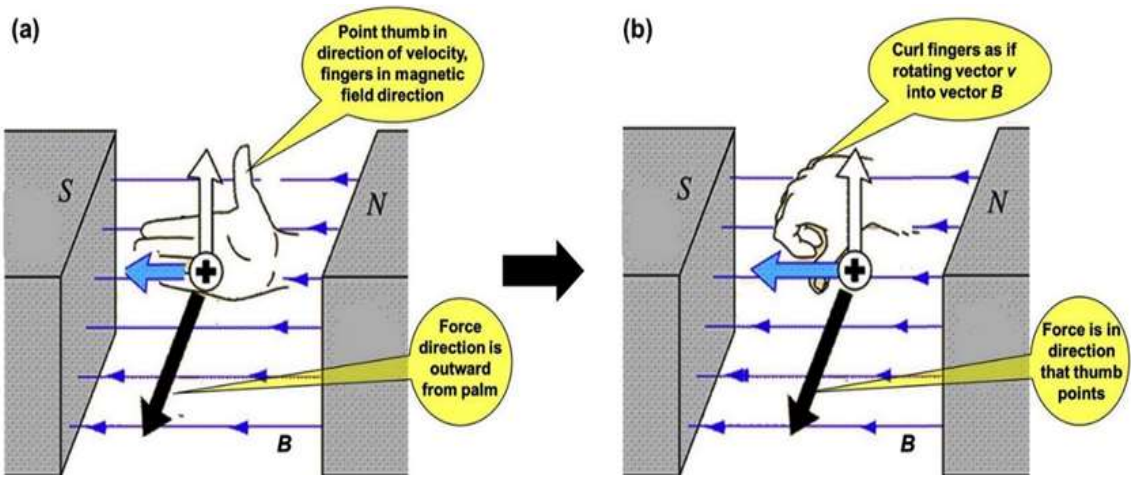

Figure 1.8*- Schematic representation of the right- hand rule governing the direction of effective force acting on charged moving particle in the direction of perpendicular B. This Lorentz force acting at the interface reduces the thickness of EDL, and thereby increases the* i_L *of the bath (D.Marett 2013)*

1.9. COMPOSITION MODULATED MULTILAYER (CMM) COATING

The materials with ultrafine microstructure are emerging as new generation materials. Such a group of materials are commonly known as compositionally modulated multi-layer. CMM has aroused high level of interest in surface engineering. CMM coatings consists of a large number of thin laminar deposits of metal or alloy layers and each layer has its own distinctive role in achieving preferred performance (Kalantary, M. R. et al 1995). A representative diagram of CMM coatings is shown in Figure 1.9, where different layers may be of few nanometers in thickness. Due to the layering at a near-atomic dimension, multilayers can exhibit remarkable and, at times, unique properties that are not achievable in conventional metallurgical alloy. These properties include magneto-optical properties, X-ray optical properties, perpendicular magnetism, novel electronic transport, superconducting properties, super modulus, improved strength, and wear and corrosion resistance. Potentiodyanamic and galvanostatic stripping techniques are usually used to characterize these CMM deposits (Wilcox and Gabe 1993).

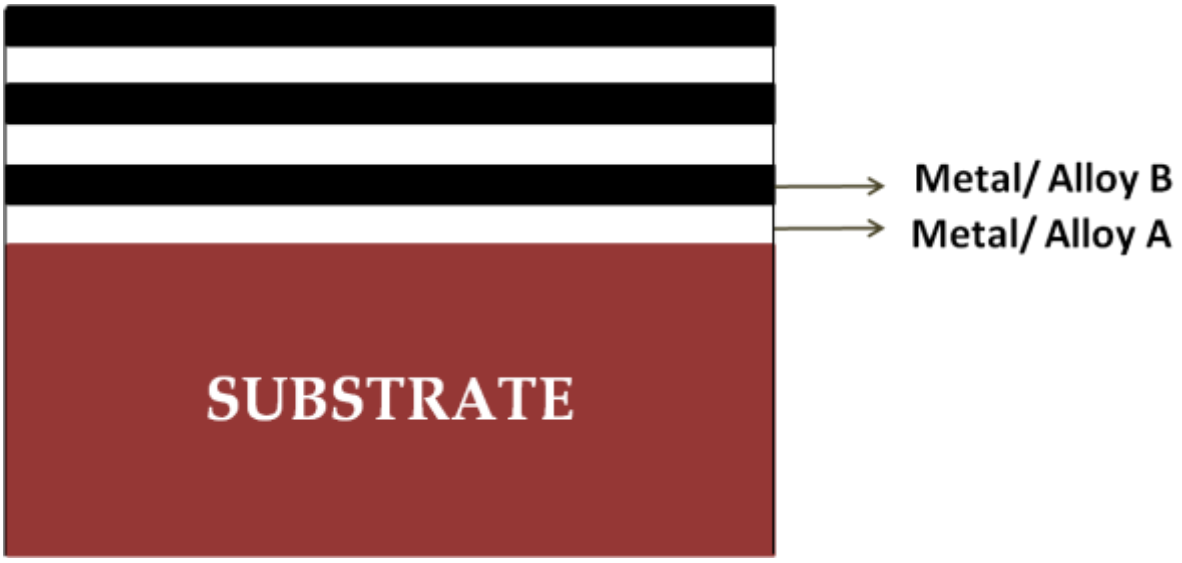

Figure 1.9 *Schematic depiction of multilayer coating having alternate layers of two metals/alloys, or two alloys of different composition, A and B*

Baral and Maxmovitch were one of the first investigators to examine this particular system. They operated a dual bath configuration depositing successive layers of zinc and nickel with individual layer thicknesses of 20-500 nm using a rotating disc electrode. CMM coatings for protection of steel substrate from corrosion have been extensively investigated (Jensen, J. D. 1998 and Mursel Alper 2002) obtained Zn-Ni CMM coating with an overall thickness of 8 pm by electrodepositing alternate layers of zinc and nickel. The zinc-nickel alloy deposition process and product has been reported by (Swathirajan 1986). The stripping responses have employed to determine the chemical and phase compositions of electrodeposited zinc-nickel alloys, evaluate their corrosion resistance, and estimate the equilibrium potentials of various zinc—nickel phases. The electrodeposition of Cu-Ni compositionally modulated multilayer with sub layers' thickness in nanometer range has been carried out (Haseeb et al. 1994). The deposition was conducted under galvanostatic conditions using dual bath technique. The structure of multilayer was characterized by SEM and higher resolution transmission electron microscopy (TEM). They found that Cu and Ni sub layers grow epitaxially on the top of one another. The local variation in the growth of copper leads to faceted morphology of the multilayer. The extent of this faceting is reduced as the sublayer thickness is decreased. Thus enormous amount of literature is available in the field of CMM deposits with the similar

conclusions that the strengths and thereby the properties of deposits obtained depends mainly on the sequence and thickness of the individual layers.

1.9.1 Development Technique of CMM Materials

There are two approaches for the development of CMM materials. One is through dry process based on vacuum technique. Sputtering, molecular beam epitaxy, laser ablation and normal temperature evaporation are all coming under this category. Though method is technically good, its prohibitive cost made to find other alternative for the development of CMM materials. Though there are different techniques of CMM deposition, all are having inherent advantages and disadvantages with regard to the quality of multilayers they create and the ease of their production, such as:

- Lower processing cost and the applicability to curved and recessed substrates
- Utilizes Simple Equipment: The process makes use of uncomplicated equipment, making it accessible and cost-efficient
- Deposition control is precise and has high reproducibility
- Precise Deposition Control and High Reproducibility: The method offers precise control over deposition, ensuring accuracy and consistency in the coating process, leading to high reproducibility.

However, in wet process the solution used will often have complicated composition (metal salts, buffering agents, complex agents, additives and inert electrolyte). Another major drawback of the process is that the substrate on which the film has to be deposited should be conducting one as magneto resistance measurement requires the substrate not to be a bulk material. Therefore, this technique of 'electrolytic method' is much more promising approach to deposit the multilayer onto a semi conducting substrate. The semiconductors can conduct sufficiently well to allow film to deposit as a metal substrate would, due to Schottky barrier for conductor of n-type. Electrochemical wet processes make use of either single bath technique (SBT), or dual bath technique (DBT) for deposition of multilayer.

i) Single Bath Technique

In SBT the deposition is done in one plating solution containing ions of different constituents of the multilayer by alternately changing the plating current/potential,

sometimes in combination with a modulation of the mass transfer towards the cathode. To avoid the simultaneous deposition, a large potential span must exist between the deposition potential of the metals. One of the major requirement of this technique is deposition potential of bath components must be far enough apart to allow a separate electrodeposition of each without any alloy formation. In spite of a suitable difference in deposition potential, alloying of the less noble metal with the nobler one is almost inevitable which has been treated as one of the limitations of this technique.

ii) Dual Bath Technique

This technique is conceptually simple and involves the deposition of the constituents from two separate plating baths in an alternate manner. Method is advisable for the deposition of two metals or alloys having almost nearer deposition potential value. This technique has many disadvantages such as, the deposition process must be continually interrupted as the sample is transferred between baths. There may be cross contamination due to drag out from each other.

1.10 CHARACTERIZATION OF ELECTRODEPOSITED ALLOY COATINGS

1.10.1 Surface characterization

The characterization of all coatings in terms of their structure at micro-level provides a keen understanding of the relationship between their structures (Girão et al. 2017). In the present study, the composition and surface morphology of electrodeposited coatings are studied by Energy-dispersive X-ray spectroscopy (EDS) and scanning electron microscopy (SEM) techniques. The micro or nanostructural features of alloy coatings, based on their surface roughness is carried out by Atomic Force Microscopy (AFM). Along with these techniques, the X-ray diffraction (XRD) technique is used to examine the phase structure of the deposit (Shetty and hedge 2018).

SEM is a powerful tool to analyze both the morphological and micro or nano-structural details of alloy coatings (Di Girolamo et al. 2016). Generally, in SEM, a high-energy electron beam is formed, and is allowed to scan the sample surface to get its surface morphology images. Then, there occurs elastic and inelastic scattering due to the interaction of the electron beam with sample. However, some parts of the electron beam

are left un-scattered. If the interaction between the sample and the electron beam is elastic, electrons reflect and are called backscattered electrons (BSE). But, inelastic interaction of the electron beam with the sample produces secondary electrons (SE) from the atoms of the sample itself. Hence, the image can be obtained by using secondary electrons as well as backscattered electrons. Since the BSEs originate from the deeper portion of the sample, BSE images are very sensitive to the variation in the atomic number in the sample, and a high atomic number of the element in the material leads to a brighter image. But, the SE that originates from the surface peripheral region, shows the image with details of the surface information. If the electron beam source is a field emission gun, and is highly focused and narrow, giving rise to high-resolution images it is called FESEM image (Girão et al. 2017).

Micro-structural information is generally obtained using an energy dispersive X-ray spectrometer (EDS) detector attached to the SEM. When an incident electron beam interacts with the sample surface, it produces X-rays and the EDS detector measure the energy and intensity distribution of the X-ray signal. Generally, the incident electron knocks out an electron knocks out an electron from the K shell of an atom in the sample. Then the electron vacancy created at the K shell (n=1) is filled by the electrons in another shell of the atom and there occurs an electron transition resulting in the emission of X-rays. The X-rays produced by the electronic transition to the K shell are called $K_{X\ rays}$, and the L shell (n=2) are $L_{X\ rays}$ and to the M shell (n=3) are called $M_{X\ rays}$ and so on. These emitted X-rays are the characteristic of each chemical element in the sample, and are thus helpful in both qualitative and quantitative analysis by providing the identification of the elements present in the coatings, and their composition in it.

Atomic force microscopy (AFM) is one of the useful techniques to examine and estimate the surface structure of a material. Unlike other microscopic techniques, the AFM technique uses a sharp probe to scan the sample surface. Hence, the light and electrons are not involved in the surface imaging (Eaton and West 2010). AFM analysis can be used to study the surface morphology and roughness of coating on a smaller scale. This experimental information can be used to predict/assess the factors responsible for

improved corrosion resistance/kinetics of electrocatalytic reactions of electrodeposited alloy coatings. (Shetty and Hegde 2018).

XRD technique is the commonly used non-destructive technique to analyse the phase structure of the electrodeposited alloy coatings. It gives information about the phase structure, preferred crystal orientations, and other structural parameters including average grain size, crystallinity, strain and crystal defects. During XRD analysis, the monochromatic X-rays are allowed to fall on the sample surface and it forms a diffraction pattern by constructive interference of X-rays scattered from the lattice planes of surface atoms. The X-ray diffraction follows Bragg's law: $n\lambda = 2d \times \sin\theta$, where 'n' is an integer, λ is the wavelength of the incident X-rays, d is the interplanar distance and θ is the angle of diffraction. These diffracted X-rays are then detected, processed and counted for structural information.

1.10.2 Corrosion monitoring techniques

Ulick R. Evans, British Scientist who is considered as the *Father of Corrosion Science* has said that "Corrosion is a largely an electrochemical phenomenon, may be defined as destruction by electrochemical or chemical agencies". Corrosion in an aqueous environment and in an atmospheric environment is an electrochemical process which involves the transfer of electrons between the metal surface and an aqueous electrolyte solution. It is an inherent, spontaneous destructive process that occurs on the surface of a metal or alloy due to its interaction with environmental elements such as oxygen, water, salts, and gases. Through the impact corrosion, about one fifth of steel production is degraded, gets lost or disappears. Under favorable corrosion conditions, all metals corrode and the most serious offender is iron and its alloys. Chemicals, soils, atmosphere (rural, industrial, marine or combination of these), food stuffs, organic materials, acids, oxidizing agents, water, dissimilar metal contacts and high temperature are the most common causes of corrosion (Paul Wynn, 1960). Most of corrosion phenomenon can be best explained by *Electrochemical theory of corrosion***.** According to this theory, corrosion reaction is the transfer of metal atoms from the solid to the solution where they exist as ions. The reaction at the less stable anodic sites (A) on metal M (e.g., where there are dislocations, imperfections) can be explained by simple equation.

$$M \rightarrow M^{n+} + ne^- \text{ ……..(1.12)}$$

At the cathode, depending on the nature of the corrosion environment, reduction takes place. The most common types are: hydrogen type corrosion and oxygen type corrosion.

Liberation of hydrogen takes place in the absence of oxygen.

i) In acidic medium, the cathodic reaction is:

$$2H^+ + 2e^- \rightarrow H_2 \uparrow \text{ ……(1.13)}$$

ii) In neutral or alkaline medium alkaline medium,

$$2H_2O + 2e^- \rightarrow 2OH^- H_2 \uparrow \text{.....(1.14)}$$

Absorption of oxygen occurs in the presence of oxygen.

i) In acidic medium,

$$4H^+ + O_2 + 4e^- \rightarrow 2H_2O \text{……..(1.15)}$$

ii) In neutral or alkaline medium,

$$2H_2O + O_2 + 4e^- \rightarrow 4OH^- \text{ .....(1.16)}$$

Thus, Fe^{+2} ions formed at anode, and OH^- ions formed at cathode combines to form $Fe(OH)_2$.

$$Fe^+ + OH^- \rightarrow Fe(OH)_2 \text{ .....(1.17)}$$

This $Fe(OH)_2$ eventually transforms into $Fe_2O_3.3H_2O$, as rust. Corrosion reactions are in general electrochemical in nature, the reasons for the popularity of electrochemical techniques for corrosion measurement are due to the fact that they are fast, sensitive and versatile. Corrosion can be separated into two types: a) uniform or general corrosion, and b) localized corrosion. General corrosion occurs uniformly over the entire surface. Localized corrosion occurs at small (dimensions ranging from 1 to 10 microns to several orders of magnitude faster than general corrosion.

i) Electrochemical Impedance Spectroscopy (EIS)

EIS is a widely utilized technique for obtaining valuable insights into electrode processes, such as double-layer capacitance for enhanced corrosion protection and the role of inhibitors. This electrochemical method assesses the system's response to a voltage perturbation. While polarization resistance can be measured with a smaller perturbation, EIS applies a small varying perturbation across a range of frequencies, allowing for a comprehensive exploration of the system's response, not just the resistive components. EIS employs a spectrum of alternating current (AC) voltage frequencies, cycling from peak anodic to cathodic

magnitudes. Capacitance and resistance values are obtained at each frequency, offering insights into corrosion behavior, rates, diffusion, and coating properties. EIS finds application in various corrosion measurement areas, including the

- Rapid estimation of corrosion rates.
- Assessment of low corrosion rates and metal contamination
- Estimation in low conductivity media
- Rapid estimation of corrosion inhibitor performance in aqueous and non-aqueous media.
- Rapid assessment of coatings.

In the EIS process, the system undergoes excitation with a small amplitude AC sinusoidal signal of potential or current across a wide range of frequencies. The resulting response is measured, and impedance is calculated as Equation 1.18. The impedance is expressed in terms of real Z'|(ω) and imaginary Z"|(ω) components. Nyquist plots or Bode plots are employed to analyze the impedance behavior, depicting a semicircle in Nyquist plots with increasing frequency in a counterclockwise direction. An "equivalent circuit" is then created to model the corrosion system using resistors, capacitors, and inductors. By fitting this circuit to the impedance spectra, values of circuit elements are extracted, offering insights into the physical behavior of the corrosion system.

$$Z(\omega) = Z' (\omega) + Z'' (\omega) \ldots\ldots\ldots\ldots\ldots\ldots (1.18)$$

The Nyquist plot exhibits a semicircle, with increasing frequency in a counterclockwise direction. At very high frequency, the imaginary component Z" disappears, leaving only the solution resistance, R_S. At very low frequency, Z" disappears, leaving a sum of R_S and the Faradic reaction resistance or polarization resistance, R_P. R_P, inversely proportional to the corrosion rate, can be subtracted from R_S measured at high frequency to obtain the compensated value of R_P, free of ohmic interferences

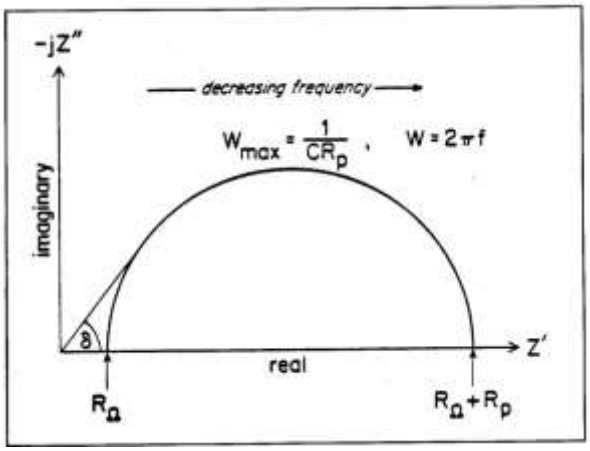

Figure 1.10 – *Representative Nyquist plot showing real and imaginary axes with impedance over range of frequency*

Since the amplitude of the excitation signal is small enough for the system to be in the equilibrium state, EIS measurements can be used to effectively evaluate the system properties without significantly disturbing them. Frequency sweeping in a wide range from high-to low frequency enables the reaction steps with different rate constants, such as mass transport, charge transfer, and chemical reaction, to be separated.

ii) Potentiodynamic polarization (Tafel's extrapolation method)

This technique is based on a three-electrode system where the sample specimen is the working electrode, calomel as a reference electrode and platinum auxiliary or counter electrode. The electrode assembly is immersed in the corrosive medium, and the corrosion potential is recorded. Tafel plots are constructed by applying a potential of 250 mV in both positive and negative directions from the open circuit potential against the reference electrode. An illustrative Tafel's plot is presented in Figure 1.11.

The corrosion plot comprises an anodic (βa) and a cathodic (βc) branch. The intersection of these branches can be extended to project onto the X and Y axes.

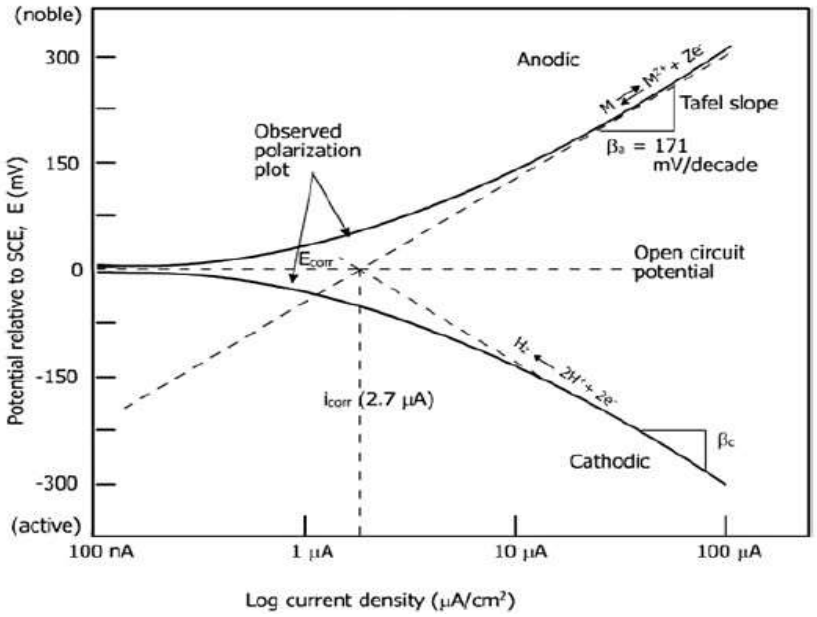

Figure 1.11*- Representative potentiodynamic polarization plots showing the extrapolation of anodic and cathodic curves to obtain and E_{corr} and i_{corr} values (Adapted from Amin et al. 2014)*

The relationship for anodic and cathodic processes under activation polarization is given in Equation 1.19 and 1.20.

$$\eta_a = \alpha_a + \beta_a \log i \qquad (1.19)$$

$$\eta_c = \alpha_c + \beta_c \log i \qquad (1.20)$$

The extrapolation method for determining corrosion rates involves extending the linear portion of either the anodic or cathodic branch of a polarization curve to intersect with the Open Circuit Potential (OCP). In this method, ηa represents anodic polarization or, ηc represents cathodic polarization, αa and αc are anodic and cathodic Tafel constants, βa and βc are anodic and cathodic Tafel slopes, and log i is the logarithm of current density By extending the linear segment and determining the intersection with the OCP, the current value obtained provides icorr, representing the rate of either the anodic or cathodic reaction under freely corroding conditions. This method is particularly useful when the polarization curve displays a well-defined linear region on either the cathodic or anodic side. The corrosion rate can be measured from the i_{corr} value by using the given Equation.

$$CR\ (mm\ y^{-1}) = \frac{K \times i_{corr} \times EW}{\rho}$$

1.11 ELECTROCATALYSIS

Electro-catalysis is the term that generally refers to the catalysis of electrode reactions (Trasatti and Doubova 1995). It means the enhancement of the rate of electrochemical reactions with the reduction in the over potential. It is because of catalytic acceleration of slow chemical reaction, through fast charge transfer steps which together constitute an electrochemical reaction (Wendt 1994). It should be noted that electro-catalytic reactions will normally involve both the formation and cleavage of the metal-adsorbate bond. Therefore, when the bond is of intermediate strength, the most effective catalysis occurs. Too low free energy of adsorption will lead to insufficient coverage by adsorbate for it to be an effective catalyst while too high a free energy of adsorption will cause the rate of the cleavage step to become too low. Generally, transition metal species play a significant role in the field of electro-catalysis because of their unpaired d-electrons and unfilled d electrons which are available for forming bonds per metal atom and also on their energy levels, and, hence, both on the choice of transition metal and its detailed environment. In the limit, the surroundings (i.e. the adjacent metal atoms in a metal or alloy, the ligands to a metal complex, or the oxide ions in an ionic lattice) and the adsorbate may be considered as ligands to the central transition metal ion acting as the catalyst center, and the surroundings will moderate all the properties of the metal-adsorbate (Pletcher 1984).

1.11.1 Water Splitting Reaction

Hydrogen has been considered as a promising alternative to unsustainable fossil fuels as it is vital for ammonia production, petroleum refining, metal refining, and electronics fabrication, with average worldwide consumption of about 40 million tons and has great potential as a clean burning fuel. Currently, reformation of natural gas, heavy oil, gasification of coal and petroleum coke contribute towards 90% of the world's hydrogen. However, in return, an enormous amount of energy gets utilized and CO_2 gets emitted (Santos et al. 2013). To realize a hydrogen-based economy, hydrogen must be efficiently and sustainably produced. Two of the most common methods used for the production of hydrogen are water splitting and steam forming. Although, steam forming is less expensive method, the advantage of steam reforming is that this reaction will produce the highest yield of hydrogen. The disadvantage is the increased heat load resulting from the large endothermic reaction and the continuous supply

of heat to the reaction. Another method is *water splitting reaction* or *water electrolysis*, where passage of electric current is involved to separate water into its basic elements, hydrogen and oxygen. This method in spite of not being a cheapest kind, it is preferred due to its high degree of purity. Room-temperature water electrolysis can take place under acidic or alkaline conditions. An electrolyzer with Proton exchange membrane (*PEM*) is used to perform water electrolysis in acidic condition, which is commonly known as *PEM water electrolysis*. Although PEM water electrolysis systems offer several advantages, such as high energy efficiency, a great hydrogen production rate and a compact design, their application remains hampered by the high cost of the catalysts and short durability of the membranes. Therefore, alkaline electrolyzers are commonly preferred. A major setback of this method is it involves high HER over potential which can be a hindrance towards large scale hydrogen production. But an efficient electrocatalyst can overcome this difficulty. An electro-catalyst is an electrode material that interacts with some certain species during a Faradaic reaction but still remain unaltered. Since electrode reactions are heterogeneous, electrocatalysts are usually heterogeneous catalysts, which means that the reactions take place on the surfaces of catalysts, and there exist adsorption/desorption steps on the surfaces of electro-catalysts.

1.11.2 Pre-requisite of electro-catalysts

For efficient electrolysis process, the most stable, abundant and active materials should be developed. The fundamental requirements of an ideal electro-catalyst are as follows (Sapountzi et al. 2017). Low intrinsic over potential for the desired reaction (hydrogen or oxygen evolution)

- The high active surface facilities both good accessibility to the reactants and sufficiently fast removal of products (gases, liquids, ions)
- High electrical conductivity (providing pathways for electrons)
- Proper chemical stability (compatibility with the electrolyte)
- Electrochemical stability (i.e. not being corroded at high over potentials)
- Good mechanical stability (especially for high-temperature electrolysis

It is well known that platinum is known to exhibit best electro-catalytic activity for HER. But due to its high cost, there is a need to replace the noble metals with low cost novel materials that can exhibit high activity for HER. Three categories of non-noble metal

electrocatalysts are under heavy investigations: Transition metal alloys, transition metal compounds, and carbonaceous nanomaterials. The most practical option, based on the electrocatalytic activity and electrochemical stability, seems to be the transition metal alloys. Most of the transition metal alloys that are characterized as hydrogen electrodes in water electrolysis are nickel-based binary or ternary co-deposits. The high activity, good corrosion resistance and low cost of Ni-based electrode materials make them efficient for HER. In oxygen evolution reaction (*OER*), main energy loss is due to high over potential occurring at the anode. IrO_2, RuO_2 though considered as the most active materials for OER, they are least abundant. So, research is going on in a direction where more abundant materials with lower cost can be obtained. This has been achieved in alkaline electrolysis by the use of transition metal catalysts. Non-platinum metals like Fe, Ni, Co are considerably cheaper but they tend to corrode and passivate under reaction conditions. So alloying them with the same group or other group metals increases the intrinsic electro-catalytic activity, changes the surface morphology and enhances the corrosion stability.

1.11.3 Volcano plot

Sabatier Principle (named after French Nobel laureate, Paul Sabatier), is a qualitative way to predict the activity of heterogeneous catalysts. The principle states that in order to have high catalytic activity, the interaction between reactants and catalysts should neither be too strong nor too weak. If the interaction is too weak, then there will be no reaction on the surface because it is difficult for catalyst surface to bind with the reactants. Suppose the interaction is too strong, then the reactant or product is difficult to get desorbed from catalyst surface, which also lowers the activity. This phenomenon has been cast into an intuitive tool termed as '*volcano plots*', which pictorially characterize catalytic activity with respect to catalyst/intermediate interactions. Volcano plots was first introduced by Balandin in 1969, and is shown in Figure 1.12.

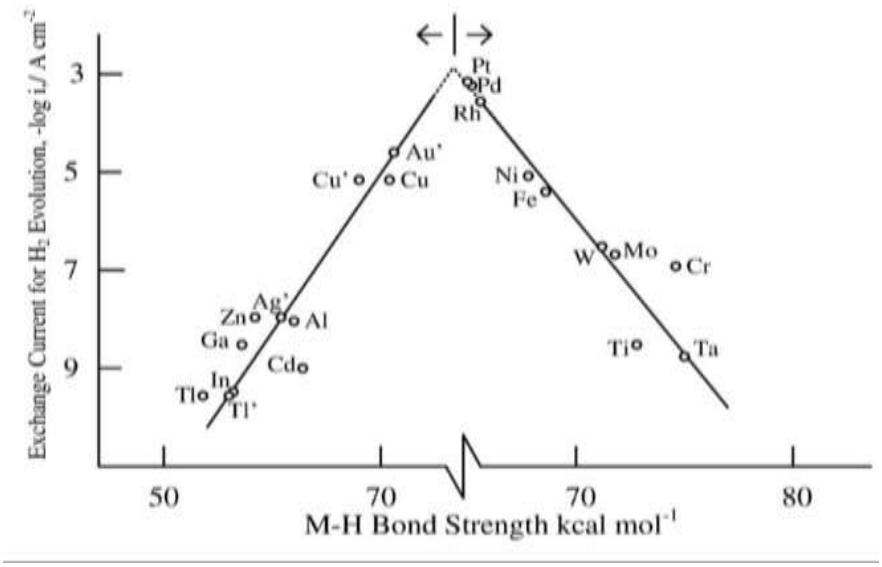

Figure 1.12 *- Typical volcano plot for HER (Adapted from Bockris et. al., 2002)*

The basic idea is that if plotting rate of a chemical reaction on a heterogeneous catalyst with some adsorption property, say adsorption enthalpy, then according to Sabatier's principle, the plot will have a maximum, showing the shape like a volcano. Volcano plots contain a minimum of two slopes, meeting at the top. The volcano shape aids comparison of the thermodynamics between different catalysts, thereby facilitating identification of '*good*' candidates. Thermodynamically optimal candidates are those fulfilling Sabatier's principle, which appear near the highest point of the volcano. The volcano slopes delineate situations in which the catalyst/substrate interaction is either too strong (left slope) or too weak (right slope) (Busch et. al. 2015).

1.11.4 Kinetics of a Reaction

In order to understand the kinetics of any electro-catalytic reaction, it is necessary to understand its mechanism. Some of the techniques frequently used for kinetic study of an electrodic reaction are: 1. Steady-state polarization (Tafel) curves, 2. Potential step charging, 3) Galvanostatic pulse, 4) Potential relaxation in an open circuit (potential decay), 4) AC impedance spectroscopy. The characterization techniques unveiled the mechanism governing the Hydrogen Evolution Reaction (HER) in strongly alkaline environments consists of the following three steps (Jakšić et al. 2000) and is represented in the Figure 1.13, and steps involved are:

i) Electroreduction of water molecules with hydrogen adsorption (Volmer reaction)

ii) Electrochemical hydrogen desorption (Heyrovsky reaction)

iii) Chemical desorption (Tafel reaction)

$$M + H_2O + e^- \rightarrow {}^{M}H_{ads} + OH^- \quad \text{..... (1.19)}$$

$$M\,H_{ads} + H_2O + e^- \rightarrow M + H_2\uparrow + OH^- \quad \text{..... (1.20)}$$

$$M\,H\,ads + M\,H\,ads \rightarrow 2M + H_2\uparrow \quad \text{.....(1.21)}$$

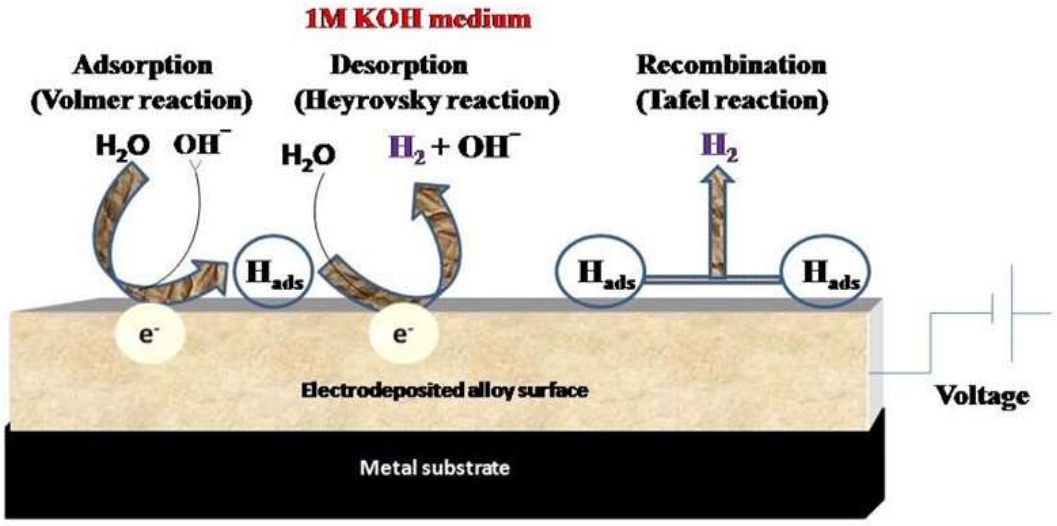

Figure 1.13*- Schematic representation of mechanisms for hydrogen evolution reaction*

1.11. 5 Electro-catalytic study of water splitting

The electro-catalytic efficiency of electrode materials can be studied by well-known methods, namely cyclic voltammetry and chrono-potentiometry methods.

i) Cyclic voltammetry (CV)

CV is a method used to investigate the electrochemical characteristics of a system, providing insights into the thermodynamics of redox processes and the rate of heterogeneous electron transfer reactions, and adsorption process. It can be used to study the electrochemical behavior of different species diffusing to an electrode surface, interfacial process, and bulk properties of the material at the surface (Li and Miao 2013). The CV test is carried out by applying a linear potential sweep, which is a potential that increases/decreases with time to the working electrode, when the potential moves back and forth above the formal potential of the analyte,

a current flow occurs through the electrode, which oxidizes or reduces the analyte. The experimental setup to carry out the CV analysis consists of three electrodes (working, reference, and auxillary electrode) immersed in an electrolyte solution, which is connected to a potentiostat. The function of the potentiostat is to apply and maintain the potential between the working and reference electrode. For an oxidation process to take place a positive potential ramp is applied to the working electrode and the electroactive species undergoes electron loss at the electrode that results in the anodic peak current along with an oxidation peak at the given potential (E_{pa}). At the same time when the potential applied at the working electrode is in the negative direction, the reduction process occurs at the electrode. This further leads to the cathodic peak current (i_{pc}) at a potential (E_{pc}) (Swaminathan and Meiyazhagan 2020). Hence, CV technique can be used to study the electrocatalytic study of an electrode towards HER and OER during the water-splitting reaction.

ii) Chronopotentiometry

Chronopotentiometry (CP) is a method employed to investigate the mechanism and kinetics of an electrochemical reaction. In this technique, a constant current is applied between the working electrode and counter electrode for a specific duration, and the resulting potential developed at the working electrode is measured relative to the reference electrode as a function of time. The electrolyte solution is usually kept unstirred and it contains supporting electrolytes in excess to facilitate the mass transport process is inferred from the variation in the potential response (Lingane and Peters 1971). This can be used to investigate the mechanism of a redox process occurring at the surface of electrodeposited alloy coatings during the electrochemical water-splitting reaction. Hence the role of the working electrode as an electro-catalyst to facilitate HER and OER can be well understood by the nature of the chronopotentiogram obtained. To study the HER activity of an electrode during water splitting, a cathodic current is passed through the working electrode which leads to the evolution of hydrogen at the electrode surface and the corresponding chronopotentiogram is obtained. Similarly, to carry out the OER at the corresponding chronopotentiogram is obtained. Similarly, to carry out the OER at the electrode surface, an anodic current is passed and that liberates the oxygen gas. The corresponding chronopotentiograms obtained for both

HER and OER manifest the long term stability of the electrode material towards the particular reaction and it robustness during the reactions (Elias and Hegde 2016).

LITERATURE REVIEW, SCOPE AND OBJECTIVES

This chapter presents the literature review of electrodeposited Ni/Co - based alloy coatings for their applications for both corrosion protection and electro-catalytic activities of water electrolysis. A literature review on how exactly the corrosion protection efficiency of binary alloy coatings can be improved substantially through modern approaches such as, composition modulated multilayer (CMM) technique and magneto-electrodeposition (MED) method. The motivation behind the work embodied in the thesis is given at the end, with scope and objectives.

The process of electrodeposition dates back to 1800 by availing of first voltage generator (Volta pile), and was improved later in 1803 by Brugnatelli. The first materials to be deposited were Au and Ag, and consequently initial applications of this technique were limited to decorative purposes. The first process for producing an alloy coating was patented in England in 1838 by Elkington and Barratt. A diffusion coating of zinc and copper was formed by immersing copper articles attached to a piece of zinc which served as internal anode, into a boiling solution of zinc chloride. This process involved the deposition of zinc. The reaction occurred because the free energy liberated by the dissolution of zinc anode to form zinc ions was greater than the free energy required to deposit zinc ions into a copper lattice. As the process did not involve the simultaneous deposition of two metals, it is not alloy deposition. The first electrodeposition of alloys probably took place at the same time that cyanides were introduced into electroplating. De Ruolz is generally credited with having been the first to deposit brass and bronze. The bronze bath which was described in 1842 was apparently similar to the modern bath, which contains a cyanide copper complex and a stannate.(Brenner 1963). From that time, electroplating technology has grown in length and breadth to meet various scientific, industrial technological applications.

Although nickel electrodeposition has been studied since the beginning of 20^{th} century, there has been an increased interest in recent years, and is now considered as one of the most frequently used method in surface finishing treatments. Metals, alloys, and composite layers can be deposited electrochemically to form in single or multicomponent layers. Out of many

Ni-based alloys, electrodeposition of Ni-M (where M = Ni, Co and Fe) alloy coatings are of great importance due to their excellent corrosion protection efficiency, and reasonably good electro-catalytic activity of HER and OER.

2.1 Electrodeposition of Ni-Ti alloy coatings

Nickel is known to be a very versatile metal for its good corrosion resistance, temperature and wear resistance properties. Electrodeposited Ni-based alloy coatings exhibit better properties compared to its single metal coatings. Ni-Ti alloy coatings have different properties like good biocompatibility (Toker et al. 2014), shape memory effect (Braz Fernandes et al. 2013), good wear resistance, and corrosion resistance (Aydoğmuş et al. 2020). These alloys have wide number of applications in bio-medical, aerospace and automobiles. Titanium and its alloys are suitable for environmental use due to their behavior from getting reduced mildly to undergo oxidation readily. They form spontaneously a protective oxide films on surface, which remain stable. Titanium exhibits excellent corrosion resistance in both marine and industrial environments (Seo et al. 2023). Though, titanium metal cannot be electrodeposited alone from any of its aqueous solutions, and it can only be co-deposited with iron group metals such as nickel, cobalt, or iron to form an alloy. This phenomenon is named as *induced co-deposition* as named by Brenner (Eliaz and Gileadi 2008).

2.2 Electrodeposition of Co-P alloy coatings

Cobalt (Co) and its alloys have been developed by different methods (Vicenzo and Cavallotti 2004), (Armyanov 2000), (Cavallotti *et al*. 2003) (Frieze et al. 1968), (Hono and Laughlin 1989) including through electrochemical deposition method. Electrodeposited cobalt-phosphorous Co-P alloy coatings have been investigated extensively for years, owing to their enhanced physical, chemical and magnetic properties. Due to these added properties, they are used as a corrosion and wear resistant material, alongside their use as soft magnetic materials for magnetic recording. Co-P alloy coatings were also used as good electro-catalysts for HER and OER in water electrolysis. Due to their excellent mechanical and wear-resistant properties, nano-crystalline Co and Co-based alloys have recently been identified as promising candidate to replace hexavalent-Cr plating (Hono and Laughlin 1989). In recent years, there is a growing interest in the electrochemical deposition of Co-based alloys, due to their applications in both basic and applied research (Kosta et al. 2012). Among various binary alloy coatings, Co-P

alloy coatings have been identified as suitable materials to replace environmentally unfriendly hard chromium. Due to impressive appearance, good corrosion and wear resistance of these coatings, they find extensive technological applications in industries. The phenomenon of co-deposition of reluctant metal with an Fe-group metal is called induced co-deposition, and the concept was first envisaged by Brenner (Brenner 1963a). Accordingly, Brenner and his co-workers developed many electrolytic baths, following induced co-deposition. They have developed a Co-P alloy coating by simultaneously depositing cobalt with the less readily deposited metal phosphorus. (Shervedani and Lasia 1997), (Elias et al. 2016), (Armyanov 2000),(Barnett et al. 2012).

In this regard, research is being carried out in order to increase the production of renewable energy sources, which are more abundant and cleaner than fossil fuels (Cavallotti et al. 2003). There is an increasing demand of energy globally due to massive utilization of nuclear fossil fuels. Hydrogen is considered as a clean-burning fuel because of its high energy density, electrochemical reactivity (Elias and Hegde 2016), and wide availability and is regarded as one of the most beneficial replacements to unsustainable fossil fuels. But the major problem with hydrogen is its less availability in pure form on earth atmosphere, but it is available in large quantity in combined form with oxygen, *i.e.* in the form of water. Water is the most abundant source for the production of hydrogen (H_2) and oxygen (O_2) by water electrolysis (Hono and Laughlin 1989), (Kanani 2006). Since water electrolysis is a very effective method for production of H_2 and O_2, and it can be achieved by development of proper electrode materials(Hono and Laughlin 1989). The main requisite of the effective electrode material is their lower over potential for hydrogen evolution reaction (HER) and oxygen evolution reaction (OER), as cathode and anode (Kosta et al. 2012). Owing to the fact that precious-metal based electro-catalysts have been found to be the best for the HER (Pt-based), and OER (Ru-based) electrode materials, and their widespread usage continues to be restricted due to its less availability and high cost (Li et al. 2018).

2.3 Electrodeposition of Co-Fe alloy coatings

Nanocrystalline materials exhibit unique and improved properties in terms of mechanical, chemical, and physical aspects compared to their conventional polycrystalline counterparts (Nik Rozlin and Alfantazi 2012). The electrodeposition technique is found to be the best and

simpler method to generate nanocrystalline materials because of its straight-forward and low cost process, and the possibility of deposition is feasible on almost any geometry of a conductive substrate (Lallemand et al. 2005). Electrodeposited cobalt-iron Co-Fe alloys have attracted considerable attention in various applications such as magnetic recording, electronics industries, and protective coatings due to their high saturation of magnetic flux and high Curie temperature (E. E. Kalu et al., 2005). The properties of electrodeposited Co-Fe alloys can be significantly influenced by homogeneous magnetic fields, affecting their microstructure, roughness, internal stress state, and chemical composition (J George et al., 2013). Studies on tensile stress have indicated that grain size plays a crucial role, with smaller grain sizes leading to higher tensile stress in electrodeposits. Additionally, decreasing the grain size can contribute to better-localized corrosion resistance due to highly distributed current (Kim et al., 2001). An increase in iron content has also been shown to result in increased stress in the alloy deposit. While extensive research has been conducted on the magnetic properties and stress of Co-Fe coatings, only a few studies have focused on the development of nanocrystalline Co-Fe alloys. Recent research involved synthesizing nanocrystalline Co-Fe through the electrodeposition method in a water bath, varying iron concentration, and other deposition parameters on stainless steel and mild steel substrates (Nor Fazil et al., 2017). Anomalous co-deposition was observed, indicating that the reduction of cobalt is inhibited while the deposition of iron is enhanced. The iron content of the deposits was found not to be affected by applying various temperatures during the electrodeposition process, although high deposition temperatures led to the formation of pits on the surface (Nik Rozlin and Alfantazi 2012). In this work, the investigation focused on understanding the effects of varying iron content in the sulfate bath on various aspects such as microstructure, crystallographic structure, grain size, surface roughness, and microhardness of substrate materials. The objective was to determine which substrate materials exhibit the best corrosion resistance under these conditions. Previous studies on the electrodeposition and characterization of Co-Fe alloy coatings, along with other alloys of iron group metals, have reported that the magnetic saturation of Co-Fe alloy increases with a rise in iron content in the deposit. Homogeneous magnetic fields have been shown to significantly impact the properties of electrodeposited Co-Fe, influencing microstructure, roughness, internal stress state, and chemical composition. Tensile stress studies emphasized the role of grain size, indicating that smaller grain sizes lead to higher tensile stress in

electrodeposits. Decreasing grain size contributes to uniform and improved localized corrosion resistance due to highly distributed current. Additionally, an increase in iron content has been linked to increased stress in the alloy deposit. While extensive research has been conducted on the magnetic properties and stress of Co-Fe alloys, only a few studies have delved into the development of nanocrystalline Co-Fe alloys. The current work aims to fill this gap by examining the effects of varying iron content in the sulfate bath on multiple material characteristics and determining which substrate materials exhibit optimal corrosion resistance.

Thus it has been reported that Ni, Co, Fe containing alloys/composites of non-precious metals, available at lower cost are emerged as good electro-catalysts for HER activity (Luo et al. 2016), (Pagliaro 2009). Due to their excellent mechanical and wear-resistant properties, nano-crystalline Co and Co-based alloys (Platatorres et al. 2007), (Pu et al. 2016), (Reddy et al. 2016) have recently been identified as promising candidate material for the replacement of hexavalent-Cr plating (Safavi and Walsh 2021). In recent years, there has been an interest in the electrochemical deposition of Co-based alloys due to both basic and applied research (Turner, 2004). Among various binary alloy coatings, cobalt-phosphorous Co-P alloy coatings have been identified as suitable materials for replacing environmentally un-friendly hard chromium. Attractive appearance, good corrosion, wear resistance, soft magnetic materials for magnetic recording and electro-catalysts for hydrogen evolution and oxidation reactions(Vicenzo and Cavallotti 2004), (Safavi and Walsh 2021) are the characteristic features of Co-P alloy coatings.

2.4. Modern methods of electrodeposition

2.4.1 Composition modulated multilayer alloy coating

A novel category of materials characterized by alternating layers of different metals or alloys, each with a thickness of a few nano/micro meters and exhibiting an ultrafine microstructure, is referred to as composition modulated multilayer (CMM) or compositionally modulated alloys (CMA), or simply multilayer coatings (Krishnan et al. 2002),(Chawa et al. 1998). As a result of layering in nano/micro metric dimensions, they exhibit improved electrical, magnetic, mechanical, and corrosion properties (Bhat et al. 2022),(Cohen et al. 1983). The changed properties of CMA coatings are found to be unique, and are impossible to get through any other conventional methods. The performance of alloy coatings can be improved drastically using

different layering schemes (in terms of thickness and composition of individual layers) to meet a number of applications, like improved corrosion resistance, wear resistance and magnetic properties (Pavithra and Chitharanjan Hegde 2013). There are number of reports on development of CMM coatings and Ni-based alloy coatings in which alloys of two different compositions are deposited layer by layer on the substrate by periodic modulation of the current density. Experimental results revealed that multilayer coatings can be used to improve the corrosion resistance property of mild steel against harsh marine environments (Venkatakrishna and Chitharanjan Hegde 2010) (Elias and Hegde 2016) (Anwar et al. 2018) (Bhat et al. 2020)

2.4.2 Magneto-electrodeposition

Off late, use of magnetic field (*B*) effect on the process of electrodeposition has been used to improve different physical and chemical properties of alloy/metal coatings. In this direction, only very few reports are available with respect to Ti-containing Ni alloys. The superimposition of external magnetic field on the process can achieve better results on the nature of electrodeposit (Fahidy 1983; Ragsdale et al. 1998). It has been described that the applied magnetic field primarily effects the transport of ions towards cathode, and consequently alters the thickness of electrical double layer (EDL). This change in mass transport process is responsible for change in surface morphology of the deposit, by altering the thickness of the double layer. Notable reports on this topic include works by Ganesh et al. in 2005a, Monzon and Coey in 2014, and Tacken and Janssen in 1995. The Lorentz force, expressed as $FL = qvB \sin\theta$, reaches its maximum magnitude when applied perpendicular ($\theta = 90^{o}$) to the applied current density or the velocity of the moving charged species, as highlighted by Monzon and Coey in 2014. Therefore, the efficient electrolysis of water can be achieved by carefully designing the electrode material and introducing an external magnetic field of optimal strength to minimize polarization effects. A comprehensive study on the magnetic field effects on water electrolysis was conducted by Wassef and Fahidy in 1976. Subsequently, researchers have successfully utilized the magnetic field as a tool to enhance electrochemical reaction kinetics. Examples of such studies include the works of Aaboubi and Msellak in 2017, Devos et al. in 1998, and Matsushima et al. in 2006.

Waskaas and Kharkats (1999) have reported the mechanism of influence of magnetic fields on electrochemical processes and also the effect of magnetic field on the polarization of nickel or cobalt systems. The more striking effect on magneto electrodeposition is limiting current. Thus, increase in limiting current changes the surface morphology of electrodeposits. Titanium is highly corrosion resistant material and easy to handle. In this regard, effect of magnetic field with respect to corrosion properties on electrodeposition of Titanium have been studied (Ganesh et al. 2005), (Koza et al. 2008), (Koza et al. 2010), (Koza et al. 2011) (Krause et al. 2007).

2.5 Electro-catalytic study of alloy coatings

Electro-catalysis is a specific branch of electrochemistry which details on the use of catalysts to modify the rates of electrochemical reactions. Electrolysis of water splitting for hydrogen evolution reaction (HER) and oxygen evolution reaction (OER) is a promising and efficient process, where catalysts play a key role. Therefore, the use of cathode and anode materials with strong stability and high reactivity is a prerequisite to guarantee the increased conversion efficiency of hydrogen and oxygen production from electrolytic water. Though Pt with a low over potential close to zero, and a Tafel slope of about 30 mV dec^{-1} is good electrocatalytic material, its prohibitive cost prevents its extensive use as electro-catalyst. In this direction several electro-catalysts have been established for several electro-catalysis reactions, like HER and OER and fuel oxidation. There are several reports in the literature on electro-catalytic performance of electrodeposited Ni-Ti alloy coatings developed under different conditions of bath chemistry. The catalytic properties of materials mainly depend on the density of active sites embedded in it, which are responsible for their redox activities (Wu et al. 2010).Generally, IrO_2 or RuO_2 for the O_2 evolution reaction (OER) and Pt for the H_2 evolution reaction (HER) are currently the most advanced electro-catalysts for water splitting in acidic solutions. In this regard, the transition metals and their alloys are used as best electrode materials for water splitting reactions. Ni and its alloys have been considered as efficient electrode materials due to their special properties, such as low cost, high strength, good wear resistance and good electro-catalytic activity (Wang et al. 2005).The electrodeposited alloys of transition metals like Ni, Co, Ti, Fe and Mo are proved to be the efficient electro catalysts towards water splitting reaction than bare Ni coatings (Fan et al. 1994) , (Rosalbino et al. 2008). Apart from this, many

reports are available in literature to support the fact that electro-catalytic efficiency of electrode materials can be improved drastically by adding nano-particles into the metal/ alloy matrix, through nanoparticles co-electrodeposition.

2.5.1 Equipment/Instruments used for the present study

The instruments and equipment employed in the current study, with their corresponding model numbers and intended applications, are organized in Table 2.1.

Table 2.1- The list of various instruments/equipments used for the present investigation

Name of the equipment/ instrument	**Model No. and manufacturer/supplier**	**Purpose used for**
Electronic Weighing Balance	SC-391, Scientech, India	To measure the quantities of salts used in bath preparation and to weigh the plated samples
pH Meter	EQ-611, Equiptronics, India	To adjust the plating bath pH
Magnetic stirrer	EQ-771, Equiptronics, India	To achieve a uniform blending of the plating bath prior to the plating process
Bench Polisher	BPP/A, Sugama Machine Tool, India	Primary mechanical polishing of the substrates
DC Power source	Aplab-LD3202, India	Conventional electrodeposition
DC Power Analyzer	Agilent-N6705, Agilent Technologies, USA	Development of CMMA coatings
Electromagnet	EM 100, Polytronics, India	For the development of Magneto electrodeposited (MED) coatings
SEM	JSM–7610F from JEOL, USA	Surface structure analysis
EDS	JEOL, Oxford Instruments, UK	Elemental composition analysis
FESEM	Neon 40 Crossbeam, Carl Zeiss, Oberkochen, Germany	Surface structure analysis

XRD	JDX–8P, JEOL, Japan	Phase structure analysis
Digital Thickness Tester	Coatmeasure M&C, ISO–17025, India	Measuring the thickness of coatings
Vickers Microhardness Tester	CLEMEX, CMT. HD, Canada	Testing microhardness of the coatings
Potentiostat/Galvanostat	Biologic SP- 150, Biologic Science Instruments, France	Electrochemical characterization of the coatings

2. 6 SCOPE OF THE WORK AND OBJECTIVES

Having inspired by the technologic importance of Ni/Co - based alloy plating, and exclusive claims of multilayer coating and magneto-electrodeposition techniques, electrodeposition of (Ni/Co-M, where M = Ti, P, Fe) alloy coatings on steel/copper for better corrosion protection is intended to be achieved here. In this direction, optimization of three new baths namely Ni-Ti, Co-P and Co-Fe were tried, using suitable additives. Ni-Ti alloy coatings of high corrosion performance was developed by exploring the advantages of multilayer and magneto-electrodeposition approach. The corrosion behavior of monolayer and multilayer Ni-Ti and Co-Fe were studied, and reasons of facts responsible for enhanced corrosion performance of composition modulated multilayer (CMM) alloy coatings were analyzed. The effect of the composition and thickness of individual layers on the corrosion performance of alloy coatings were analyzed and results are discussed. Similarly, in case of magneto-electrodeposition, the effect of intensity of magnetic field (*B*), applied both parallel and perpendicular on the process of electrodeposition were studied, and experimental results detailed in the light of magneto-hydrodynamic (MHD) effect. The incredible claims of electroplating (like effect of operating parameters) were tried to explore effectively for electro-synthesis of Ni-Ti, Co-P and Co-Fe alloys as electrocatalytically active material for water splitting applications. The electro-catalytic activity of these coatings, in terms of hydrogen evolution reaction (HER) and oxygen evolution reaction (OER) in complete alkaline water electrolysis were studied. The effect of addition of Ag nanoparticles into the binary alloy coatings matrix were studied, and optimum conditions were identified for best performance of alloy coatings for water splitting applications.

Thus, as the conventional metal plating is becoming insufficient to meet many of the recent technological demands, Ni/Co-M (where M = Ti, P and Fe) alloy coatings with improved properties are to be tailored to cater the needs of advanced applications. The philosophy of the work present in this thesis is to maximize the corrosion protection ability and electro-catalytic activity of the deposited alloy coatings from the proposed baths, namely Ni-Ti, Co-P and Co-Fe by proper manipulation of deposition conditions. In this direction, the title project is driven by the following objectives.

1. To optimize few new electrolytic baths of Ni/Co-based binary alloys, for developing a bright, smooth, uniform coatings, using suitable additives and to optimize the deposition conditions (like current density, temperature and pH of the bath) for peak performance of the coatings, in terms of their electrochemical properties, namely corrosion and electro-catalytic activity.
2. To study the corrosion behavior of all electrodeposited alloy coatings (monolayer, multilayer and magneto-electrodeposited), deposited for same duration (10 min) by electrochemical AC and DC methods in 3.5% NaCl solution, for comparison purpose.
3. To develop a comprehensive approach to improve significantly the corrosion resistance property of Ni-Ti and Co-Fe alloys by multilayer approach by modulating the mass transport process at cathode film, by pulsing the cathode current densities.
4. To optimize the deposition conditions of CMM coatings of Ni-Ti and Co-Fe binary alloys, in terms of number of layers and composition of each layer for best performance against corrosion.
5. To improve the corrosion resistance property of monolayer Ni- Ti alloy coatings using the benefit of *magneto-electrolysis. i.e.,* by applying magnetic field (*B*), in both parallel and perpendicular to the direction of electric field.
6. To validate the effect of intensity and direction of magnetic field (*B*) on the properties of electrodeposited alloy coatings, and to optimize the conditions for their best performance against corrosion.

7. To study the electro-catalytic activity of Ni-Ti and Co-P alloy coatings to use as electrode material for alkaline water electrolysis for HER and OER using CV (Cyclic Voltammetry) and CP (Chrono-potentiometry) techniques.
8. To study the effect of incorporation of Ag-nanoparticles into Ni-Ti and Co-P alloy matrix towards their efficiency for water splitting applications, in terms of HER and OER.
9. To compare the corrosion protection efficiency and electro-catalytic activity of electrodeposited alloy coatings, by conventional electrodeposited (ED), composition modulated multilayer (CMM), and magneto-electrodeposited (MED) methods, and to understand the reasons responsible for improved properties, through principles of alloy deposition and magneto-hydrodynamic (MHD) effect.
10. To compare and characterize the monolayer, multilayer and electro-deposited alloy/composite alloy coatings using different instrumental methods such as FESEM, EDS, XRD and AFM and to analyze the reasons responsible for their improved corrosion resistance and electro-catalytic properties.

CHAPTER-3

EXPERIMENTAL

This chapter speaks about the methods and materials used for the production and characterization of electrodeposited Co/Ni-based alloys' and their nanocomposite coatings. The experimental results on improvisation of corrosion resistance behavior of monolayer alloy coatings through multilayer approach is presented here, and a comparison is made among the Ni-Ti and Co-Fe multilayered alloy coatings, and with their monolayer counterparts. Experimental results on improvisation of corrosion performance of Ni-Ti alloy coatings, through magneto-electrodeposition technique, in relation to its monolayer counterpart is presented here. The effect of magnetic field (B), in terms of intensity and direction on its corrosion resistance is given. The experimental results on electro-catalytic efficiency of different alloy coatings towards water splitting applications of HER and OER are presented here. A comparison of electro-catalytic efficiency of different alloy coatings, and their nanocomposite coatings are made, followed by a concise description of the characterization techniques used. The corrosion resistance and electro-catalytic efficiency of alloy coatings, developed through different deposition methods have been summarized, and the results are discussed.

During experimental study of corrosion and electro-catalytic performance of all binary alloy coatings through different methods of deposition, the operating variables and composition (current density, temperature, pH and duration of deposition) of a given bath was kept constant, for comparison purpose. All chemical reagents used are of LR grade (Merck, Mumbai, India). The pH of the bath is adjusted with NH_4OH or HCl, using Micro pH Meter (Systronics, 362). All depositions were carried out at room temperature for 10 minutes, under the constant condition of agitation on the polished substrate in a customized rectangular PVC cell**.** The substrate (mild steel or copper) is polished metallurgically to get the mirror finish, degreased with trichloroethylene, and then pickled in 1:1 HNO_3. The anode surface has been activated each time by immersing in 10% HCl followed by water wash. The deposition is carried out on a known active surface area of substrate, keeping other region covered with cellophane tape. The anode used in electrodeposition process is of same exposed surface area as that of the cathode (substrate). The cathode and anode are placed parallel to each other in

the PVC cell. washed with distilled water, followed by air drying, and then stored in desiccator till further analyses. The electrodeposited binary alloy coatings, obtained through different methods, like conventional method using DC, composition modulated multilayer (CMM) or simply multilayer using pulsed DC and magneto-electrodeposition by inducing magnetic field (*B*) were analyzed for their phase structure, composition and surface morphology using XRD EDX and FESEM techniques.

3.1 Hull Cell Study

The optimization of bath composition and operation variables (like pH, temperature and current density) of all newly reported electrolytic baths for Ni-Ti, Co-P and Co-Fe, mentioned in the thesis were accomplished by well-known Hull cell method (Parthasaradhy 1989). The Hull cell of 267 mL capacity was used for the optimization of bath. The polished mild steel substrate was used as cathode; and the metallic/graphite anode, activated each time by immersing in 10% HCl followed by water wash was used. The bath was optimized to get bright, smooth, uniform and homogeneous deposit of Ni-Ti, Co-P and Co-Fe using Hull cell method by varying concentration of metal ions, complexing reagents and addition agents (to act as brighteners, levelers, wetting agent etc. to impart better appearance to coating). The various steps followed in optimization of bath composition and operating variables, using conventional Hull cell is shown schematically in Figure 3.1

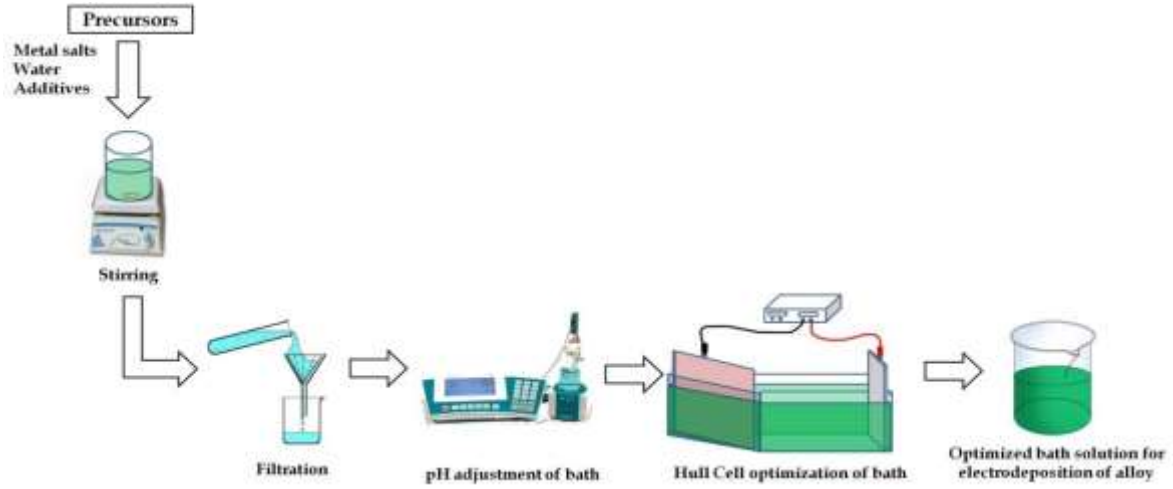

Figure 3.1 *- Flow chart showing the steps involved in optimization of bath using Hull cell*

3.2 Conventional electroplating

The optimized bath of different binary alloys (in terms of the composition and current density to get bright, smooth, uniform coating) were then used for their electroplating, starting from conventional monolayer alloy coating till different methods of deposition. Binary alloy coatings were applied to a substrate under various current density conditions (arrived by Hull cell method), on passing direct current (DC) through power source, by keeping anode and cathode parallel as shown in Figure 3.2. The plating process is conducted by maintaining constant pH, temperature and the deposition rate. The electrochemical behavior of the alloy coatings were analyzed by EIS and Tafel techniques in 3.5% NaCl medium. The coatings that exhibited the least corrosion rate (CR) was considered as the optimal current density, which is the characteristic of the given bath and the same was used for other deposition process.

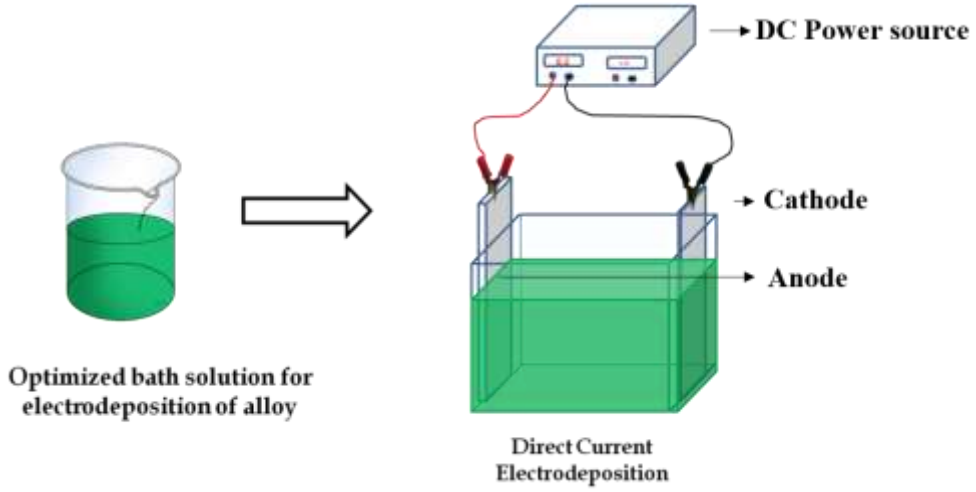

Figure 3.2*- Schematic representation of set up used for conventional electrodeposition*

3.3 Development of multilayered alloy coatings

Driven by the fact that periodic modulation in mass transport process at cathode film (by periodic change in the current density) leads to the development of multilayer coatings on the surface of cathode, multilayer coatings of binary alloys can easily be developed. Hence, in order to improve corrosion resistance property of Ni-Ti and Co-Fe alloy coatings by taking the advent of modern multilayer technique, their CMMA coatings were developed electrolytically by pulsing periodically the DC, between two different current strengths. This enabled the development of coatings in layered manner, by having a periodic modulation in composition (Leisner et al. 1996a). In the deposition process, the current is alternated among different current densities, referred to as cyclic cathode current densities (CCCD's). Accordingly,

multilayer Ni-Ti and Co-Fe alloy coatings have been developed using square current pulses (pulsed DC) as shown in Figure. 3.3(b). The current pulse used for conventional monolayer alloy coating is also shown in Figure 3.3(a). The cross sectional view of multilayer and monolayer alloy coatings are also shown on the right of Figure 3.3(b).

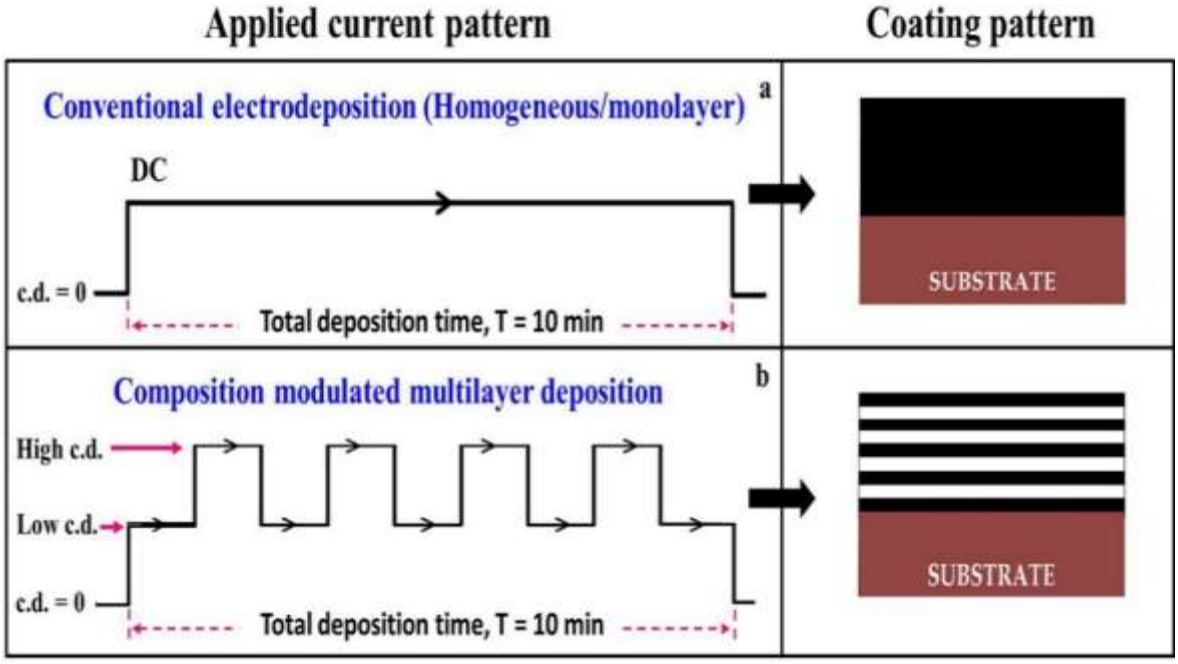

Figure. 3.3 *- Schematic diagram showing the power pattern used for deposition of multilayer alloy coatings, and the cross sectional view of multilayer alloy coating developed (lower right) in comparison with that of its monolayer coating (on top)*

Here, multilayer or CMM coatings with alternate layers of different compositions are conveniently expressed as $(Ni/Co\text{-}M)_{1/2/n}$. Where M = Ti or Fe, 1 and 2 denote the first and second (or cyclic) cathode current densities chosen to be applied for the layers of deposition of alloys with differing compositions, and 'n' denotes the number of layers created during the whole plating time, which is 10 minutes. The DC power source (DC Power Analyzer, Agilent Technologies, Model: N6705) was programmed to alternately change CCCDs in order to generate multilayer coatings. As a result, multilayer binary alloy coatings of various configurations, i.e., under distinct sets of CCCDs and with varying numbers of layers, were created and their corrosion resistance behavior was investigated.

3.4 Magneto-electrodeposition

Magneto-electrodeposition (MED) refers to the electrodeposition that occurs under the influence of an induced magnetic field (B). MED is a promising technology for improving the mass transfer constraints during deposition, and thus the characteristics and performance of alloy coatings. As a result, magnetic fields can be employed to impart certain qualities to electrodeposited coatings. The MED Ni-Ti and Co-Fe coatings were created utilizing a DC power source at the desired current density in combination with a magnetic field. MED studies were carried out with an electromagnet (Polytronics, Model: EM 100) including intensities ranging from 0.1 T to 0.4 T and ion flow directions (parallel and perpendicular). The schematic diagram for the setup is given in Figure 3.4

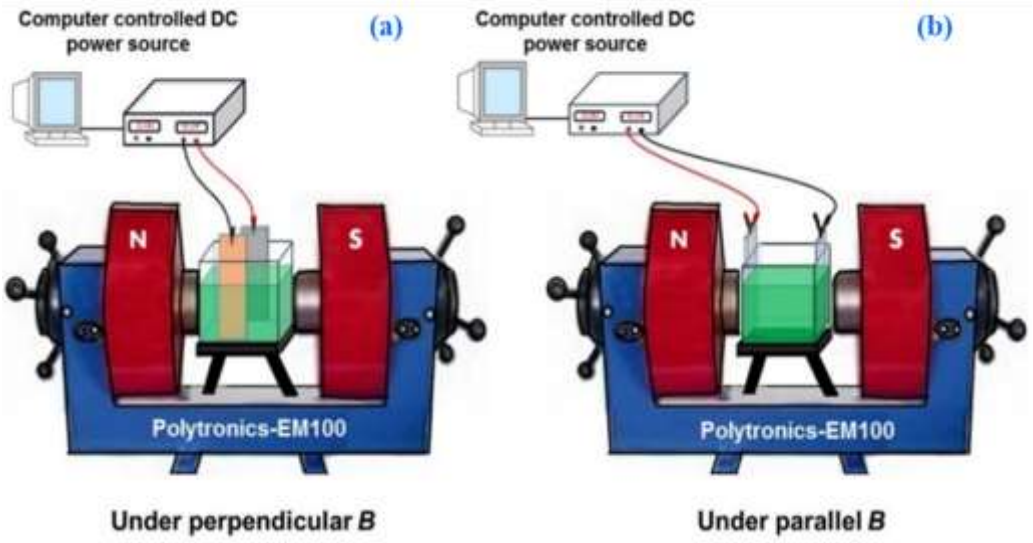

Figure. 3.4 *- Experimental setup to use for MED of binary alloy coatings under conditions magnetic field B is perpendicular (a), and parallel (b) to the direction of electric field. It may be noted that current density is kept constant throughout the process of deposition*

MED coatings of Ni-Ti alloy coatings were deposited, under different conditions of *B* (both intensity and direction) by keeping the deposition current density as constant, (depending on the optimal condition of the bath). The coatings were applied through two different methods: normal and conventional electrodeposition (ED), carried out under natural convection, and magnetoelectrodeposition (MED), conducted under forced

convection. These will be denoted as Ni-Ti B=0 T and Ni-Ti B = 0.1 T/per (or par), depending on the intensity and direction of the induced magnetic field (B) relative to the flow direction of ions. All depositions were conducted on a mild steel substrate after surface preparation. A 250 mL PVC vessel was utilized for the plating process, with a graphite anode and the substrate was positioned parallel, 5 cm apart. The deposition duration for all experiments was 10 minutes at room temperature using the optimal bath conditions for comparison purposes.

3.5 Development of Ni/Co-M (M = P and Fe) alloy coatings for electro-catalytic study

To examine the electro-catalytic properties of electrodeposited alloy coatings for water splitting applications, the coatings were applied onto a copper rod with a cross-sectional area of 1 cm^2. This is accomplished using a specially designed electrodeposition setup, depicted in Figure 3.5.

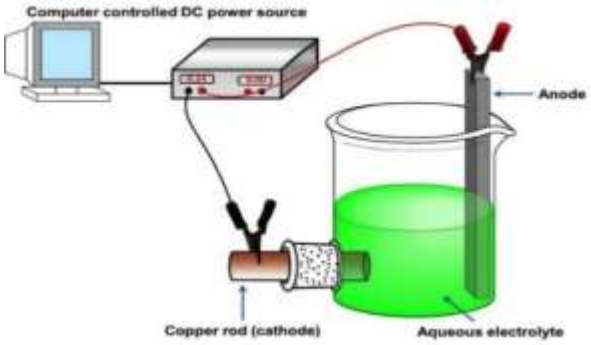

Figure 3.5 - *Experimental setup used for electrodeposition of alloy coatings for electro-catalytic study. Here, polished copper rod was used for electrodeposition of binary alloy coatings to enable quantitative measurement of their electro-catalytic efficiency*

3.6 Study of corrosion and electro catalytic behavior of Ni/Co-M alloys

The corrosion behavior of monolayer, multilayer (CMM) and magneto-electrodeposited (MED) Ni/Co-based alloy coatings (all coatings deposited at 1.0 – 4.0 A/dm^2 for 10 mins duration) were studied in 3.5 % NaCl solution by potentiodynamic polarization and electrochemical impedance spectroscopy (EIS) methods, using potentiostat/galvanostat. Potentiodynamic polarization study was carried out in a potential ramp of ±250 mV around equilibrium potential, at scan rate of 1 mVs^{-1}. EIS study was made using 10 mV perturbing AC voltage, and corresponding Nyquist and Bode plots were used to understand the corrosion

efficiency of alloy coatings. Corrosion rates of alloy coatings were calculated by Tafel's extrapolation method. The improved corrosion rates of CMM and MED coatings in relation to its monolayer counterpart were discussed, and the reasons contributing to the enhanced corrosion resistance were analyzed and the results were discussed. Similarly, the electro-catalytic performance of monolayer and magneto-electrodeposition (MED) Ni/Co-based alloy coatings developed on a copper rod were investigated using a custom-designed three-electrode tubular glass cell, illustrated in Figure 3.6. The working electrode was an electrodeposited copper rod, the counter electrode was platinized platinum with the same surface area (1.0 cm^2), and a saturated calomel electrode (SCE) served as the reference electrode are analysed cyclic voltammetry (CV) and chronopotentiometry (CP) were utilized to determine

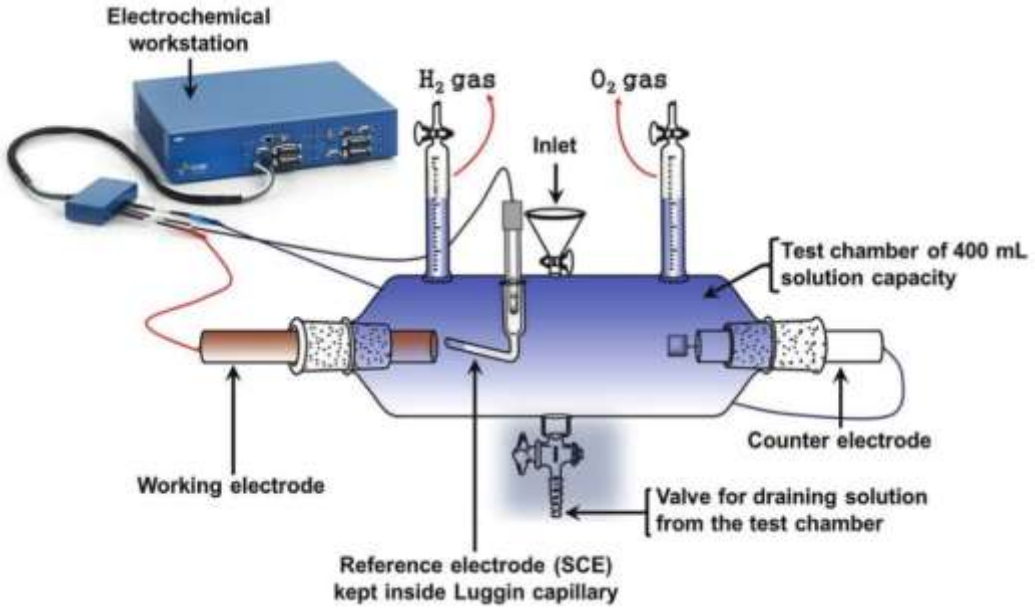

Figure. 3.6 - *Customized three-electrode glass cell to use for quantification of electro-catalytic activity of alloy coatings, in terms of the volume of H_2/O_2 gases liberated while using them as cathode and anode material, respectively*

ELECTROCHEMICAL DEPOSITION OF MONOLAYER AND MULTILAYER Ni-Ti ALLOY COATINGS FOR IMPROVED CORROSION PROTECTION OF MILD STEEL

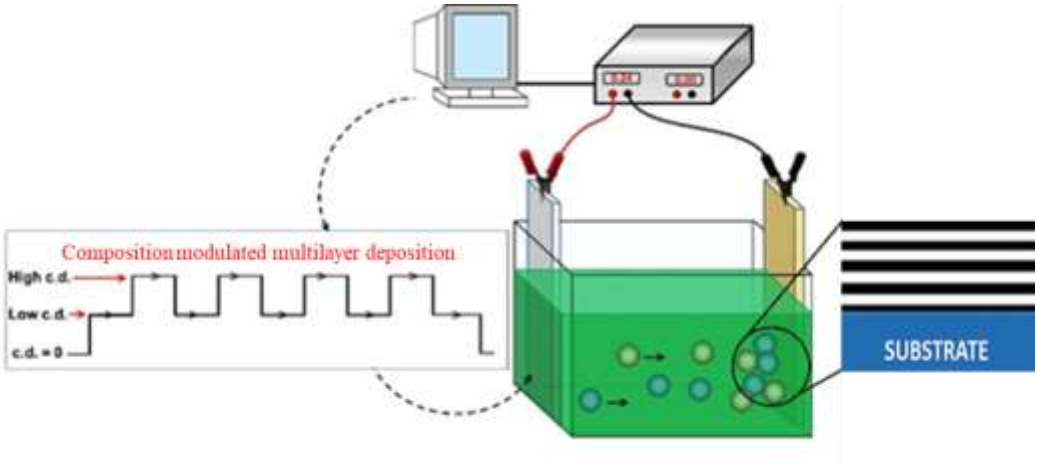

This chapter details the optimization of a new electrolytic bath of Nickel-Titanium Ni-Ti alloy, using glycerol as additive. The experimental results of present study unfold in two parts. In the first part, optimization of bath composition and operating parameters of a new bath is studied using Hull cell method. Conventional monolayer Ni-Ti alloy coatings were electrodeposited from the optimized bath using direct current (DC). The current densities were optimized for the deposition of the most corrosion-resistant monolayer alloy coatings. In the second part, the discussion focuses on enhancing the corrosion resistance of monolayer Ni-Ti alloy coatings through a method known as Composition Modulated Multilayer Alloy (CMMA), while using the same bath. The multilayer Ni-Ti alloy coatings, having alternate layers of different compositions and thickness were developed by periodic modulation of the DC during process of deposition. Coatings configurations were optimized, in terms of current pulse height and duration of deposition of each layer to maximize their corrosion protection efficiency, compared to its monolayer counterpart. The better corrosion resistance of multilayer Ni-Ti alloy coatings was explained with plausible mechanism.

4.1 INTRODUCTION

Titanium and its alloys are known to have certain specific properties, such as aerospace, bio-medical, good biocompatibility, shape memory effect, good wear resistance, and corrosion

resistance. Among many methods of fabrication of these alloys, electrodeposition is of particular significance due to genuine reason of its low cost and high deposition rate. They form spontaneously a protective oxide films on surface, which remain stable. Titanium exhibits excellent corrosion resistance in both marine and industrial environments (Seo et al. 2023). Though, titanium metal cannot be electrodeposited alone from any of its aqueous solutions, and it can only be co-deposited with iron group metals such as nickel, cobalt, or iron to form an alloy. This phenomenon is called as *induced co-deposition* as named by Brenner (Eliaz and Gileadi 2008). Ni-Ti alloy coatings have different properties like good biocompatibility (Toker et al. 2014), shape memory effect (Braz Fernandes et al. 2013), good wear resistance, and corrosion resistance (Aydoğmuş et al. 2020). These alloys have wide number of applications in bio-medical, aerospace and automobiles.

In this direction a novel bath of Ni-Ti alloy has been proposed. Ni-Ti alloy coatings have been developed using glycerol as the brightner. In the first part of this chapter, direct current (DC) has been used as the driving force for deposition conventional monolayer Ni-Ti alloy coatings. The surface morphology, compositional data and phase structure of alloy coatings corresponding various current densities were characterized by utilizing SEM, EDS and XRD techniques. The experimental results of investigations were correlated with the phase structure, morphology, and chemical composition of the coatings. In the second part, how the corrosion resistance of monolayer Ni-Ti alloy coatings can be further improved by multilayer approach using the same bath is explained. The corrosion performance of both monolayer and multilayer Ni-Ti alloy coatings were assessed by electrochemical AC and DC method, using 3.5 % sodium chloride solution (to mimic the intense corrosion medium) for comparison purpose.

4.2 EXPERIMENTAL

4.2.1 Optimization of Ni-Ti alloy bath

A new Ni-Ti alloy bath containing nickel sulphate ($NiSO_4$), titanium oxy sulphate ($TiOSO_4$), tri-sodium citrate ($Na_3C_6H_5O_7 \cdot 2H_2O$) and glycerol has been proposed here. Individually, all chemicals are dissolved in double distilled (DD) water before, after being thoroughly combined and agitated. Using a Micro-pH Meter (Systronics-362), the bath pH was maintained to 4.0 using either H_2SO_4 or NH_4OH (depending on the necessity). The usual Hull cell approach was

used to optimize the bath composition and plating factors, as discussed elsewhere (Kanani 2006). The bath conditions and plating variables of the optimized Ni-Ti alloy bath, arrived after Hull-cell experiment is reported in Table 4.1. All electroplating of Ni-Ti alloy coatings were carried out using power source (DC Power Analyzer, Agilent N6705C, USA). The power patterns used for the development of monolayer and multilayer Ni-Ti alloy coatings are illustrated in Figure 4.1.

Table 4.1 - The composition and operating variables of newly optimized Ni-Ti alloy bath

Bath Ingredients	*Composition (g/L)*	*Operating Variables*
Nickel Sulphate ($NiSO_4$)	49.8	Anode: Graphite
Titanium Oxy Sulphate ($TiOSO_4$)	39.9	Cathode: Mild steel
Tri Sodium Citrate ($Na_3C_6H_5O_7 \cdot 2H_2O$)	16.5	Temp: 303K
Glycerol	3.3 mL/L	pH: 4.0 current density range: 1.0-4.0 A/dm^2

It may be noted that constant current, or direct current (DC) was used for development of monolayer alloy coatings as shown in Figure 4.1 (a); and pulsed current of different pulse height was used to develop layered coatings (having different composition) as shown in Figure 4.1(b). The cross-sectional view of monolayer and multilayer alloy coatings formed are shown on right.

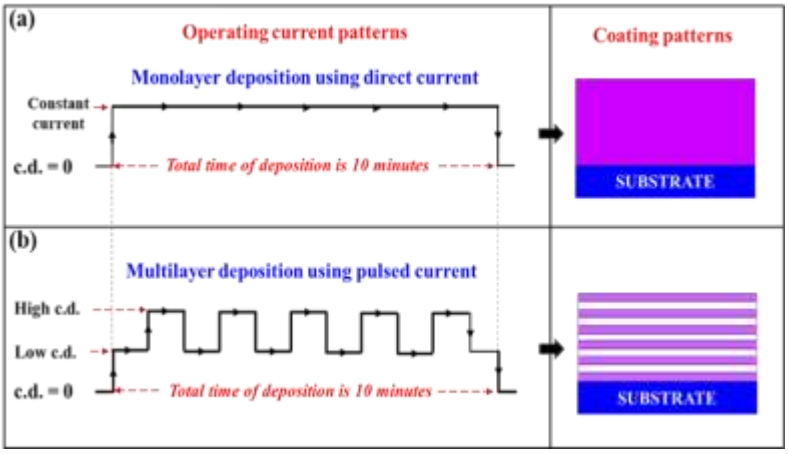

Figure 4.1- *Schematic diagram showing the current patterns used for development of a) monolayer, and b) multilayer Ni-Ti alloy coatings, and the cross-sectional view of their coatings (on right)*

Electroplating was carried out in a 200 mL capacity cell (made of PVC). Mild steel (MS) plates (C-0.17%, Si-0.43%, Mn-0.54%, P-0.16% and Fe -98.7%) having dimensions of (7.5 cm ×2.5 cm × 0.2 cm) were used as cathode. The surfaces were mirror polished using emery wheels of gradually decreasing grit size. Finally, surfaces were cleaned with a cotton swab dipped in the trichloroethylene (TCE), as solvent. All depositions were carried out on same active surface area of (3.0 × 3.0 cm^2) of polished MS plate at 303 K, keeping other area masked by means of cellophane tape. Ni-Ti alloy coatings of various compositions were plated galvanostatically at various current densities while maintaining the parallel alignment of anode and cathode. Substrates after being electroplated were washed under running water, rinsed with distilled water, and then dried in hot air. Before being taken for additional analysis, it is finally dried in a desiccator. All electroplating reported here were carried at pH 4.0 and current densities (1.0 – 4.0 A/dm^2) for a time period of 600 s (for comparison purpose). To validate the relative performance of all coatings, the duration of all depositions was kept constant

All electrochemical investigations of Ni-Ti alloy coatings were performed in a three-electrode cell, where electrodeposited Ni-Ti alloy coatings were used as working electrode, saturated calomel electrode (SCE) as reference electrode and platinum foil (having the same active surface area as that of working electrode) as counter electrode using a computer controlled electrochemical workstation, potentiostat/galvanostat (*Biologic SP-150, Biologic Science Instruments, France*). The electrochemical impedance spectroscopy (EIS) experiment was carried out with a small amplitude (± 10 mV) AC pulse in the frequency range of 100 kHz to 10 mHz. The corrosion rate (CR) of Ni-Ti alloy coatings were measured using the potentiodynamic polarization method at a scan rate of 1 mVs^{-1} in a potential window of ± 250 mV around open circuit potential (OCP). Using Nyquist plots, the relative EIS responses for different Ni-Ti alloy coatings were used to determine their polarization resistance (R_p) values. The change in composition and surface morphology of alloy coatings with deposition current density was investigated using Scanning Electron Microscope (SEM), interfaced with an Energy Dispersion X-ray Spectroscopy (EDS) instrument. The drift of phase structure of alloy coatings with current density was investigated using X-Ray Diffraction (XRD) technique (Rigaku, Miniflex 600, with CuK radiation having = 1.5418 as the X-ray source) and results are discussed.

4.3. RESULTS AND DISCUSSIONS

4.3.1 Development of monolayer Ni-Ti alloy coatings

On taking the optimized bath, electrodeposition of conventional monolayer Ni-Ti alloy coatings were accomplished using direct current (DC) using power source (DC Power Analyzer, Agilent N6705C, USA). The nature of power pulse used for deposition of monolayer Ni-Ti alloy coatings is shown in Figure 4.1(a), with cross sectional view of the deposit (on right). The electrodeposition of Ni-Ti alloy coatings was carried out at different current densities. *i.e.* from 1.0 A/dm^2 to 4.0 A/dm^2. A sound, bright, and homogeneous Ni-Ti alloy coatings were obtained in the studied range of current densities. The proposed Ni-Ti alloy bath known to follow induced type co-deposition as explained by Brenner (Brenner, 1963). According to this process, deposition of alloys containing metals, such as molybdenum, tungsten, or germanium and titanium cannot be deposited as such. However, these metals can readily be co-deposited with the iron group metals (Ni, Co and Fe) (Brenner 1963),(Eliaz and Gileadi 2008). Hence, due to inherent nature of induced type of codeposition that the proposed bath follows, variations in properties of electrodeposited Ni-Ti alloy coatings with current density is quite unpredictable. Accordingly, the scope for studying the structure-property relationship of Ni-Ti alloy is quite vagarious. In this regard, in the present study Ni-Ti alloy coatings corresponding to different current densities are first characterized for their basic properties, such as composition, surface morphology, phase structure, and corrosion resistance.

4.3.2 Compositional analysis

The key factors affecting the composition of the electrodeposited alloy are operating variables of the bath and the bath composition. Moreover, the composition of any binary or ternary alloy coatings often determines the extent to which it protects against corrosion. In this context, Table 4.2 reports the composition of electrodeposited Ni-Ti alloy coatings corresponding to various current densities. From the compositional data, it may be noted that the Ni content decreased with an increase in current density, while the Ti content in the deposit increased. It may also be noted that the deposit is found to be very porous, with a globular structure.

Table 4.2 - Compositional change and corrosion rates (CR) of Ni-Ti alloy coatings with current density deposited from optimized bath

Deposition current density (A/dm^2)	Thickness (μm)	Ni content in the deposit (wt. %)	Ti content in the deposit (wt. %)	$-E_{corr}$ (mV vs SCE)	i_{corr} (μAcm^{-2})	$CR \times 10^{-2}$ (mm/y)
1.0	5.3	99.1	0.9	-370.8	19.4	19.67
2.0	8.6	98.6	1.4	-308.8	17.1	18.20
3.0	10.2	97.7	2.3	-267.6	16.8	16.97
4.0	12.1	96.5	3.5	-257.6	13.8	14.02

4.3.3 Surface morphology

The microstructure of Ni-Ti alloy coatings deposited at different current densities is shown in Figure 4.2

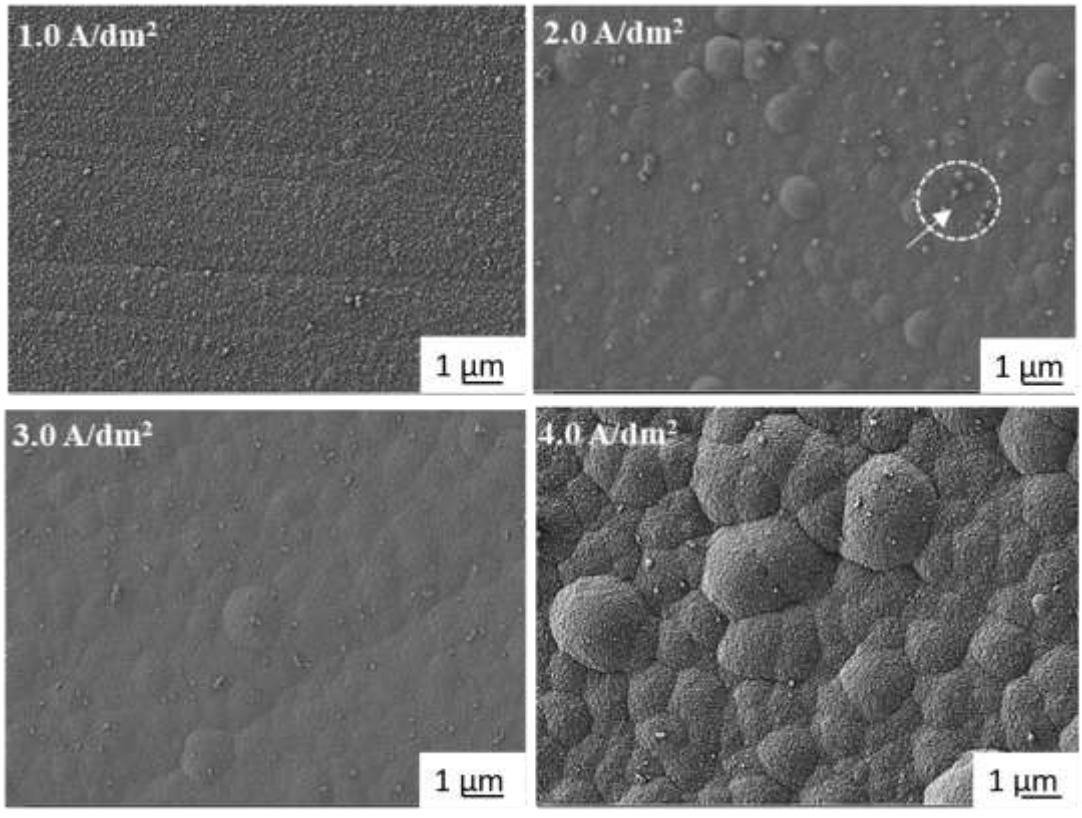

Figure 4.2 - *SEM images depicting the Ni-Ti alloy coatings deposited at different current densities from optimal bath*

From the surface morphology of alloy coatings deposited at current densities ranging from 1.0 A/dm^2 to 4.0 A/dm^2 one can observe that current density plays a significant role on the surface morphology and pattern of electrodeposits. It is seen that Ni-Ti coating electrodeposited at lower current densities exhibits a particulate-like structure on their surface as shown on coating corresponding to 2.0 A/dm^2 in Figure 4.2 These features indicate that the co-deposited Ti particulates were uniformly distributed in the Ni matrix of the coating. Further, it may be noted that the presence of metal particles embedded into the nickel matrix distinctly enlarge the real surface of the coating (Sun et al. 2016). The increased roughness of the alloy coatings at higher current density may be explained by the fact that at high current density excessive evolution of H_2 gas on the surface leaves the cathode film to be more alkaline. As a result, precipitation of metal hydroxides takes place due to the availability of excessive hydroxyl ions.

The thickness of Ni-Ti alloy coatings were found to be increased with current densities, and is in the range of 5-12 μm. The thickness of coatings were calculated from Faraday's law and was verified using Digital Thickness Tester (*Coatmeasure, 2016, 629-643 632, M&C, ISO–17025*), and is reported in Table 4.2. It may be noted that thickness of alloy coatings increased with current density. It is due to obvious reason of increase in rate of deposition with increase of current density (as per Faraday's first law), supplemented by excessive evolution of H_2 at cathode during deposition. It is confirmed by the porosity of coating as shown in Figure 4.2(d).

4.3.4 AFM Study

The surface roughness is an equally important factor to influence the properties of alloy coatings. Hence, the surface topography of electrodeposited alloy coatings is studied using three dimensional Atomic Force Microscopy (AFM) technique. Accordingly, were AFM image of Ni-Ti alloy coatings, deposited at different current densities are shown in Figure 4.3. The topographical study of alloy was carried out by measuring their average roughness (Ra) and root mean square roughness (Rq) values (Ashraf et al. 2016). Accordingly, Ra and Rq values of electrodeposited Ni-Ti alloy coatings corresponding to different current densities are measured, considering their 5 μ m × 5 μ m surface area, and experimental data are reported in the Table 4.3.

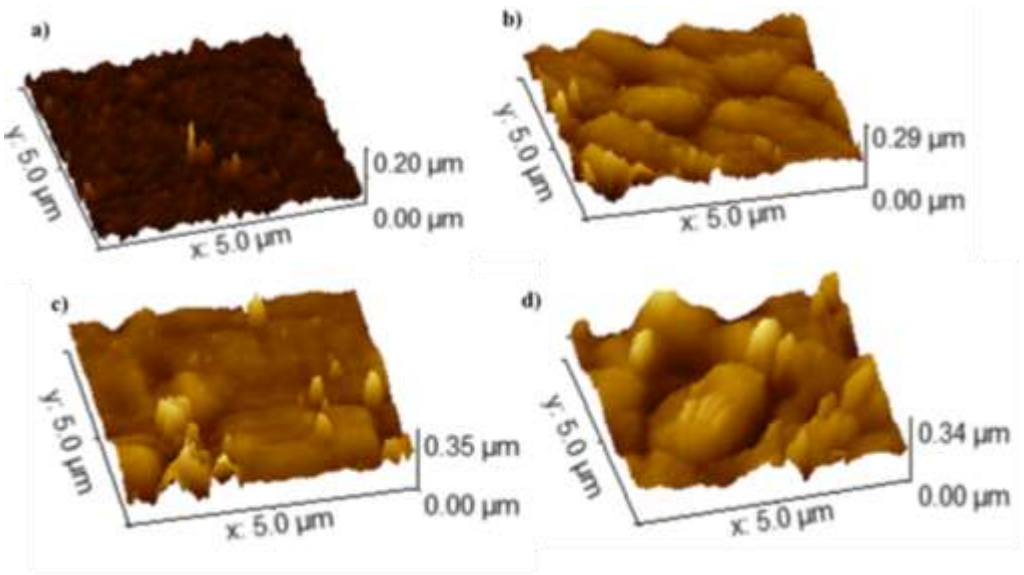

***Figure 4.3** - The AFM image showing the topography of Ni-Ti alloy coatings deposited from the optimized bath at: a) 1.0 A/dm^2, b) 2.0 A/dm^2, c) 3.0 A/dm^2 and d) 4.0 A/dm^2*

It may be seen that the surface smoothness of Ni-Ti alloy coatings decreased with current density, as seen in AFM images from Figure 4.3, and it is in support of the morphological study of alloy coatings using SEM technique.

Table 4.3. - The surface roughness data of Ni-Ti alloy coatings developed at different current densities, using optimized bath

Coating configuration	*R_q (nm)*	*R_a (nm)*
Ni-Ti $_{1.0\ A/dm^2}$	11.0	8.2
Ni-Ti $_{2.0\ A/dm^2}$	24.5	18.7
Ni-Ti $_{3.0\ A/dm^2}$	30.8	20.9
Ni-Ti $_{4.0\ A/dm^2}$	41.5	32.0

4.3.5 X-Ray diffraction study

XRD technique was used to analyse the phase structure of Ni-Ti alloy coatings, deposited at different current density. The characteristic XRD peaks of Ni-Ti alloys deposited from 1.0

A/dm^2 to 4.0 A/dm^2 is presented in Figure 4.4. Sharp signals of X-ray reflections confirm that electrodeposited Ni-Ti alloy coatings are crystalline in nature.

The XRD peaks at 2θ = 43.3°, 44.0°, 51°, 53°, 73°, 75° and 89.7° represents the phase angles of Ni-Ti alloy coatings electrodeposited at different current densities, corresponding to the planes (110), (411), (200), (111), (110), (220) and (200), respectively. These multiple peaks of Ni-Ti alloy coatings may be attributed to the formation of a mixed-metal complex containing both metals and citrate as a complexing agent as explained in the mechanism of co-deposition of Ti and Ni ions. It may be seen that intensity of peaks corresponding to different scattering angles remained to be almost constant even with change of current density. This stands for the reason that change of composition of alloys is minimal with current density and is supported by composition data, in Table 4.2. It may also be seen that phase angles corresponding to different reflections of all coatings remains constant regardless of the current density at which they are deposited. This constancy of phase angles of Ni-Ti alloy coatings corresponding to different current densities indicates the formation of solid solution of Ni with Ti.

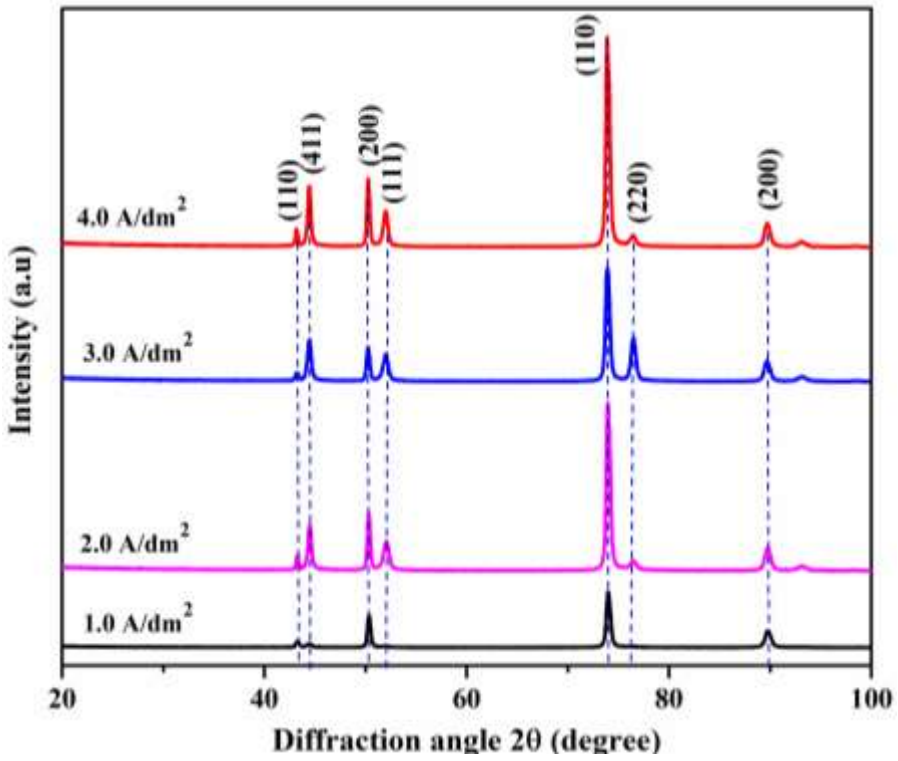

Figure 4.4- *X-ray diffraction peaks of Ni-Ti alloy deposited at different current densities from optimal bath. Constancy of phase angles of coatings corresponding to different current density indicate the formation of solid solution of Ni with Ti*

4.3.6 Corrosion study

The very purpose of this experimental study is to develop the most corrosion resistant Ni-Ti alloy coatings from the optimized bath. As titanium and titanium alloys have been used in engineering and medical applications due to their unique combination of mechanical properties and corrosion resistance. Moreover, as light metals, titanium and titanium alloys provide high specific strength, exceptional biocompatibility and excellent corrosion resistance. In this regard, the experimental work embodied in this work is to formulate a new electrolytic bath Ni-Ti alloy, for development of high corrosion resistant coatings, using the glycerol as additive to protect MS in marine environment. Hence, electrochemical corrosion behaviour of Ni-Ti alloy coatings were studied through EIS and Tafel's methods. The experimental results of corrosion study are reported below.

i) EIS Study

EIS technique can be used as a powerful tool to explore information with regard to the electrode processes such as double layer capacitance, solution resistance and polarization resistance, etc. The best adaptable tool to study the corrosion performance of electrodeposited coatings is the Nyquist plot. This basically consists of studying the impedance (AC resistance) over a range of frequency, on passing AC current of small amplitude (Yuan et al. 2010). In popular Nyquist plots, impedance (Z) is represented as complex number, having real impedance part (Z') and imaginary impedance part (Z"), and such representation is provided with provision to distinguish the contribution of solution resistance (R_s) versus polarization resistance (R_p) of a test electrode (Hegde and Rao 2014). Accordingly, Nyquist plots of Ni-Ti coatings deposited at different current densities are shown in Figure. 4.5, and their electrochemical impedance parameters calculated are reported in Table 4.4. It may be noted that at lower frequency limit, imaginary component gradually increases as the deposition current density is increased. In other words, polarization resistance (R_P) value of Ni-Ti alloy coatings increased with current density, and is maximum for coating corresponding to 4.0 A/dm^2, and supported by the highest value reported in Table 4.4. It is supported by the fact that, higher the corrosion resistance, higher the charge transfer resistance of the coating. Hence, it may be inferred that it is the most corrosion-resistant, compared to all other coatings.

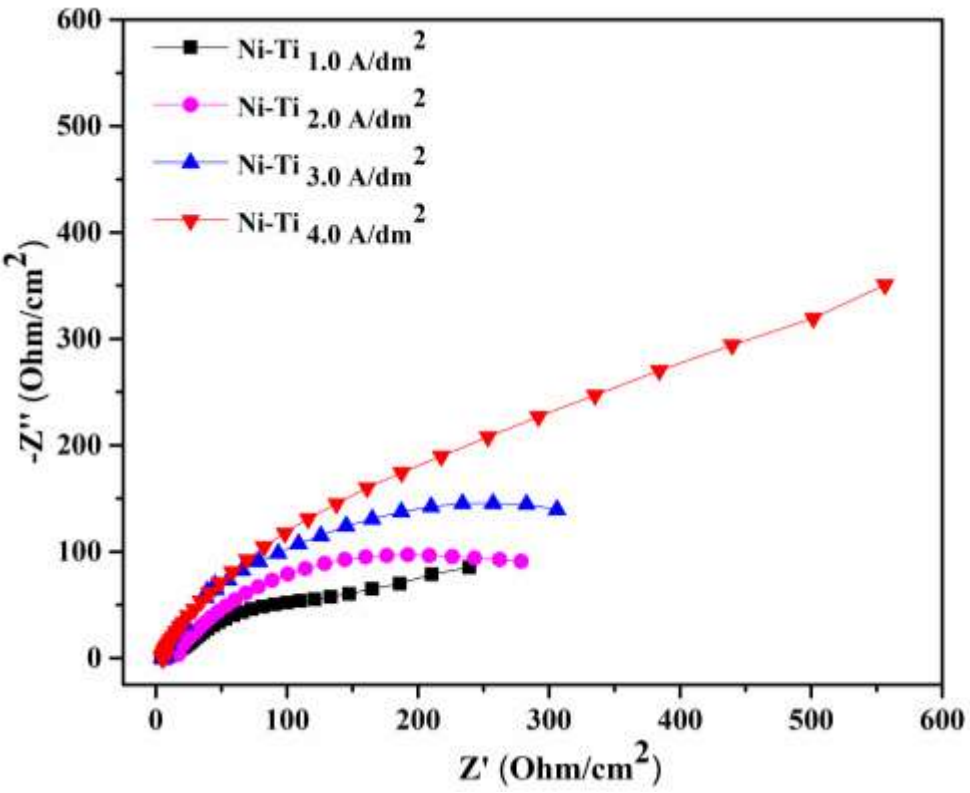

Figure 4.5. *Nyquist plots of Ni-Ti coatings deposited at different current densities. Highest polarization resistance (R_P) of Ni-Ti coating corresponding 4.0 A/dm^2 may be seen, compared to other coatings*

Table 4.4 - The electrochemical impedance parameters of Ni-Ti alloy coatings corresponding to different current density deposited from optimized bath

Coating configuration	R_s (Ω)	R_c (Ω)	Q_c(μF)	R_{ct}(Ω)	Q_{dl}(μF)	R_p(Ω)	χ^2 (10^{-3})
Ni-Ti $_{1.0\ A/dm^2}$	4.49	108	294	283	796	391	8.48
Ni-Ti $_{2.0\ A/dm^2}$	5.31	741	781	345	982	1086	6.36
Ni-Ti $_{3.0\ A/dm^2}$	5.57	931	887	413	1077	1344	5.68
Ni-Ti $_{4.0\ A/dm^2}$	5.74	1053	970	715	1278	1768	4.66

*B*ode plot is an alternative representation of the impedance in terms of the frequency represented directly along the X-axis. There are two types of Bode diagram, called magnitude plot (log |*Z*| *vs* log *f*) and phase angle plot (phase angle (θ) vs log *f*), describing the frequency dependencies of the |*Z*| and phase, respectively. A Bode plot is normally depicted

logarithmically over the measured frequency range because the same number of points is collected at each decade. Accordingly, Bode's magnitude and phase angle plot of all Ni-Ti alloy coatings are drawn and are shown in Figure 4.6. The highest value of log |Z| at lower limit of frequency recorded by Ni-Ti $_{4.0\ A/dm^2}$ alloy coatings, shown in Figure 4.6 (a) endorses the fact that it is the most corrosion resistant compared to all other coatings. It is evidenced further by Bode's phase angle (θ) plot shown in Figure 4.6(b).

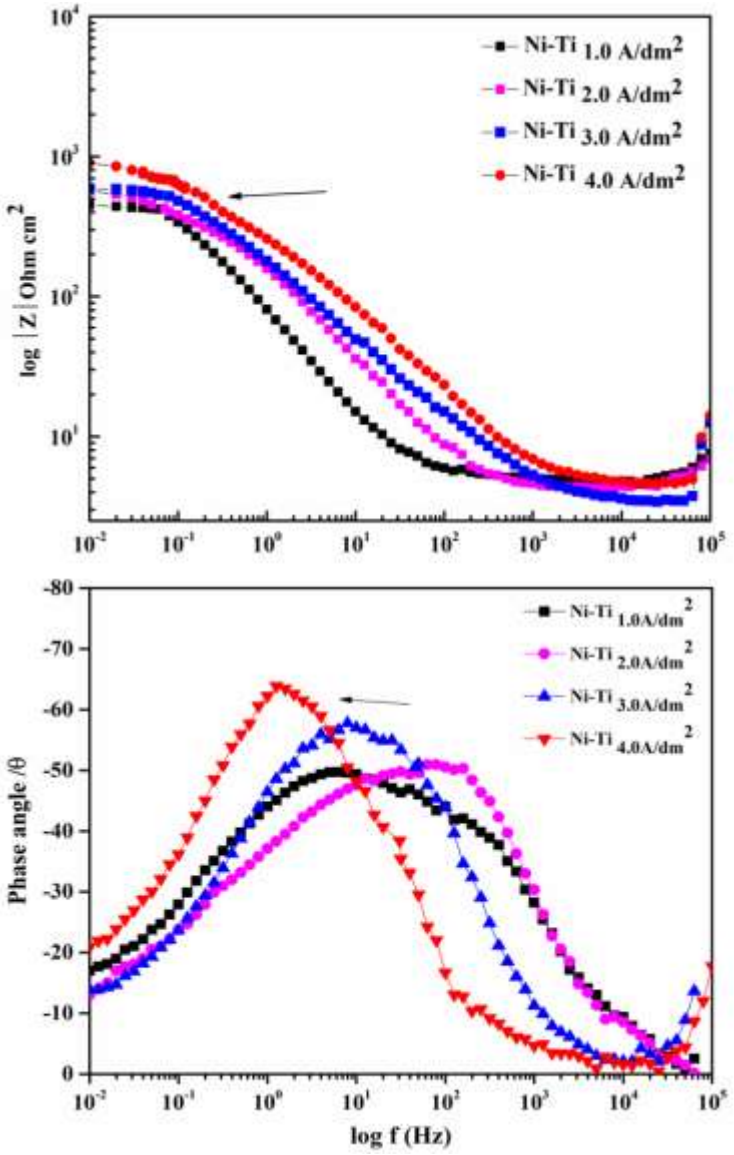

Figure 4.6 - *Bode's magnitude and phase angle plots of Ni-Ti alloy coatings corresponding different current density shown respectively in (a) and (b), demonstrates that Ni-Ti $_{4.0\ A/dm^2}$ coating is the most corrosion resistant than all other coatings*

It may be noted that Ni-Ti $_{4.0\ A/dm}{}^{2}$ coating is more capacitive in nature (with highest negative phase angle) compared to other coatings. The analysis of Electrochemical Impedance Spectroscopy (EIS) data typically involves fitting it to an Equivalent Electric Circuit (EEC) model. An equivalent circuit model comprises resistances, capacitances, and/or inductances, along with specialized electrochemical elements like Warburg diffusion elements and constant phase elements. This combination replicates the response of the electrochemical system when subjected to the same excitation signal (Jones DA.2016). Hence, an EEC is modelled to study the electrochemical behaviour of the interface of Ni-Ti coating (optimal) in the test solution environment and is shown in Figure 4.7.

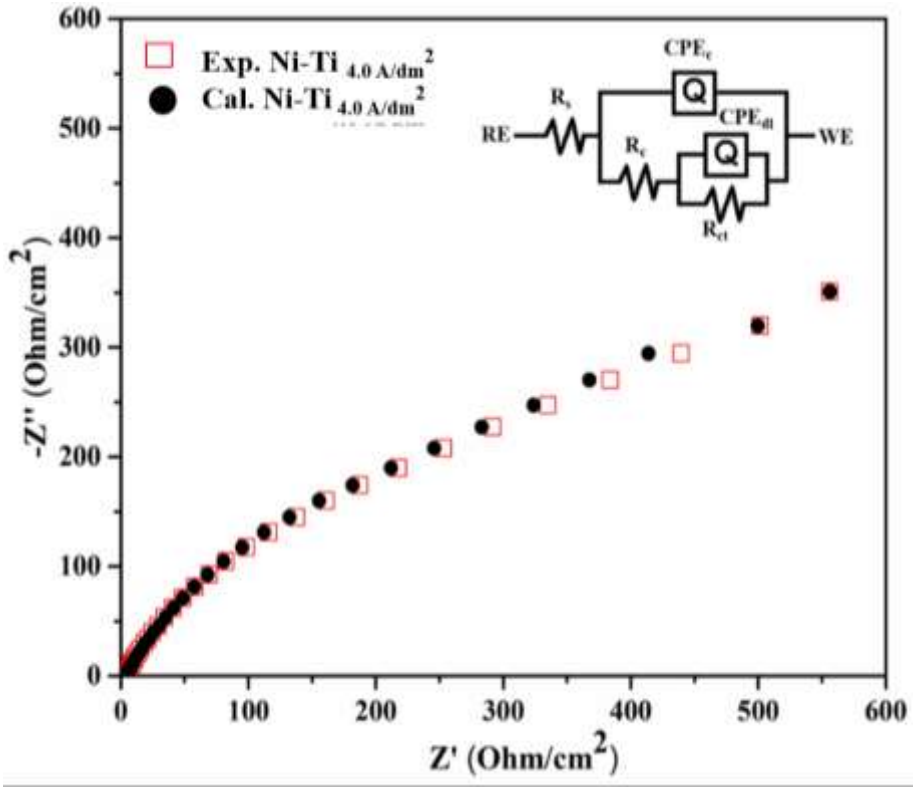

Figure 4.7 - *Nyquist plot of Ni-Ti $_{4.0\ A/dm}{}^{2}$ alloy coating showing its simulation, and equivalent circuit (in the inset)*

A best agreement between experimental data and fitted data was obtained, and corresponding equivalent circuit is shown in the inset of Figure 4.7. The equivalent circuit indicates the porous nature of the deposit attributed to the presence of a passive film on the

surface. In this representation, R_s represents the solution resistance, R_c represents the resistance of the coating, and R_{ct} represents the charge transfer resistance, CPE_{dl} - capacitance of the electrical double layer (EDL) involved in the equivalent circuit.

ii) Potentiodynamic polarization study

The corrosion behaviour of Ni-Ti alloy coatings was evaluated quantitatively by potentiodynamic polarization method. The Tafel plots of Ni-Ti alloy coatings deposited at various current densities are shown in Figure 4.8

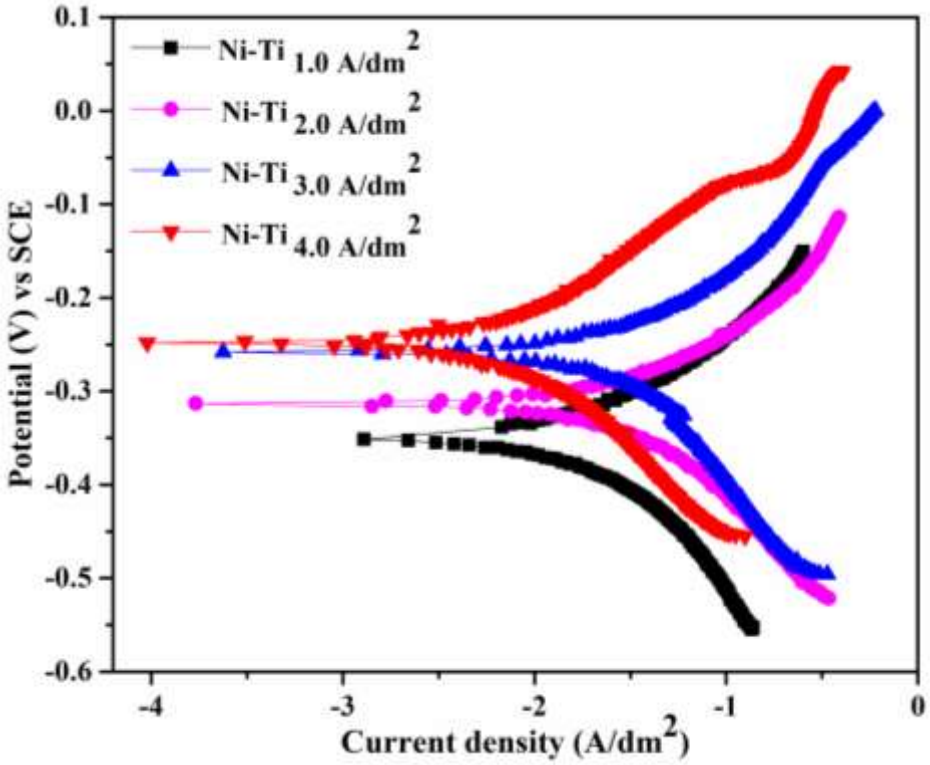

Figure 4.8 *- Potentiodynamic polarization behaviour of Ni-Ti alloy coatings deposited at different current densities. Tafel plot corresponding to 4.0 A/dm^2 showing different behavior, compare to other current density may be seen*

Table 4.2 reports the corrosion data of all alloy coatings, evaluated using Tafel's extrapolation method. The corrosion rate values of different Ni-Ti alloy coatings, reported in Table 4.2 reveals that Ni-Ti alloy deposited at 4.0 A/dm^2 is the most corrosion resistant, compare to all other coatings, and is in agreement with the trend observed in case of EIS study. Thus it may be summarized that among the Ni-Ti alloy coatings deposited at different current

density, Ni-Ti alloy corresponding to 4.0 A/dm^2 (14.02 $\times 10^{-2}$ mm/y), is the most corrosion resistant. Further, small change in corrosion rates of alloy coatings with current density is due to marginal change in its composition. *i.e.* from 0.8 wt. % to 3.5 wt. % of Ti. Thus both EIS and potentiodynamic polarization study reveals that increase of corrosion resistance of Ni-Ti alloy coatings with current density is due to increased Ti content of the alloy as reported in Table 4.2. In addition, from the literature it is evident that Ti has electrochemical properties superior to other metals due to the passive surface TiO_2 layer.

Driven by the observed phenomenon that there can be a substantial enhancement in the corrosion resistance of alloy coatings, when coating is changed from monolayer to multilayer type (Thangaraj et al. 2009),(Wilcox and Gabe 1993) (Bull and Jones 1996), multilayer Ni-Ti alloy coatings have been developed from the same optimized bath. Experimental results of investigation on development of multilayer Ni-Ti alloy coatings is presented below.

4.4 Electrodeposition of multilayer Ni-Ti alloy coatings

4.4.1 Optimization of cyclic cathode current densities (CCCD's)

The multilayer Ni-Ti alloy coatings have been developed from the same bath (Table 4.1). Coating has been affected by periodic modulation of direct current (DC) between two values, called cyclic cathode current densities (CCCD's), during process of deposition. The power patterns used for deposition of multilayer Ni-Ti alloy coatings is shown in a representative diagram in Figure 4.1(b), with cross sectional view of the coating on right. Here, cyclic cathode current density refers to change of cathode current density between two values in a cyclic manner (periodically). Thus, multilayer Ni-Ti alloy coatings were produced at different sets of pulsed current densities by proper setting up of the power source.

To optimize the Cyclic Cathode Current Densities (CCCDs) for the creation of highly corrosion-resistant coatings, they are formulated at various sets of CCCDs with 10 layers (chosen arbitrarily for right composition of alternate layers). The corrosion performance were of 10 layered multilayer coatings, deposited at different CCCD's were evaluated by electrochemical impedance spectroscopy (EIS) and potentiodynamic polarization methods. The corrosion response of alloy coatings, in terms of Nyquist and Tafel's methods are shown

in Figures 4.9. The corrosion rates (CR's) determined by Tafel's method are reported in Table 4.4.

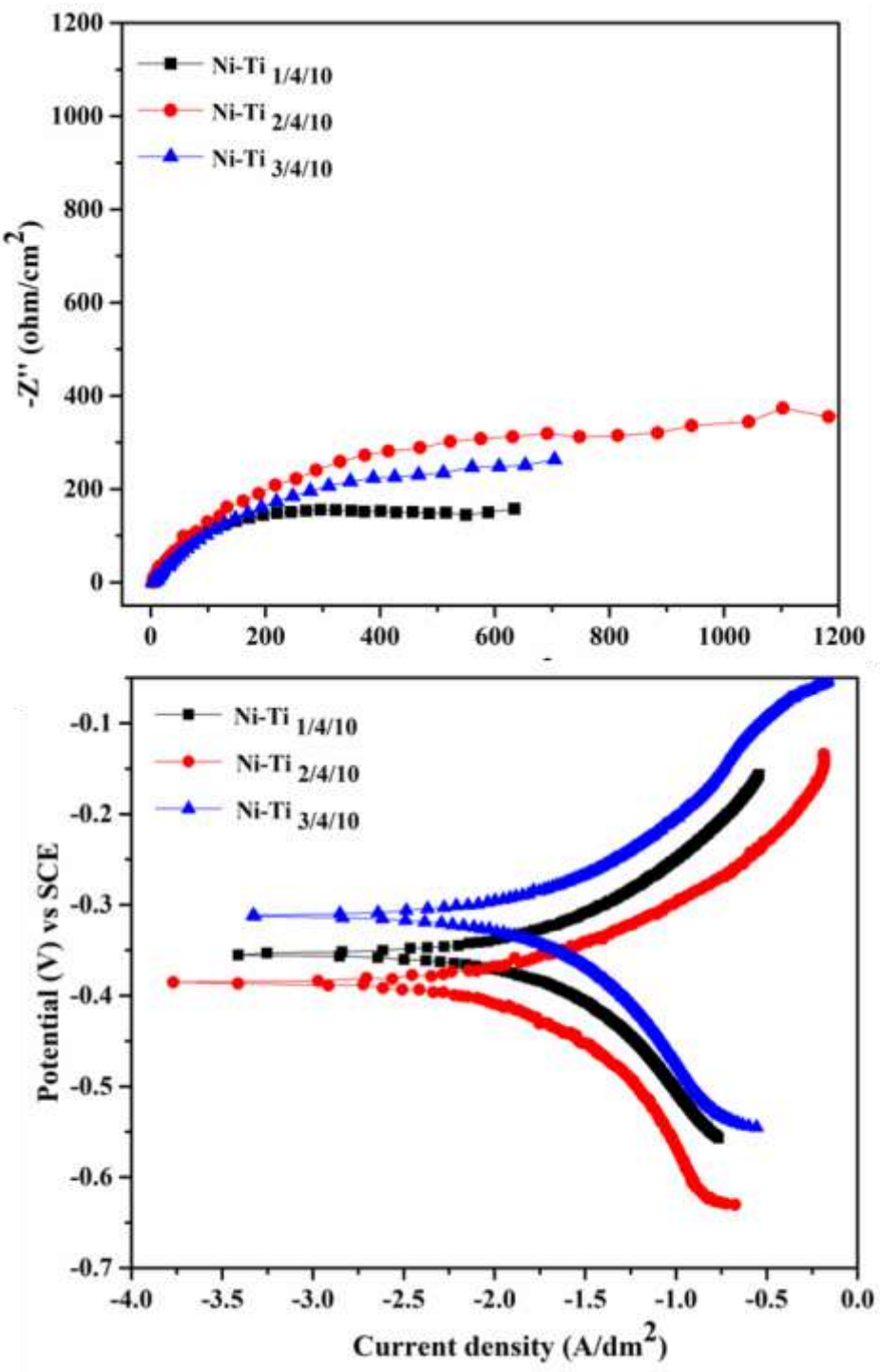

Figure 4.9 - *Corrosion response of multilayer Ni-Ti alloy coatings having 10 layers, deposited at different CCCD's using same bath, evaluated by a) Nyquist plots, and b) Tafel plot.*

The higher capacitive loop corresponding to Ni-Ti $_{2/4/10}$ configuration, shown in Figure 4.9(a) indicates that it is the maximum corrosion resistant compared to all other coatings. It amounts to the fact that this set of CCCD's is the most suggested for formation alternate layers of different composition, to form coatings with clear demarcation between layers. This is supported by the corrosion data exhibited in Table 4.5.

Table 4.5. Corrosion data of 10 layered Ni-Ti alloy coatings having different compositions, deposited at different CCCD's from the optimized bath

Coating configuration	- E_{corr} (mV vs. SCE)	i_{corr} ($\mu A\ cm^{-2}$)	CR ($\times 10^{-2}\ mmy^{-1}$)
Ni-Ti $_{1/4/10}$	-378.24	13.55	13.75
Ni-Ti $_{2/4/10}$	-370.14	10.33	10.11
Ni-Ti $_{3/4/10}$	-372.90	11.29	11.91
Ni-Ti $_{4.0}$ (monolayer)	-257.7	13.81	14.02

From the values of CR, it may be inferred that corrosion rate of multilayer Ni-Ti alloy coatings at different CCCD's is much lower than that of its monolayer alloy coating deposited from the same bath. Among three sets of CCCD's tried, the least CR was observed case of 2.0 & 4.0 A/dm^2 (9.45×10^{-2} mmy^{-1}). Therefore, this set of CCCD has been selected to examine the effect of layering on the corrosion protection efficiency of their coatings.

4.4.2 Optimization of total number layers

The properties of CMM alloy coatings are principally determined by the reduced grain size and large number of interfaces, affected due to pulsing of direct current (DC) during deposition. Hence, based on the preliminary work, 2.0 and 4.0 A/dm^2 were selected as CCCD's for production of CMM Ni-Ti alloy coatings having 10, 60, 120, 300 and 600 layers. Here, the number of layers are selected based on the equal distribution of total time 600 secs (used for both monolayer and multilayer alloy coatings). Accordingly, the corrosion behaviour of electrodeposited multilayer Ni-Ti alloy coatings having different number of layers (10- 600 layers) were studied by EIS and Tafel's method, and experimental results are discussed below.

i) Electrochemical impedance study

The Electrochemical Impedance Spectroscopy (EIS) technique operates on the principle that an interface can be modeled as a combination of passive electrical circuit elements, including resistance, capacitance, and inductance. When an alternating current is applied to these elements, the resulting current is obtained using Ohm's law. Using this principle, many valuable information with regard to kinetics of electrode reaction including the rate corrosion at the interface can be explored. In this method, generally a small perturbation of AC voltage is impacted at the interface, and its response as impedance (time dependent resistance) is measured. In EIS, the most versatile, commonly illustrating the data as imaginary impedance (Zimg) versus real impedance (Zreal). This plot provides the capability to differentiate the contributions of polarization resistance (Rp) versus solution resistance (Rs) in the electrochemical system under investigation (Yogesha et al. 2011). Accordingly, Nyquist plots of multilayer Ni-Ti alloy coatings with different number of layers were studied and is shown in Figure 4.10.

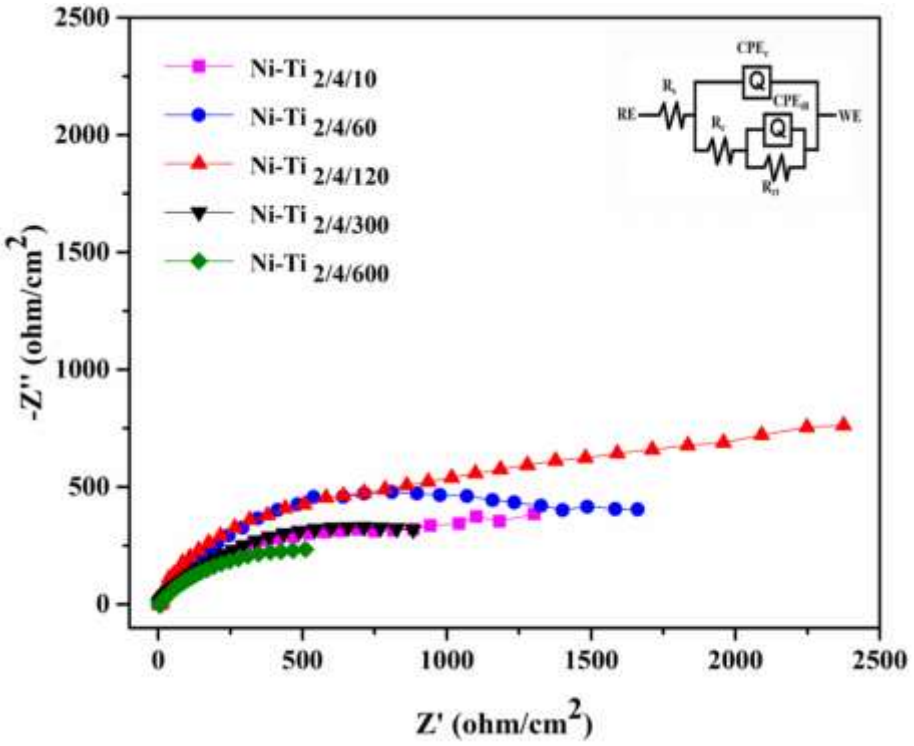

Figure 4.10*- Nyquist plots of multilayer Ni-Ti alloy coatings having different number of layers (from 10 to 600 layers), deposited from the same optimized bath using pulsed current*

The impedance study has been carried out at AC frequency, ranging from 10 KHz to 0.01 Hz. Impedance responses corresponding to all multilayer coatings were found to be a depressed semicircle, with one capacitive loop as shown in Figure 4.10. These depressed semicircles are attributed to the frequency dispersion of the interfacial impedance, and this unusual flattening behaviour is due to the inhomogeneity of the metal surface arising from surface roughness or interfacial phenomena arises during plating (Yuan et al. 2010). The shape of Nyquist plots in Figure 4.10 indicates that the same corrosion protection mechanism is followed in all coatings of different configurations. High polarization resistance (R_{ct}), or charge transfer resistance corresponding to Ni-Ti $_{2.0/4.0/120}$ configurations with large capacitive loop indicates that it is the most corrosion resistant of all the coatings examined. The solution resistance R_s was found to be almost constant as shown in Figure 4.10. This consistency can be attributed to the utilization of the same bath chemistry and cell configurations for the corrosion study. The observed values of Rp indicate that the corrosion protection effectiveness of Ni-Ti $_{2.0/4.0}$ coatings increased progressively with increasing number of layers and it continues up to 120 layers, and then decreased.

ii) Tafel's polarization study

Tafel's extrapolation method was employed for determining the corrosion current density (i_{corr}), and thereby the corrosion rate (CR) of the coatings. The potentiodynamic polarization behaviour of CMM Ni-Ti $_{2.0/4.0}$ coatings having different number of layers are shown in Figure. 4.11, and their corrosion data are reported in Table 4.6.

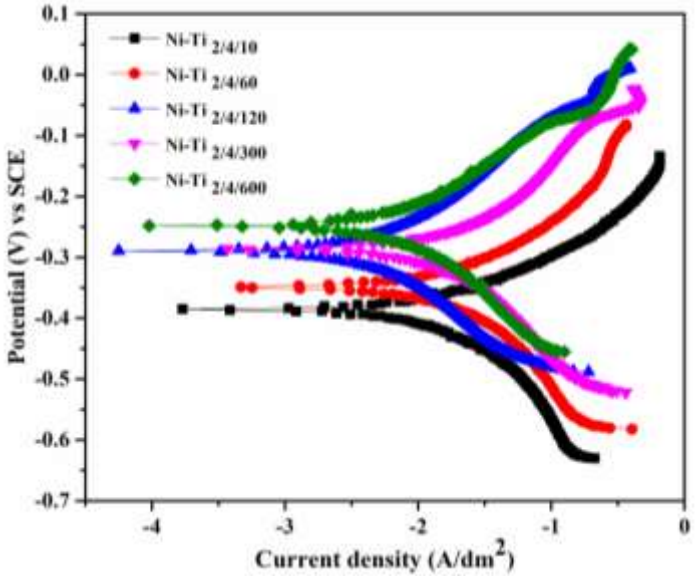

Figure 4.11 *- Tafel's plots of multilayer Ni-Ti alloy coatings having different number of layers (from 10 to 600 layers) deposited from same bath for same duration of time*

It is important to note that corrosion rates of multilayer coatings, having Ni-Ti $_{2/4/120}$ coating matrix is least compared to its monolayer Ni-Ti $_{4.0}$ coating, deposited by conventional method as shown in Table 4.6. This indicates that layering has its effect in decreasing the CR of alloy coatings. Thus, it may be inferred that the improved corrosion protection of multilayer Ni-Ti alloy coating has bearings with both the thickness and composition of individual layers.

Table 4.6 - Corrosion parameters of multilayer Ni-Ti alloy coatings of different configuration of layering, deposited using the same bath

Coating configuration	$-E_{corr}$ (mV vs. SCE)	i_{corr} ($\mu A\ cm^{-2}$)	CR ($\times 10^{-2}$ mm y^{-1})	R_p	χ^2 (10^{-3})
Ni-Ti $_{2/4/10}$	-370.1	10.33	10.11	2548	5.48
Ni-Ti $_{2/4/60}$	-359.6	7.27	7.66	3298	4.86
Ni-Ti $_{2/4/120}$	-290.5	2.54	2.66	7380	2.89
Ni-Ti $_{2/4/300}$	-287.8	8.32	8.78	5286	4.32
Ni-Ti $_{2/4/600}$	-252.2	12.86	12.98	2538	5.24
Ni-Ti $_{4.0}$ (monolayer)	-257.7	13.81	14.02	1768	4.66

It is interesting to note that the CR's of multilayer Ni-Ti alloy coatings decreased with the number of layers up only to 120 layers, and then started increased (Table 4.6). i.e., at 300 and 600 layers. It may be attributed to the diffusion of layers due to rapid change of current pulses, and it may be explained as follows: As larger numbers of layers are allowed to form in same total time duration (600 s), the time for deposition of each layers, *i.e*. for both Ni-Ti $_{2.0}$ and Ni-Ti $_{4.0}$ are small. Owing to short pulse duration time (2 and 1 second, respectively in case of 300 and 600 layers), there is no sufficient time for metal ions to relax (against diffusion under given current density) and to deposit on the cathode to form a distinct interface. As a result, at high degree of layering no modulation in the composition of layers is likely to happen, and at a higher degree of layering, the multilayer coating tends to become a monolayer coating. Hence, it may be noted that CR's of multilayer Ni-Ti alloy coatings are tending towards that of monolayer coatings as number of layers has increased *i.e.* from 300 and 600 as shown in Table 4.6. This early attainment of homogeneity of multilayer Ni-Ti alloy coatings, *i.e.* at only 120 layers may be attributed by the limitation of induced type of co-deposition of Ni with Ti, where effect of current density on alloy composition is very marginal. In other words, multilayer coating tends to become monolayer soon due to small effect of current density on the composition of alloy coatings.

Thus electrochemical corrosion data showed that CMM Ni-Ti alloy coatings deposited at 2.0 and 4.0 A/dm^2 CCCD's, having 120 layers, represented by Ni-Ti $_{2.0/4.0/120}$ showed the least CR (2.66×10^{-2} mmy^{-1}), compared to its monolayer Ni-Ti $_{4.0}$ alloy coating (14.02×10^{-2} mmy^{-1}), deposited from the same electrolytic bath for same length of time. Therefore, the optimal coating configuration for multilayer coating from the proposed bath is CMM Ni-Ti $_{2.0/4.0/120.}$ The total thickness of the coating under optimal configuration, *i.e*., for Ni-Ti $_{2.0/4.0/120}$, was found to be about 8 μm. Therefore, the average thickness of the individual layers was estimated to be in the range of 66 nm. However, when the thickness of individual layers is taken below this limit, overlapping of layers are expected to take place due to short period of diffusion during deposition of individual layers.

4.4.3 Comparison of monolayer and multilayer Ni-Ti alloy coatings

A substantial improvement in the corrosion resistance behaviour of Ni-Ti alloy coatings were found when monolayer coating is changed to multilayer type, and are supported by data shown

in Table 4.6. The corrosion response of monolayer and multilayer Ni-Ti alloy coatings are compared in terms of impedance response as Nyquist and Bode's plot as shown in Figures 4.12 and 4.13, respectively.

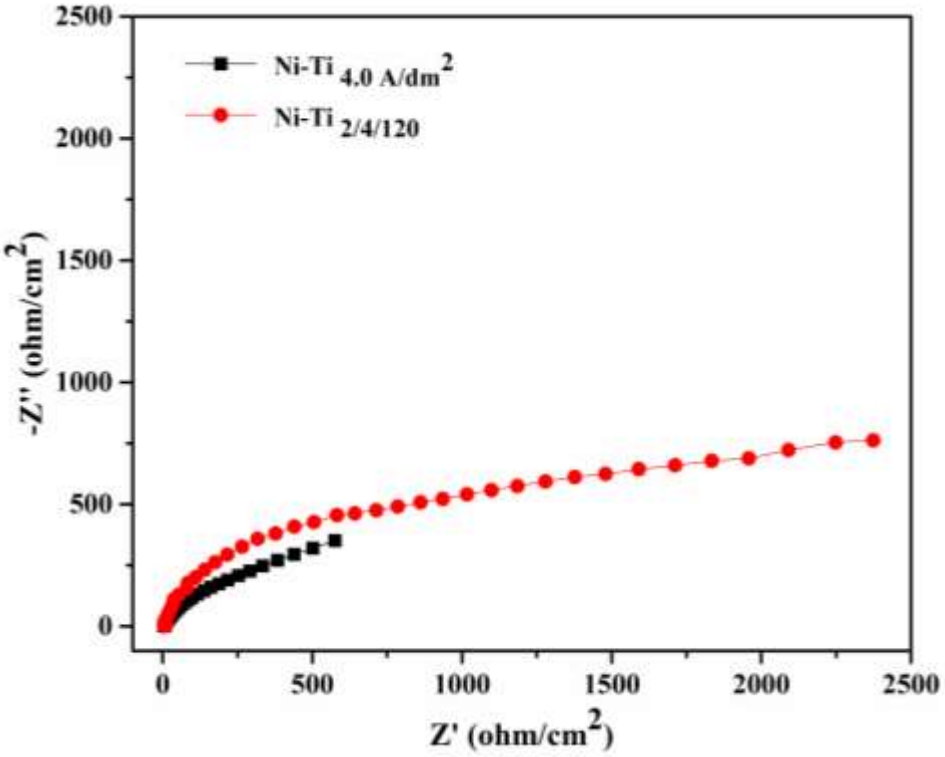

Figure 4.12 *- Impedance response of monolayer Ni-Ti $_{4.0}$ and multilayer Ni-Ti $_{2.0/4.0/120}$ alloy coatings, deposited from the same bath for same duration*

The Nyquist diagrams showing impedance response of both monolayer and multilayer coatings clearly indicates that multilayer Ni-Ti $_{2.0/4.0/120}$ alloy coating is much more corrosion resistant than its monolayer counterpart, *i.e.* Ni-Ti $_{4.0}$ demonstrated higher R_P value.

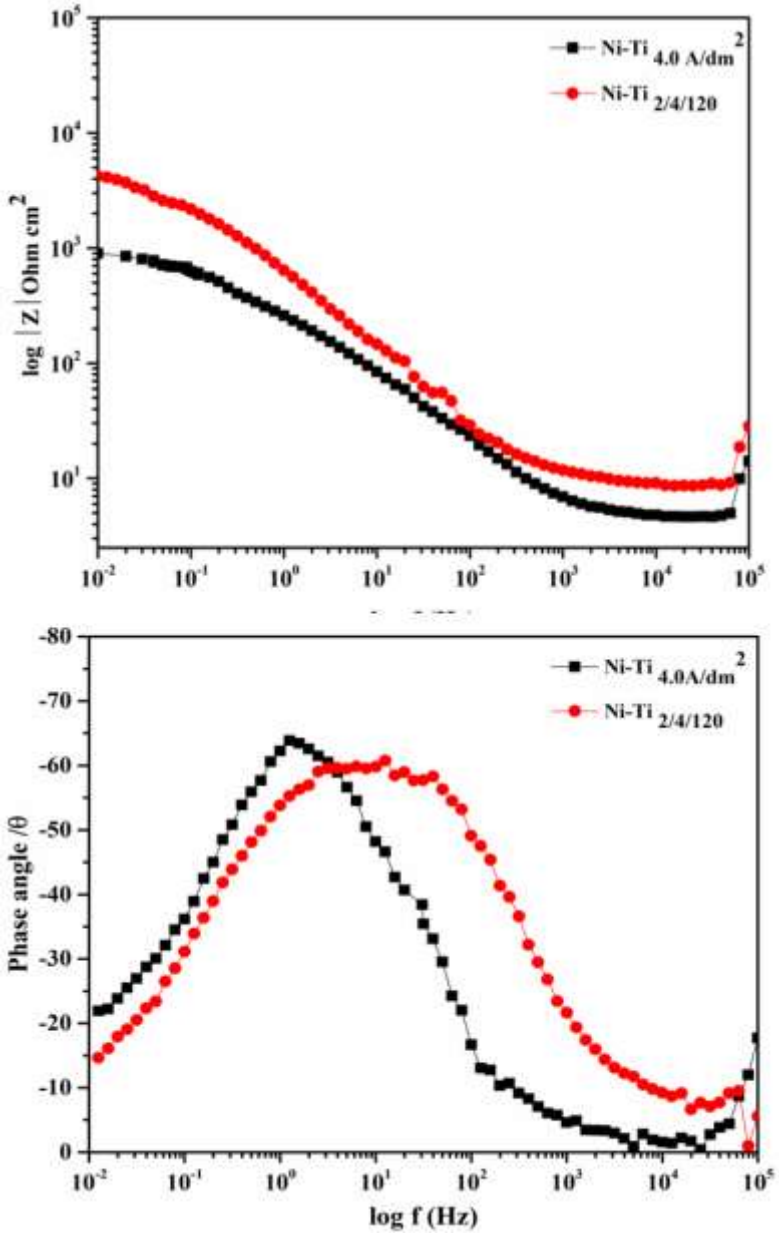

Figure 4.13- *Bode's plots of monolayer Ni-Ti* $_{4.0}$ *and multilayer Ni-Ti* $_{2.0/4.0/120}$ *coatings: a) Magnitude plot showing high value of |Z|, and b) phase angle plot showing wider peaks in case of multilayer coatings, compared to its monolayer counterpart deposited from the same bath*

Bode plots help in understanding the interfacial/corrosion behavior of electrode system under study, using the same same data points which are used in Nquist plots. Accordingly, two types of Bode plots, called magnitude plot (log $|Z|$ *vs* log f) and phase angle plot (phase angle (θ) vs log f), describing the frequency dependencies of the $|Z|$ and phase, respectively have been studied. Bode's magnitude and phase angle plot of both monolayer Ni-Ti $_{4.0}$ and

multilayer Ni-Ti $_{2.0/4.0/120}$ coatings are shown in Figure 4.13. The highest value of log |Z| at lower limit of frequency recorded by Ni-Ti $_{2.0/4.0/120}$ alloy coatings, shown in Figure 4.13(a) endorses the fact that it is the most corrosion resistant compared to its monolayer alloy coating. It is evidenced further by Bode's phase angle (θ) plot shown in Figure 4.13(b). It may be noted that Ni-Ti $_{2.0/4.0/120}$ coating is more capacitive in nature (due to wider peak), compared to its monolayer counterpart.

Similarly, the anticorrosion behaviour of both monolayer and multilayer Ni-Ti alloy coatings are compared through Tafel's plots, and is shown in Figure 4.14.

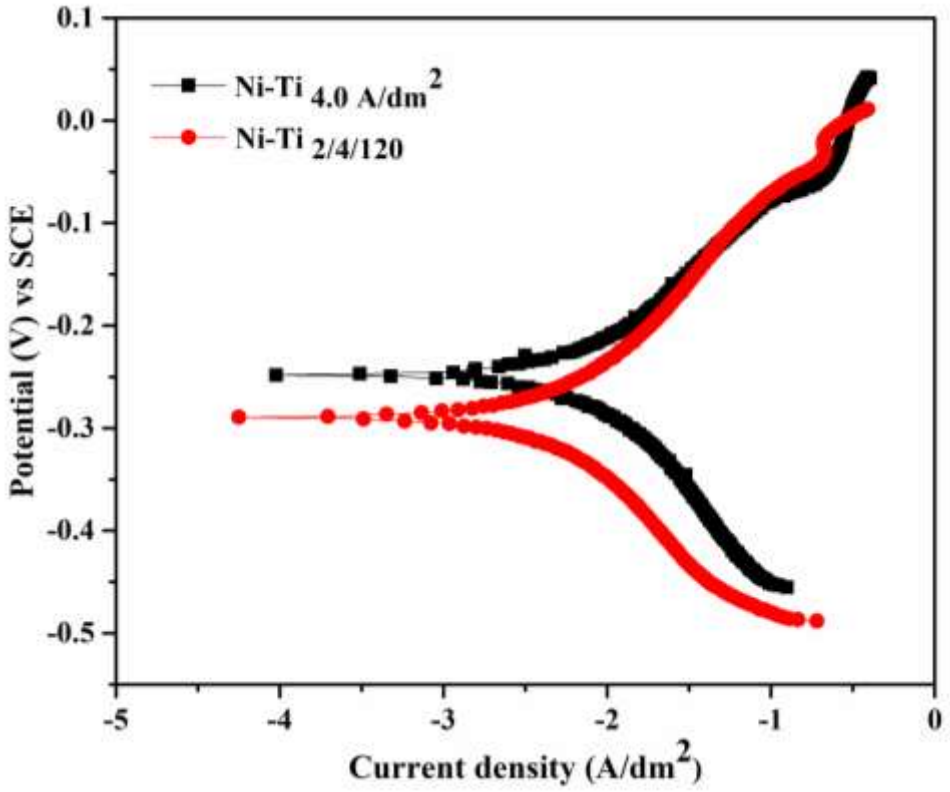

Figure 4.14- *Comparison of Tafel's responses of monolayer Ni-Ti $_{4.0}$ and multilayer Ni-Ti $_{2.0/4.0/120}$ coatings, deposited from same bath for same duration*

It may be noted from the behaviour of Tafel's plots of multilayer Ni-Ti $_{2.0/4.0/120}$ alloy coating is more corrosion resistant than Ni-Ti $_{4.0}$. It is supported by their change of $i_{corr,}$ and E_{corr} and CR values (Table 4.6). There is no much work reported on electrodeposition of Ni-Ti alloy coating in the literature. However, few experimental results reported are under different conditions of bath compositions and operating parameters. The corrosion data revealed that

Ni-Ti $_{2.0/4.0/120}$ is about 7 times (CR= 2.66×10^{-2} mm y^{-1}) more corrosion resistant than Ni-Ti $_{4.0}$ alloy coatings (CR=14.02×10^{-2}mmy^{-1}).

4.4.4 SEM analysis of multilayer coating

The formation of layered coatings having successive layers of alloys of different compositions was confirmed by scanning electron microscopy (SEM) analysis. The cross-sectional view of Ni-Ti $_{2.0/4.0/10}$ coating was examined under SEM and is shown in Figure 4.15. The close inspection of the microscopic appearance of Ni-Ti $_{2.0/4.0/10}$ alloy coating, under SEM displayed the formation of 10 layers, having alternatively different compositions as shown in Figure 4.15. Poor demarcation between layers is due to residues deposited during Polishing.

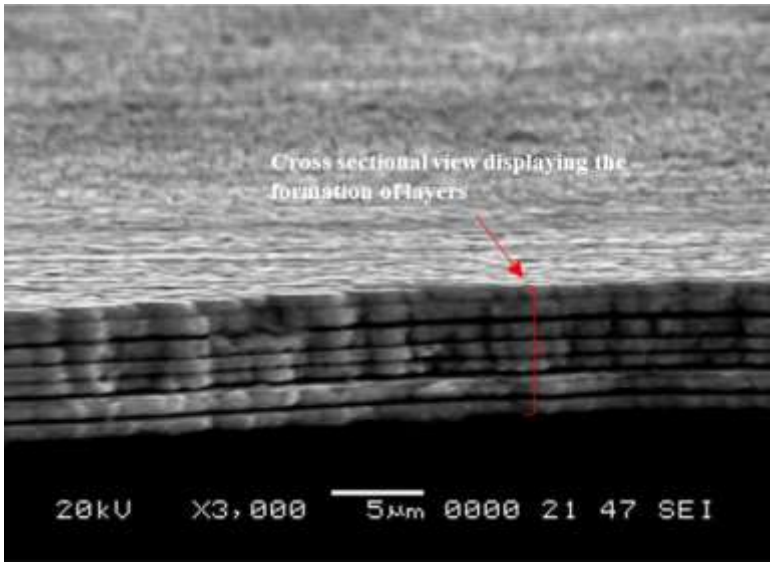

Figure 4.15- *Cross-sectional view of Ni-Ti $_{2.0/4.0/10}$ coating under SEM displaying the formation of coatings in layered pattern*

4.4.5 Reasons for improved corrosion resistance of multilayer Ni-Ti alloy coating

The better anticorrosion performance of multilayer Ni-Ti alloy coatings in relation to its monolayer alloy coating may be attributed to its coatings having layers of alternatively different composition. The mechanism of corrosion in multilayer Ni-Ti alloy coating in relation to its monolayer alloy coating, is shown pictorially in Figure 4.16. In case of monolayer Ni-Ti alloy coating, *i.e.,* in Ni-Ti $_{4.0}$, the coating being homogeneous or non-nanostructured, corrosion occurs unabatedly and corrosion medium reaches the substrate very quickly, as shown in Figure 4.17(a). Improved corrosion protection of multilayer Ni-Ti alloy coatings

were attributed to the increased number of interfaces, affected due to layers of alloys having low and high Ti content. Hence in multilayer Ni-Ti alloy coatings, layers are getting dissolved selectively depending on their composition. The corroding medium spreads laterally at the interface, and delays the corrosion process as shown pictorially in Figure 4.16(b). In multilayer coating, i.e. in Ni-Ti $_{2.0/4.0/10}$, owing to the presence of well-defined phase boundaries between layers, electrolyte spreads both laterally and vertically as shown in Figure 4.16(b). Thus, due to multilayer structure the lower layer will come in contact with the corrosion medium only after the complete destruction of top layers. Consequently, substrate will get exposed to the corrosion medium layer by layer. Therefore, substrate is well protected from the corroding medium much better in case of multilayer coating than in monolayer coating.The increase of CR at higher degree of layering of course beyond optimal number of layers is due to diffusion of layers, due to rapid change of CCCD's as explained earlier.

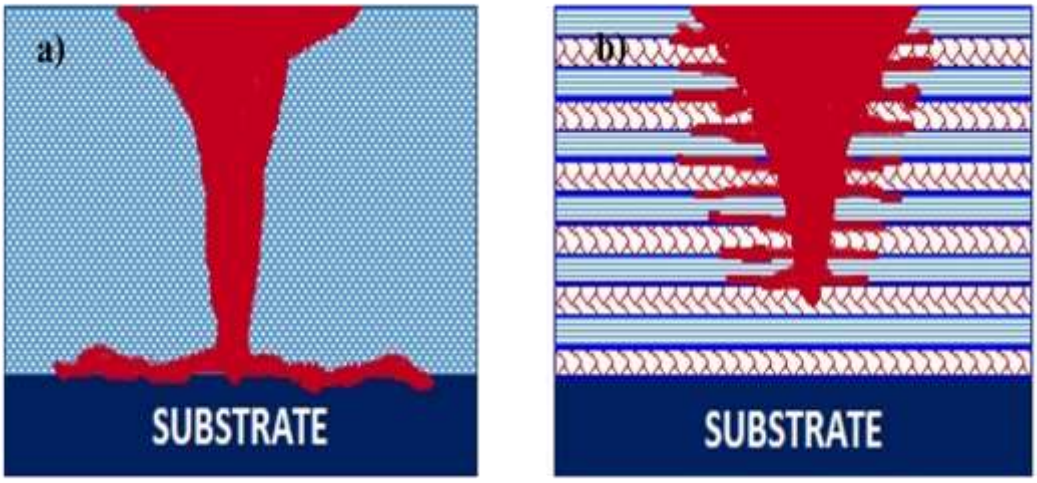

Figure 4.16- *Schematic diagram showing the mechanism for decreased corrosion rate of multilayer Ni-Ti alloy coating, compared to monolayer Ni-Ti alloy coating deposited for the same duration. It may be seen that in case of multilayer coating the corroding medium takes more time to reach substrate due to its lateral spreading across interfaces*

4.5 Conclusions

A new electrolytic bath of Ni-Ti alloy has been proposed using the glycerol, as additive. The current density for development of the most corrosion resistant monolayer alloy coatings have been developed using direct current (DC). The poorer corrosion performance of monolayer Ni-Ti alloy coatings (due to inherent induced type of co-deposition) has been improved by multilayer approach. Experimental results of investigation has evidenced the following facts:

1. The corrosion protection efficiency of monolayer Ni-Ti alloy coatings have improved further by composition modulated multilayer (CMM) approach by proper selection of cyclic cathode current densities (CCCD's).
2. Experimental study revealed that the corrosion stability of multilayer Ni-Ti alloy coatings is increasing with degree of layering up to certain level and then decreased.
3. The improved corrosion protection efficiency of multilayer alloy coatings were attributed to the increased number of interfaces, affected due to layers of alloys having low and high Ti content.
4. Under optimal condition, multilayer Ni-Ti alloy coating, having Ni-Ti $_{2.0/4.0/120}$ configurations is approximately seven times more corrosion resistant than its monolayer Ni-Ti $_{4.0}$ deposited from the same bath for same duration.
5. Increase of CR, higher degree of layering (after 120 layers) is due to the diffusion of layers. It may be attributed to the rapid change of current pulse, where no significant compositional change of individual layers are likely to happen.
6. Early attainment of homogeneity of multilayer Ni-Ti alloy coating, at only 120 layers may be attributed by the limitation of induced type of co-deposition of Ni with Ti. In other words, it is due to a small change of alloy composition with change of current pulse.
7. The corrosion mechanism to support the fact that better corrosion protection of multilayer Ni-Ti alloy coating is due to selective dissolution of alternate layers of alloys, having low and high Ti content and due to lateral spreading of the corrosion medium.

IMPROVISATION OF CORROSION PERFORMANCE OF Ni-Ti ALLOY COATING THROUGH MAGNETO ELECTRODEPOSITION

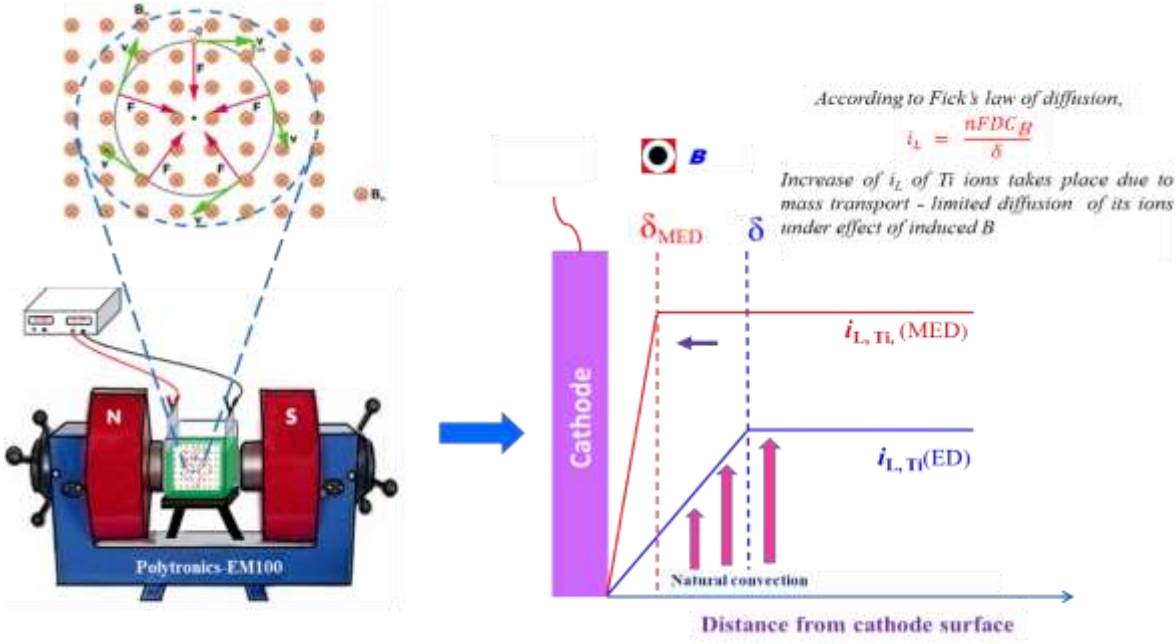

This chapter discusses the improvisation of corrosion protection efficiency of Ni-Ti alloy coatings through magneto-electrodeposition (MED). The conditions of MED were optimized by inducing a magnetic field (B), in both intensity and direction. The magnetic field, applied simultaneously to the process of electrodeposition was used as the tool to alter the crystallinity, composition and thereby the corrosion resistance of Ni-Ti alloy coatings. It was demonstrated that the corrosion resistance of Ni-Ti alloy coatings can be improved to seven folds of its magnitude by MED approach. A significant increase in corrosion resistance of MED alloy coatings was found, under both parallel and perpendicular B. It was attributed to the increased Ti content of the alloy affected due to its limiting current density (i_L) value. The high corrosion resistance of the MED Ni-Ti alloy coatings was explained in the light of MHD effect, caused due to increased mass transport process at cathode. The inherent limitations of the bath, like induced type of co-deposition which impedes the development of Ti-rich alloy coatings were successfully resolved by MED method. Drastic improvement in corrosion resistance is ascribed to the basic difference in the process of electrocrystallization and phases formed during MED, confirmed by SEM and XRD study.

5.1 INTRODUCTION

The effect of magnetic field (*B*) on the process of electrodeposition of metals/alloys/polymer/ composite coatings is of great interest for many researchers for past several years. The application of magnetic field on the process of electrodeposition can improve the quality of deposit, and thereby its physico-mechanical properties including the corrosion behavior. It is well established fact that under normal conditions of electrodeposition, Ni-Ti alloy follows induced type of co-deposition. Here, as titanium metal cannot be electrodeposited from its aqueous solutions, and it can only be co-deposited with Fe - group metals such as nickel, cobalt, or iron to form an alloy. This phenomenon is called as *induced co-deposition*, named by Brenner (Brenner 1963c). Here, the metal which stimulate the deposition is called inducing metal, and the metal which do not deposit by itself is called reluctant metal. Generally, in induced type of co-deposition, effects of plating variables on the composition of alloys are more vagarious and unpredictable, than in any other types of co-deposition. As a result, in induced type of co-deposition current density has negligible effect on their composition, and hence corrosion protection efficiency.

Therefore, possible means to improve the corrosion resistance of Ni-Ti alloy coating to a large extent by varying the current density is quite unrealistic. In this regard, the poorer corrosion performance of Ni-Ti alloy coatings was tried to improve by taking the advantage of magnetic field effect. *i.e.,* by carrying out the electrodeposition under the influence of induced magnetic field. The advantage of magnetic field effect on the process of electrodeposition was reviewed in detail by Fahidy et al (Fahidy 2001). It has been described that the applied magnetic field primarily effects the transport of ions towards cathode, and consequently alters the thickness of electrical double layer (EDL). This change in mass transport process is responsible for change in surface morphology of the deposit, by altering the thickness of the double layer. Thus, corrosion performance of Ni-Ti alloy coatings can be improved by altering the mass transport process at the electrode-electrolyte interface, during their deposition. This can be brought about by applying magnetic field during process of electrodeposition, and process is called magneto-electrodeposition, and is explained by phenomenon called *magneto-hydrodynamic (MHD) effect*. Thus, superimposition of magnetic field develops a new route for

development of coatings/materials with higher/better corrosion resistance properties. The effect on deposit characteristics is mainly dependent on intensity and direction (parallel and perpendicular) of the applied magnetic field.

Therefore, in continuation of the previous study on electrodeposition of Ni-Ti alloy coatings (Chapter 4), here an attempt has been made to improve the corrosion resistance properties of monolayer Ni-Ti alloy coating through magneto-electrodeposition technique. Effect of inducing the magnetic field (*B*), both intensity and direction on the corrosion behaviour of Ni-Ti alloy coatings have been studied.

5.2. EXPERIMENTAL

5.2.1 Magneto-electrodeposition of Ni-Ti alloy coatings

The magneto-electrodeposition of Ni-Ti alloy coatings was carried out using the proposed bath, which contained Nickel sulphate ($NiSO_4$), titanium oxysulphate ($TiOSO_4$), tri-sodium citrate ($Na_3C_6H_5O_7 \cdot 2H_2O$), and glycerol (Table 4.1). Initially, monolayer Ni-Ti alloy coatings were electrodeposited at different current densities by conventional methods using direct current (DC). The current density at which the Ni-Ti alloy coating exhibited the lowest corrosion rate was identified. It was found that the monolayer Ni-Ti alloy coating electrodeposited at 4.0 A dm^{-2}, abbreviated as ED Ni-Ti $_{4.0\ A\ dm^{-2}}$, had the highest corrosion resistance compared to all other coatings. Subsequently, magneto-electrodeposited Ni-Ti alloy coatings, abbreviated as MED Ni-Ti, were electrodeposited under varying conditions of induced magnetic field B (parallel and perpendicular to the direction of the electric field lines, as required). An electromagnet (Polytronics, Model: EM 100, India), as shown in Figure 5.1, was used as the source of the magnetic field for this study. The magneto-electrodeposition was performed on polished mild steel under both magnetic field conditions, with the electrolytic cell positioned in the uniform magnetic field located between the poles of the electromagnet, as depicted in Figures 5.1(a) and 5.1(b). All depositions were conducted for 600 seconds, similar to the conventional electrodeposited Ni-Ti alloy coatings, to facilitate comparison. The magneto-electrodeposited alloy coatings were developed at different magnetic field intensities ranging from 0.1 to 0.4 T (Tesla), both parallel and perpendicular at the optimal current density of 4.0 A dm^{-2}, using the same bath. The current density of 4.0 A dm^{-2} was selected based on the lowest corrosion rate observed among different current densities (ranging from 1.0 to 4.0 A

dm^{-2}). The corrosion performances of all the coatings were evaluated in a 3.5% NaCl solution at 298 K using electrochemical AC and DC methods. This was accomplished with a potentiostat/galvanostat (VersaSTAT-3, Princeton Applied Research) in a three-electrode cell, with MED coatings as the test electrode (TE), a platinized platinum electrode as the counter electrode (CE), and a saturated calomel electrode (SCE) as the reference electrode.

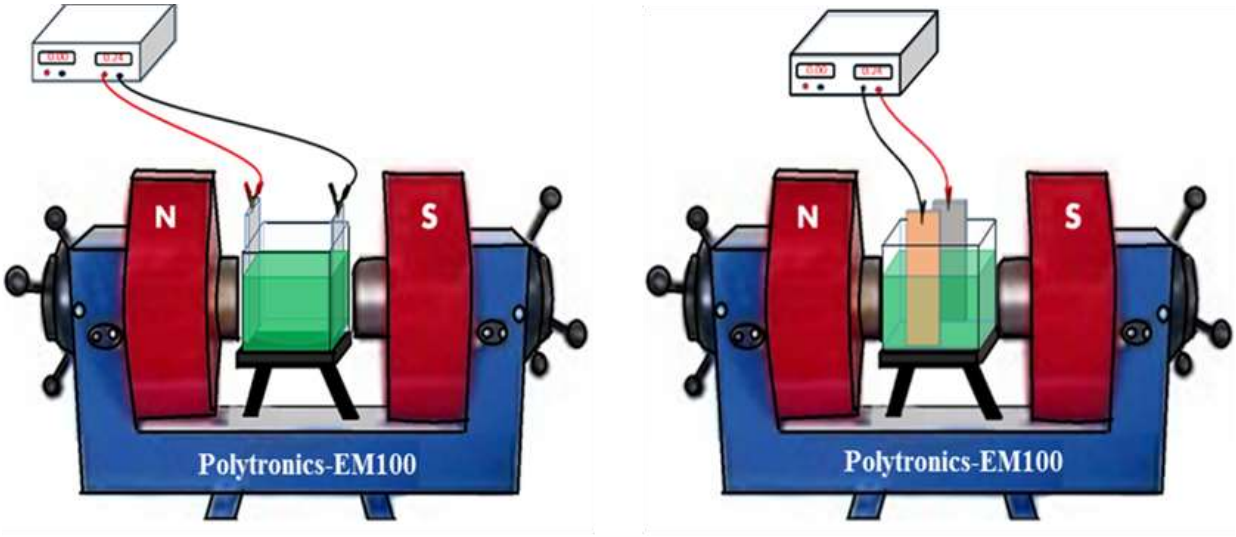

Figure 5.1 - *The experimental set up used for magneto-electrodeposition of Ni-Ti alloy coating under two conditions magnetic field (B): a) parallel and b) perpendicular to the direction of electrical field. It may be noted that in a) lines of electric field and magnetic field are parallel, and in b) they are perpendicular to each other*

The corrosion rates (CR's) of all coatings were evaluated by Tafel extrapolation method. Conventionally electrodeposited Ni-Ti alloy coatings are represented conveniently as ED Ni-Ti, with current density as subscript. Magneto-electrodeposited Ni-Ti coatings under conditions of parallel (||) field as MED || Ni-Ti $_{x,}$ and under conditions of perpendicular (⊥) field as MED ⊥ Ni-Ti $_{x}$. Here, 'x' denotes the intensity of *B* at which magneto-electrodeposition is carried out.

5.3 RESULTS AND DISCUSSION

Electrodeposition of Ni-Ti alloy coatings under the effect of induced magnetic field (*B*) were carried out using optimized bath (Table 4.1), under conditions of both parallel and perpendicular *B*, and experimental observations are described below.

5.3.1 FESEM – EDS study

To understand the effect of magnetic field on the surface morphology, process of electro-crystallization and their compositions, MED Ni-Ti alloy coatings were developed at different intensity of *B* (both parallel and perpendicular in the range of 0.1 T – 0.4 T), and their FESEM-EDS analyses were made. The FESEM images of MED Ni-Ti alloy coatings developed under conditions of parallel field, represented as MED || Ni-Ti, and under conditions of perpendicular field, represented as MED ⊥ Ni-Ti are shown in Figures 5.2 and 5.3, respectively.

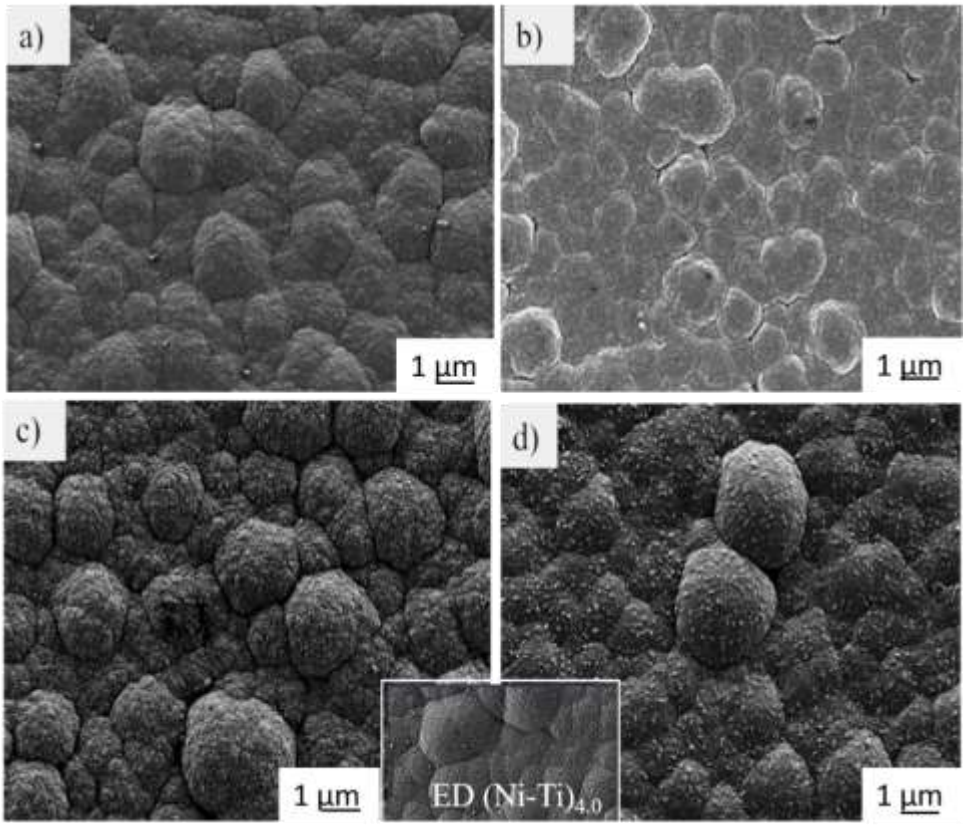

Figure 5.2 - *The surface morphology of MED || Ni-Ti alloy coatings deposited under different conditions of applied B: (a) 0.1 T, (b) 0.2 T, (c) 0.3 T and (d) 0.4 T. The surface feature of ED Ni-Ti* $_{4.0}$ *(without the effect of B) is shown in the inset for comparison purpose*

It may be noted that, under conditions of both parallel and perpendicular conditions, magnetic field intensity (*B*) has significant effect on surface features of alloy coatings. The surface morphology of conventional ED Ni-Ti $_{4.0\ A/dm^2}$ coating (developed without the effect of

B) shown in the inset of Figures 5.2 and 5.3 (for comparison purpose) confirms that magnetic field has significant influence on the surface feature of alloy coatings. It is further confirmed that change of surface features increased with increase of intensity of *B*, in both parallel and perpendicular condition as shown in Figures 5.2 and 5.3.

5.3.2 Effect of magnetic field *(B)* on composition

The effect of magnetic field, in both direction and intensity on the composition of MED Ni-Ti alloy coatings have been studied by EDS technique. The wt. % change of noble metal (Ni) content in the deposit with intensity and direction of *B* are shown in Table 5.1. From the composition data, it may be noted that wt. % of Ti in the deposit increased substantially with intensity of *B*, in both parallel and perpendicular magnetic field. As already been indicated in induced type of co-deposition, plating variable like current density hardly effects wt. % of the reluctant metal in the deposit (Table 4.2), and hence its corrosion behavior. However, from the composition data (Table 5.1), it may be noted that wt. % of Ti in the MED coatings has increased significantly with intensity of *B*, in both parallel and perpendicular field.

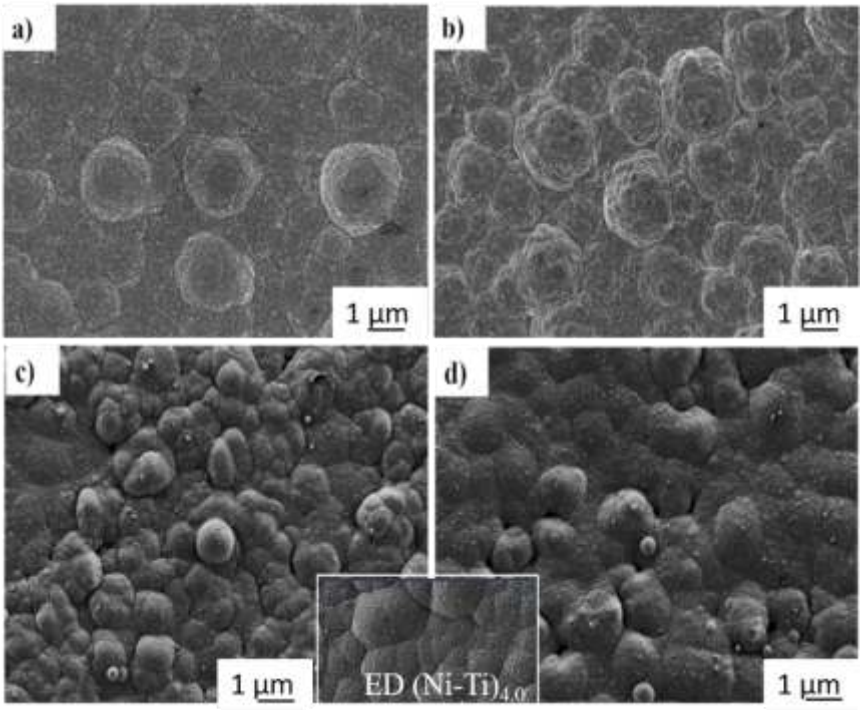

Figure 5.3- *The surface morphology of MED ⊥ Ni-Ti alloy coatings, under different conditions of applied B: (a) 0.1 T, (b) 0.2 T, (c) 0.3 T and (d) 0.4 T. The surface feature of ED Ni-Ti* $_{4.0}$ *(without the effect of B) is shown in the inset for comparison purpose*

In addition, from the literature it is evident that Ti has electrochemical properties superior to other metals due to the passive surface TiO_2 layer. Thus the composition data reveals that the superimposition of magnetic field *B* increased the wt. % Ti in the deposit from 3.5 wt. % to about 7.3 wt. % in both parallel and perpendicular field is due to induced co-deposition as explained in the preceding section.

Table 5.1. Composition and corrosion data of magneto-electrodeposited Ni-Ti alloy coatings under different conditions of *B* in relation to its conventional alloy coating

Coating configuration	wt. % of Ni	wt. % of Ti	$-E_{corr}$ (mV vs CE)	i_{corr} ($\mu A\ cm^{-2}$)	$CR \times 10^{-2}$ ($mm\ y^{-1}$)
ED Ni-Ti	96.5	3.5	-257.68	13.81	14.02
Effect of Parallel B					
MED|| Ni-Ti $_{0.1T}$	95.4	4.6	306.1	10.1	10.7
MED|| Ni-Ti $_{0.2T}$	94.8	5.2	282.1	6.6	6.9
MED|| Ni-Ti $_{0.3T}$	92.7	7.3	255.8	2.8	3.0
MED|| Ni-Ti $_{0.4T}$	93.6	6.4	263.6	4.6	4.8
Effect of Perpendicular B					
MED ⊥ Ni-Ti $_{0.1T}$	95.3	4.7	292.4	5.8	6.1
MED⊥ Ni-Ti $_{0.2T}$	94.7	6.2	279.2	4.5	4.7
MED ⊥ Ni-Ti $_{0.3T}$	92.5	7.5	245.1	2.1	2.3
MED⊥ Ni-Ti $_{0.4T}$	93.3	6.7	262.2	3.4	3.6

5.3.3 XRD Study

The XRD signatures of MED Ni-Ti alloy coatings developed at different field strengths, under parallel and perpendicular directions are shown in Figures 5.4 and 5.5, respectively. It was observed that MED Ni-Ti alloy coatings, regardless of the intensity and direction of the field exhibit the same crystal structures. The intensity of peaks, corresponding to the planes 200 and

410 has increased progressively with increase of intensity of *B*, and is attributed to the increase in the wt. % of Ti in the deposit. The intensity of reflections corresponding to (110) and (200) planes was found to be decreased with increase of *B*, and is due to the decrease of Ni content in the deposit. Hence, from the intensity of peaks, it may be inferred that decrease of peak intensity with increase of *B* is due to the decrease of Ni content in the deposit. Thus, XRD study of MED Ni-Ti alloy coatings, under both parallel and perpendicular condition reveals that applied magnetic field has a distinct role to alter the composition of the alloy coatings, but not in their phase structures. Hence, similarities of XRD patterns of MED Ni-Ti alloy coatings (under both parallel and perpendicular field) reveals that magneto-electrodeposition is more a mass transport controlled process, without bringing change in the crystallinity of deposits.

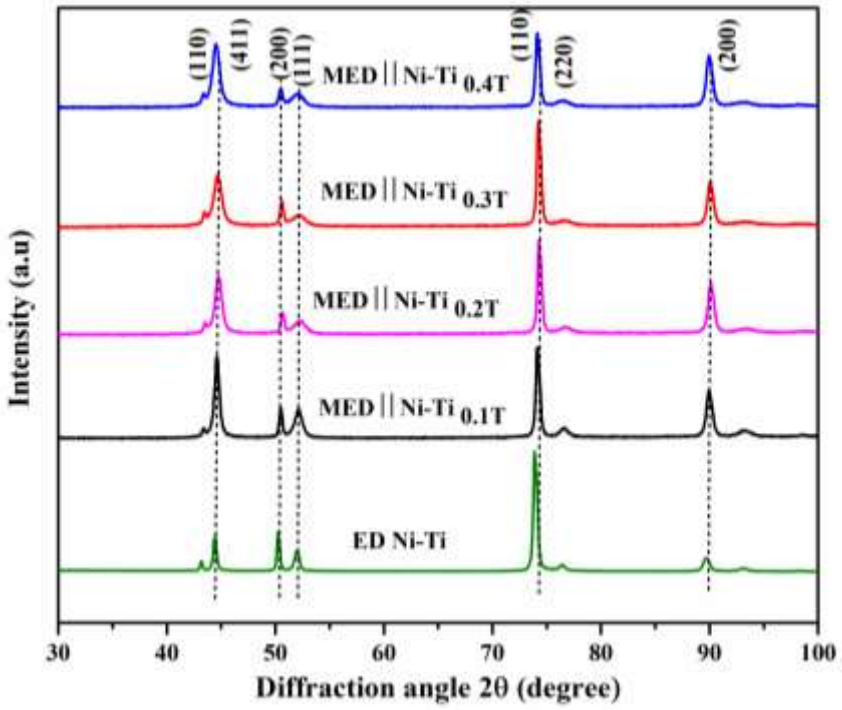

Figure 5.4 - *X-ray diffraction spectra of MED || Ni-Ti alloy coatings deposited under different intensities of B using optimal bath*

The constancy of diffraction angles (θ) in XRD patterns of all Ni-Ti alloy coatings is due to alloy deposits from the solid solution of individual metals (Cullity 1978). Solid solutions are characterized by the fact that atoms in the lattice of a metal are substituted by atoms of another metal.

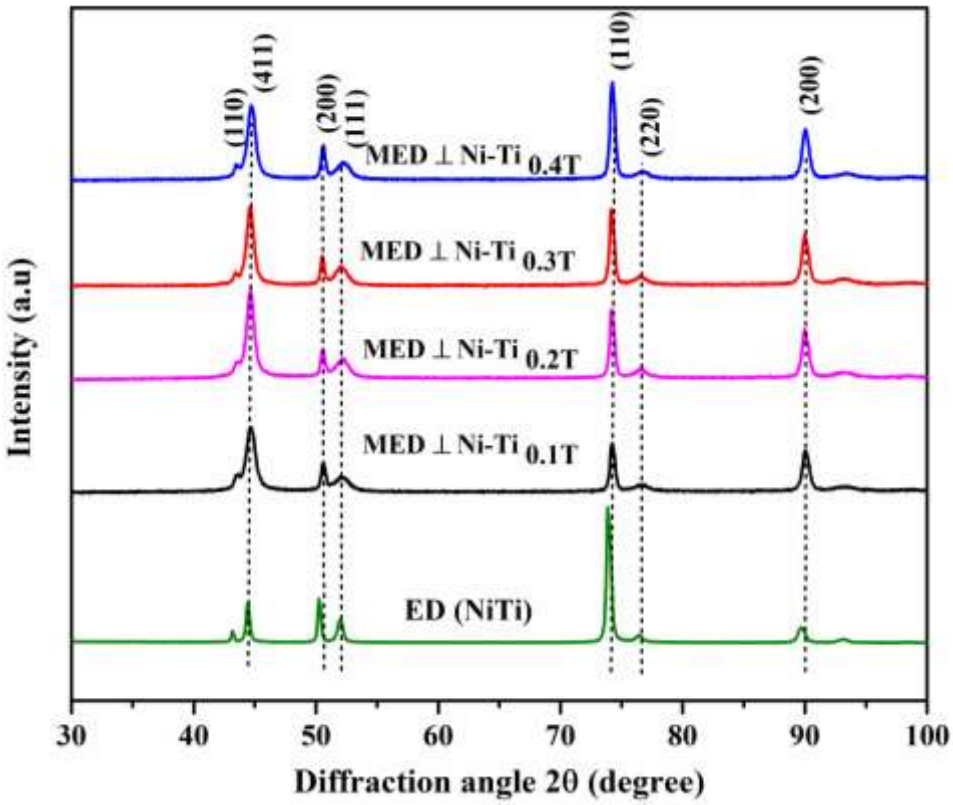

Figure 5.5 - *X-ray diffraction spectra of MED ⊥ Ni-Ti alloy coatings deposited under different intensities of B using optimal bath*

This substitution changes the dimension of the unit cell, without the change in the type of cell, and this substitution may occur either over a limited range of composition or over the complete range of composition from one pure metal to the other. A gradual increase in the intensity of peak, and slight increase in diffraction angle was found with increase of *B*, in both parallel and perpendicular field as seen in Figures 5.4 and 5.5. This shift of scattering angle to right may be attributed to increase in the wt. % Ni in the deposit with *B*; supported by the composition data, given in Table 5.1.

5.4 Corrosion study

The very objective of the magneto-electrodeposition is to improve the corrosion protection efficiency of Ni-Ti alloy coatings by overcoming the limitation of induced co-deposition. Accordingly, the corrosion performance of MED Ni-Ti alloy coatings were studied by the electrochemical AC and DC techniques, and experimental results are discussed.

5.4.1 EIS study

Nyquist plots of MED Ni-Ti alloy coatings, deposited under both parallel and perpendicular field effect are shown in the Figures 5.6 (a) and 5.6 (b).

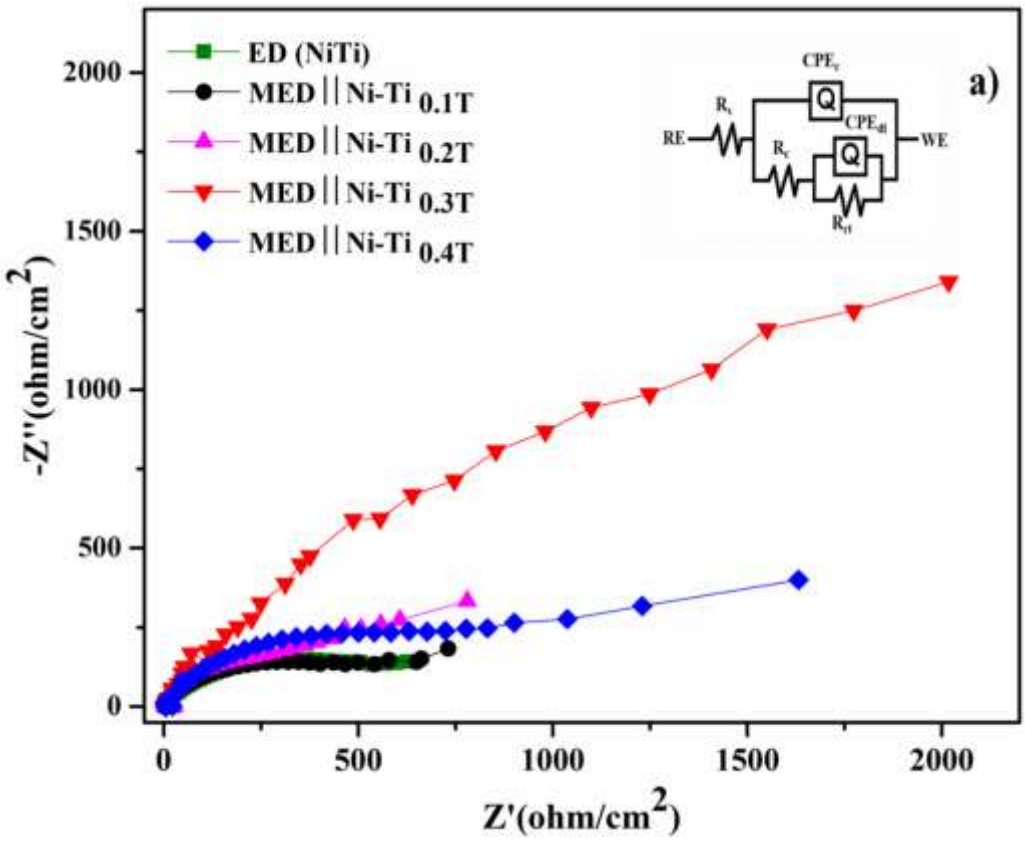

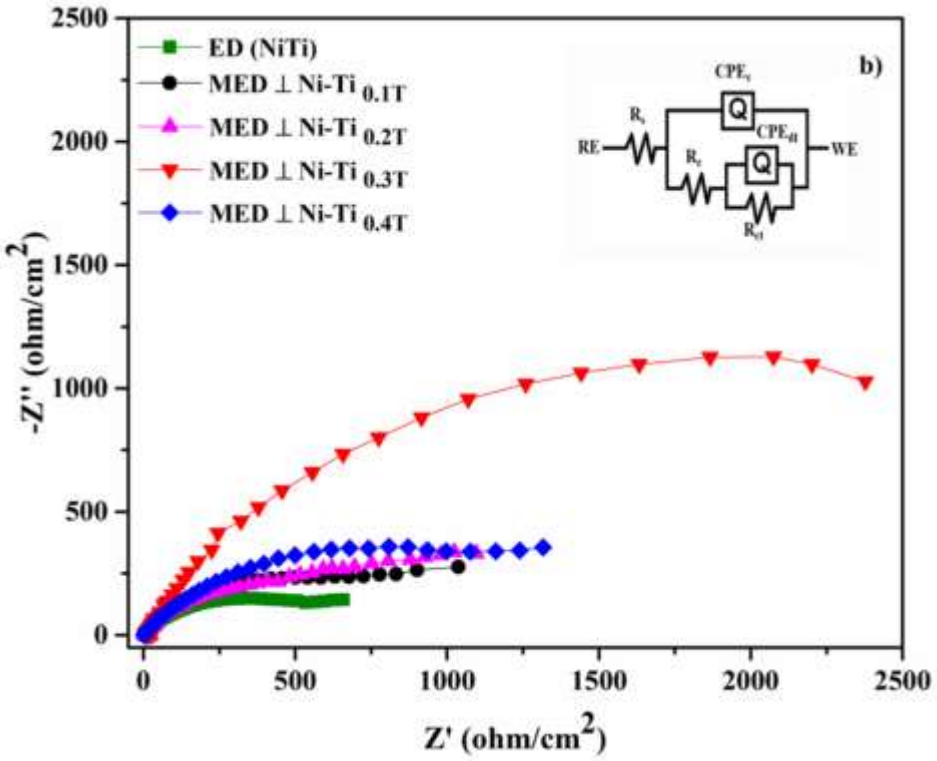

Figure 5.6 – *Nyquist responses of MED Ni-Ti alloy coatings deposited at different intensities of B under conditions of (a) parallel, and (b) perpendicular field*

The impedance responses of alloy coatings were used to understand their corrosion protection efficiency, in terms of various electrical components present in fitted electrochemical equivalent circuit (EEC). Nyquist plots of MED Ni-Ti alloy coatings, corresponding to both parallel and perpendicular field (Figures 5.6 (a) and 5.6 (b)) showed a single semicircle loop for all samples, this indicates only single charge transfer process is taking place at the interface. At higher frequencies the interception of real axis is ascribed to the solution resistance (R_s) and at the lower frequencies, the interception with real axis is ascribed to the charge transfer resistance (R_{ct}). Impedance responses of MED Ni-Ti alloy coatings, corresponding to both parallel and perpendicular field indicates that the value of (R_{ct}), *i.e.*, the length of semicircle increased with increase of intensity of *B*, and it is maximum for MED|| Ni-Ti $_{0.3T}$ and MED⊥ Ni-Ti $_{0.3T}$ coatings. Hence, they have been taken as the optimal configuration of the coating showing highest corrosion resistance.

Table 5.2- EIS data obtained from equivalent circuit simulation of Ni-Ti alloy coatings electrodeposited under different conditions of magnetic field *(B)*

Coating configuration	R_S (Ω)	R_C (Ω)	Q_C (μF)	R_{ct}(Ω)	Q_{dl}(μF)	χ^2 (10^{-3})
MED || Ni-Ti $_{0.1T}$	10.8	1056	914	778	1350	4.12
MED || Ni-Ti $_{0.2T}$	12.3	1372	998	956	1486	3.89
MED || Ni-Ti $_{0.3T}$	14.6	1651	1189	1250	2512	2.34
MED || Ni-Ti $_{0.4T}$	13.2	1442	1053	1123	1508	3.54
MED ⊥ Ni-Ti $_{0.1T}$	11.2	1286	1082	875	1425	4.86
MED ⊥ Ni-Ti $_{0.2T}$	12.6	1492	1259	1068	1682	4.56
MED ⊥ Ni-Ti $_{0.3T}$	15.6	1892	1725	1348	2651	2.89
MED ⊥ Ni-Ti $_{0.4T}$	13.4	1539	1337	1216	1758	3.96

From the impedance responses of MED|| Ni-Ti $_{0.3T}$ and MED⊥ Ni-Ti $_{0.3T}$ coatings, electric circuit elements (EED) were evaluated from their EEC (shown in inset of Figures 5.6 (a) and 5.6 (b)). The values of those circuit elements, like solution resistance (R_S), coating resistance (R_c), constant phase element (CPE) of the alloy coatings (Q_c), charge transfer resistance (R_{ct}) and constant phase element (CPE) of the coatings-substrate interface (Q_{dl}) of all coatings are reported in Table 5.2. It may be noted that the value of R_c and R_{ct}, put together constitute the polarization resistance of alloy coatings, and they are responsible for their corrosion resistance behaviors. The diameter of capacitive loops of Nyquist plots represents the polarization resistance of the work electrode (Liu et al. 2013). Hence, it may be seen that in both parallel and perpendicular *B*, axial radius of the semicircle keeps increasing with the intensity of *B*, till 0.3 T and then decreased. This clearly suggests that the polarization resistance (R_p) of MED coatings increased with intensity of *B*. But at high intensity of *B*, the value of R_p was found to be decreased. This is further supported by the data listed in the Table 5.2. Hence MED Ni-Ti $_{4.0/0.3T/per}$ coating, with highest charge transfer resistance (Rct) and less capacitance value shows that it is the least corrosive compared to all other coatings. Further MED Ni-Ti alloy coatings developed under all other parallel magnetic field are comparatively less corrosion resistant than MED Ni-Ti $_{4.0/0.3T/per}$. The increased corrosion resistance of alloy

coatings may be explained on the basis of their alloy composition, surface roughness and crystallite size. Thus, an increased Ti content of the alloy towards higher *B*, lead to an increase of electrochemical activity, roughness and strain of the Ni-Ti alloy matrix, and hence these factors are found to be responsible for their decreased corrosion resistance(Bakhit et al. 2014). The corrosion inhibition efficiency of MED alloy coatings, obtained from the impedance responses are in agreement with values obtained from EEC fitment (San et al. 2012).

5.4.2 Potentiodynamic polarization study

The potentiodynamic polarization behavior of MED Ni-Ti alloy coatings, corresponding to different intensities of magnetic field, applied in both parallel and perpendicular directions are shown in Tafel's plots Figures 5.7 (a) and 5.7(b). The rate of corrosion rates calculated by Tafel's extrapolation method, and corresponding data are reported in the Table 5.1. It was observed that regardless of the direction of applied magnetic field, its increase of strength, *i.e.*, up to 0.3 T, the i_{corr} and corresponding CR's were decreased, but later it increased in its values. Hence, it may be realized that super imposition of magnetic field during electrodeposition process can enhance the corrosion resistance properties of alloy coatings by bringing changes in the deposit characteristics such as composition and surface morphology affected due to magneto-convection. The increasing corrosion resistance of the coating is attributed to the increase in limiting current density (i_L) of Ti in the bath, due to superimposition of magnetic field. However, it was observed that CR's of MED Ni-Ti alloy coatings decreased with the intensity of *B* only up to 0.3 T, under both parallel and perpendicular B, and then decreased.

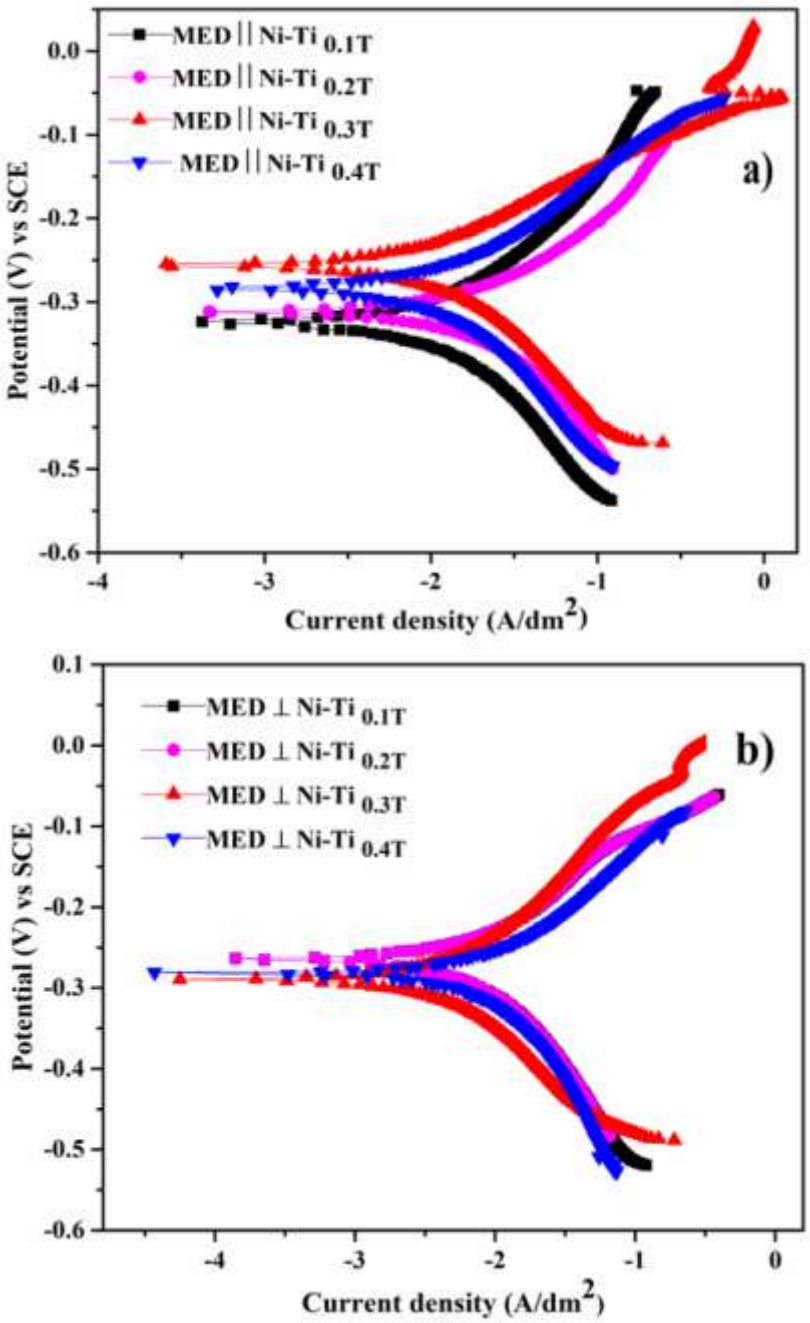

***Figure 5.7** – Potentiodynamic polarization behavior of MED Ni-Ti alloy coatings deposited at different conditions of applied magnetic field: (a) parallel and (b) perpendicular*

But, on applying *B* greater than its limiting value (of the bath), it started giving an adverse effect on the deposit characteristics, may be due to increase in the hydrogen evolution reaction (HER) on its surface. As a result, the coatings were shown to be rougher at higher limits of induced *B* at (0.4 T) with decreased Ni content. Hence, alloy coatings at higher intensity of *B* showed greater CR in both parallel and perpendicular fields (Table 5.1). In conclusion, MED

⊥ Ni-Ti $_{0.3T}$ coating has the least corrosion rate (2.3 x 10^{-2} mmy^{-1}) and MED ‖Ni-Ti $_{0.3T}$ with CR value of (3.0 x 10^{-2} mmy^{-1}). Hence, it may be noted that higher CR value (14.02 x 10^{-2} mmy^{-1}) of conventional Ni-Ti alloy coating, represented as ED Ni-Ti $_{4.0}$ has been improved to greater extent by magneto-electrodeposition. The lower corrosion rate of magneto-electrodeposited MED⊥ Ni-Ti $_{0.3\,T}$ compared to MED ‖Ni-Ti $_{0.3T}$ may be due to the additional magnetic convective effect governed by Lorentz force (Bund et al. 2003), (Jha and Aina 2016), (Koza et al. 2010). It accounts the fact that in case of parallel *B*, a non-electrostatic field parallel to the surface of the working electrode is generated, which makes the solution to move near to the interface. In case of perpendicular *B*, both non-electrostatic and electrostatic forces are being operated. Hence, magneto convection effect is maximum for perpendicular *B*.

5. 5 Comparison of ED and MED Ni-Ti alloy coatings

The corrosion data of Ni-Ti alloy coatings under optimal conditions of magneto reveals that MED ‖Ni-Ti $_{0.3T}$ and MED ⊥ Ni-Ti $_{0.3T}$ coatings are of highest corrosion resistance (least CR), compared to its conventional alloy coating, represented as Ni-Ti $_{4.0}$. This increased corrosion resistance of MED Ni-Ti alloy coatings may be attributed to the changed composition (Table 5.1), phase structure and surface morphology of alloy coatings, affected due to induced magnetic field.

The microstructure and the phase structure of ED Ni-Ti $_{4.0}$, MED ‖ Ni-Ti $_{0.3T}$ and MED⊥Ni-Ti $_{0.3T}$ alloy coatings, showing the highest corrosion resistances (all optimal) are shown comparatively in Figure 5.8. It may be seen that surface morphology of alloy coatings, responsible for better corrosion resistance has changed as the mode of deposition is changed, from conventional type to magneto-electrodeposition type. Thus, it may be seen from the FESEM image that ED Ni-Ti alloy coating (deposited under no effect of magnetic field) is rougher than MED ⊥ Ni-Ti $_{0.3T}$. This may be attributed to the fact that when *B* is oriented perpendicular to the electrode surface, the magneto convection effect is found to be maximum due to inclusion of Lorentz force. Hence, coating corresponding to MED ⊥ Ni-Ti $_{0.3T}$ configuration found to be the most uniform, with least corrosion rate.

The observed facts amount to state that the Lorentz force acting, under condition of perpendicular *B* is responsible to increase the mass transfer process towards cathode. This in turn is responsible for decrease in diffusion layer thickness in the vicinity of the electrode.

Hence, it may be concluded that induction of magnetic field during deposition, improved the corrosion resistance of alloy coatings by smoothening its surface.

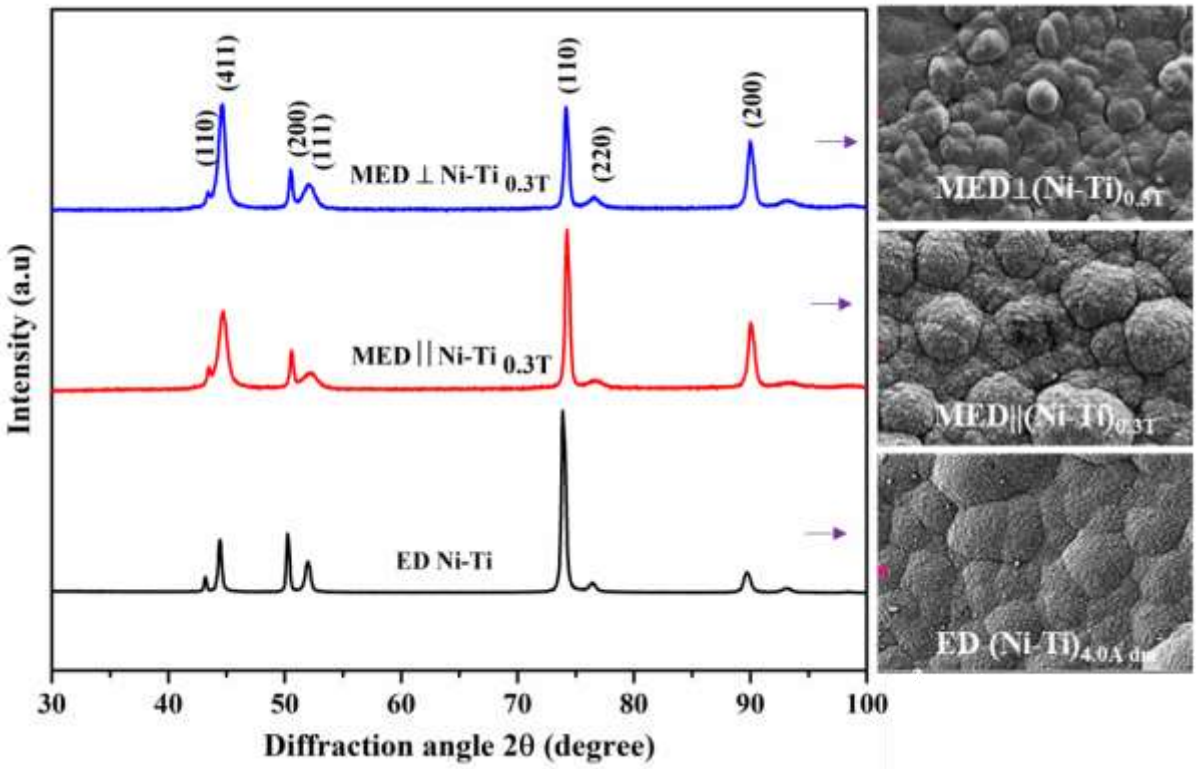

Figure 5.8- *Comparison of XRD patterns and surface morphology of MED Ni-Ti alloy coatings deposited under optimal conditions of parallel and perpendicular B, in comparison with ED Ni-Ti alloy coatings deposited from the same bath*

The corrosion resistance behavior of ED Ni-Ti, MED ‖ Ni-Ti $_{0.3T}$ and MED ⊥ Ni-Ti $_{0.3T}$ coatings showing the least CR (optimal) are shown in Figure. 5.8. The Nyquist plots, with distinct difference in the diameter of the capacitive loops indicates that magneto-electrodeposited Ni-Ti alloy coatings (both parallel and perpendicular) are far more corrosion resistant than their conventional alloy counterpart. This further supported by their potentiodynamic polarization response shown in the inset of Figure 5.9, with having a clear difference between their i_{corr} and E_{corr} values. Thus, from the corrosion data it may be summarized that, if ED Ni-Ti $_{4.0\ A/dm^2}$ alloy coating, having 3.5 wt.% Ti showed CR = 14.02 x 10^{-2} mmy^{-1}, MED coatings having MED ‖ Ni-Ti $_{0.3\ T}$ and MED ⊥ Ni-Ti $_{0.3\ T}$ configurations (having respectively 7.3 wt.% and 7.5 wt.% Ti) showed CR's = 3.0 x 10^{-2} mmy^{-1} and 2.3 x 10^{-2} mmy^{-1}, respectively. Thus CR values demonstrates that MED Ni-Ti alloy coatings are about

seven times more corrosion resistant than conventional ED alloy coatings deposited from same bath for same duration.

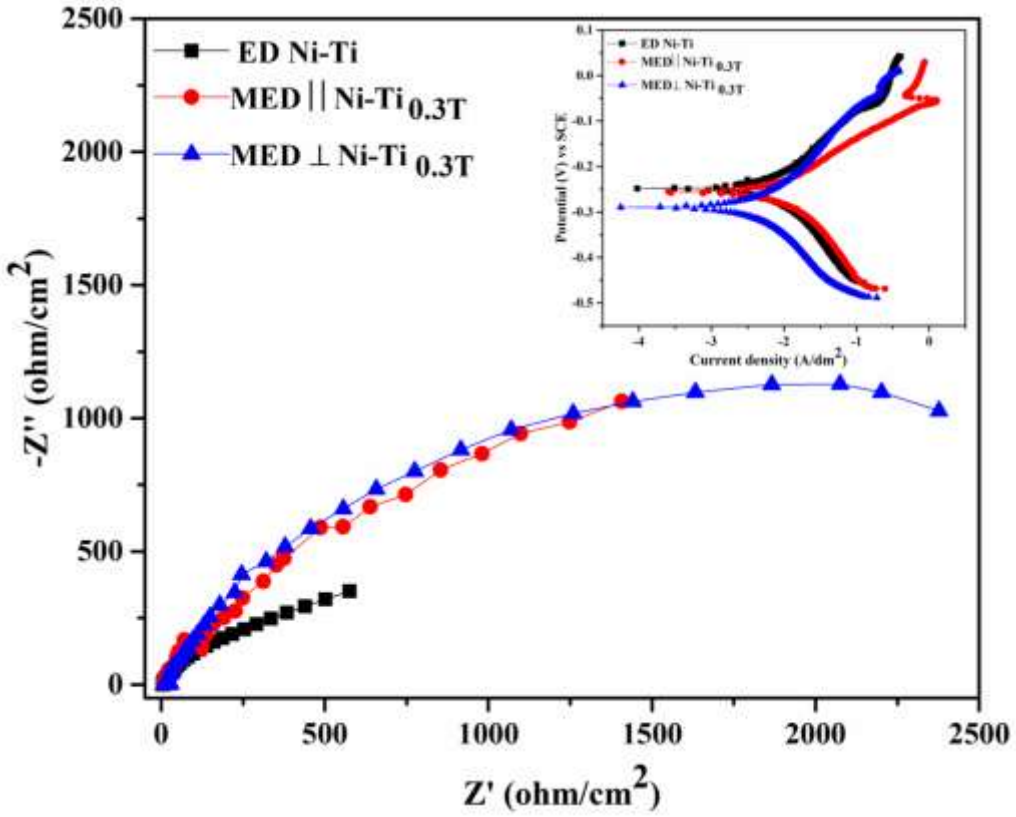

***Figure 5.9** – Comparison of impedance responses of MED Ni-Ti alloy coatings (under parallel and perpendicular B) in relation of ED Ni-Ti coating deposited from same bath (all under optimal condition), with Tafel's responses (inset)*

5.6 Discussion

From the composition data (Table 5.1), it may be noted that Ti content of conventional alloy coating has increased substantially from 3.5 wt. % to a maximum of 7.3 wt. % and 7.5 wt. %, for parallel and perpendicular *B*, respectively. Thus, on superimposition of *B* (both parallel and perpendicular), the reluctant metal (Ti) content has increased drastically, and it started decreasing at higher limits of *B* as reported in Table 5.1 Hence, increase of Ti content in the deposit, affected due to magnetic field effect is responsible for improved corrosion resistance of MED Ni-Ti alloy coatings. The factor responsible for the increase in wt. % Ti in the deposit may be explained as below. The basic principle of electroplating states that the composition of electrodeposits are determined by the limiting current density (i_L) of metal ions in the bath.

Here, it may be recalled that i_L is the current density at which the rate of electrodeposition is maximum. It follows the statement that i_L is the measure of maximum reaction rate that cannot be exceeded by increasing the current density. Therefore, when the electrode process is mass-transfer controlled, the value of the current density is given by Equation 5.1

$$i_L = \frac{n F D_z C_B}{\delta} \qquad (5.1)$$

Where, *n* is the valency of the metal ions, and F is the Faraday constant (96,400 C), D_z is the diffusion coefficient of the reacting species, C_B is the concentration and δ is the thickness of electrical double layer (EDL). Thus, superimposed magnetic field creates an artificial convection, and thereby increase of mass transport process at EDL. This increased mass transport process decreases the thickness of EDL (δ), and thereby increases the value of i_L (Equation 5.1). Increase in the limiting current density (i_L) of Ti in the bath, due to induction magnetic field is shown schematically in Figure 5.10. It may be seen that limiting current density (i_L) of Ti under condition of magnetic field (both parallel and perpendicular), represented as $i_{L,Ti}$ (MED) is much higher than that of conventional Ni-Ti alloy coating, represented as $i_{L,Ti}$ (ED). Thus increase of Ti content in the MED deposit is due to increase of its limiting current density (i_L).

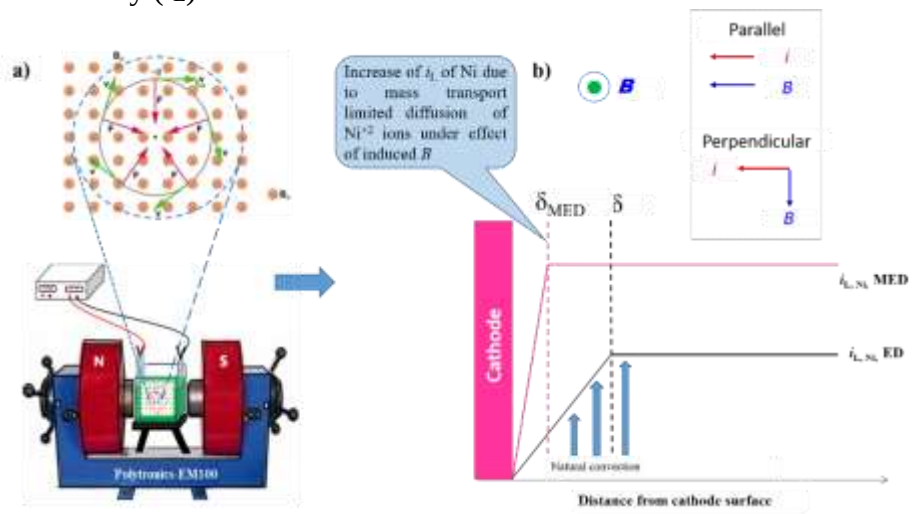

Figure 5.10 *– Schematic representation showing: a) Process of magneto-electrodeposition and b) decrease of diffusion layer thickness (δ) due to increase of limiting current density (i_L) on superimposition of magnetic field, B*

The lines of ionic movement responsible for change of EDL thickness, during conventional electrodeposition (ED) and magneto-electrodeposition (MED) are shown in the Figure 5.11.

Generally, in conventional ED, lines of ionic movement are parallel, and perpendicular to the plane of the cathode, as shown in Figure 5.11(a). When magnetic field applied is parallel to the direction of movement of ions, an increase in the rate of mass transport is affected due to formation of a hydrodynamic boundary layer at the E-E interface due to tangential velocity, induced by the field that actually decreases the diffusion layer thickness, and increases the flux of the ionic species (Ganesh et al. 2005). This situation is shown in Figure 5.11(b). When the applied *B* is perpendicular to the direction of movement of ions, the improved deposition patterns of MED coatings may be attributed to the magneto-hydrodynamic (MHD) effect, which may be explained from the Lorentz force due to the interaction of velocity field of charged species with electromagnetic field (Koza et al. 2008), (Koza et al. 2010), (Koza et al. 2011) (Krause et al. 2007). The total force on a charged particle, moving in an electromagnetic field is the Lorentz force, and is given by,

$$F_L = qE + qvBSin\theta \qquad (5.2)$$

Where, F_L is the Lorentz force, q is the charge of an ion, E is the electric field strength, v is the velocity of the ions and B is the magnetic flux density. When a *B* is applied perpendicular to the direction of the flow of ions (Where Sin 90º = 1), the Lorentz force is exerted on the moving ions, and thereby induces a convective force operating during magneto-electrodeposition, with perpendicular field is shown in Figure 5.11 (c).

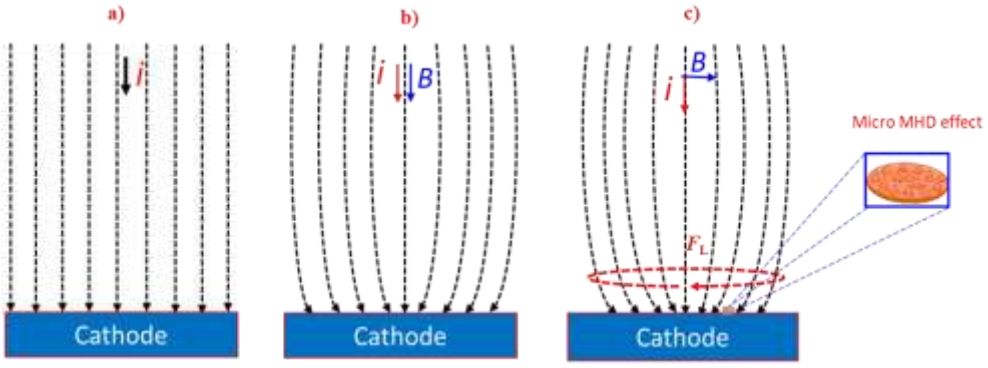

Figure 5.11 *- Diagrammatic representation showing lines of ionic movement responsible for change in EDL thickness during electrodeposition of Ni-Ti alloy coatings: a) ED Ni-Ti natural convection b) MED Ni-Ti Parallel B, and c) MED Ni-Ti Perpendicular B (Gonsalves and Hegde 2021)*

Thus in the light of principles of magneto-electrodeposition, it may be summarized that MED ⊥ Ni-Ti $_{0.3T}$ coating obtained in a perpendicular direction was found to be more corrosion resistant, compared to ED Ni-Ti alloy coatings of other configurations. The highest effect of perpendicular field, compared to parallel field is due to the combined effect of non-electrostatic force and Lorentz force. The Lorentz force is at its maximum when field is applied perpendicular to the direction of flow of ions (Equation 5.2). This is responsible for highest decrease of EDL thickness during deposition. The thickness of the cathode film decreased from δ to δ_{MED} when the coating mode shifted from ED (Electrodeposition) to MED (Magnetoelectrodeposition) as shown in the Figure 5.10. Additionally, the increase in titanium (Ti) content in the alloy, resulting from a higher initial Ti concentration (i_L), contributes to the enhanced corrosion resistance of the magneto-electrodeposited (MED) Ni-Ti alloy coatings.

5.7 CONCLUSIONS

The lower corrosion protection efficiency of conventional ED Ni-Ti alloy coatings, due to the induced type of co-deposition of Ni and Ti ions has been increased substantially by superimposition of magnetic field (*B*) parallel to the process of electrodeposition. Magneto-electrodeposited (MED) Ni-Ti alloy coatings have been developed by using the optimal bath by inducing the magnetic field (both parallel and perpendicular to the lines of electric field). From the experimental results, the following conclusions are drawn:

1. The corrosion protection efficiency of conventional ED Ni-Ti alloy coatings can be increased drastically through magneto-electrodeposition (MED) approach by inducing the magnetic field *B*, simultaneously to the process of electrodeposition.
2. Under optimal conditions, MED Ni-Ti alloy coating is about seven times more corrosion resistant compared to its electrodeposited (ED) counterpart, deposited from the same bath for the same duration at the same current density.
3. Drastic improvement in the corrosion protection efficiency of MED Ni-Ti alloy coatings, (under both parallel and perpendicular field) is attributed to increase of wt. % Ti in the deposit, affected due to the MHD effect.
4. The improved corrosion resistance of MED Ni-Ti alloy coatings, in relation to its conventional alloy coatings were attributed to their changed composition, and surface morphology, supported by EDS, FESEM and XRD study, respectively.

5. The Ti content in the deposit is found to be increased with *B* (in both parallel and perpendicular field) due to increase of its limiting current density (i_L) value, affected due to magneto convection effect.
6. The constancy of XRD patterns of MED Ni-Ti alloy coatings, regardless of the direction and intensity of *B* is due to formation of solid solution of Ni-Ti alloy. Only change of intensity of XRD peaks were found due to change in the composition of alloy.
7. The lesser corrosion protection efficiency of conventional ED Ni-Ti alloy coatings due to the inherent induced type of co-deposition of Ni and Ti ions has been improved effectively by superimposition of magnetic field parallel to the process of electrodeposition.

ELECTRO-CATALYTIC STUDY OF ELECTRODEPOSITED Ni-Ti ALLOY COATINGS AND EFFECT OF ADDITION OF Ag NANOPARTICLES

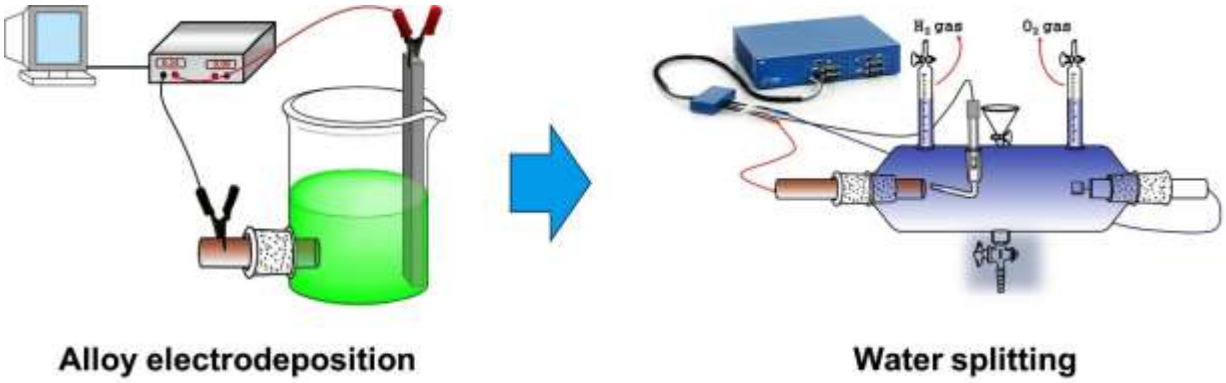

The present chapter aims to study the electro-catalytic activity of electrodeposited Ni-Ti alloy coatings using the alkaline water as electrolyser. The Ni-Ti alloy coatings deposited at different current densities were used as electrode material as both cathode and anode for hydrogen evolution reaction (HER) and oxygen evolution reaction (OER), respectively. The electro-catalytic performance of alloy coatings were evaluated in 1M KOH medium using cyclic voltammetry (CV) and chronopotentiometry (CP) techniques. The factors responsible for changed electro-catalytic activity of Ni-Ti alloy coatings with deposition current densities were explained in terms of their changed surface morphology, composition and phase structure, evidenced by SEM, AFM, EDS and XRD analyses. The effect of addition of Ag nanoparticles into bath on electro-catalytic activity of HER was tested. The enhanced electro-catalytic activity of Ni-Ti-Ag composite coating has been attributed to the incorporation of Ag-nanoparticles into alloy matrix. The deposition conditions for best electro-catalytic activity of Ni-Ti and Ni-Ti-Ag coatings were proposed and results are discussed. The poorer electro-catalytic response of Ni-Ti alloy coatings for change of current densities were attributed to the obvious limitations of induced type of co-deposition prevailing in the bath. The observed small change of electro-catalytic response of Ni-Ti alloy coatings with deposition current densities is attributed to small change of its composition, linked to the obvious limitation of induced type of co-deposition prevailing in the bath.

6.1 INTRODUCTION

Electro-catalytic water splitting driven by renewable energy input to produce clean H_2 has been widely regarded as a promising future energy portfolio. Hence, synthesis of high performance and economically viable electro-catalysts for overall water splitting applications is of high priority (You and Sun 2018). The electro-catalytic properties of electrode materials mainly depend on the density of active sites embedded in it, which are responsible for their redox activities (Wu et al. 2010).Generally, IrO_2 or RuO_2 for the O_2 evolution reaction (OER) and Pt for the H_2 evolution reaction (HER) are currently the most advanced electro-catalysts for water splitting in acidic solutions. In this regard, the transition metals and their alloys are used as best electrode materials for water splitting reactions. Ni and its alloys have been considered as efficient electrode materials due to their special properties, such as low cost, high strength, good wear resistance and good electro-catalytic activity (Wang et al. 2005).The electrodeposited alloys of transition metals like Ni, Co, Ti, Fe and Mo are proved to be the efficient electro catalysts towards water splitting reaction than bare Ni coatings (Fan et al. 1994) , (Rosalbino et al. 2008). Apart from this, many reports are available in literatures to support the fact that electro-catalytic efficiency of electrode materials can be improved drastically by incorporation of colloidal nano-particles into the metal/ alloy matrix, through nanoparticles co-electrodeposition.

In this direction, Ni-Ti alloy coatings electrodeposited from the proposed optimal bath of Ni-Ti (Table 4.1) has been subjected to electro-catalytic study. Ni-Ti alloy coatings were accomplished on copper substrate (for electro-catalytic study) from acid sulphate bath at different current densities, and their efficiency for water electrolysis of hydrogen evolution reaction (HER) and oxygen evolution reaction (OER) were studied. The performance of Ni-Ti deposit as bipolar electrode material has been evaluated quantitatively, and electro-catalytic kinetic parameters were assessed by conventional cyclic voltammetry (CV) and chrono-potentiometry (CP) methods. Further, in view of many reports on improved electro-catalytic activity of nanoparticles induced transition metals alloy coatings, it was attempted to improve the electro-catalytic performance of Ni-Ti for HER by incorporating the Ag-nanoparticles into the bath. Here, Ni-Ti-Ag composite coatings have been developed through co-electrodeposition, where Ag-nanoparticles are dispersed in optimal Ni-Ti bath. The electro-

catalytic efficiency of composite coatings was investigated, in relation to its binary alloy matrix to evaluate effect of Ag nanoparticles. The electro-catalytic activity of Ni-Ti alloy and Ni-Ti-Ag composite coatings were evaluated under different conditions of their depositions. Different factors responsible for varied electro-catalytic activity are correlated with their composition, phase structure and surface topography, evidenced through EDS, XRD, AFM and SEM analyses, and experimental results are discussed.

6.2. EXPERIMENTAL

6.2.1 Electrodeposition of Ni-Ti alloy coatings

The electro-catalytic study of Ni-Ti alloy coatings have been were carried out, after they are being deposited from the proposed bath, mentioned in Chapter 4. The electrolytic bath containing nickel sulphate ($NiSO_4$), titanium oxysulphate ($TiOSO_4$), tri-sodium citrate ($Na_3C_6H_5O_7 \cdot 2H_2O$) and glycerol were used in the preparation of electrolytic solution. The bath composition and operating parameters, arrived using standard Hull cell method is reported in Table 4.1. Electro-catalytic characterization of Ni-Ti alloy coatings were studied by depositing them on the cross-sectional area of the copper rod having 1.0 cm^2 surface area (shown by the arrow mark in Figure 6.1(a)), using a specially made electrodeposition setup as shown in Figure 6.1(a). The Ni-Ti alloy coatings so deposited, now treated as electrodes are tested for their electro-catalytic activity of water splitting behavior in 1.0 M KOH, using the electrolyser as shown in Figure 6.1(b). The electro-catalytic behavior of water splitting, in terms of HER and OER were studied quantitatively by collecting the H_2 and O_2 gases liberated at cathode and anode, respectively. The Ni-Ti alloy coatings were developed on the cross sectional area of mirror finished copper rod at different current densities (from 1.0 to 4.0 A/dm^2), using it as cathode, and graphite sheet as anode as shown in Figure 6.1(a). All electrochemical studies made here are by using a three electrode system, where test electrode was working electrode, platinum electrode was counter electrode, and saturated calomel electrode (SCE) was reference electrode. A Luggins capillary with KCl Bridge was used to minimize the ohmic polarization. The electrolytic cell fitted with graduated burettes on top Figure 6.1 (b), enables quantitative measurement of hydrogen and oxygen gases, liberated during water electrolysis.

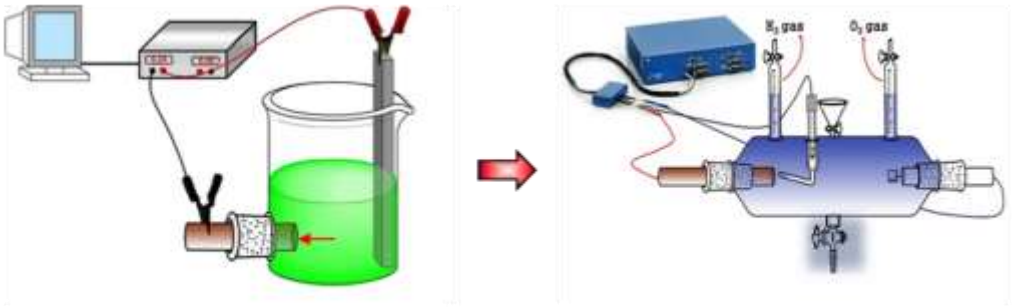

Figure 6.1*- Schematic of the experimental setup used for: a) Electrodeposition of Ni-Ti alloy coating, and b) Electrolyser set up used for water splitting of HER and OER*

All depositions of Ni-Ti alloy coatings were carried out using constant current power source (DC Power Analyzer, Agilent Technologies, N6705C, USA). All coatings were carried out for same duration 10 mins, keeping both temperature and pH constant, for the purpose of comparison. The pH of the bath was adjusted to 4.0 using pH meter (Systronics-362), on addition of either sulphuric acid (H_2SO_4) or ammonium hydroxide (NH_4OH) solution, depending on the requirement.

6.3. RESULTS AND DISCUSSION

6.3.1 Characterization of Ni-Ti alloy coatings

The compositional and structural characterization of Ni-Ti alloy coatings were carried out using EDS, FESEM, AFM and XRD analyses. Further, their electro-catalytic behaviors for alkaline water splitting (for both HER and OER) were studied in 1M KOH, using a custom made tubular glass set up having three electrodes as shown Figure 6.1(b). The conventional CV and CP techniques were employed to study the electro-catalytic efficiency of alloy coatings, using computer controlled potentiostat/galvanostat (VersaSTAT-3 (Princeton Applied Research, USA). The electro-catalytic stability of the electrodeposited coatings were tested by chronopotentiometry method by monitoring the electrode reaction for duration of 1800 s. The efficiency of electrode reactions, both as cathode and anode for HER and OER were evaluated quantitatively by measuring the volume of H_2 and O_2 evolved on 1.0 cm^2 surface area of the test electrode for duration of 300 s electrolysis time.

6.3.2 Surface morphology and phase structure of alloy coatings

Knowing the fact that electro-catalytic activity of alloy coatings are based on their composition, surface roughness and positivity, the composition of Ni-Ti alloy coatings corresponding to different current densities are reported in Table 4.2, evidenced by EDS analyses. The phase structure of Ni-Ti coatings corresponding to different current densities were examined by XRD techniques and corresponding X-ray peaks are shown in the Figure 6.2. The observed lattice planes are (110), (411), (200), (111), (110), (220) and (200) matched with the JCPDS File No: 03-065-5744 corresponding to Ni-Ti alloy coatings. In addition, change in the surface morphology of alloy coatings with deposition current densities are shown in the Figure 6.2 (right). It may be seen that Ni-Ti alloy coatings electrodeposited at different current densities exhibits morphology with particulate-like structure on its surface as shown in Figure 6.2.

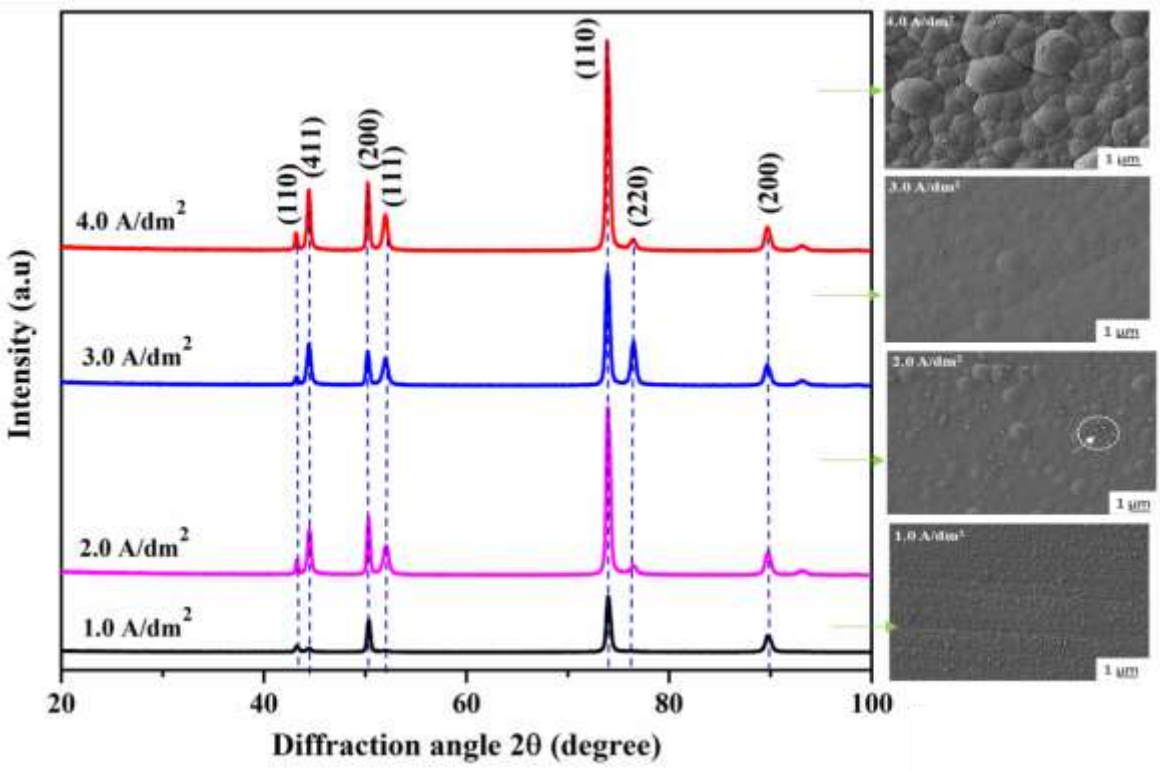

Figure 6.2 *- X-ray diffraction peaks of Ni-Ti alloy coatings deposited at different current densities from the optimized bath. On the right are given their FESEM image showing different surface morphology responsible for their different electro-catalytic activities*

The surface features of these Ni-Ti alloy coatings indicate that the co-deposited Ti has distributed uniformly in its Ni matrix. Further, it may be noted that the presence of metal particles embedded into the nickel matrix distinctly enlarge the real surface of the coatings, which is requirement of any coatings for good electro-catalytic property (Sun et al. 2016).

6.3.3 Electro-catalytic study

The electro-catalytic behaviour of Ni-Ti alloy coatings from the proposed bath, electrodeposited at different current densities have been studied for their efficiency to electrolyse water. Electro-catalytic study has been done in 1.0 M KOH, in terms of their HER (hydrogen evolution reaction) and OER (oxygen evolution reaction).

6.3.3.1 Hydrogen Evolution Reaction

The steady state equilibrium is the state at which water splitting occurs as HER and OER, due to the act of electro-catalyst. Accordingly, Ni-Ti alloy coatings deposited at different current densities are subjected to electro-catalytic study through cyclic voltammetry (CV) and chrono-potentiometry (CP) techniques, and are discussed below.

i) Cyclic voltammetry study

The electro-catalytic behaviour of Ni-Ti coatings has been studied for HER by making coatings as the cathode in electrolyser. The cyclic voltammetry (CV) study was made in a potential range of 0.0 V to -1.6 V at 50 mV/sec scan rate, after being stabilized on 20 cycles. The CV curves of alloy coatings, deposited at different current densities are as shown in the Figure 6.3, and corresponding kinetic parameters of HER are listed in the Table 6.1.

During the Cyclic Voltammetry (CV) study, a consistent observation was made regarding the gradual decrease in current responses with an increase in the number of cycles. Eventually, the current values reached a stable state near -1.6 V. This reduction in current density could be attributed to the resistance posed by the hydrogen gas formed on the cathode surface. The attainment of stable and reproducible CV curves towards the end suggests the establishment of equilibrium between the attached and detached hydrogen gas on the electrode surface *i.e.* a state of steady liberation of H_2 gas from the surface of cathode. The current density corresponding to this equilibrium is called cathodic peak current density, denoted by i_{pc} and the potential at which desorption of hydrogen gas started is called onset potential. From

the CV curves, shown in Figure 6.3, it may be noted that Ni-Ti alloy coating deposited at 4.0 A/dm^2 showed the highest cathodic peak current density with least onset potential for HER, compared to all other coatings.

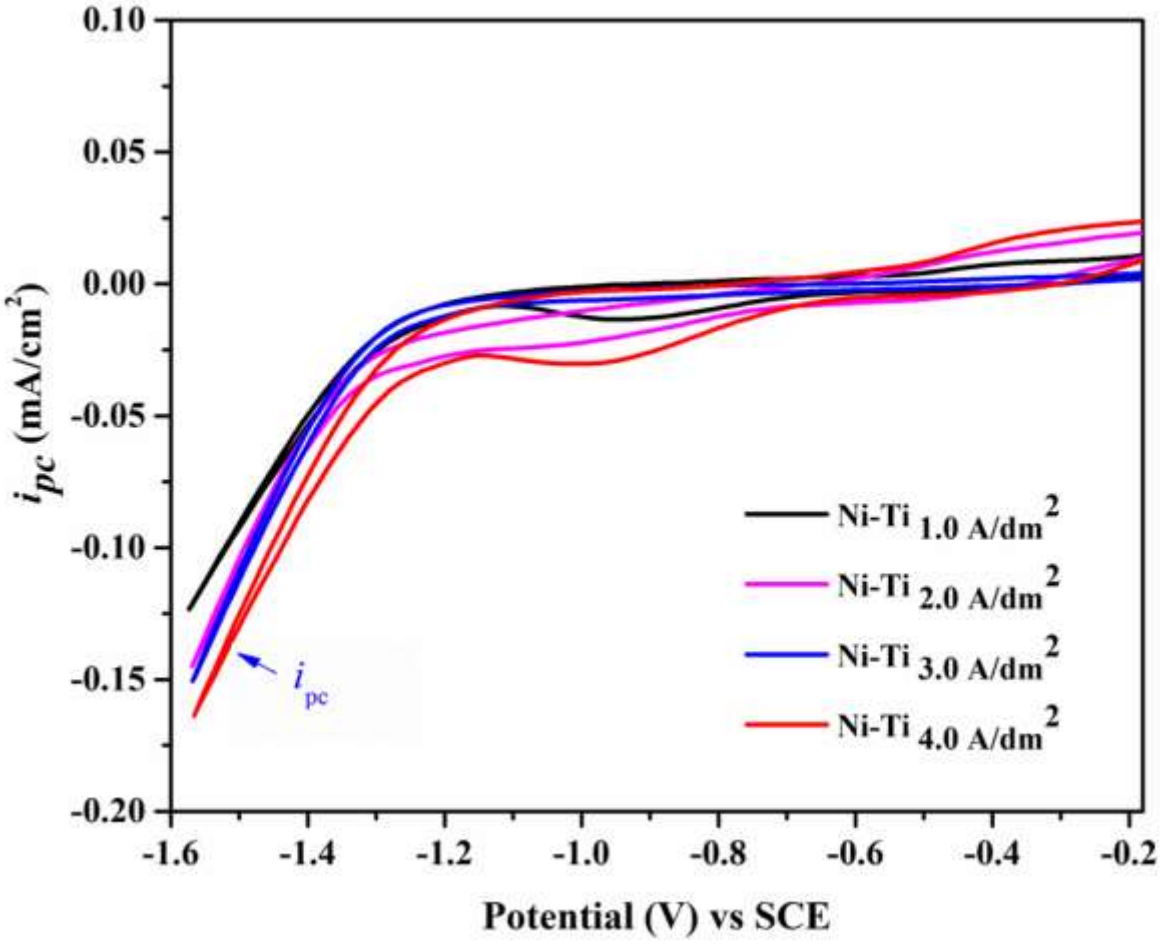

Figure 6.3 *– Cyclic voltammetry curves of HER of Ni-Ti coatings deposited at different current densities from the optimized bath*

Hence, it may be inferred that this particular coatings having Ni-Ti $_{4.0\ A/dm^2}$ configuration has the highest efficiency for HER. The highest efficiency of Ni-Ti $_{4.0\ A/dm^2}$ coatings for HER may be attributed to its highest Ti content, which is responsible for more number of active sites for evolution of hydrogen. It is important to note that the tendency of HER of alloy coatings bears a close relationship with its surface roughness. Hence, the highest efficiency of Ni-T i$_{4.0\ A/dm^2}$ coating towards HER, compared to all other coatings may be attributed to its highest roughness and porosity, as shown in Figure 6.2 (right). It was further evidenced by its highest average

roughness value as reported in Table 4.3. The average roughness value of Ni-Ti alloy coatings were found to be increased with deposition current density as shown in the Figure 6.2.

Figure 6.1- The electro-kinetic parameters for HER on the surface of Ni-Ti alloy coatings deposited at different current densities using same bath

Deposition current density (A/dm^2)	Ti content in the deposit (wt. %)	Cathodic peak c.d. (i_{pc}) ($mA\ cm^{-2}$)	Onset potential for H_2 evolution (V vs SCE)	Volume of H_2 Evolved in 300 s (cm^3)
1.0	0.81	-0.11	-1.20	9.4
2.0	1.40	-0.14	-1.23	10.6
3.0	2.32	-0.16	-1.27	11.2
4.0	3.50	-0.18	-1.30	11.9

ii) Chronopotentiometry

To examine the thermodynamic stability of Ni-Ti alloy coatings corresponding to different current densities, they have been subjected to chrono-potentiometry (CP) analysis. Chrono-potentiometric technique is basically monitoring the potential change as a function of time by applying a constant current between test electrode and reference electrode. The CP study was carried out by applying a constant current of 0.3 A on working electrode for a period of 1800 s. The CP behaviour of Ni-Ti alloy coatings corresponding to different current densities are shown in the Figure 6.4. The CP curves corresponding to all current densities demonstrated that there exists a sudden decrease of potential with time in the very beginning (before 5 seconds which is not seen in Figure 6.4), which eventually reached a steady state as shown in Figure 6.4. This sudden decrease of potential in the beginning of electrolysis is due to the attainment of equilibrium between H^+ ions in the solution and H_2 gas on the surface of cathode.

Here, it may be noted that Ni-Ti alloy coating at 4.0 A/dm^2 attained the steady state condition very quickly, compared to all other coatings. This behaviour confirms the fact that Ni-Ti coating at 4.0 A/dm^2 is electrocatalytically more active, and stable for HER. Hence it is better electrode material for HER. Further, the electro-catalytic behaviour of Ni-Ti coatings were evaluated quantitatively on the basis of the amount of hydrogen liberated for 300 s, on its surface. The quantity of hydrogen evolved on the surface of alloy coatings deposited at 1.0 A/dm^2, 2.0 A/dm^2, 3.0 A/dm^2 and 4.0 A/dm^2 is reported in Table 6.1, and same is shown in the

inset of Figure 6.4. Thus, the experimental data demonstrated that Ni-Ti $_{4.0\ A/dm^2}$ alloy coating is most favourable for HER, compared to coatings at other current density. In addition, CP study established the fact that Ni-Ti alloy coatings, deposited at 4.0 A/dm^2 is the most stable and efficient electrode material for HER, in compliance with CV study.

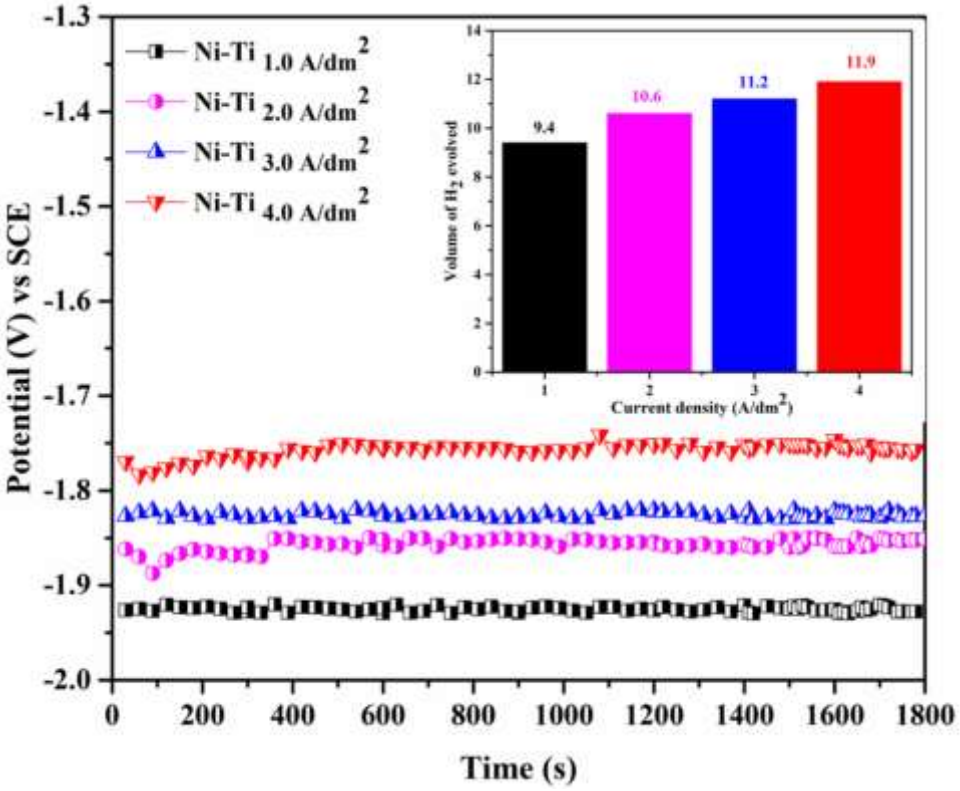

Figure 6.4 *- Chronopotentiograms for Ni-Ti alloy coatings deposited at different current densities. Given in the inset are volumes of H_2 gas liberated on their surfaces*

6.3.3.2 Oxygen Evolution Reaction

The electro-catalytic behavior of Ni-Ti alloy coatings at different current densities were tested for their efficiency for OER by using them as anode, in the same line as for HER. The experimental studies were carried out using CV and CP methods.

i) Cyclic voltammetry

The cyclic voltammetry technique has been employed to study the electro-catalytic behaviour of electrodeposited Ni-Ti alloy coatings, at different current densities. A potential window of 0 to 0.75 V, and a scan rate of 50 mV sec^{-1} for 20 cycles was used. The corresponding voltammograms are shown in Figure 6.5. From the graph, it is clear that Ni-Ti alloy deposited

at current density equal to 1.0 A/dm^2 showed the maximum peak anodic current density (i_{pa}) as shown in Figure 6.5. It demonstrates the fact that it has better OER activity compared to coatings at other current densities. The i_{pa} value is found to be decreased with the increase of deposition current density. Hence, it may be inferred that Ni-Ti $_{1.0\ A/dm^2}$ coating has highest efficiency for even OER.

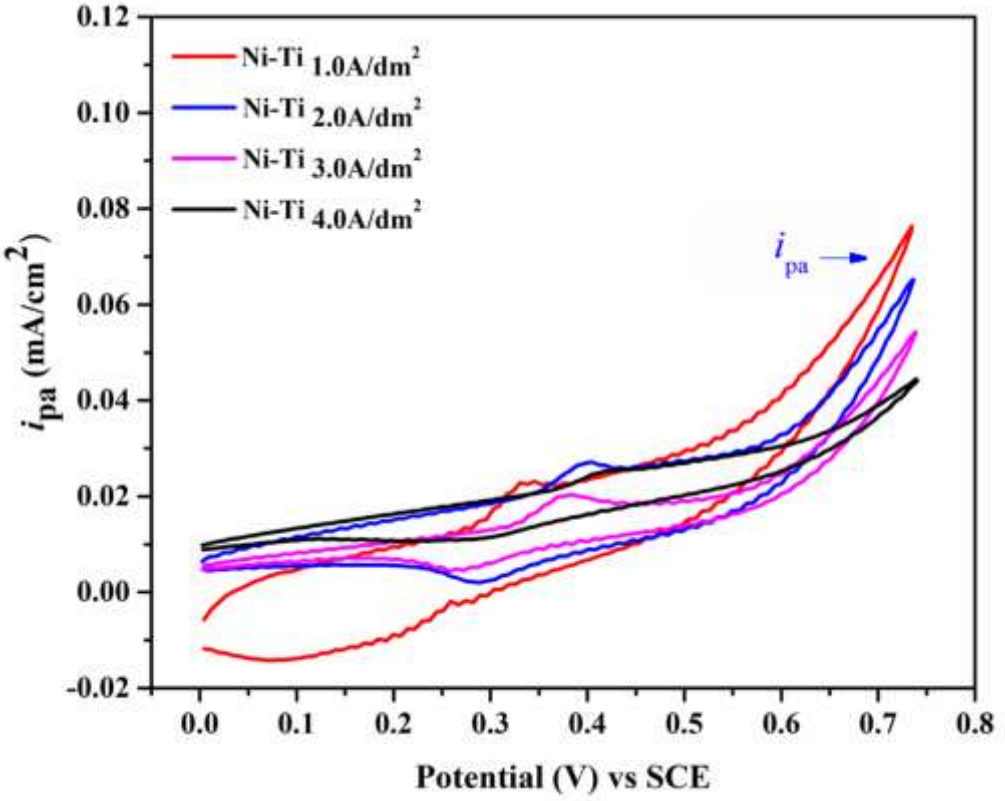

Figure 6.5 – *Cyclic voltammograms of OER on the surface of Ni-Ti alloy coatings deposited at different current densities*

ii) Chronopotentiometry

Chronopotentiometry (CP) study for evolution of OER on the surface of Ni-Ti alloy coatings were carried out at a positive current + 0.3 A cm^{-2}, and corresponding electrochemical responses are shown in Figure 6.6.

It may be observed that initially the potential has increased drastically, and then remained almost constant indicating the establishment of an equilibrium between adsorbed OH^- and liberated O_2. The amount of O_2 liberated in the initial 300 s on different coatings were measured, and is reported in Table 6.1. It may be noted that there is no significant change in

the volume of oxygen liberated with deposition current density. This is may be attributed to the small change in the composition of alloy coatings with current density, and inherent sluggish OER. However, from the volume of O_2 liberated, it may be noted that Ni-Ti $_{1.0A/dm^2}$ coating is more efficient for OER, than other coatings. The least wt. % Ti in Ni-Ti $_{1.0\ A/dm^2}$, supported by EDS study may be responsible for its better efficiency for even OER (Table 6.2).

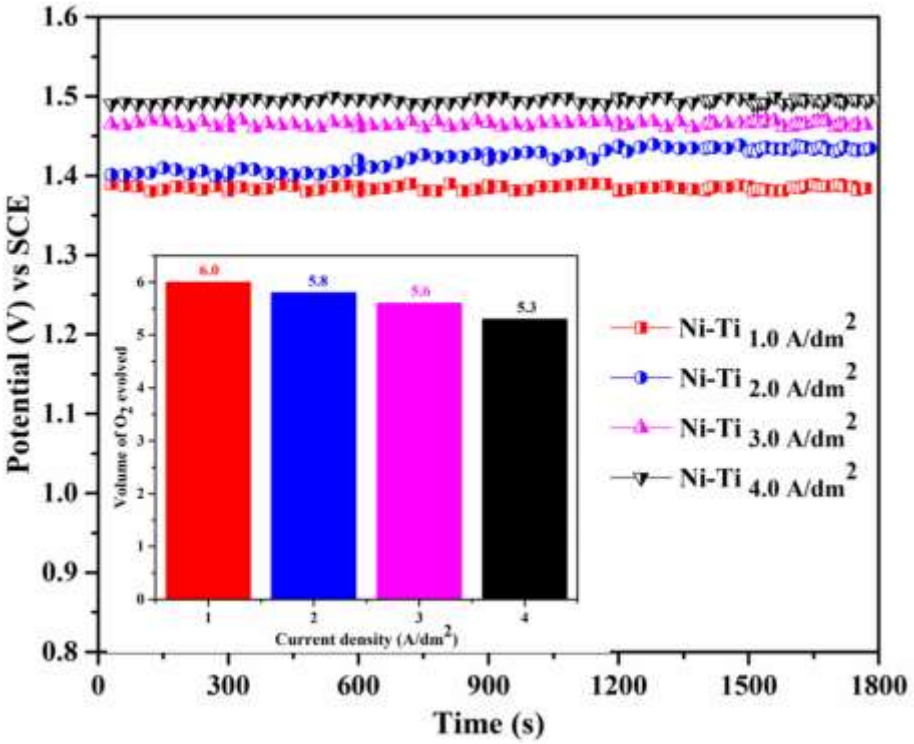

Figure 6.6 *- Chronopotentiograms of Ni-Ti alloy coatings deposited at different current densities showing different responses for OER*

Table 6.2- Electro-catalytic parameters for OER on the surface of Ni-Ti alloy coatings deposited at current densities

Deposition Current density (A/dm^2)	Ti content in the deposit (Wt. %)	Anodic peak c.d. (i_{pa}) ($mA\ cm^{-2}$)	Onset potential for O_2 evolution (V vs SCE)	Volume of O_2 Evolved in 300 s (cm^3)
1.0	0.81	0.077	0.36	6.0
2.0	1.40	0.063	0.22	6.8
3.0	2.32	0.052	0.19	5.6
4.0	3.50	0.044	0.15	5.3

Here, it is important to note that among different electrodeposited Ni-Ti alloy coatings studied, Ni-Ti $_{4.0\ A/dm^2}$ coating (having highest Ti content) is electro-catalytically highest active for HER; and Ni-Ti $_{1.0\ A/dm^2}$ coating (having least Ti content) is electro-catalytically highest active for OER. This inverse response of Ni-Ti alloy coating is due to the underlying reduction and oxidation processes on electrode surface during HER and OER, respectively.

6.4 EFFECT OF ADDITION OF SILVER NANO-PARTICLES

Guided by the literature that incorporation of nanoparticles into the electroactive alloy matrix can improve their electrocatalytic activity to large extent, Ag nanoparticles (<100 nm) were added into the bath (Table 4.1). The improvement in its electro-catalytic activity, in terms of its efficiency for HER have been tested, using it as cathode. The experimental study has been made and their catalytic efficiency and stability has been tested by studying their CV and CP study. Experimental results are discussed as below.

6.4.1 Development of Ni-Ti-Ag composite coating

The effect of addition of silver (Ag) nanoparticles on electro-catalytic activity of Ni-Ti-Ag nanocomposite coating has been tested, by adding a known amount of it into the bath solution. Ag-electrodeposited Ni-Ti coatings, represented as Ni-Ti-Ag composite were developed by conventional electrodeposition method, by adding known amounts of three different concentrations of Ag nanoparticles, like 0.5 g/L, 1.0 g/L and 2 g/L (Table 6.3). The electrolyte was stirred over night for uniform dispersion of Ag nanoparticles and for 15 minutes before every use. The Ni-Ti-Ag composite coatings were developed on the cross sectional area of mirror finished copper rod, having exposed surface area of 1 cm^2 as cathode; and graphite sheet as anode at an optimal deposition current density of 4.0 A/dm^2, using the same electrolyser. Here, it may be noted that current density of 4.0 A/dm^2 was selected as the deposition current density at which Ni-Ti alloy showed is highest electro-catalytic activity for HER as discussed in the Section 6.3.3.1. All other deposition conditions, like pH and duration of deposition are kept constant for comparison purpose. Here, Ni-Ti-Ag composite coatings are conveniently denoted as Ni-Ti-Ag_x, where X stands for the amount of Ag nanoparticles (in g/L) added into the optimized Ni-Ti bath.

Table 6.3 – Change in the wt.% of Ni, Ti and Ag in Ni-Ti-Ag composite coatings due to addition of varied amount of Ag nanoparticles into the bath, deposited at 4.0 A/dm^2

Coating configuration	Ni content in the deposit (wt. %)	Ti content in the deposit (wt. %)	Ag content in the deposit (Wt. %)	Volume of H_2 evolved in 300 s (cm^3)
Ni-Ti	96.50	3.50	-	11.9
Ni-Ti-Ag $_{0.5}$	94.90	3.12	1.98	12.2
Ni-Ti-Ag $_{1.0}$	93.68	3.28	3.04	13.6
Ni-Ti-Ag $_{2.0}$	94.28	3.18	2.54	12.5

6.4.2 Characterization Ni-Ti-Ag composite coating

As catalytic process is a surface phenomenon, and it depends on its very surface morphology. Hence, to explain the electro-catalytic behaviour of the Ni-Ti-Ag composite coating, they are subjected to surface and compositional analyses, like SEM-EDS, XRD and AFM study.

6.4.2.1 SEM-EDS Analysis

The microstructure of electrodeposited Ni-Ti-Ag composite coatings were analysed using SEM, and the corresponding SEM micrographs are shown in the Figure 6.7. A clear difference in the surface morphology of composite coatings may be seen, when they are deposited without, and with Ag nanoparticles (in different amounts). As seen in SEM images, the Ag nanoparticles were spread over the surface of the alloy coatings almost uniformly by giving almost rougher surface to earlier smooth Ni-Ti alloy coating. It may also be noted that the adsorption of Ag nanoparticles onto the Ni-Ti deposit results in the formation of granules at higher amount of Ag nanoparticles as shown in the Figure 6.6. Further, from the EDS analysis of Ni-Ti-Ag composite coatings, it was found that metals content of composite coating has changed due to the addition of Ag nanoparticles into the bath. Change of metals content in the composite coatings with different amount of Ag nanoparticles is shown in Table 6.3. From the composition data, it may be seen that incremental change in nano-Ag particle content in the bath resulted in the change of wt.% of both Ni and Ti in the deposit. The presence of wt.% of Ag confirms the incorporation of nano sized Ag particles onto the surface of substrate, alongside the coatings. Electro-catalytic study of Ni-Ti-Ag composite coatings revealed that

the addition of only 1.0 g/L of Ag nanoparticles into the bath has good effect on its electro-catalytic performance of HER.

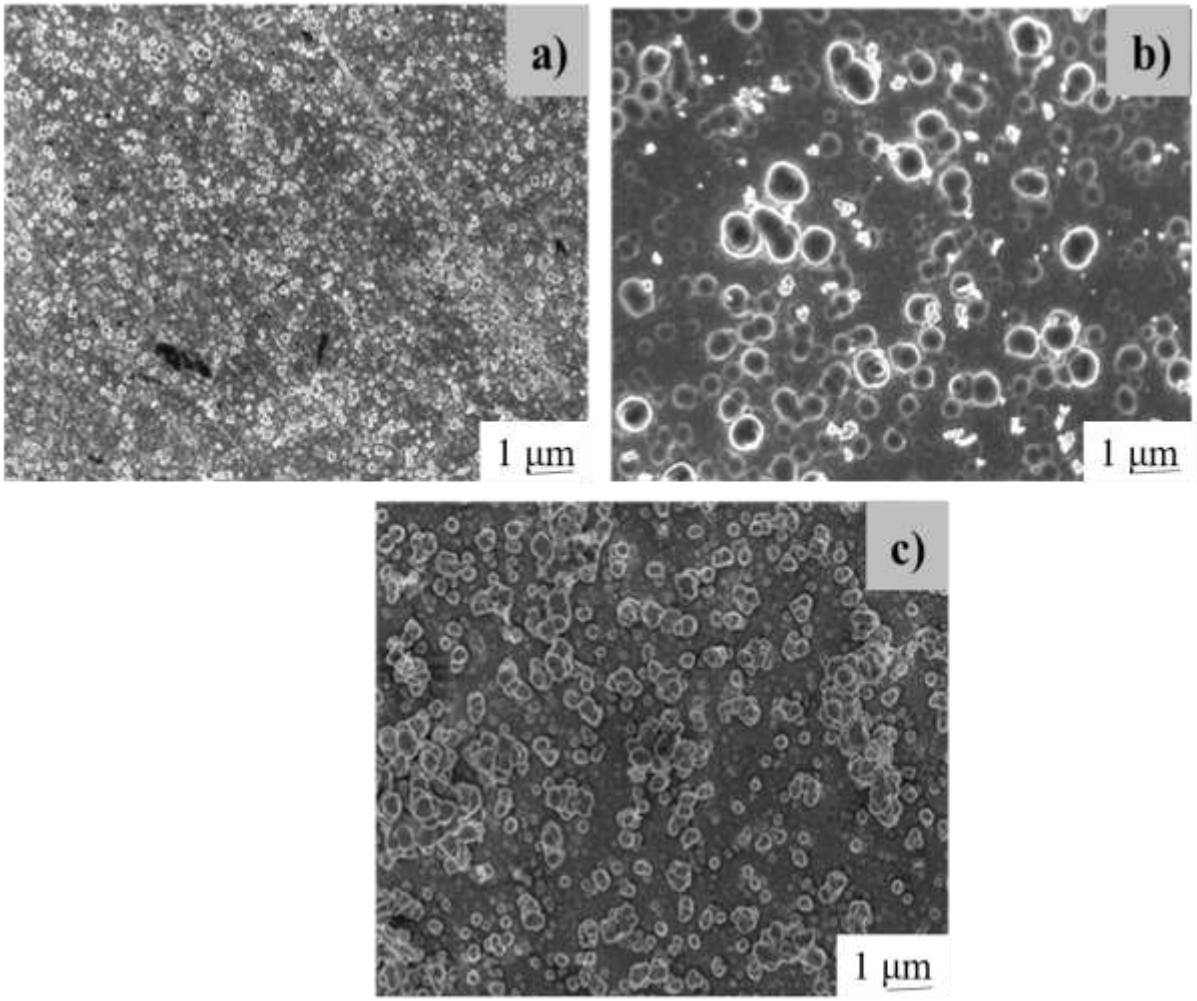

***Figure 6.7** - SEM image of Ni-Ti-Ag composite coatings developed under different conditions: (a) Ni-Ti-Ag $_{0.5g}$, b) Ni-Ti-Ag $_{1.0g}$ and c) Ni-Ti-Ag $_{2.0g}$*

6.4.2.2 XRD study

Crystallographic study of Ni-Ti-Ag composite coatings have been made in relation to that bare-Ni-Ti alloy coatings, and is shown in the Figure 6.8. It may be seen that there are no significant peaks corresponding to Ag is observed in the diffractograms. However, it may be noted that the position of the peaks remains unaltered, on addition of Ag nanoparticles into the alloy matrix, except the change in peak intensity. This change of peak intensity may be ascribed for

the change in the wt. % metal ions in alloy matrix, due to incorporation of Ag. Thus, increase in intensity of diffraction peaks corresponding to Ni of Ni-Ti-Ag composite coatings are corresponding to the slight increase of Ni, which increased with increase in concentration of Ag.

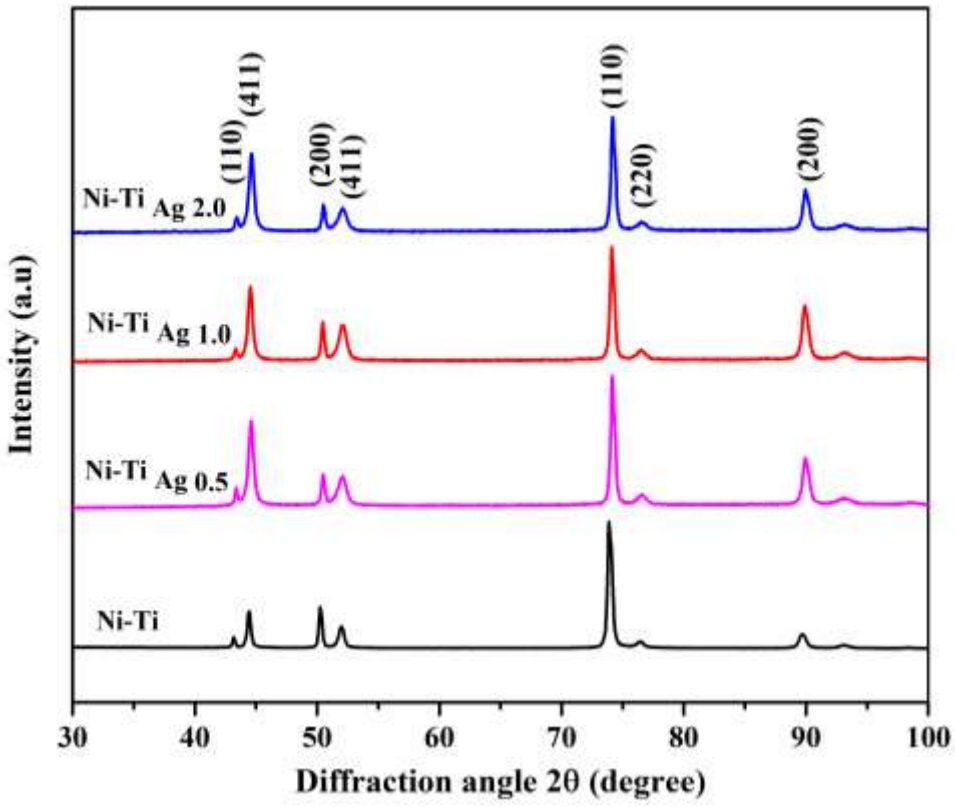

Figure 6.8 *- XRD of Ni-Ti alloy coatings under different conditions: Ni-Ti, Ni-Ti-Ag $_{0.5g}$, Ni-Ti-Ag $_{1.0g}$ and Ni-Ti-Ag $_{2.0g}$*

6.4.2.3 AFM Study

Surface roughness is considered to be an important parameter that influences HER of electrode materials. Accordingly, Atomic Force Microscopy (AFM) analysis was carried out for bare Ni-Ti and Ni-Ti-Ag$_{1.0}$ composite coatings to get valuable information about the surface properties, particularly surface average roughness. Figure 6.9 (a) and 6.9 (b), gives the AFM images for bare Ni-Ti and Ni-Ti-Ag$_{1.0g}$ composite coatings deposited at 4.0 A/dm^2, respectively. The surface roughness data, revealed that average surface roughness of bare - Ni-Ti alloy coating is increased from 32.08 nm 49.62 nm due to addition of 1.0 g of Ag nanoparticles into the bath. Thus, substantial improvement in the electro-catalytic efficiency

of Ni-Ti-$Ag_{1.0g.}$ composite coatings for HER, compared to bare Ni-Ti alloy coatings may be due to increased active sites and surface roughness of alloy coatings.

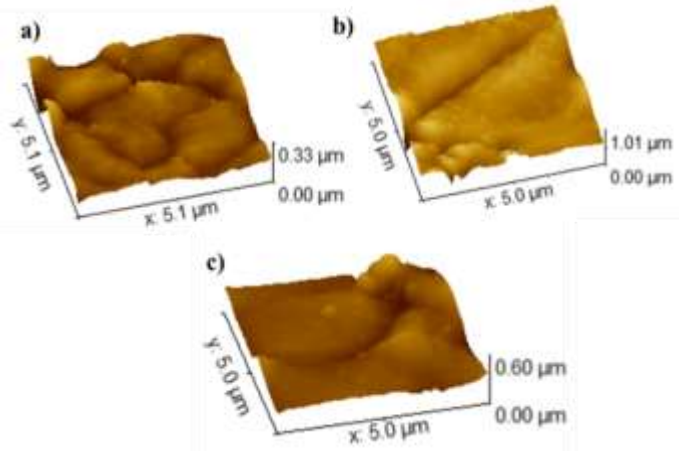

***Figure 6.9** – AFM image of Ni-Ti-Ag composite coatings developed under different conditions: Ni-Ti-$Ag_{0.5g}$, Ni-Ti- $Ag_{1.0g}$ and Ni-Ti-$Ag_{2.0g}$*

6.5 Evaluation of HER activity of Ni-Ti-Ag composite coatings

i) Cyclic voltammetry

Cyclic voltammetry technique was employed to understand the HER activity of Ni-Ti-Ag composite coatings, and their CV responses are as shown in Figure 6.10. From the value of cathodic peak current density (i_{pc}), it may be noted that among the composite coatings, Ni-Ti-$Ag_{1.0g}$ coating shows the highest efficiency of HER reactions.

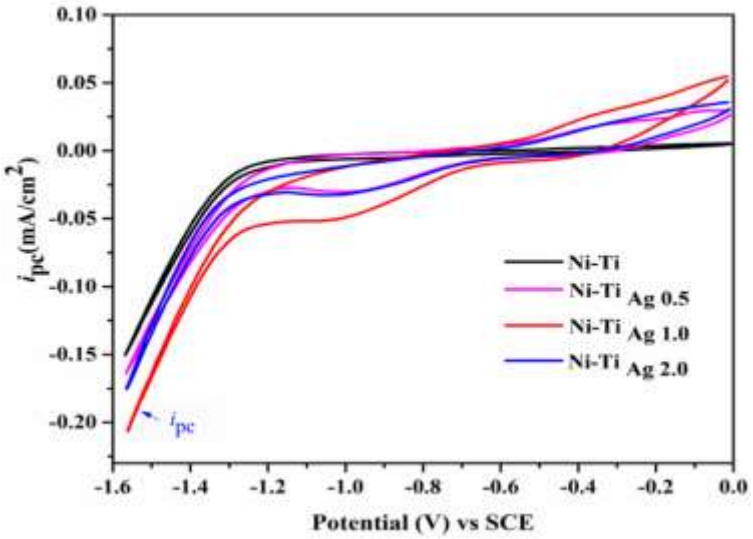

***Figure 6.10** – CV responses for HER activity of Ni-Ti and Ni-Ti-Ag composite coatings having varied concentrations of Ag- nanoparticles, developed at 4.0 A/dm^2*

ii) Chronopotentiometry

The chrono-potentiometry (CP) study of Ni-Ti-Ag composite coatings was made to test their thermodynamic stability, and ability to liberate oxygen on its surface. CP response of all composite coating in relation to its bare - Ni-Ti alloy coating was carried out at a positive current + 0.3 A cm^{-2}, and their corresponding electrochemical responses are shown in Figure 6.11. The CP study has been made by applying a constant current of -300 mA for a time interval of 1800 s, and the nature of their chrono-potentiograms are shown in Figure 6.11. From the data reported in Table 6.4, it may be noted that among Ag- nanoparticles added coatings, Ni-Ti-Ag $_{1.0g}$ alloy coatings highest efficiency for HER with having the highest i_{pc} and lowest onset potential values as shown in Figure 6.10.

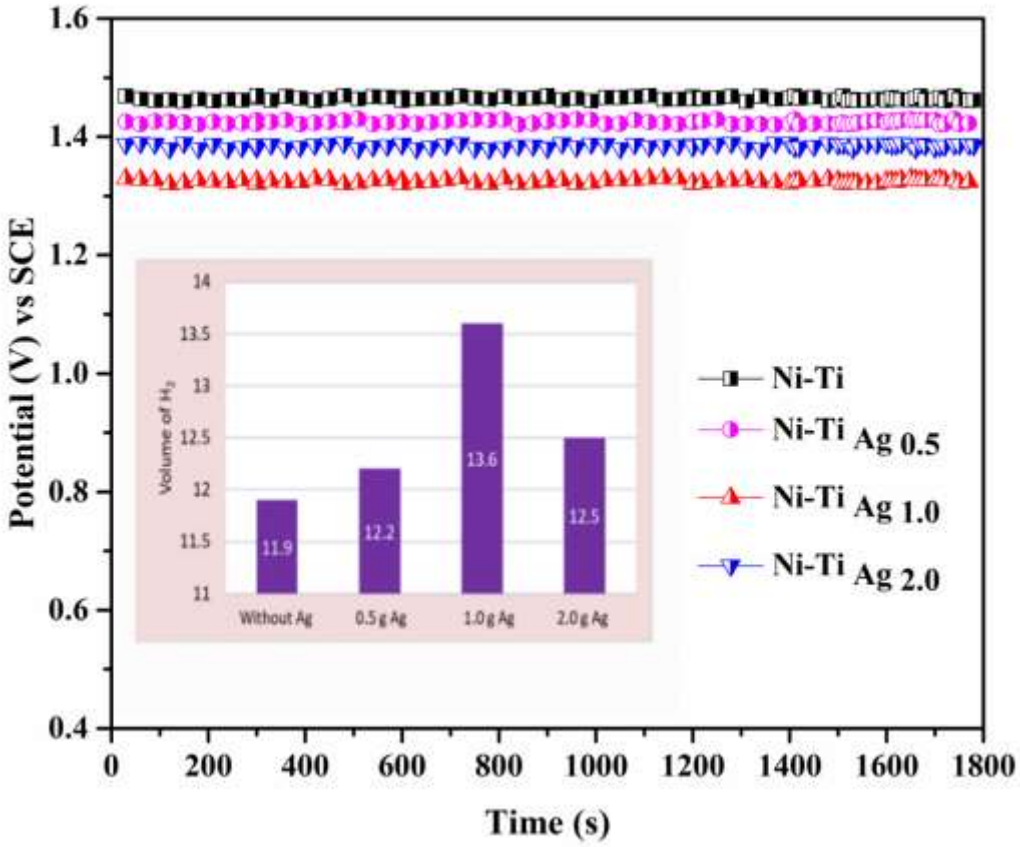

Figure 6.11 *- CP responses of Ni-Ti-Ag composite coatings for HER showing their electro-catalytic stability for 1800 s, and volume of H_2 gas liberated (in the inset) on the electrode surface at varied amount of Ag nanoparticles, in relation to Ni-Ti alloy coating. All coatings were deposited at 4.0 A /dm^2*

Table 6.4 – Electro-catalytic parameters of Ni-Ti-Ag composite coatings in different composition for HER alkaline water electrolysis

Coating configuration	Cathodic peak current density i_{pc} (mA cm^{-2})	Onset potential for H_2 evolution (V vs SCE)	Volume of H_2 Evolved in 300s (cm^3)
Ni-Ti-Ag $_{0.5}$	- 0.15	-1.29	12.2
Ni-Ti-Ag $_{1.0}$	- 0.20	-1.33	13.6
Ni-Ti-Ag $_{2.0}$	- 0.17	-1.31	12.5
Ni-Ti	- 0.14	-1.30	11.9

The value of cathodic peak current density (i_{pc}) and onset potentials for HER of all Ni-Ti-Ag composite coatings are reported in the Table 6.4, with the volume of H_2 gas evolved during initial 300 s. It may be seen that Ni-Ti-$Ag_{1.0}$ coatings showed the highest performance of HER, by liberating 13.6 cm^3 of H_2 gas in initial 300 s, compared to other coatings. Thus from the electro-catalytic study of Ni-Ti-Ag composite coatings, Ni-Ti-$Ag_{1.0}$ alloy coating is electrocatalytically more active for HER, than other coatings, it is supported by the highest volume of H_2 gas (13.6 cm^3) liberated during electrolysis, compared to bare- Ni-Ti alloy deposited at same current density. It may be attributed to the characteristic surface feature of the Ag-particles interposed composite coating of Ni-Ti alloy, as shown in Figure 6.7.

6.6. CONCLUSIONS

The electro-catalytic study of electrodeposited Ni-Ti alloy coatings for alkaline water electrolysis, and the effect of addition of Ag nanoparticles on its HER efficiency have been studied, and following conclusions have been arrived.

1. The Ni-Ti alloy coatings have been deposited at different current densities and their electro-catalytic study has been made by using them as electrode material as both cathode and anode, for HER and OER respectively.
2. The electro-catalytic performances were evaluated in 1.0 M KOH medium using electrochemical techniques such as cyclic voltammetry (CV) and chronopotentiometry (CP).
3. Quantitative measurement of H_2 and O_2 gases evolved at cathode and anode revealed that Ni-Ti alloy coatings, having high wt. % Ti (deposited at high current density) is good electrode

material for HER; and the one having low wt.% Ti (deposited at low current density) is good electrode material for OER, respectively, supported by CV and CP study.

4. Thus changed electro-catalytic activity of Ni-Ti alloy coatings, developed at different current densities were also attributed to their changed composition, integrated with changed surface morphology, and phase structures, confirmed through SEM, AFM, EDS and XRD analysis.

5. The observed small change of electro-catalytic response of Ni-Ti alloy coatings with deposition current densities is attributed to small change of its composition, linked to the obvious limitation of induced type of co-deposition prevailing in the bath.

6. Addition of Ag nanoparticles into Ni-Ti bath found to increase the electro-catalytic efficiency of both HER. It was observed that Ni-Ti-$Ag_{1.0}$ coatings showed the highest efficiency for HER. *i.e.* 13.6 cm^3.

7. The high electro-catalytic activity of Ni-Ti-Ag composite was found to be affiliated to the incorporation of Ag nanoparticles in the Ni-Ti alloy matrix, confirmed by SEM, EDS and AFM studies.

ELECTROCHEMICAL DEPOSITION OF Co-P ALLOY COATINGS AND THEIR CORROSION AND ELECTRO-CATALYTIC STUDIES

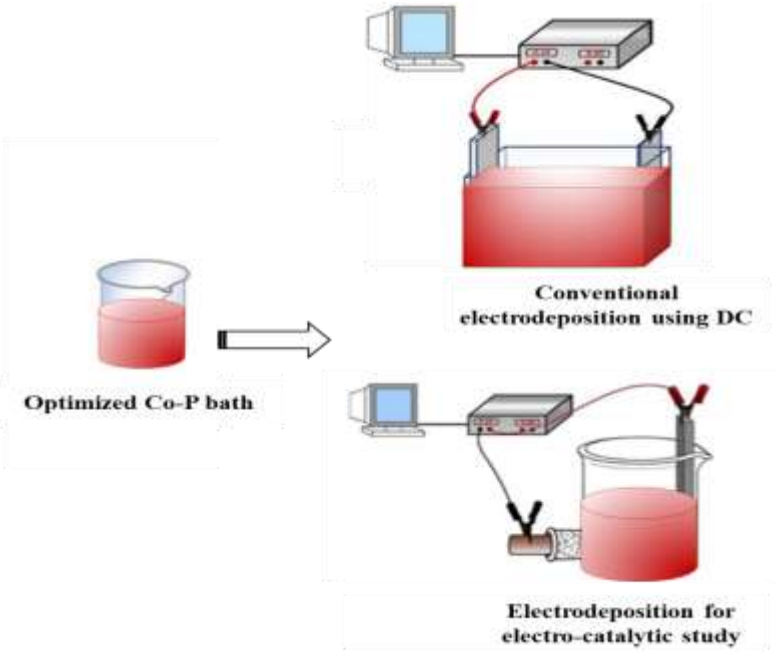

This chapter details the formulation of new electrolytic bath of Co-P alloy using glycine as the additive, through standard Hull cell method. The Co-P alloy coatings were deposited at different current densities using the optimized bath, and their corrosion behaviors were studied by electrochemical AC and DC methods. Further, electro-catalytic behavior of these coatings were studied, using them as electrode material for water splitting of hydrogen evolution reaction (HER) and oxygen evolution reaction (OER), respectively. An optimal current density has been proposed for electrochemical deposition of Co-P alloy coating for its highest performance against corrosion. The compositional change of alloy coatings with current density has been studied. The experimental results of investigation has been discussed using the evidences from SEM-EDS and XRD analyses. The effect of addition of Ag-nanoparticles into the bath on the electro-catalytic activity of HER has also been studied. The deposition conditions for best electro-catalytic activity of both Co-P and Co-P-Ag coatings were proposed, and results are discussed.

7.1 INTRODUCTION

Electrodeposition method of material development has numerous advantages, including precise control over the thickness and microstructure of the film, a low operating temperature, and a low cost. This method has the potential to create alloy and particle-reinforced composite coatings. The operational variables involved in electrodeposition, are like current control type, cathode current density, electrolyte pH, modulation of mass transport process, temperature etc. have a significant impact on the final properties of the deposit (Al-Bat'hi 2015). Cobalt (Co) and its alloys have been developed by different methods (Vicenzo and Cavallotti 2004), (Armyanov 2000), (Cavallotti *et al*. 2003) (Frieze et al. 1968), (Hono and Laughlin 1989) including through electrochemical deposition method. Electrodeposited cobalt-phosphorous Co-P alloy coatings have been investigated extensively for years, owing to their enhanced physical, chemical and magnetic properties. Due to these added properties, they are used as a corrosion and wear resistant material, alongside their use as soft magnetic materials for magnetic recording. Co-P alloy coatings were also used as good electro-catalysts for HER and OER in water electrolysis. Due to their excellent mechanical and wear-resistant properties, nano-crystalline Co and Co-based alloys have recently been identified as promising candidate to replace hexavalent-Cr plating (Hono and Laughlin 1989).

In recent years, there is a growing interest in the electrochemical deposition of Co-based alloys, due to their applications in both basic and applied research (Kosta et al. 2012). Among various binary alloy coatings, Co-P alloy coatings have been identified as suitable materials to replace environmentally unfriendly hard chromium. Due to impressive appearance, good corrosion and wear resistance of these coatings, they find extensive technological applications in industries. From the principle of alloy plating, it is well known that elements such as P, Mo and W cannot be electrodeposited by themselves independently from their electrolyte solution. However, these elements can be co-deposited with Fe-group metals, like Fe, Co, Ni and Mn. This phenomenon of co-deposition of reluctant metal with an Fe-group metal is called induced co-deposition, and the concept was first envisaged by Brenner (Brenner 1963a). Accordingly, Brenner and his co-workers developed many electrolytic baths, following induced co-deposition. They developed Co-P alloy coating, by co-depositing Co with reluctant metal, P and succeeded in resolving their obvious limitations of electro-less

plating such as the use of expensive reducing agent, a high operating temperature and difficulty in controlling the deposition rate. Thus, enormous number of publications on the electrodeposition of phosphorous alloys with Fe-group metals have already been reported (Shervedani and Lasia 1997), (Elias et al. 2016). (Armyanov 2000),(Barnett et al. 2012).

In this regard, research is being carried out in order to increase the production of renewable energy sources, which are more abundant and cleaner than fossil fuels (Cavallotti et al. 2003). There is an increasing demand of energy in the globe due to massive utilization of nuclear fossil fuels. Hydrogen is considered as a clean-burning fuel due to its high electrochemical reactivity, energy density (Elias and Hegde 2016), and wide availability and is regarded as one of the most beneficial alternatives to unsustainable fossil fuels. But the major problem with hydrogen is its less availability in pure form on earth atmosphere, but it is available in large quantity in combined form with oxygen, *i.e.* in the form of water. Water is the most abundant source for the production of hydrogen (H_2) and oxygen (O_2) by water electrolysis (Hono and Laughlin 1989), (Kanani 2006). Since water electrolysis is a very effective method for production of H_2 and O_2, and it can be achieved by development of proper electrode materials(Hono and Laughlin 1989). The main requisite of the effective electrode material is their lower over potential for hydrogen evolution reaction (HER) and oxygen evolution reaction (OER), as cathode and anode (Kosta et al. 2012). Owing to the fact that precious-metal based electro-catalysts have been found to be the best for the HER (Pt-based), and OER (Ru-based) electrode materials, and their widespread usage continues to be restricted due to its less availability and high cost (Li et al. 2018).

It has been reported that Ni, Co, Fe containing alloys/composites of non-precious metals, available at lower cost are emerged as good electro-catalysts for HER activity (Luo et al. 2016), (Pagliaro 2009). Due to their excellent mechanical and wear-resistant properties, nano-crystalline Co and Co-based alloys (Platatorres et al. 2007), (Pu et al. 2016), (Reddy et al. 2016) have recently been identified as promising candidate material for the replacement of hexavalent-Cr plating (Safavi and Walsh 2021). In recent years, there has been an interest in the electrochemical deposition of Co-based alloys due to both basic and applied research (Turner 2004). Among various binary alloy coatings, cobalt-phosphorous Co-P alloy coatings have been identified as suitable materials for replacing environmentally un-friendly hard

chromium. Appealing appearance, good corrosion, wear resistance, soft magnetic materials for magnetic recording and electro-catalysts for hydrogen evolution and oxidation reactions(Vicenzo and Cavallotti 2004), (Safavi and Walsh 2021) are the characteristic features of Co-P alloy coatings.

Keeping those unique properties of Co-P alloy coatings, a new electrolytic bath of Co-P alloy has been proposed. Co-P alloy coatings of high corrosion resistance have been developed on mild steel, using glycine as the additive. The current density, the driving force of electroplating has been used as tool to develop coatings of highest corrosion resistance. The compositional data, phase structure and surface morphology of alloy coatings corresponding various current densities were characterized using SEM, EDX and XRD techniques. The experimental results of investigations were correlated with the morphology, chemical and phase composition of the coatings. The work is mainly focused on the galvanostatic development of Co-P alloy coatings on mild steel at different current densities, and to optimize the current density for better corrosion protection of alloy coatings in 3.5% NaCl solution (to mimic the intense corrosion medium). The electro-catalytic performance of Co-P alloy coatings, and the effect of addition of Ag nanoparticles into the Co-P alloy matrix were studied. The electro-catalytic kinetic parameters of alloy coatings were evaluated using cyclic voltammetry (CV) and chrono-potentiometry (CP) study, and experimental results were discussed. The effect of Ag-nanoparticles on electro-catalytic performance for HER has been studied, and experimental results are discussed.

7.2 EXPERIMENTAL

A new Co-P alloy bath having cobalt chloride (Metal salt), sodium hypophosphate (Metal salt) When metal salt concentration is maximum, higher c.d. is often utilized for deposition to occur, which can lead to an increase in grain size. Further, reduced metal ion concentration decreases the grain size and leads to the formation of fine, adherent coating films, potassium sodium tartrate (Rochelle salt) acts as a complexing agent results in a fine-grained, and more adherent deposit. The main purpose of using the complexing agent in electroplating are: i) To make the deposition potential more negative, enabling plating to take place at a lower potential. ii) To prevent the passivation of anodes, allowing them to dissolve easily and improve current efficiency. iii) To enhance the throwing power of the plating bath. iv) To prevent the reactivity

of plating ions with the cathode metal, ammonium chloride acts as a supporting electrolyte which enhances the conductivity of the plating bath and glycine acts as a brightener, as bath constituents has been proposed. Individually, all chemicals were dissolved in double distilled water, then mixed thoroughly on stirring, to ensure complete dissolution. The pH of bath was maintained to be 8.5, using either dilute H_2SO_4 or NH_4OH, depending on the requirement using Micro-pH Meter (Systronics-362). The composition and operating variables were optimized for deposition of smooth, bright and uniform Co-P alloy coatings by conventional Hull cell method as reported elsewhere (Kanani 2006). The bath conditions and plating variables of optimal bath, arrived after Hull-cell experiment is reported in Table 7.1. Thin coatings of Co-P alloy have been accomplished on mild steel substrate using optimized bath in a 200 mL capacity cubic cell (made of PVC material). A direct current (DC) power source (DC Power Analyzer, Agilent N6705A, USA) was used to drive the process of electrodeposition. Mild steel plates having dimensions of (7.5 cm ×2.5 cm × 0.2 cm) were metallurgically polished to obtain a mirror finish and then degreased with trichloroethylene (TCE), as solvent. Conventional Co-P alloy coatings were accomplished by keeping anode and cathode parallel at distance of 5 cm.

Table 7. 1- The composition and operating variables of optimized Co-P alloy bath

Bath Ingredients	*Composition (g L^{-1})*	*Operating Variables*
Cobalt Chloride ($CoCl_2$)	13.2	Anode: Graphite
Sodium hypophosphate ($NaPO_2H_2$)	22.5	Cathode: mild steel
Potassium sodium tartrate (PST) ($KNaC_4H_4O_6.4H_2O$)	104.5	Temp: 303 K
Ammonium chloride (NH_4Cl)	49.5	pH: 8.5
Glycine (NH_2-CH_2-COOH)	4.4	Current density range: 1.0 - 4.0 A/dm^2

All depositions were carried out on same active surface area of (3.0 × 3.0 cm^2), keeping other part masked by means of cellophane tape at 303 K, pH = 8.5 for 10 minutes for comparison purpose. The polished substrate was electro-cleaned before plating, and then pickled in 0.5 M HNO_3. After deposition, coatings were rinsed multiple times with distilled water, and dried in hot air, and then desiccated until further testing. The anti-corrosion behavior

of all electrodeposited Co-P alloy coatings were studied by electrochemical AC and DC methods in 3.5% NaCl solution, to mimic aggressive corrosion environment. All electrochemical investigations of Co-P alloy coatings were carried out using a computer controlled electrochemical workstation, potentiostat/galvanostat (*Biologic SP-150, Biologic Science Instruments, France*), in a three-electrode cell by having the electrodeposited Co-P alloy as working electrode, platinum foil (having same surface area as active surface area of working electrode) as counter electrode, and saturated calomel electrode (SCE) as reference electrode. The electrochemical impedance spectroscopy (EIS) study was made using AC pulse of small amplitude (± 10 mV) in the frequency range of 100 kHz to 10 mHz. The corrosion rates (CR) of Co-P alloy coatings were evaluated by potentiodynamic polarization method in the potential window of ± 250 mV around open circuit potential (OCP) at a scan rate of 1 mVs^{-1}. The EIS response of different Co-P alloy coatings were used to find their polarization resistance (R_p) values, using Nyquist plots. The change of surface morphology and composition of alloy coatings with deposition current density were examined using Scanning Electron Microscope (SEM), interfaced with Energy Dispersion X-ray Spectroscopy (EDS) facility. The variation in the phase structure of alloy coatings with current density were analyzed through X-Ray Diffraction (XRD) techniques (Rigaku, Miniflex 600, with CuKα radiation having λ = 1.5418 Å, as the X-ray source).

7. 3 RESULTS AND DISCUSSIONS

Generally, in induced type of co-depositions, variations in the properties of electrodeposited alloy coatings with current density is quite unpredictable. Therefore, electrodeposition of Co-P alloy coatings was carried out using optimal bath at different current densities. *i.e.* from 1.0 A dm^{-2} to 4.0 A dm^{-2}. Co-P alloy coatings corresponding to different current density are first characterized for their basic properties, like, composition, surface morphology, and phase structure and corrosion resistivity.

7.3.1 Compositional analysis

The change in composition of electrodeposited Co-P alloy coatings with current density was analyzed, in terms of their Co and P content in the deposit, and are reported in Table 7.2. From the composition data, it may be noted that Co content of the deposit decreased and with

increase of current density. Variation in the wt. % of Co and P in the deposit with current density, in relation to their content in the bath is shown in Figure 7.1. The composition reference line (CRL) corresponding to the wt. % of Co and P in the bath (based on the weight of salt in the bath) is shown by horizontal perforated lines. Thus, it may be noted that wt. % of Co in the deposit is much higher than that in the bath, whereas wt. % of P is much lower than that in bath. Further, a small change in the wt. % of both metals (Co and P) with current density was found as shown in Figure 7.1. This marginal change of metal contents in the deposit with current density is due to undergoing induced type of co-deposition. It may be recalled that in induced type of co-deposition effects of the plating variables (current density, stirring, temperature etc.) on the composition of the alloys are more vagarious and unpredictable than the effects on the composition of alloys of any of the other types of co-deposition.

Table 7. 2 - Change of composition and corrosion rates (CR) of Co-P alloy coatings with current density deposited from optimized bath

Deposition Current density (A/dm^2)	Co content in the deposit (wt. %)	P content in the deposit (wt. %)	Thickness of coating (μm)	- E_{corr} (V vs. SCE)	i_{corr} (μA cm^{-2})	CR ($\times 10^{-2}$ mmy^{-1})
1.0	93.8	6.2	6.0	-529.9	28.9	34.9
2.0	92.7	7.3	8.2	-527.1	35.6	43.7
3.0	92.6	7.4	10.3	-576.4	36.9	45.2
4.0	91.3	8.7	12.0	-540.0	37.5	46.5
In the bath	36.6	66.4				

It may be recalled that in induced type of co-deposition effects of the plating variables (current density, stirring, temperature etc.) on the composition of the alloys are more vagarious and unpredictable than the effects on the composition of alloys of any of the other types of co-deposition (Brenner, 1963).

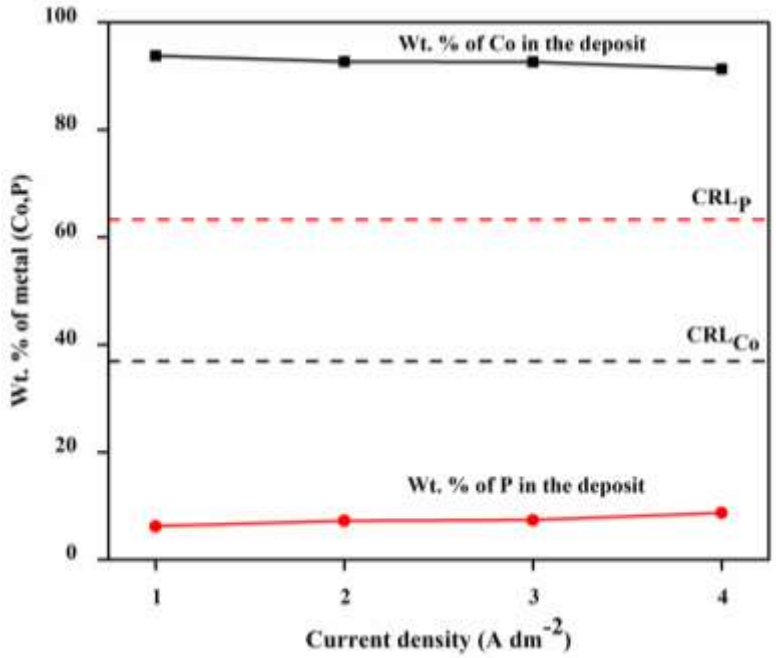

Figure 7.1- *Variation in the wt. % of Co and P in Co-P alloy coatings with change of current density. The composition reference line (CRL) corresponding to wt. % of Co and P in the bath is shown as horizontal perforated line*

7.3.2 Surface morphology

It may be seen that the surface feature of Co-P alloy coatings obtained at different current densities are characterized by the presence of crack, with few spheroids on its surface. It is important to note that these cracks of specific patterns are characteristic feature of binary alloys of Fe-group metals with Co and P. The characteristic cracks having specific patterns were found to grow with increase of current density. The cracks of Co-P alloy coatings may be attributed to hydrogen embrittlement, affected due to simultaneous liberation of H_2 on cathode during deposition. Accordingly, as the current density is increased, liberation of H_2 on the surface of cathode has also been increased. This increased liberation of H_2 on cathode, has resulted in increase of the depth and width of micro-cracks, evidenced by SEM micrographs as shown in Figure 7. 2.

The microstructure of Co-P alloy coatings deposited at different current densities are shown in Figure 7. 2. From the surface morphology of alloy coatings deposited at current density from 1.0 A/dm^2 to 4.0 A/dm^2, one can make out that current density has significant role on the process of and pattern of electrodeposition.

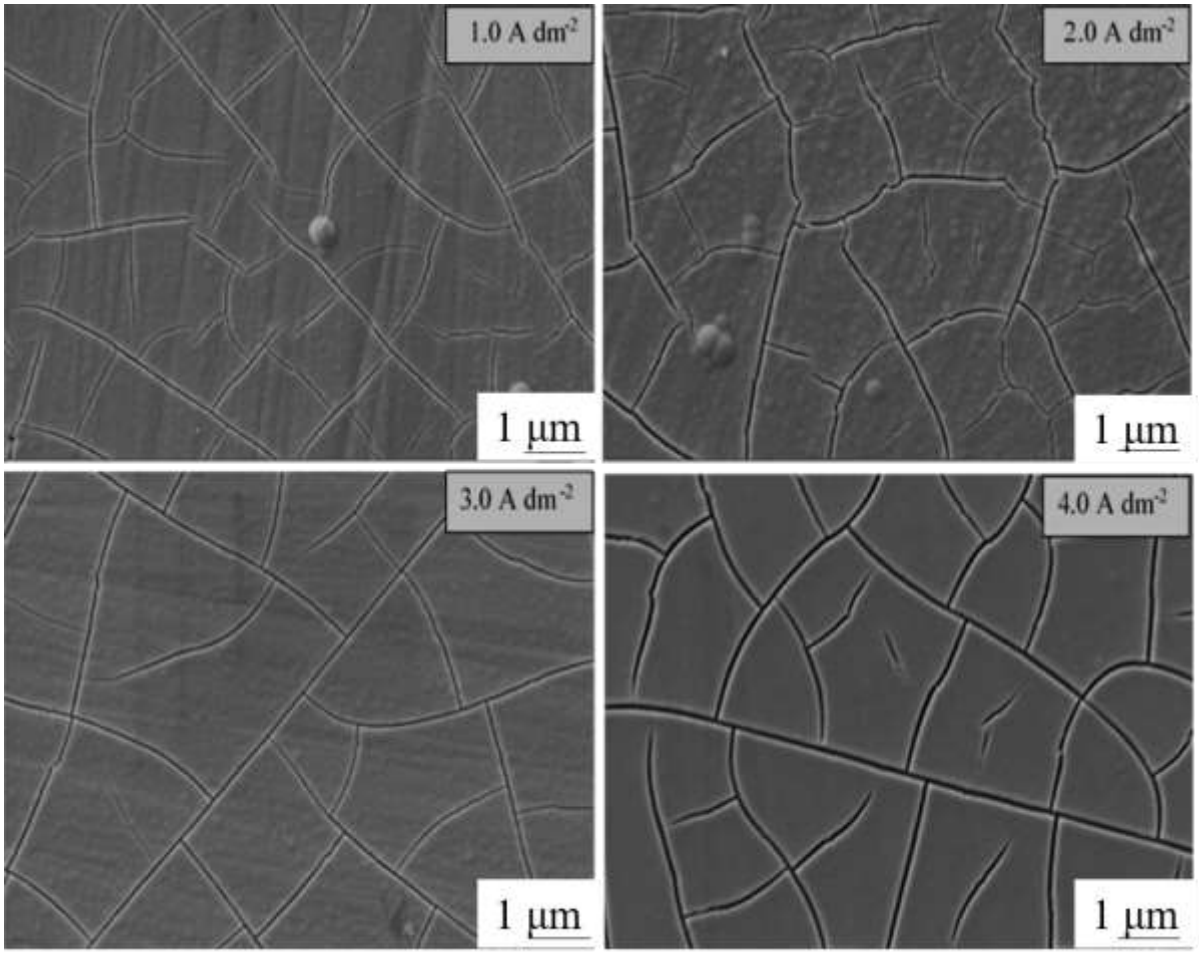

Figure 7. 2 - *Micrograph of Co-P alloy coatings showing dependency of deposition current density on surface morphology of deposits. A characteristic cracks having specific patterns, found growing with increase of current density may be seen*

7.3.3 AFM Study

The surface roughness is an equally important factor to influence the properties of alloy coatings. Hence, the surface topography of electrodeposited alloy coatings are studied using three dimensional Atomic Force Microscopy (AFM) technique. Accordingly, the AFM image of Co-P alloy coatings, deposited at 1.0 A/dm^2 and 4.0 A/dm^2 are shown in the Figure 7.3.

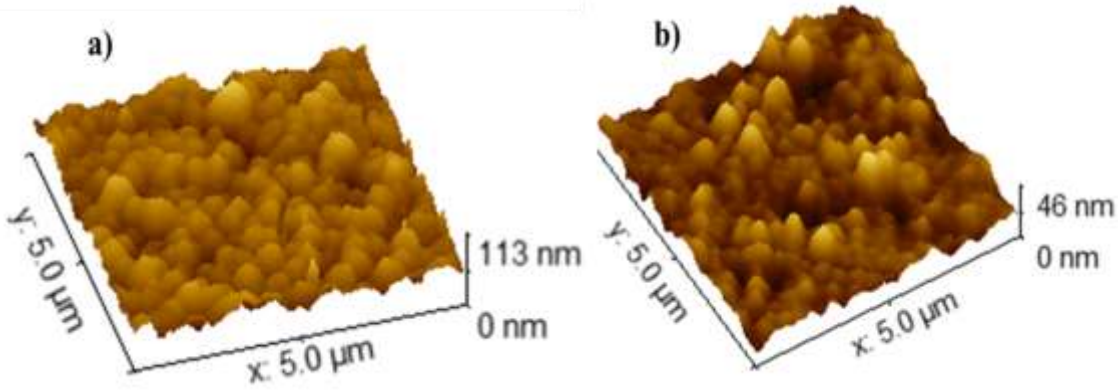

Figure 7. 3 *- The AFM image showing the topography of Co-P alloy coatings deposited from the optimized bath at: a) 1.0 A/dm^2, b) 4.0/dm^2*

The topographical information of any coatings may be carried out by measuring their average roughness (R_a) and root mean square roughness (R_q) values (Ashraf et al. 2016). Accordingly, R_a and R_q values of electrodeposited Co-P alloy coatings corresponding to 1.0 A/dm^2 and 4.0 A/dm^2 are measured, considering their 5 µ m × 5 µ m surface area, and those experimental data are reported in the Table 7.3. It may be seen that the surface smoothness of Co-P alloy coatings decreased with current density as supported by AFM images shown in Figure 7.3.

Table 7.3 - The surface roughness data of Co-P alloy coatings developed at different current densities, using optimized bath

Coating configuration	*R_q (nm)*	*R_a (nm)*
Co-P $_{1.0\ A/dm^2}$	9.6	7.5
Co-P $_{4.0\ A/dm^2}$	5.4	4.1

7.3. 4 X-Ray diffraction study

The X-ray Diffraction (XRD) technique was employed to analyze the phase structure of Co-P alloy coatings deposited at various current densities, ranging from 1.0 A dm^{-2} to 4.0 A dm^{-2}. The characteristic XRD peaks of the Co-P alloys are illustrated in Figure 7.4. The XRD peaks at 2θ = 43.3°, 50.4°, 73.9° and 89.7° represents the phase angles of Co-P alloy coatings, corresponding to the planes (111), (200), (110), and (200), respectively. It may be seen that

intensity of peaks corresponding to different scattering angles remained to be almost constant even with change of current density. This stands for the reason that change of composition of alloys is minimal with current density, and is supported by composition data in Table 7. 2. It may also be seen that phase angles corresponding to different reflections of all coatings remains constant regardless of the current density at which they are deposited. This constancy of phase angles of Co-P alloy coatings corresponding to different current densities indicates the formation of solid solution of Co with P (Li et al. 2018).

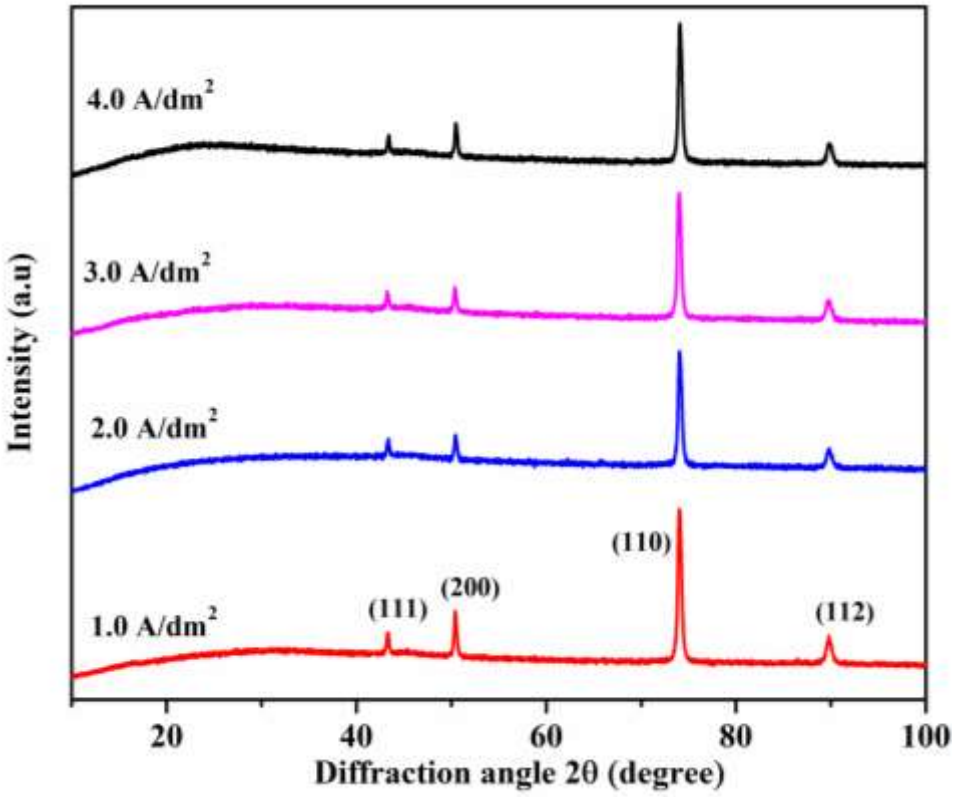

Figure 7.4 *- X-ray diffraction peaks of Co-P alloy deposited at different current densities from optimal bath. Constancy of phase angles of coatings corresponding to different current density indicate the formation of solid solution of Co with P*

7.3.5 Corrosion study of Co-P alloy coatings:

The electrochemical corrosion behavior of Co-P alloy coatings was examined using Electrochemical Impedance Spectroscopy (EIS) and potentiodynamic polarisation techniques, and the experimental results are reported below.

i) EIS Study

EIS technique can be used as a powerful tool to explore information with regard to the electrode processes such as double layer capacitance, solution resistance and polarization resistance etc. The best adaptable tool for studying the corrosion behavior of electrodeposited coatings is the Nyquist plot. This basically consists of studying the impedance (AC resistance) over a range of frequency, on passing AC current of small amplitude (Yuan et al. 2010). In popular Nyquist plots, impedance (Z) is represented as complex number, having real impedance part (Z') and imaginary impedance part (Z"), and such representation is provided with provision to distinguish the contribution of polarization resistance (R_p) verses solution resistance (R_s) of a test electrode (Hegde and Rao 2014). Accordingly, Nyquist plots of Co-P coatings deposited at different current densities are shown in Figure 7.5.

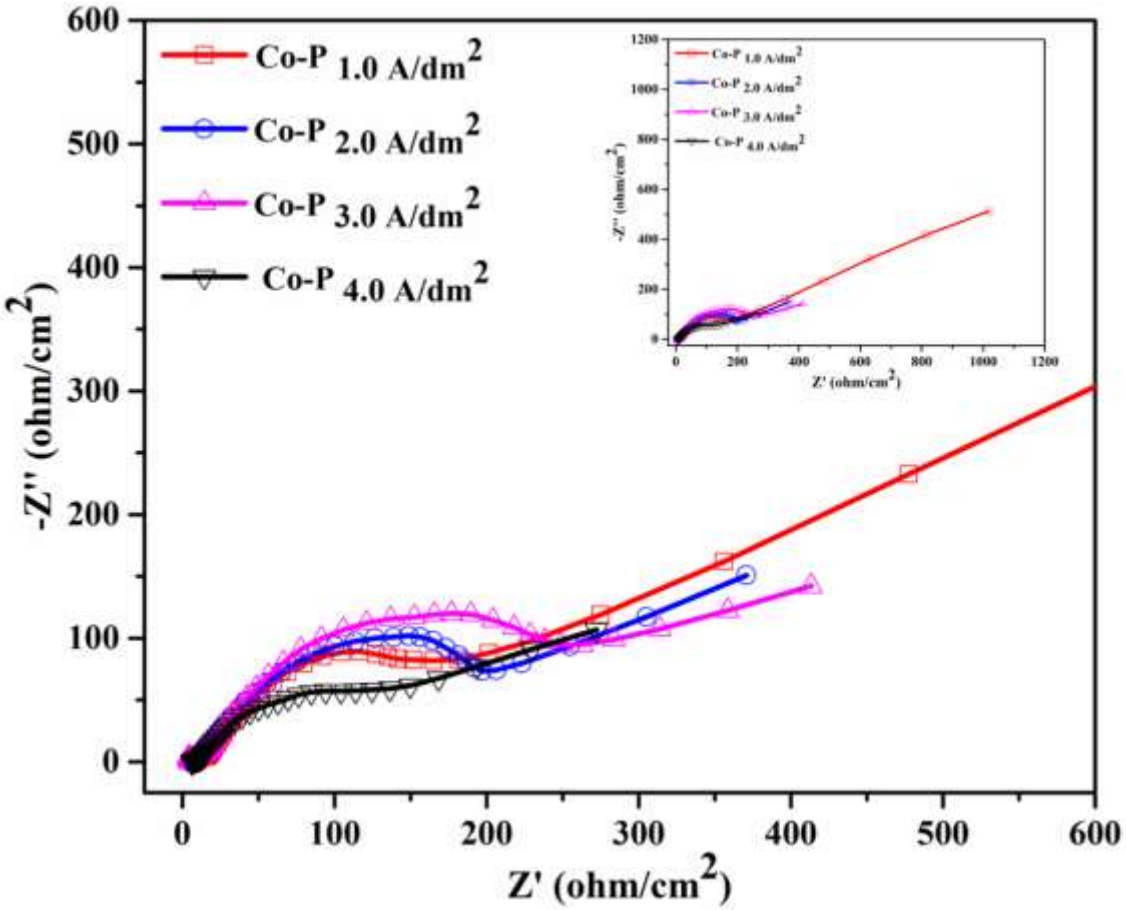

***Figure 7.5** - Nyquist plots of Co-P coatings deposited at different current densities. Highest polarization resistance (R_P) of Co-P coating corresponding 1.0 Adm^{-2} may be seen, compared to other coatings. In the inset is given impedance spectrum of all coatings in full scale*

It may be noted that impedance responses of Co-P alloy coatings decrease with increase of deposition current density. In other words, polarization resistance (R_P) value of coatings decreased with current density. Change of impedance corresponding to the different Co-P alloy coatings in full scale is shown in the inset of Figure 7. 5. Thus, on the basis of highest (R_P) value of Co-P coating corresponding to 1.0 A/dm^2, it may be inferred that it is the most corrosion resistant coatings compared to all other coatings.

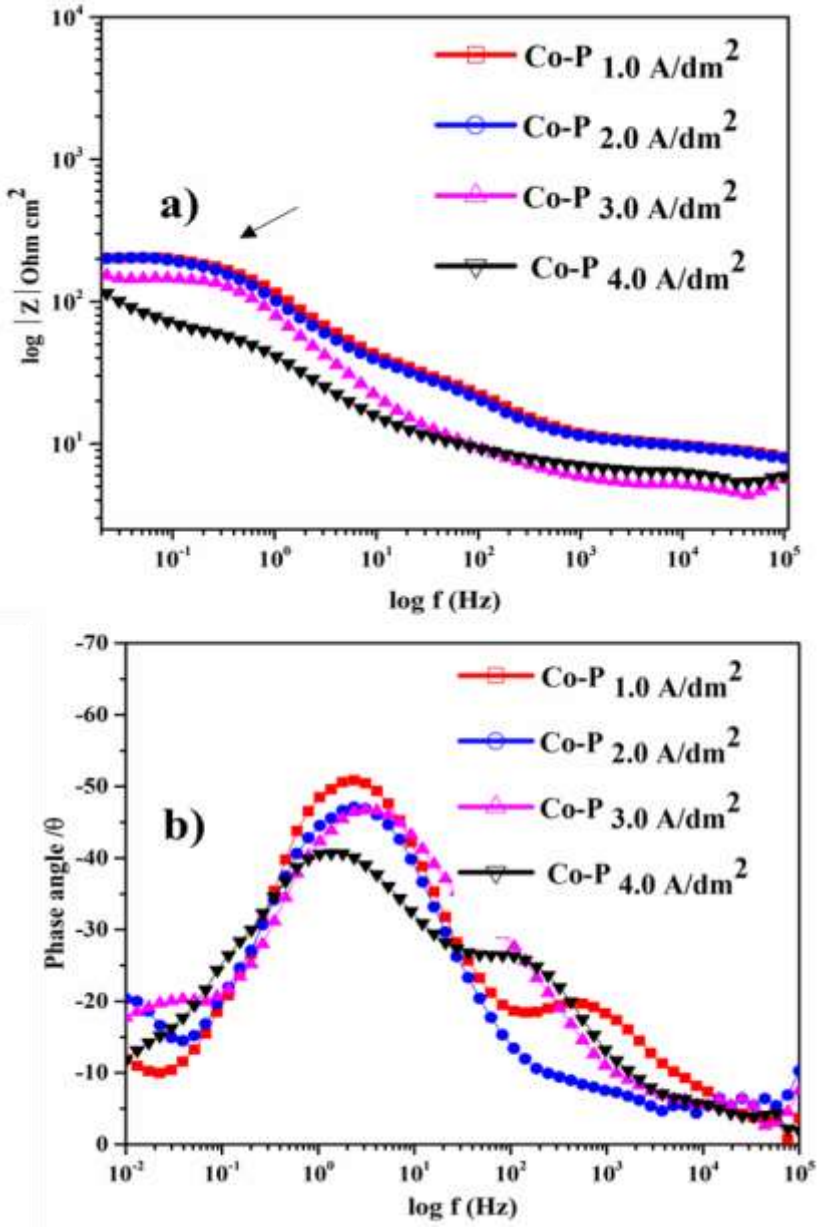

Figure 7.6 - *Bode's magnitude and phase angle plots of Co-P alloy coatings corresponding different current density shown respectively in (a) and (b), demonstrates that Co-P $_{1.0\ A/dm^2}$ coating is the most corrosion resistant than all other coatings*

Bode's plot is an alternative representation of the impedance in terms of the frequency represented directly along the X-axis. There are two types of Bode diagram, called magnitude plot (log |*Z*| *vs* log *f*) and phase angle plot (phase angle (θ) vs log *f*), describing the frequency dependencies of the |*Z*| and phase, respectively. A Bode plot is normally depicted logarithmically over the measured frequency range because the same number of points is collected at each decade. Accordingly, Bode's magnitude and phase angle plot of all Co-P alloy coatings are drawn and are shown in Figure 7. 6. The highest value of log |Z| at lower limit of frequency recorded by Co-P $_{1.0\ A/dm^2}$ alloy coatings, shown in Fig 7.6 (a) endorses the fact that it is the most corrosion resistant compare to all other coatings. It is evidenced further by Bode's phase angle (θ) plot shown in Figure 7. 6 (b). It may be noted that Co-P $_{1.0\ A/dm^2}$ coating is more capacitive in nature with highest negative phase angle, compared to other coatings.

ii) Potentiodynamic polarization study

The corrosion behavior of Co-P alloy coatings was evaluated quantitatively by potentiodynamic polarization method. The potentiodynamic polarization behavior of Co-P alloy coatings deposited at various current densities are shown in Figure 7.7, and their corresponding corrosion data are reported in Table 7. 2.

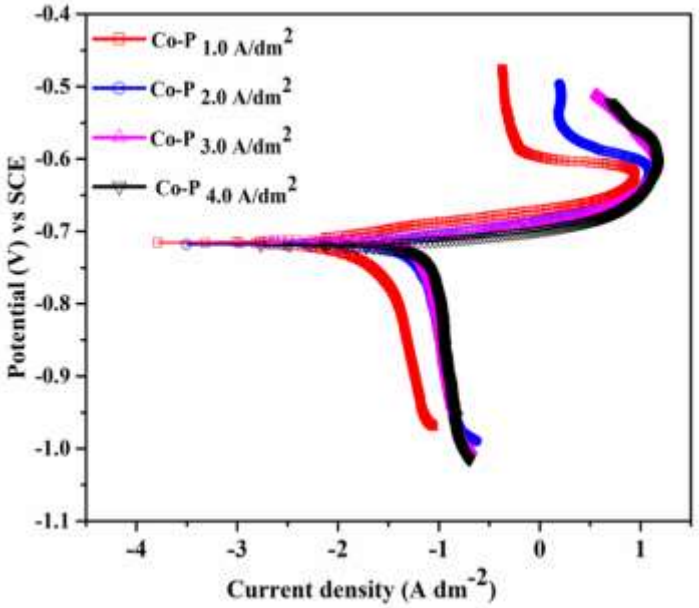

***Figure 7.7** - Potentiodynamic polarization behavior of Co-P alloy coatings deposited at different current densities deposited from the same bath*

From the corrosion rate values reveals that Co-P alloy deposited at 1.0 A/dm^2 is the most corrosion resistant, compare to all other coatings, and is in compliance with the trend established through EIS study. From the nature anodic polarization curve of all coatings, shown in Figure 7.7, it may be pointed out that Co-P alloy coating continue to dissolve rapidly in the beginning, and then forms passive film at higher potential. This indicates to propose that better corrosion protection of Co-P alloy coatings is due to formation of corrosion product to act as barrier between coating and corrosion medium, and it is more in case of coating at 1.0 A/dm^2. Thus, it may be summarized that among the Co-P alloy coatings deposited at different current density, Co-P alloy corresponding to 1.0 A/dm^2 is the most corrosion resistant, and is attributed to its highest noble metal (Co) content. Further, small change in corrosion rates of alloy coatings with current density is due to marginal change in its composition.

7.3.6 Cyclic polarization study

The highest corrosion resistance exhibited by Co-P alloy coating, deposited at 1.0 A/dm^2 was tried to understand better by cyclic polarization study in a potential ramp from -1.0 V to 0.1 V, and is shown in Figure 8. In the forward scanning, the value of current increased from negative to positive, which showed that the oxidizing reaction of passivation film occurred with increasing potential. During backward scanning, the value of current decreased from positive to negative, indicating that reduction reaction of the high valence oxide in the passivation film occurred with the falling potential. It may be noted that in the range of - 0.1 V to - 0.6 V, the current of backward scanning is higher than that of the forward scanning (it may be seen at a given potential shown by horizontal line in Figure 7.8), indicating that the dissolving of oxide film has better corrosion protection compared to the alloy coatings. In addition, E_{corr} value corresponding to corrosion product is found to be shifted to higher (nobler) value compared to that of electrodeposited alloy as seen in Figure 7.8.

It indicates that the corrosion product by being nobler acts as a barrier, and gives better protection to the substrate. Thus cyclic polarization study demonstrates that very high corrosion stability of Co-P alloy coating deposited at 1.0 A/dm^2 is due to the inhibition effect of corrosion products formed on the electrode surface, where they act as barrier between metal and the medium.

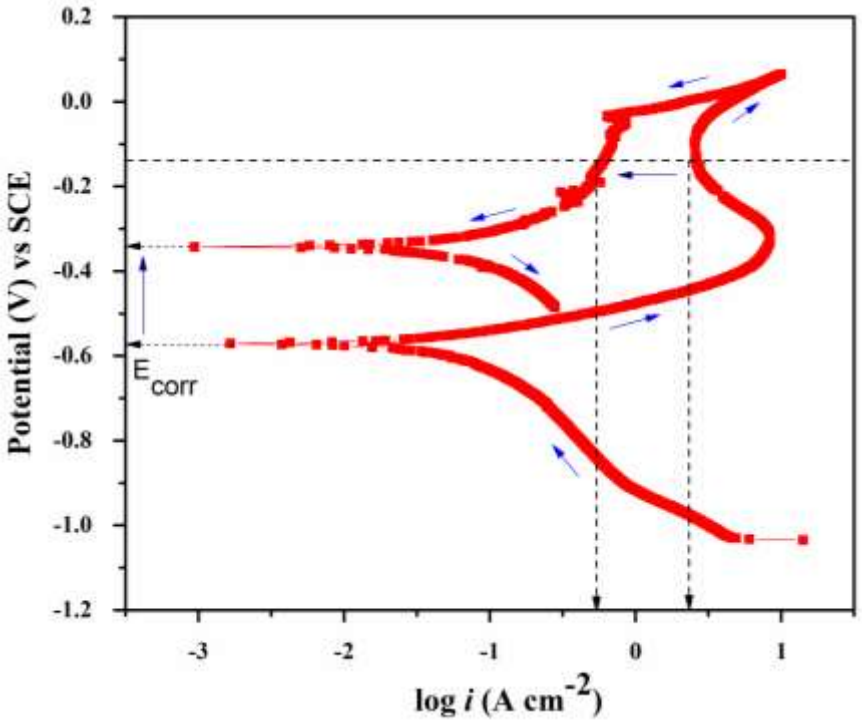

Figure 7.8 *- Cyclic polarization behavior of Co-P alloy coating deposited at 1.0* A/dm^2. *Decreased current corresponding to corrosion product of at given potential indicates the better corrosion stability of Co-P alloy coatings is due to barrier protection of corrosion product*

7. 4 Development of Co-P-Ag composite coatings

The effect of addition of Ag-nanoparticles on the electro-catalytic efficiency of bare-Co-P alloy coatings was tried to study, by adding known quantities Ag-nanoparticles into the bath. The electro-catalytic study of water electrolysis for both HER and OER of Co-P alloy coating revealed that coating corresponding to 1.0 A/dm^2 is the most electro-catalytically the active, with having maximum efficiency for HER and OER. Based on the above fact, it was tried to increase the efficiency of Co-P alloy coatings by adding Ag-nanoparticles in different quantities. This is done by dispersing Ag nano-powder (having particle size <100 nm, procured from Sigma-Aldrich) into the optimized Co-P bath (Table 7.1), in three different quantities. They are 0.5 g L^{-1}, 1.0 g L^{-1} and 2.0 g L^{-1}. The Ag-nanoparticles were added into electrolyte solution, and was kept for agitation overnight, under ultrasonic agitation. The electro-deposition of Co-P-Ag composite coatings were made on copper strip at 1.0 A/dm^2. *i.e.*, optimal current density of the bath. For convenience, Co-P-Ag composite coatings were

represented as Co-P-Ag $_x$, where 'x' stands for the amount of Ag nanoparticles added into the bath.

7.4.1 Evaluation of electro-catalytic activity of Co-P coatings

The electro-catalytic activity of Co-P alloy coatings, from the optimized bath (Table 7.1) electrodeposited at different current densities were subjected to electro-catalytic study by using them as cathode and anode for evaluating their efficiency for hydrogen evolution reaction (HER) and oxygen evolution reaction (OER), respectively in 1.0 M KOH solution. Experimental observations are recorded as below.

7.4.2 Electro-catalytic study

i) Cyclic Voltammetry Study:

The cyclic voltammetry (CV) technique has been employed to investigate electron transfer-initiated chemical reactions, particularly in catalysis. The study focused on Co-P alloy coating deposited at various current densities (1.0 A/dm^2 to 4.0 A/dm^2) for both Hydrogen Evolution Reaction (HER) and Oxygen Evolution Reaction (OER). The potential range for HER was set from 0 V to -1.6 V, and for OER from 0 V to 0.75 V, with a scan rate of 0.05 V s^{-1}. The resulting cyclic voltammogram, presented in Figure 7.9, indicates that the onset potential for HER increases with the deposition current density. In Figure 7.9 (a), it is evident that the Co-P coating deposited at 1.0 A/dm^2 (with a composition of 93.8 wt.% Co and 6.2 wt.% P) exhibits the least onset potential and the highest cathodic peak current density (i_{pc}). As the deposition current density increases to 4.0 A/dm^2, the value of i_{pc} reaches its minimum. Detailed electro-catalytic data are reported in Table 7.4

The analysis of the cyclic voltammetry (CV) results indicates that the Co-P alloy coating deposited at 1.0 A/dm^2, with the least phosphorus (P) content and highest cobalt (Co) content, exhibits the highest efficiency for the Hydrogen Evolution Reaction (HER) as a cathode. The decrease in electro-catalytic activity for HER with an increase in current density is attributed to the rise in P content, as supported by the data in Table 7.4. Conversely, the Co-P alloy deposited at 4.0 A dm^{-2}, with the highest P content, demonstrates the highest performance for the Oxygen Evolution Reaction (OER), showing the least onset potential and the highest anodic peak current density (i_{pa}), as illustrated in Figure 7.9(b). The highest value of i_{pa} for the Co-P alloy corresponding to 4.0 A dm^{-2}, with the highest P content, indicates the

surface's efficiency in facilitating the anodic reaction. Therefore, the Co-P alloy coatings exhibit different tendencies for HER and OER based on their P content, with coatings deposited at 1.0 A dm^{-2} being more prone to HER and less prone to OER, while those deposited at 4.0 A dm^{-2} exhibit the opposite behavior.

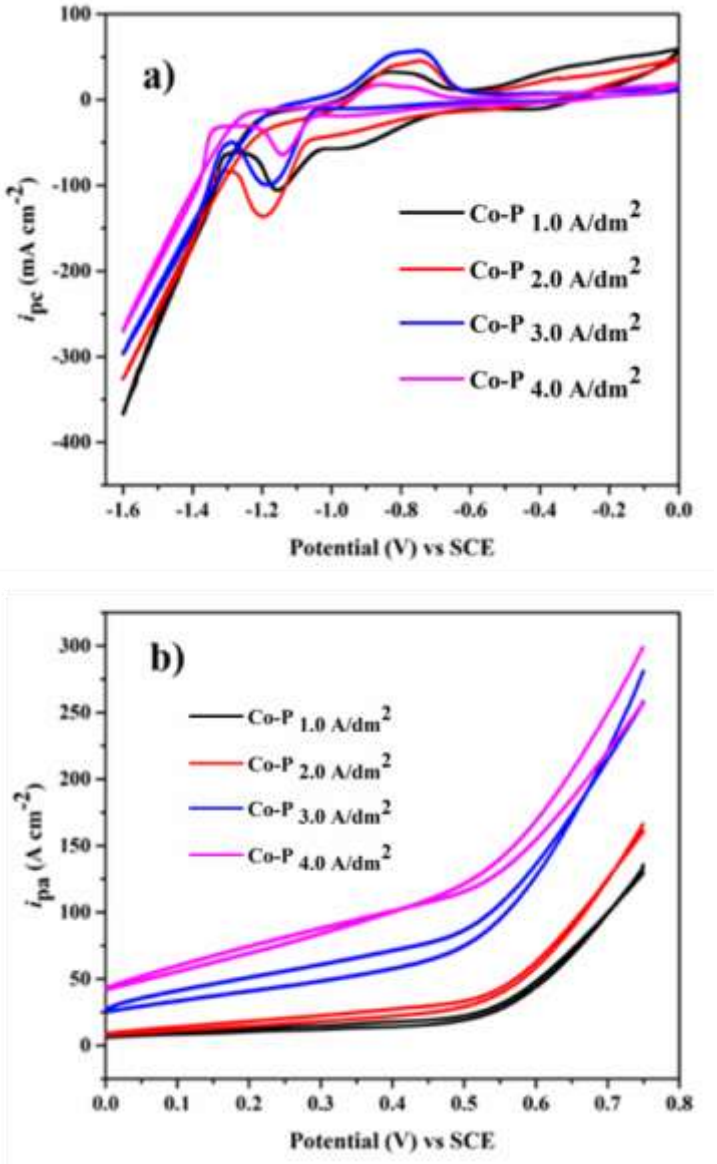

Figure 7.9 *- CV study of Co-P alloy coatings corresponding to different current densities showing their electro-catalytic efficiency for (a) HER and (b) OER*

This increase of electro-catalytic character of Co-P alloy coatings for OER, with increase of current density is due to increased P and decreased Co content of the alloy. Thus this mutually opposite electro-catalytic activity of Co-P alloy coatings towards HER and OER, which

changes with deposition c.d.'s of the alloy is attributed to change in the composition of the alloy, in terms of Co and P content. As hydrogen overpotential of P being less, Co-P alloy at deposited 1.0 A dm^{-2} (more Co) favored HER more and Co-P alloy deposited at 4.0 A dm^{-2} being having less Co, it favored OER.

Table 7.4- Electro-catalytic kinetic parameters of Co-P alloy coatings corresponding to different current density for HER, with wt. % P content in the deposit

Deposition Current density (A/dm^2)	Co content in the deposit (wt. %)	P content in the deposit (wt. %)	Cathodic peak c.d. (i_{pc}) (mA cm^{-2})	Onset potential for H_2 evolution (V vs SCE)	Volume of H_2 Evolved in 300s (cm^3)
1.0	93.8	6.2	359.2	1.23	10.8
2.0	92.8	7.2	318.0	1.25	10.4
3.0	92.6	7.4	287.4	1.26	10.0
4.0	91.3	8.7	259.8	1.28	9.8

ii) Chronopotentiometry Study

Chronopotentiometry (CP) is a technique that involves measuring the potential of the working electrode over time while a constant current is passed between the working and reference electrodes. In the study of Co-P alloy coatings deposited at current densities ranging from 1.0 A/dm^2 to 4.0 A/dm^2, CP was employed by applying a constant current of -0.3 A to 0.3 A for 1800 seconds each for both Hydrogen Evolution Reaction (HER) and Oxygen Evolution Reaction (OER). The electro-catalytic performance of these Co-P alloy coatings was assessed through chronopotentiometry, and the volume of evolved H_2 and O_2 on a 1 cm^2 surface area was quantified over a 300-second duration. The resulting chronopotentiograms for HER are illustrated in Figure 7.10 (a), and the corresponding amount of H_2 evolved is presented in the bar chart in Figure 7.10 (b).

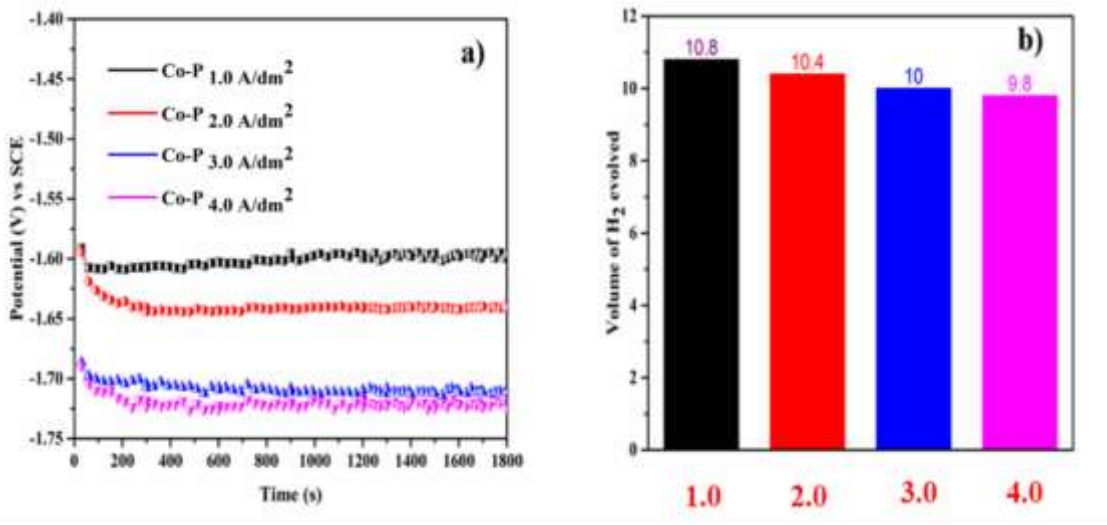

Figure 7.10 *- CP study of Co-P alloy coatings corresponding to different current densities showing their electro catalytic efficiency for (a) HER and (b) the volume of H_2 evolved for 300 s*

The chronopotentiograms of Co-P alloy coatings for HER, corresponding to different current densities is shown in Figure 7.10. The nature of chronopotentiograms clearly speaks about the stability of coatings as effective electro-catalysts. In comparison to all other coatings, the Co-P coating deposited at 1.0 A/dm^2 demonstrated its highest stability with highest electro-catalytic activity for HER with the maximum amount of H_2 gas evolution. All Co-P alloy coatings demonstrated a sudden reduction in potential at the beginning of electrolysis and eventually reaching a steady state. This is due to the sudden attainment of equilibrium between H^+ reduction on the electrode surface and H_2 gas evolution from the surface. When compared to other coatings, the coating produced at 1.0 A/dm^2 reached the steady state very quickly. This confirmed the fact that Co-P alloy coating at 1.0 A/dm^2 is electrocatalytically more stable and active for reduction reaction, and is a best electrode material for HER. Similarly, a chronopotentiogram study of Co-P alloy coatings for OER, at varying current densities obtained are shown in Figure 7. 11(a), and the amount of O_2 evolved is shown in Figure 7.11 (b) as bar chart. From the data reported in Table 7.5, it may be noted that Co-P alloy coating at 4.0 A/dm^2 demonstrated a highest activity for OER with highest volume of O_2 gas evolved at a lower potential (positive). This may be attributed to the excessive oxidation of OH^- ions, due to the highest P content of the deposit. At the same time, when current is applied to any

coating, there is an initial potential rise due to the abrupt depletion of OH^- ions from the electrolyte at the electrode surface.

Table 7.5- Electro-catalytic kinetic parameters of Co-P alloy coatings for OER during alkaline water electrolysis, with metal contents in the deposit

Deposition Current density (A/dm^2)	Co content of the deposit (wt. %)	P content in the deposit (wt. %)	Cathodic peak c.d. (i_{pc}) ($mA\ cm^{-2}$)	Onset potential for O_2 volution (V vs SCE)	Volume of O_2 evolved in 300 s (cm^3)
1.0	93.8	6.2	135.3	0.53	5.2
2.0	92.8	7.2	165.9	0.48	5.4
3.0	92.6	7.4	281.0	0.47	5.6
4.0	91.3	8.7	298.6	0.43	5.8

The oxidation of OH^- to O_2 gas processed indefinitely, the generation of O_2 gas at the electrode surface and its evolution from the surface occur simultaneously, resulting in the system's potential remaining unchanged. This small change in the electro-catalytic behavior (in terms of volume of both H_2 and O_2 gas evolved) of Co-P alloy coatings with current density is due to small change in their composition, inherited by the induced type of co-deposition in the bath.

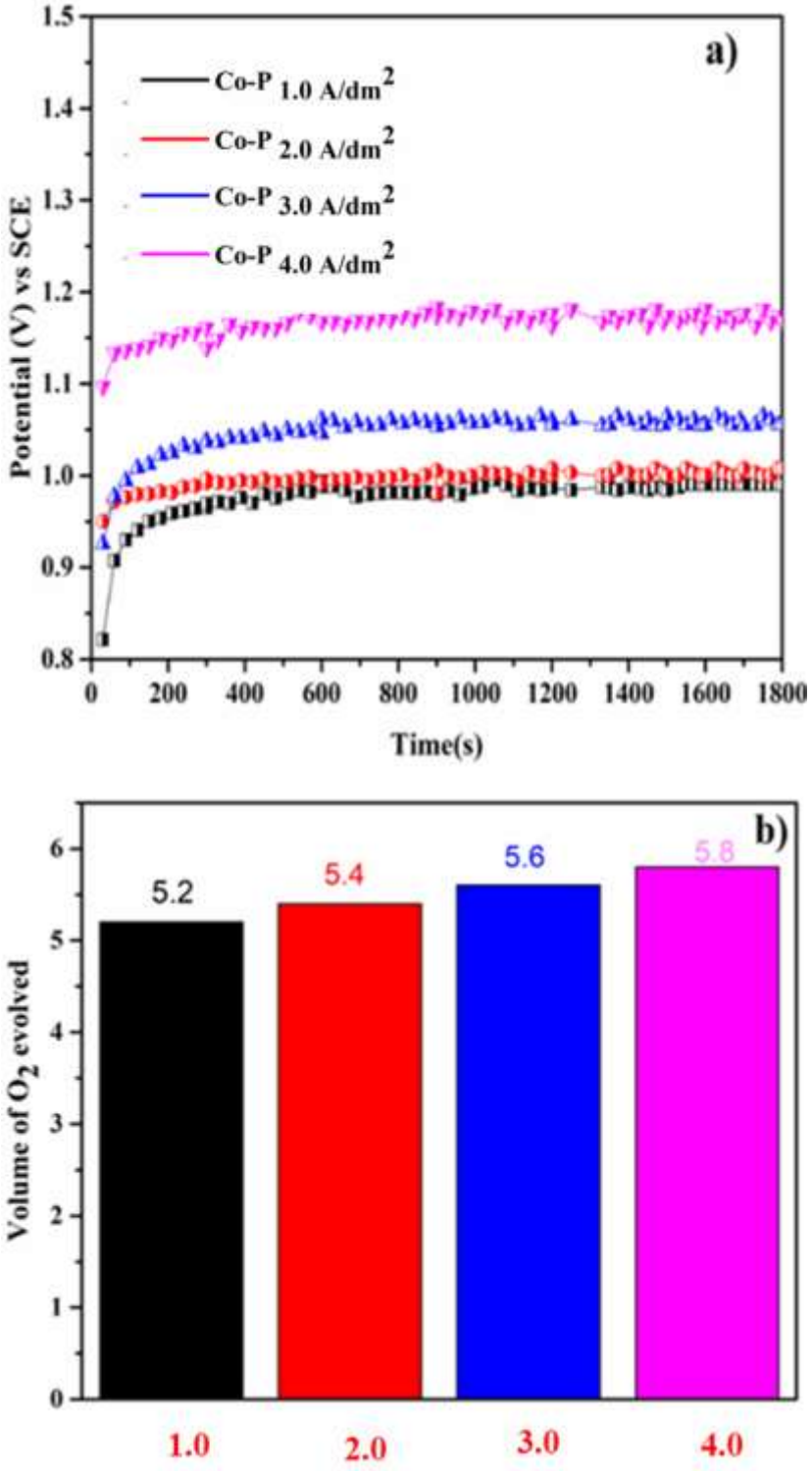

Figure 7.11 *- CP study of Co-P alloy coatings corresponding to different current densities showing their a) electro-catalytic stability for OER and (b) volume of O_2 liberated in 300 s*

7.4.3 Inverse dependency of electro-catalytic efficiency of HER and OER with composition

The electro-catalytic activity of Co-P alloy coatings for both HER and OER, deposited at different current densities are summarized in Tables 7.4 and 7.5. From the data, it may be noted that as the deposition current density of Co-P alloy coating is increased (or as Co content of the decreased), its electro-catalytic efficiency for HER (cathodic process) is decreased; whereas for OER (anodic process), it increased. This inverse dependency of electro-catalytic efficiency of HER and OER with Co content of alloy coatings may be attributed to the redox behavior of alloy coatings, having different composition. It may be explained in terms of the tendency of the electrons to transmit between working electrodes (test electrodes) and counter electrode. It is to recall here that in electrochemical study, working electrode is an electrical conductor, and by means of an external power source (potentiostat), voltage can be applied to it to modulate the energy of the electrons in the electrode. Hence, driving force of a particular reaction can be controlled, and the ease with which thermodynamic and kinetic parameters can be measured (Elgrishi et al. 2018). In the backdrop of the above principle, a conceptual diagram showing the efficiency of Co-P alloy coatings, having different Co content towards HER and OER during alkaline water electrolysis is given in Figure 7.12.

It may be noted that during alkaline water electrolysis, H_2 and O_2 gases are liberated on working electrode Co-P alloy coatings having different compositions, when relatively negative and positive potentials are applied, respectively through the potentiostat. When electrons on the Co-P alloy coatings are at a higher energy than the Lowest Unoccupied Molecular Orbital (LUMO) of the electrolyte constituent (H^+), electron from the electrode is transferred to electrolyte constituent to release H_2. Similarly, when electrons in the Co-P alloy coating is at lower energy than the Highest Occupied Molecular Orbital (HOMO) of electrolyte constituent (OH^-), electron from the electrolyte constituent is transferred to electrode to release O_2. Thus, depending on the Co content of the alloy (depending on the deposition current density), Co-P alloy coatings can assume different electrode potential values (E_1, E_2, E_3 and E_4) along the energy axis (depending on its Co content), as shown in Figure 7.11, and hence different energy gap (ΔE) between HOMO-LUMO. Therefore, transferring of electrons takes place from HOMO to LUMO to favor either HER or OER, depending on their composition. If the

efficiency of Co-P alloy coating, deposited at a particular current density, say at 1.0 A/dm^2 (having the highest Co content) is more favourable for HER (due to low energy gap ΔE), and is less favourable for OER (due to large energy gap ΔE), as shown in Figure 7.12. But Co-P alloy coating, deposited at 4.0 A/dm^2 (having less Co content) is more favourable for OER (and less favourable for HER), as may be seen in Figure 7.12. Thus, it may be summarized that a mutually opposite electro-catalytic activity of Co-P alloy coatings towards HER and OER, which changes with deposition current density is attributed to the change in composition of the alloy, in terms of their Co and P content. Thus, the driving force of electrochemical reaction of water splitting of both HER and OER of Co-P alloy coating is a function of energy difference between working electrode and counter electrode, and show mutually opposite trends. In other words, mutually opposite treands in the volume of H_2 and O_2 gas are evoloved, depending on the current density), and it is due to reduction and oxidation processes involed HER and OER, respectively.

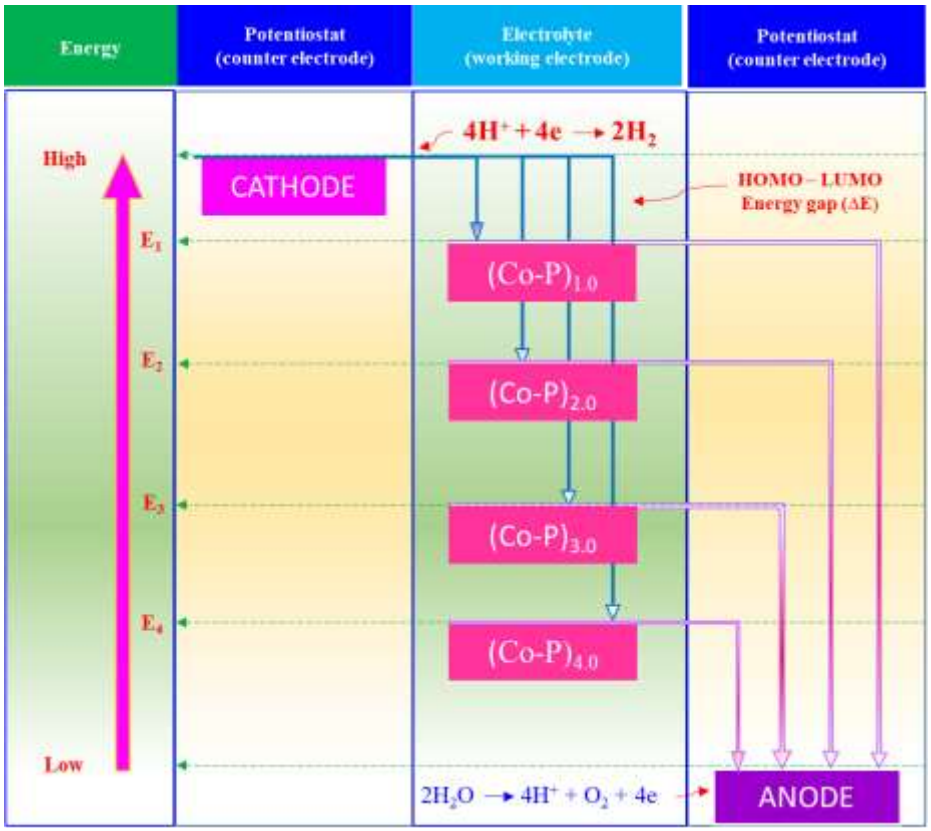

Figure 7.12 *- Representational diagram showing inverse dependancy of Co-P alloy coating, deposited at different current density for HER and OER in alkaline water electrolysis*

7.5 Effect of addition of Ag-nanoparticles

From the literature it was found that HER performance of many binary alloy coatings can be increased significantly by adding known quantity of nanoparticles into their bath solution (Pagliaro 2009). On the other hand, experimental study on electro-catalytic behavior of electrodeposited Co-P alloy coatings revealed that Co-P $_{1.0\ A/dm^2}$ shows its best performance for HER, compared to all other coatings. Hence, Co-P-Ag composite coatings were developed by adding 0.5 g L^{-1}, 1.0 g L^{-1} and 2.0 g L^{-1} of Ag-nanoparticles into the proposed bath of Co-P alloy (Table 7.1), and their electro-catalytic performances were studied.

7.5.1 Evaluation of HER activity of Co-P-Ag composite coating

Cyclic voltammetry and chronopotentiometry study

Cyclic voltammetry technique was employed to understand HER activity for Co-P-Ag composite coatings in a potential range of 0.0 V to -1.6 V at a potential scan rate of 0.05 V s^{-1} for 20 cycles. For the first 10 cycles, there was a shift in (i_{pc}) values, which at later stage retraced the path of previous cycle. Figure 7.13 represents the CV plots of Co-P-Ag composite coatings, with different quantities of Ag-nanoparticles, with that of bare - Co-P alloy coatings. The electro-catalytic parameters corresponding to HER were tabulated in Table 7.6.

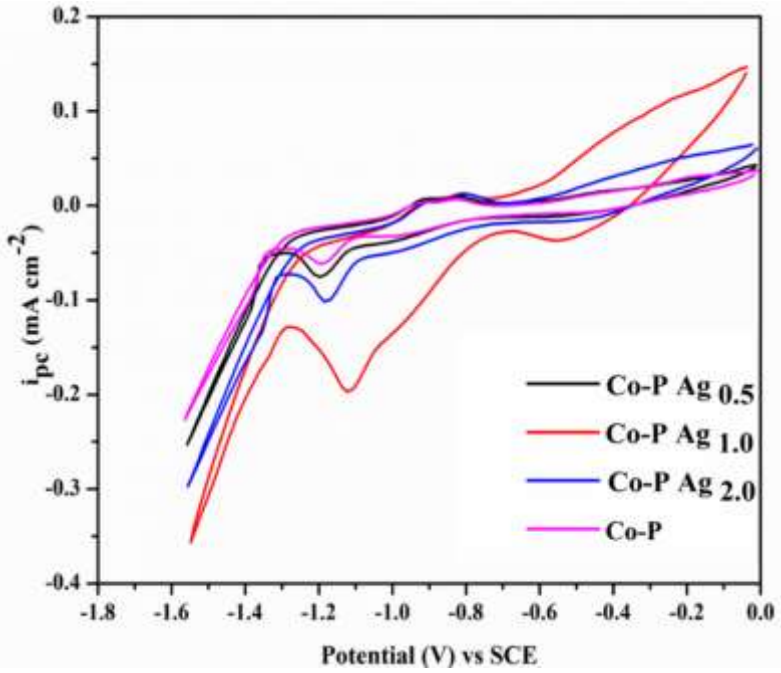

Figure 7. 13- *CV responses for HER activity of Co-P and Co-P- Ag composite coatings having varied concentrations of Ag-nanoparticles, electrodeposited*

Among Ag-nanoparticles added coatings, it may be seen that Co-P-Ag $_{1.0\ g}$ composite coatings shows the highest (i_{pc}) and lowest onset potential values as shown in the Figure 7.13. To examine the electro-catalytic stability of composite alloy coatings, their CP study have been made by applying a constant current of -300 mA for time interval of 1800 s, and nature of their chronopotentiograms are shown in the Figure 7.14. It may be seen that Co-P-Ag $_{1.0\ g}$ coatings showed highest performance of HER, by liberating 12.2 cm^3 of H_2 gas in initial 300 s, compared to other coatings. The value of cathodic peak current density (i_{pc}), and onset potentials for HER of all Co-P-Ag composite coatings are reported with the volume of H_2 gas evolved in 300 s, in Table 7. 6. Thus, Co-P-Ag composite coating corresponding to 1.0 g Ag is electro-catalytically more active for HER, than other coatings, it is supported by the highest volume of H_2 gas (12.2 cm^3) liberated during electrolysis.

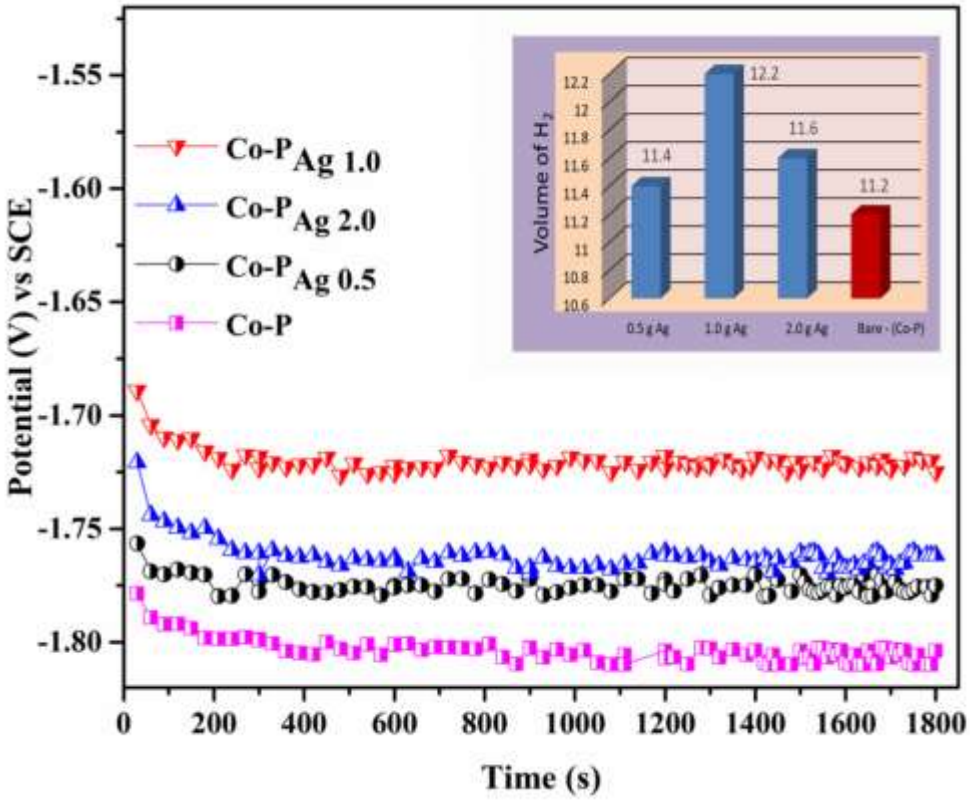

Figure 7.14 *– CP responses of Co-P-Ag composite coatings for HER showing their electro-catalytic stability, and the volume of H_2 gas liberated with varied amount of Ag nanoparticles, in relation to that of bare -Co-P alloy coating*

7.5.2 Morphological study

7.5.2.1 SEM-EDS study

The surface morphology of Co-P-Ag composite coatings with different amounts of Ag nanoparticles added, into the optimal bath. It is evident from the Figure 7. 15 that Ag nanoparticles are embedded in the Co-P alloy matrix homogenously. It may also be noted that the adsorption of Ag nanoparticles on to the Co-P deposit resulted in the formation of non-homogeneous coatings with lumps of nano-particles on the surface as shown in the Figure. 7.15.

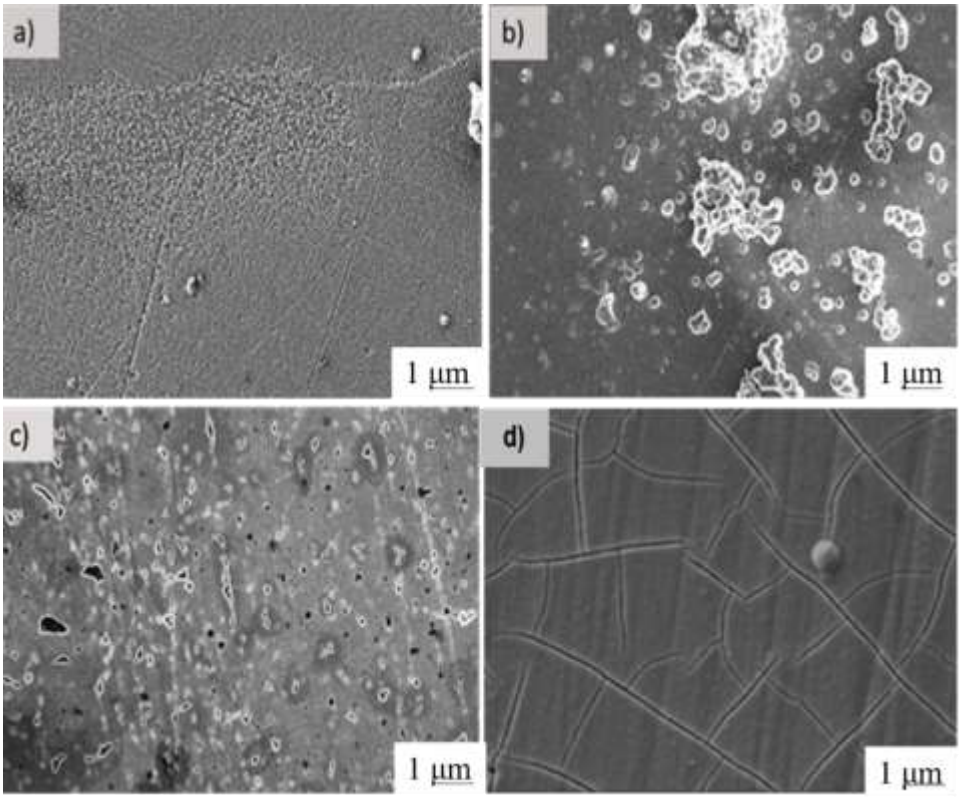

Figure 7.15 - *FESEM micrographs of Co-P-Ag composite coatings having varied amount of Ag nanoparticles incorporated: a) 0.5 g L^{-1} Ag, b) 1.0 g L^{-1} Ag, c) 0.5 g L^{-1} Ag and d) without, deposited at 1.0 A/dm^2 from the same optimal bath*

Further from the EDS analysis of Co-P-Ag composite coatings, it was found that metals content of composite coating has changed due to addition of Ag-nanoparticles into the bath. Change of metal contents in the composite coatings with different amount of Ag-nanoparticles are shown in the Table 7.6. From the compositional data, it may be seen that increment in

nano-Ag particles in the bath resulted in the variation in the wt.% of Co and P composition in the deposit.

Table 7.6 - Electro-catalytic HER parameters obtained for bare Co-P and Co-P-Ag composite coatings developed

Coating Configuration	Peak cathodic current (i_{pc}) (mA cm^{-2})	Onset potential for HER (V) vs SCE	Volume of H_2 evolved for 300 s (cm^3)
Co-P-Ag $_{0.5}$	-238.5	-1.26	11.4
Co-P-Ag $_{1.0}$	-363.2	-1.18	12.2
Co-P-Ag $_{2.0}$	232.2	1.28	11.6
Bare- Co-P	-339.2	-1.23	11.2

The presence of wt. % of Ag confirms the incorporation of nano Ag onto the substrate along with alloy deposit. Importantly, the addition of only 1.0 g L^{-1} of Ag nano-particles into the bath is good enough to bring improvement on the electro-catalytic activity of HER.

7. 5.2.2 XRD study

Crystallographic study of Co-P-Ag composite coatings have been made in relation to that bare-Co-P alloy coatings and is shown in the Figure 7.16.

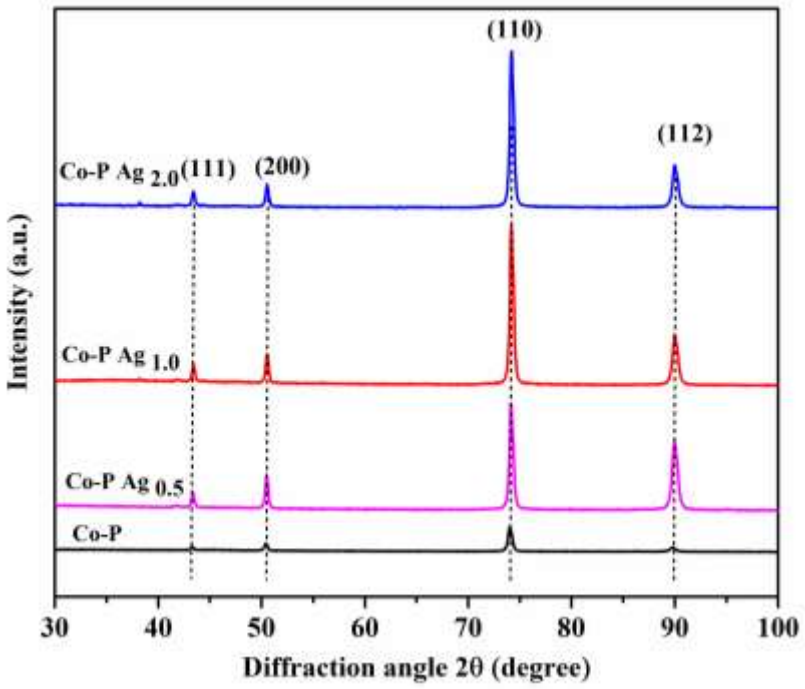

Figure 7.16 – *Comparison of XRD signals obtained for bare-Co-P and Co-P-Ag composite coatings developed at 1.0 A/dm^2*

From the nature of XRD reflections, it may be seen that there are no significant peaks corresponding to Ag is observed in the diffractograms. However, it may be noted that the position of the peaks remains unaltered, on addition of Ag nanoparticles into the alloy matrix, except the change in peak intensity. This change of peak intensity may be ascribed for the change in the wt. % metal ions in alloy matrix, due to incorporation of Ag. Thus, increase in intensity of diffraction peaks corresponding to Co-P-Ag composite coatings are corresponding to the slight increase of Ni, which increased with increase in concentration of Ag.

7.5.2.3 AFM Study

Surface roughness is considered to be an important parameter that influences HER of electrode materials. Accordingly, Atomic Force Microscopy (AFM) analysis was carried out for bare-Co-P and Co-P-Ag$_{1.0}$ composite coatings to get valuable information about the surface properties, particularly surface average roughness. Figure 7.17 a), b) and c) gives the AFM images of bare Co-P, Co-P-Ag $_{1.0\ g}$ and Co-P-Ag $_{2.0\ g}$ composite coatings deposited at 1.0 A/dm^2, respectively. The surface roughness data, revealed that average surface roughness of bare-Co-P alloy coating is increased from 7.5 nm to 8.4 nm due to addition of 1.0 g L^{-1} Ag-nanoparticles into the bath. Thus, the observed improvement in the electro-catalytic efficiency of Co-P alloy coatings, due to addition of Ag-nanoparticles may be attributed to their increased active sites and surface roughness, as evidenced by AFM images.

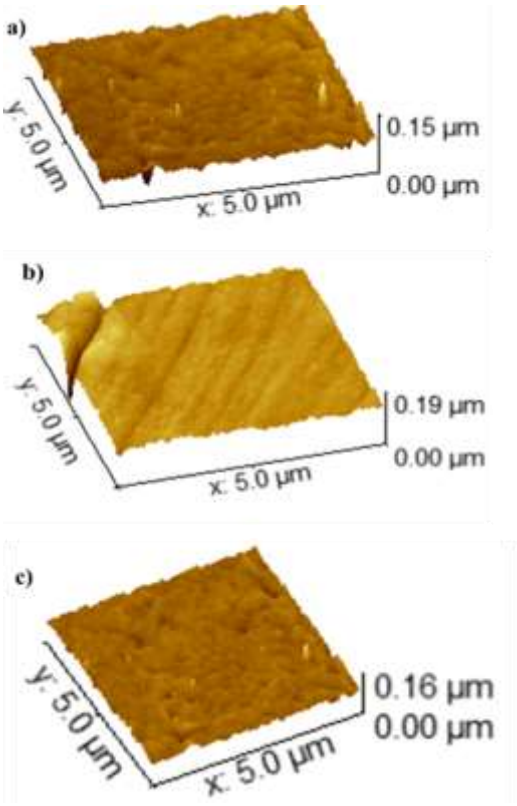

***Figure 7.17** – AFM image showing surface roughness of Co-P alloy corresponding to: a) bare - Co-P alloy, b) Co-P-Ag $_{1.0\ g,}$ and c) Co-P-Ag $_{2.0}$ deposited from the same bath.*

7.6 CONCLUSIONS

An electrolytic bath of Co-P alloy has been proposed for development of corrosion resistant coatings using glycine as additive, and following conclusions are made:

1. Very bright and sound coatings of Co-P alloy was obtained from a new bath at different current densities (1.0 A/dm^2 to 4.0 A/dm^2). The compositional data of electroplated alloy coating revealed that bath follows induced type of co-deposition.
2. Experimental study demonstrated that among Co-P alloy coatings deposited at different current density, Co-P alloy corresponding to 1.0 A/dm^2 is the most corrosion resistant, and is attributed to high wt. % of Co in the deposit
3. Increase of corrosion rate of Co-P alloy coatings towards high current density is attributed to decreased Co content, and increased cracks on surface due to liberation of hydrogen.

4. Electro-catalytic study revealed that Co-P alloy coatings for both HER and OER are highly dependent on its composition, depending on the current density at which they are deposited.
5. A small change in the electro-catalytic behaviour (in terms of volume of both H_2 and O_2 gas evolved) of Co-P alloy coatings with current density is due to small change in their composition, inherited by the induced type of co-deposition.
6. Mutually opposite electro-catalytic activity of Co-P alloy coatings towards HER and OER with deposition current density, in terms of the volume of H_2 and O_2 gas are evoloved is due to the nature of reaction. *i.e.* due to reduction and oxidation processes involed for HER and OER, respectively.
7. The composite Co-P-Ag alloy coatings have shown better efficiency for evolution of both H_2 and O_2 gases *i.e.* 12.2 cm^3 and 6.2 cm^3, respectively. Hence it is attributed to increased roughness and active sites on the surface.
8. The surface feature, phase structure and compositional change of Co-P alloy coatings, responsible for highest electro-catalytic activity of HER and OER were examined, using scanning electron microscopy (SEM), X-ray diffraction (XRD) and Energy Dispersive X-ray spectroscopy (EDS) techniques.

DEVELOPMENT OF NANO-LAYERED Co-Fe ALLOY COATINGS FOR BETTER CORROSION PROTECTION OF MILD STEEL

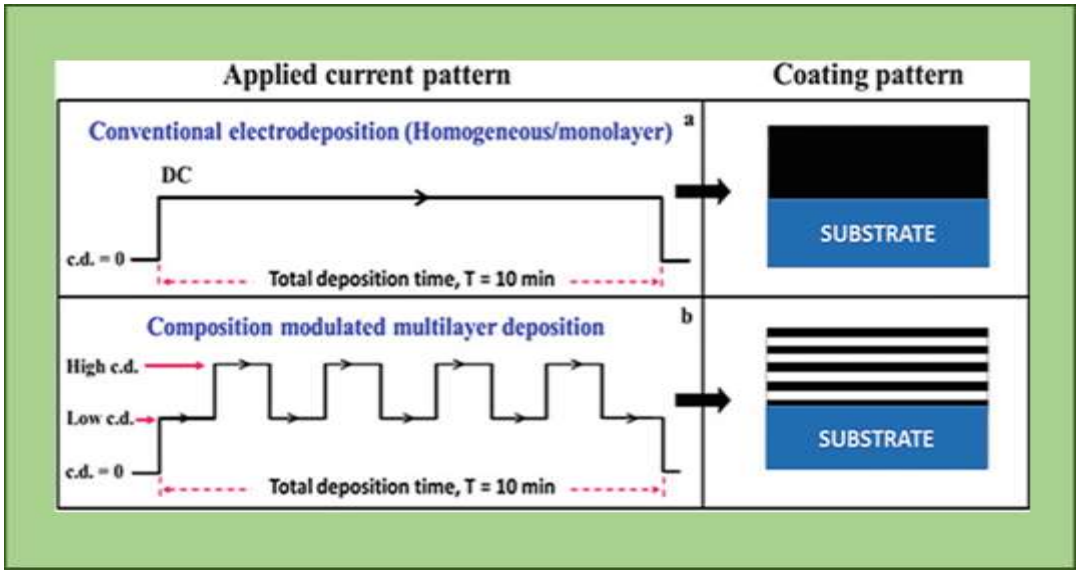

Here optimization of a new citrate bath of Cobalt- Iron Co-Fe alloy has been made, using the glycine as the additive. The experimental results are presented in two parts. The first part, details the optimization of composition and operating parameters of bath, using Hull cell method. Then monolayer Co-Fe alloy coatings were electrodeposited from the optimized bath using direct current (DC). The current densities were optimized for deposition of most corrosion resistant monolayer alloy coatings. In the second part, how the poorer corrosion resistance of monolayer Co-Fe alloy coatings can be improved further by composition modulated multilayer alloy (CMMA) method, using the same bath is explained. The multilayer, or nano-layered Co-Fe alloy coatings, having alternate layers of different compositions have been effected by periodic modulation of DC, during deposition. Coatings configurations were optimized, in terms of the composition of individual layers (by changing current pulse height) and thickness of the coatings (by changing the duration of deposition of each layer) to maximize their corrosion protection efficiency, compared to its monolayer counterpart. The experimental study revealed that corrosion resistance property of multilayer Co-Fe alloy coatings increases with number of layers only up to certain degree of layering, and then decreased. The better corrosion resistance of multilayer Co-Fe alloy coatings were explained with plausible mechanism, and results are discussed.

8.1 INTRODUCTION

Current density is an important tool of electroplating, and no study of the metal/alloy deposition is complete without the detailed data on its variation. It acknowledges that the impact of current density is less consistent compared to other operating variables when considering the variation in the composition of the electrodeposited alloy. The research specifically focuses on understanding the effect of current density on the composition of Co-Fe alloy coatings. Over the past few decades, significant progress has been made in developing soft magnetic films for industrial applications. These films exhibit desirable properties such as low coercive field, low hysteresis loss, low eddy current loss, high electric permeability, and high saturation magnetization. Co-Fe alloys, in particular, have gained attention due to their high saturation magnetization value (2.4 T), making them suitable for applications in computer memories. However, the coercivity of these alloys is relatively high. Efforts have been made to reduce the coercivity of Co-Fe alloys, and recent advancements in nano-crystalline materials have shown that reducing grain size in ferromagnetic materials can significantly decrease coercivity without affecting saturation magnetization. Electrodeposition is identified as a promising technique for producing such nano-crystalline coatings.

Recent advancements in nanostructured multilayer coatings have been driven by the emergence of new synthetic methods that offer control over the number and composition of individual layers (Bang and Suslick, 2010). The use of periodically pulsed current from a highly sensitive power source provides an accessible and versatile approach for synthesizing nanostructured multilayer coatings with extraordinary properties, not achievable through conventional methods. Multi-layered coatings represent a new class of materials with alternate layers of different metals or alloys with varying composition and phase structures (Thangaraj et al., 2009). These coatings consist of nanoscale layers and are often referred to as nano-laminated or composition-modulated coatings. Composition-modulated multilayer alloy (CMMA) coatings comprise thin layers of alloys of the same metals but with different compositions. The pulse electrodeposition method has a merit that it is possible to control the composition and layer thickness of multilayer coating in atomic scale by varying the amplitude of cathodic current (pulse), which is responsible for composition change; and deposition time, responsible for thickness of deposit (Yahalom and Zadok 1987). Thus by knowing the advent of multilayer alloy coatings, compared to monolayer alloy coatings (developed through

conventional method using direct current), a more anti-corrosive Co-Fe alloy coatings was tried to develop from the same optimized bath through multilayer approach, by pulsing periodically the cathode current density (between two values) during plating. The composition and thickness of alternate layers of alloys are manipulated by proper modulation of current densities (pulsing) and duration of pulse (time), respectively. The multilayer coatings of Co-Fe alloy having lamellar structure of nanometer scale were developed under different conditions of current densities (current pulse) and number of layers, from the optimized bath. The corrosion protection efficiency of multilayer Co-Fe alloy coatings were evaluated by electrochemical AC and DC methods. The effect of composition of alternate layers, and degree of layering on corrosion protection efficiency of multilayer alloy coatings have been discussed. The multilayer coatings with different configurations, considering variations in composition and thickness of individual layers, have been fabricated by precisely modulating the amplitude and duration of square current pulses. The coating configurations for these multilayer alloy coatings were fine-tuned to achieve optimal performance against corrosion. The factors contributing to the enhanced corrosion resistance of multilayer Co-Fe alloy coatings are elucidated, and the results are thoroughly discussed.

In this direction, present chapter unfolds in parts. In the first part, optimization of composition and operating parameters of bath, using Hull cell method is detailed. Then monolayer Co-Fe alloy coatings were developed using direct current, and current densities were optimized for deposition of most corrosion resistant alloy coatings. In the second part, how the poorer corrosion resistance of monolayer Co-Fe alloy coatings can be improved further by composition modulated multilayer alloy (CMMA) method, using the same bath is explained. The multilayer, or nano-laminated Co-Fe alloy coatings, having alternate layers of different compositions have been effected, by periodic modulation of direct current during deposition. The corrosion performance of monolayer and multilayer Co-Fe alloy coatings have been compared, reasons responsible for improved performance of multilayer coatings have been discussed.

8.2 EXPERIMENTAL

The optimization of new Co-Fe alloy bath has been carried out by Hull cell method as described elsewhere (Khanani, 2006). The coating showed bright appearance in the range of current

density from 1.0 A/dm^2 to 4.0 A/dm^2. Electrodeposition of Co-Fe alloy has been accomplished using a sulphate bath consisted of different components, shown in Table 8.1. The pH of the bath was adjusted to 3.5 using either dilute H_2SO_4 or NH_4OH, depending on the requirement using Micro-pH Meter (Systronics-362), and the solution was filtered prior to the deposition. Electrolytic bath was prepared using analytical grade reagents and double distilled water.

Table 8.1 - The composition and operating variables of new optimized bath of Co-Fe alloy

Bath Ingredients	*Composition (g L^{-1})*	*Operating Variables*
Cobalt Sulphate ($CoSo_4$)	152	Anode: Graphite
Ferrous Sulphate ($FeSo_4$)	16	Cathode: Mild steel
Tri Sodium Citrate ($Na_3C_6H_5O_7 \cdot 2H_2O$)	30	Temp: 303 K
Ammonium chloride (NH_4Cl)	8.0	pH: 3.5
Glycine (NH_2-CH_2-COOH)	1.0	Current density: 1.0 - 4.0 Adm^{-2}

Driven by the fact that there can be a significant improvement in the corrosion performance of multilayer alloy coatings, when coating is changed from monolayer to multilayer type (Benaicha et al. 2016; Tsyntasaru et al. 2012), multilayer Co-Fe alloy coatings were deposited from optimized bath using pulsed current. Multilayer coatings of different configurations have been developed with different set of cyclic cathode current densities (CCD's) *i.e.* two current densities between which cathode pulse is made to cycle repeatedly to form coatings in layered pattern. All other conditions of deposition are kept constant as that of monolayer coating. The power pattern used for deposition of monolayer and multilayer Co-Fe alloy coatings, and their homogeneity are shown by a representative diagram in Figure 8.1. The simple direct current (DC), or constant current was used for development of conventional monolayer Co-Fe alloy coating, as shown in Figure 8.1(A), with the homogeneity of coating shown below. Multilayer Co-Fe alloy coating was developed by periodic pulsing of the direct current (DC), during process of deposition. The power pattern used for development of multilayer coating is shown in Figure 8.1(B). In this study, for convenience all monolayer Co-Fe alloy coating deposited

at a particular current density ‘x’ is represented as Co-Fe $_x$ and multilayer Co-Fe alloy coating having layers of alloys of different compositions are represented as Co-Fe $_{1.0/3.0/n}$ (where 1.0 and 3.0 indicate the cyclic current density (CCCD), and ‘n’ is the number of layers formed during total plating time, *i.e.*, 10 min).

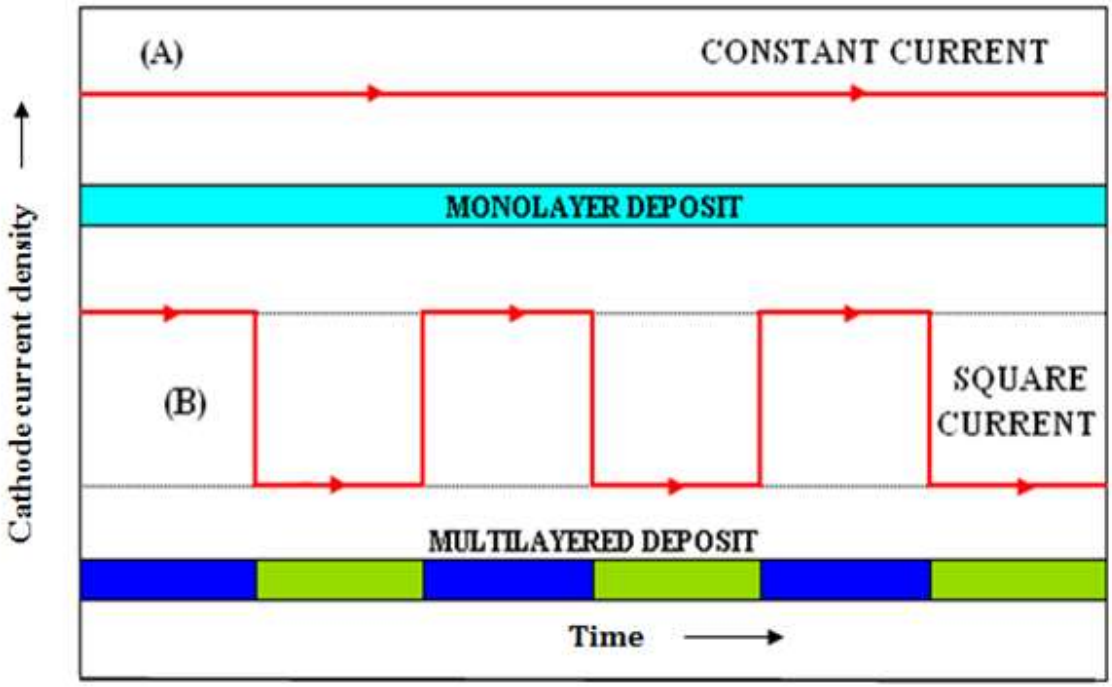

Figure 8.1*- Schematic representation of current pulses used for electrodeposition of Co-Fe alloy coatings: (A) direct current (DC) for monolayer coating, (B) pulsed DC for multilayer coating*

All the Co-Fe alloy coatings subjected to EIS analysis before potentiodynamic polarization assessment using Tafel's method. All electrochemical potentials referenced in the study are with respect to the saturated calomel electrode (SCE). EIS analysis involved a 10 mV perturbing AC voltage in a frequency range of 100 kHz to 10 mHz, and the corresponding Nyquist plots were analyzed to obtain polarization resistance (RP) values. Scanning Electron Microscopy (FESEM), coupled with Energy Dispersion X-ray Spectroscopy (EDS), was employed to examine changes in the surface morphology and composition of the alloy coatings at different deposition current densities. The variation in the phase structure of alloy coatings with current density was investigated using X-Ray Diffraction (XRD) techniques (Rigaku, Miniflex 600, with CuKα radiation, λ = 1.5418 Å, as the X-ray source.

8.3 RESULTS AND DISCUSSION

8.3.1 Development and characterization of monolayer Co-Fe alloy coatings

The monolayer Co-Fe alloy coatings were developed from the optimal bath (Table 8.1), using direct current (DC). They are subjected different analysis, and experimental results are reported in Table 8.2.

Table 8.2 - Change of composition and corrosion rates (CR) of Co-Fe alloy coatings with current density deposited from optimized bath

Deposition Current density (A/dm^2)	Co content in the deposit (wt. %)	Fe content in the deposit (wt. %)	- E_{corr} (mV vs. SCE)	i_{corr} ($\mu A\ cm^{-2}$)	CR $\times 10^{-2}$ ($mm\ y^{-1}$)	R_p
1.0	86.9	13.1	- 406.6	14.4	15.6	1735
2.0	84.7	15.3	- 422.5	18.5	16.0	1328
3.0	82.6	17.4	- 520.4	16.8	18.4	1261
4.0	80.4	19.6	- 421.8	15.6	20.3	453
In the bath	90.5	9.5				

8.3.1.1 Compositional analysis

The composition data of Co-Fe alloy coatings deposited at different current density is reported in Table 8.2. In addition, change in the composition of alloy coatings with current density is also shown diagrammatically in Figure 8.2. Further, it should be noted that wt. % of Co and Fe in the bath are, respectively 90.40 % (shown as horizontal line in Figure 8.2 based on the bath composition) and 9.52%. Hence, from the composition data, it may be noted that the wt. % of more readily deposit-able metal (Co) in the deposit has decreased with increase of current density. This behavior of decrease of more readily deposit able metal with increase of current density is in compliance with anomalous type of co-deposition, characteristic of mutual alloys of Fe-group metals (Fe, Co, Ni and Mn), as envisaged by Brenner (Brenner, 1963). Further, it was observed that at current density more than 1.0 A/dm^2, the wt. % of Co in the deposit was found to be decreased with current density. In addition, at 1.0 A/dm^2, the bath produced a bright and uniform deposit having highest wt. % of Co (86.9 %). This increase of Co content with decrease of current density (Figure 8.2) indicates that the deposition process is tending

towards the normal type. It is supported by the fact that in anomalous type of co-deposition (Brenner 1963). Hence, at lower current density the wt. % of Co in the deposit is more due to effect of anomalous type of co-deposition in the bath.

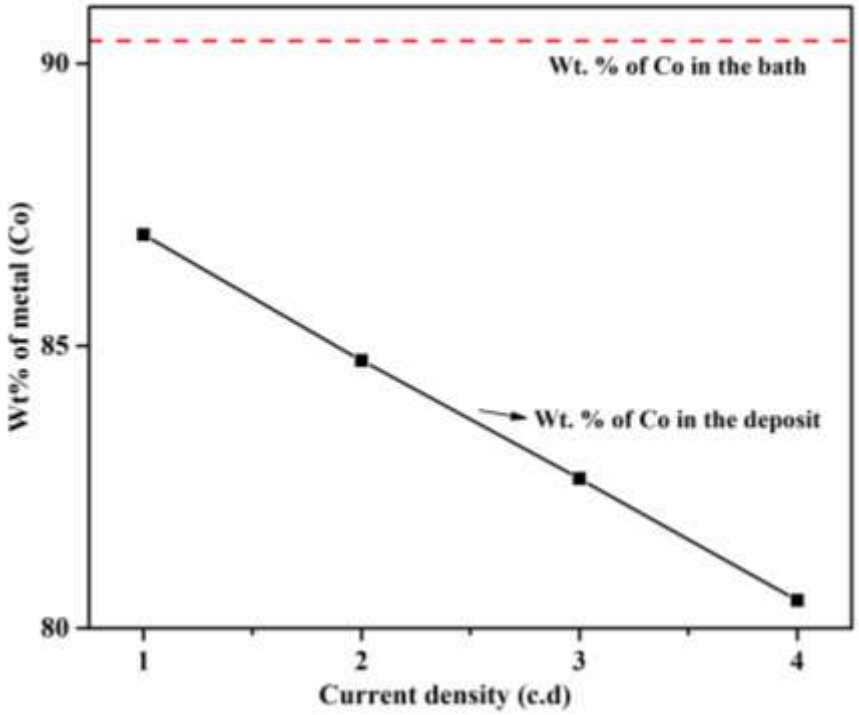

Figure 8.2- *Change in wt. % of Co in the deposit with current density, deposited from optimal Co-Fe bath. Horizontal line represents wt. % of Co in the bath based on bath composition*

8.3.1.2 Surface Morphology

The variation in the surface morphology of Co-Fe coatings with current densities is shown in the Figure 8.3. At high current density *i.e.,* 4.0 A/dm^2 it was observed that the deposit is uniform with smooth surface. The surface morphology at low current density reveals that the initial growth of fresh nuclei randomly distributed over the surface of substrate. At lower current density, like at 1.0 A/dm^2, one can observe irregular granule shapes, these granules are made up of a number of small crystallite spherical clusters. Hence, the brightness and surface structure of the coatings were determined mainly by deposition current density as a function of its Co content in the deposit.

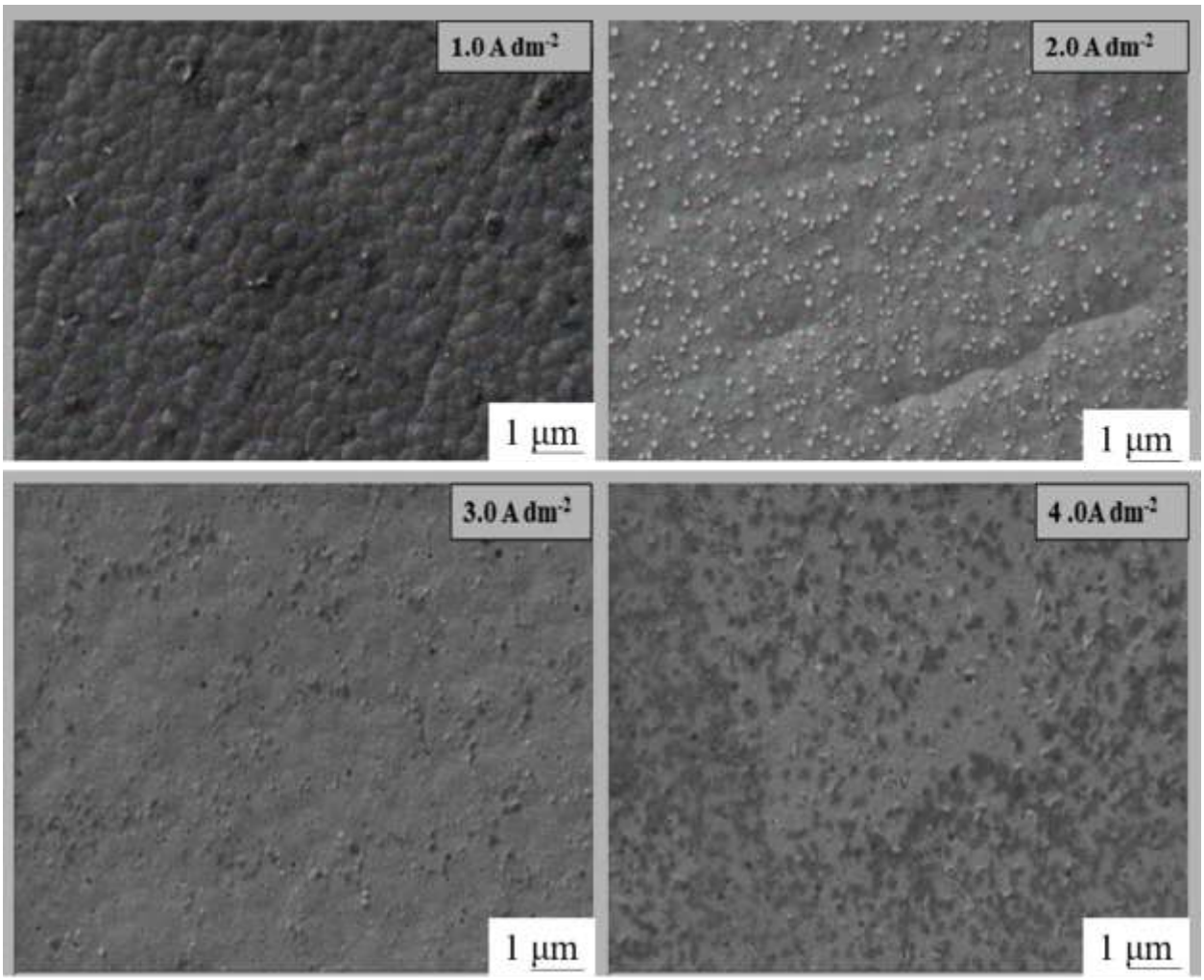

Figure 8.3 – *Surface morphology of Co-Fe alloy coatings showing dependency of deposition current density on their surface features*

8.3.1.3 AFM Study

The surface roughness of alloy coatings is an important factor which can greatly influence their properties. In this regard, the surface topography of electrodeposited Co-Fe alloy coatings were studied using three dimensional Atomic Force Microscopy (AFM) technique The three dimensional AFM image of Co-Fe alloy coatings corresponding to 1.0 A/dm^2 and 4.0 A/dm^2 are shown in the Figures 8.4 (a) and 8.4 (b). The topographical characterization was carried out by measuring the amplitude parameters, like surface roughness (R_a) and root mean square roughness (R_q) value, and they are important experimental parameters to assess the surface features of the coatings (Ashraf et al. 2016). Accordingly, it may be noted that surface

roughness of alloy coatings decreased from 15.35 nm to 5.60 nm with increase in the current density as can be seen in the AFM images depicted in the Figure 8.4.

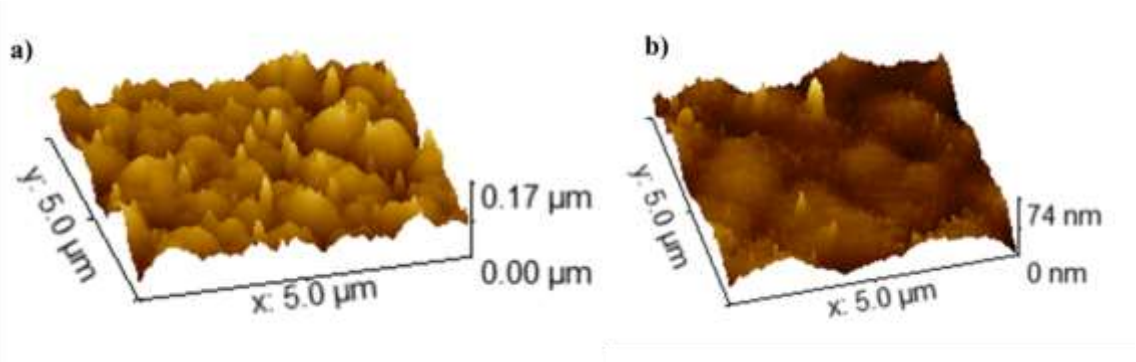

Figure 8.4 *- AFM images of Co-Fe alloy coating deposited at two different current densities: (a) 1.0 A/dm^2, and (b) 4.0 A/dm^2*

8.3.1.4 X-ray diffraction study

The crystal orientation of Co-Fe alloys with varying metal contents has been analyzed using the XRD technique. The phase structures of the alloy coatings at different current densities are determined by examining the peak profiles of X-ray reflection plotted against 2θ, as illustrated in Figure8.5

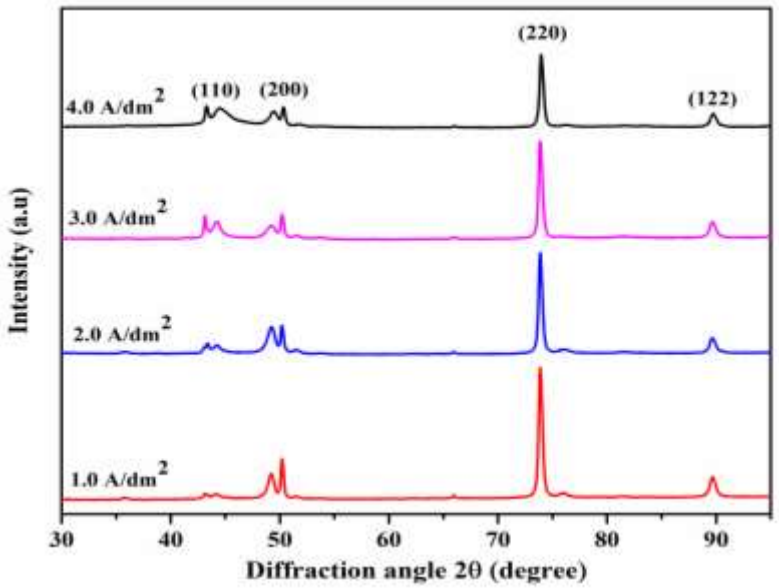

Figure 8.5 - X-ray diffraction peaks of Co–Fe alloy deposited at different current densities from optimal bath. Constancy of phase angles of coatings corresponding to different current density indicate the formation of solid solution of Co and Fe

The XRD peaks of Co-Fe alloy indicates that alloy coatings consists of a substitutional solid solution of Co and Fe. The XRD peaks at 2θ = 43.3°, 50.4°, 73.9° and 89.7° represents the phase angles of alloy coatings at different current densities, corresponding to the planes (110), (200), (220), and (122) respectively. It may be seen that intensity of peaks corresponding to different scattering angles remained to be almost constant, even with change of their deposition current density. This stands for the reason that change of composition of alloys is minimal with current density, and is supported by composition data in Table 8.2. It may also be seen that phase angles corresponding to different reflections of all coatings remains constant regardless of the current density at which they are deposited. This constancy of phase angles of Co-Fe alloy coatings at different current densities indicates the formation of solid solution of Co with Fe in the deposit(Li et al. 2018).

8.3.1.5 Corrosion study of Co-Fe alloy coatings

The electrochemical corrosion behavior of Co-Fe alloy coatings was examined using Electrochemical Impedance Spectroscopy (EIS) and potentiodynamic polarisation techniques, and their experimental results are reported below.

i) EIS study

EIS is employed to assess the barrier properties of the electrical double layer capacitance and determine the polarization resistance. In this technique, the Nyquist plot is a versatile tool, commonly representing imaginary impedance (Z') versus real impedance (Z''), allowing for the differentiation of polarization resistance (R_p) from solution resistance (R_s). The Nyquist plots for Co-Fe coatings deposited at various current densities, ranging from 1.0 A/dm^2 to 4.0 A/dm^2, are illustrated in Figure 8.6. The presence of a single semicircle for all coating configurations suggests the involvement of a single charge transfer process in the corrosion mechanism (Ullal and Hegde 2014). The capacitive loop observed at higher frequency limits indicates that the corrosion protection of the coatings is attributed to double layer capacitance (C_{dl}). Moreover, an increase in the semicircle's radius with current density suggests a close relationship between corrosion rate (CR) and the current density used for deposition. The maximum diameter of the capacitive loop at the optimal current density (1.0 A/dm^2) indicates that the deposit is the most corrosion-resistant.

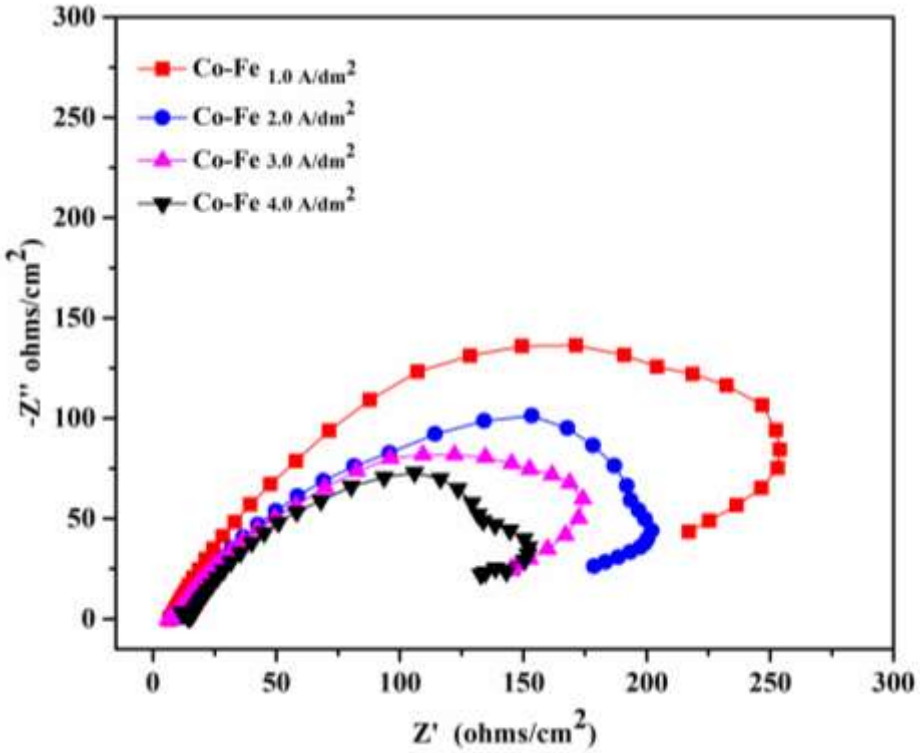

Figure 8.6- *Nyquist plots of Co-Fe coatings deposited at different current densities Highest polarization resistance (R_P) of Co-Fe coating corresponding 1.0 A/dm^2 may be seen, compared to other coatings.*

ii) Potentiodynamic Polarization study

The corrosion performance of Co-Fe coatings deposited at varying current density was evaluated by potentiodynamic polarization study. Corrosion rates (CR's) were evaluated by Tafel's extrapolation method, and corresponding plots are shown in Figure 8.7. The observed corrosion potential (E_{corr}), corrosion current density (i_{corr}) and CR are reported in Table 8.2.

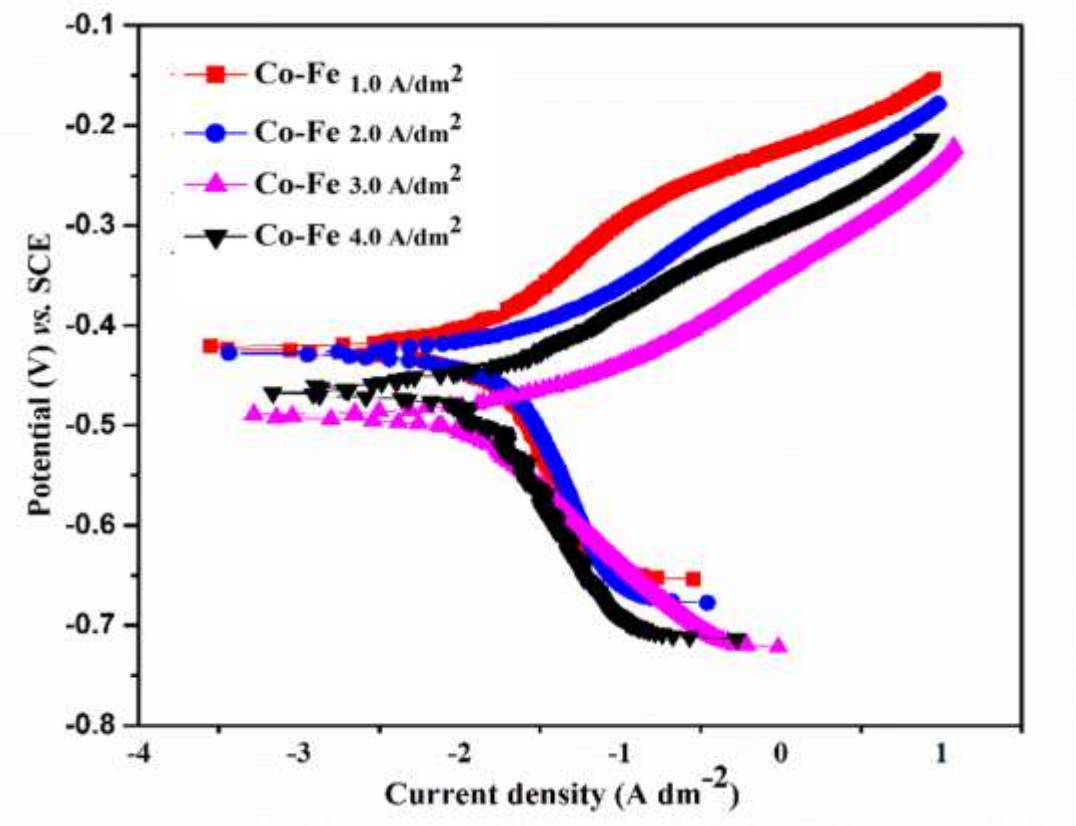

Figure 8.7- *Tafel plots of Co-Fe coatings deposited at different current densities from the optimal bath.*

The corrosion data revealed that the optimized bath given in the Table 8.1 could produce bright coating at current density of 1.0 A/dm^2, showing minimal corrosion rate (15.6 × 10^{-2} mmy^{-1}), compared to those produced at different current densities as may be seen in Table 8.2. This least corrosion rate of Co-Fe $_{1.0}$ alloy coating may be attributed to its highest Co content (Table 8.2).

8.3.2 Development of multilayer Co-Fe alloy coatings

Knowing the fact that the physico-mechanical properties, including corrosion behavior of electrodeposited metal/alloy coatings can be improved to many fold of its magnitude by composition modulated multilayer method (Benaicha et al. 2016; Tsyntasaru et al. 2012). Hence, corrosion performance of monolayer Co-Fe alloy coatings was tried to improve further by multilayer technique, using the same bath. Accordingly, multilayer coatings of Co-Fe alloy, having different configurations have been developed by selection different sets of cyclic cathode current densities (CCCD's). CCCD's are current densities of different heights,

between which cathode pulse is made to cycle repeatedly to form Co-Fe alloy coatings in layered pattern on the substrate as shown in Figure 8.9.

8.3.2.1 Optimization of cyclic cathodic current densities (CCCD's)

The preliminary investigation on electrodeposition and characterization of Co-Fe alloy coatings indicated that the proposed bath could generate coatings with varying composition, morphology, and phase structure, as detailed in Table 8.1. The composition of Co-Fe alloy ranged from 13.1 to 19.6 wt.% of Fe over current densities from 1.0 to 4.0 A/dm^2. To enhance the anticorrosion performance of monolayer Co-Fe alloy coatings through a multilayer approach, coatings were deposited at different sets of Cyclic Cathode Current Densities (CCCDs). To determine the optimal composition of alternate layers in multilayer coatings for the highest corrosion resistance, coatings were developed at various CCCD sets. Initially, coatings were developed with ten layers (chosen arbitrarily) at three different CCCD sets, and their corrosion performances were evaluated using Electrochemical Impedance Spectroscopy (EIS) and potentiodynamic polarization techniques. The corresponding Nyquist and Tafel plots for Co-Fe alloy coatings with ten layers, utilizing different CCCD sets, are presented in Figures 8.8 and 8.9, respectively. The corrosion data are reported in Table 8.3. This coating procedure at various CCCD sets provides a means to optimize the composition of individual layers, aiming for the best configuration of multilayer coatings with the highest corrosion resistance.

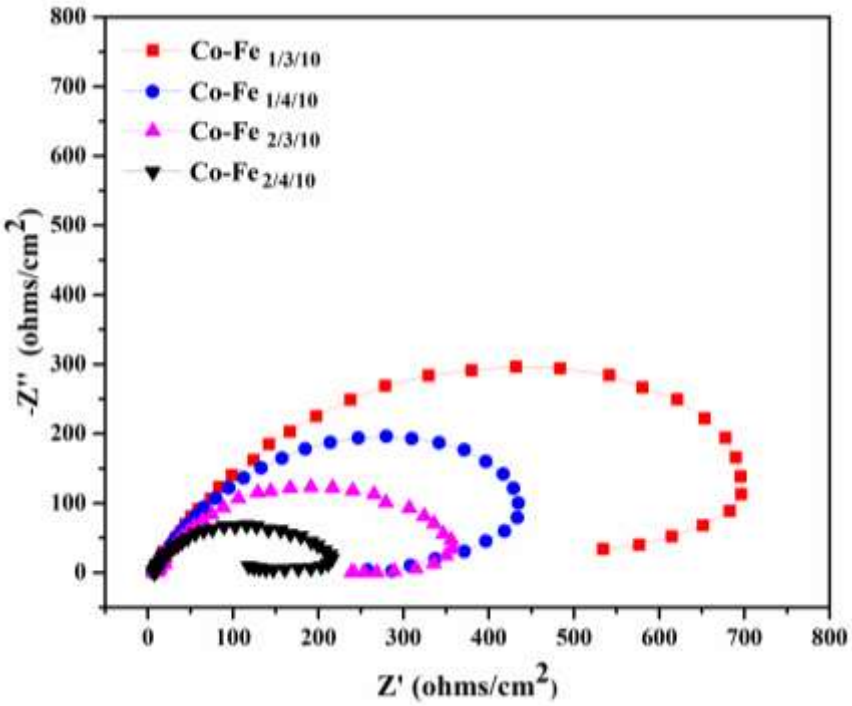

Figure 8.8 *- Nyquist plots of multilayer Co-Fe alloy coatings having 10 layers, deposited at different CCCD's from the same optimal bath*

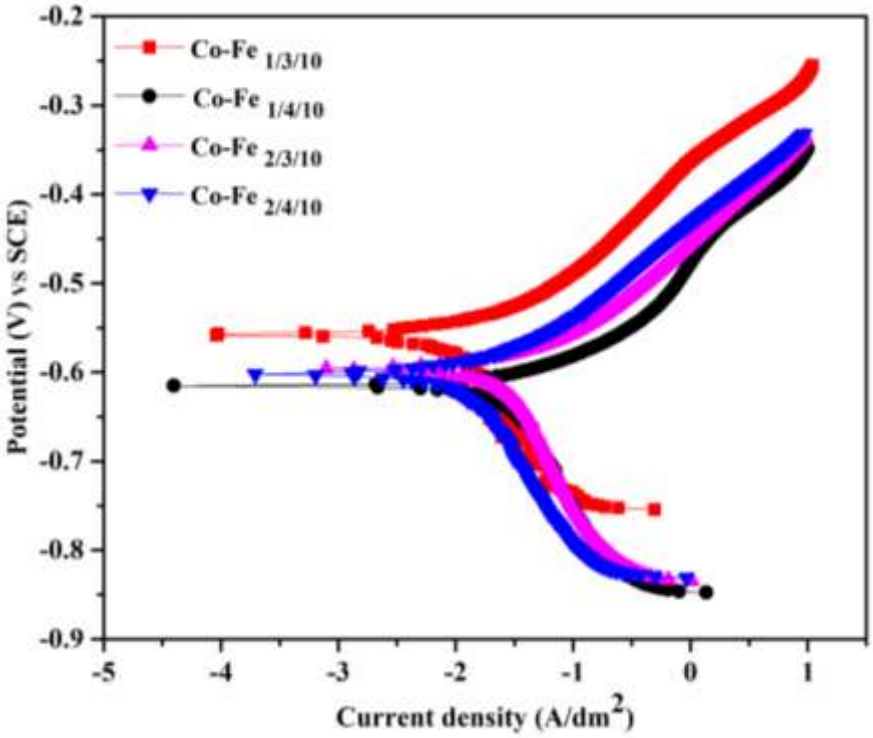

Figure 8.9 *- Tafel's plots of multilayer Co-Fe alloy coatings having 10 layers, deposited at different CCCD's from the same optimal bath*

Table 8.3 - Corrosion data of multilayer Co-Fe alloy coatings having 10 layers of alloys, having different compositions, deposited from the optimal bath

Coating configuration	wt.% of Co	wt.% of Fe	- E_{corr} (mV vs. SCE)	i_{corr} ($\mu A\ cm^{-2}$)	CR $\times 10^{-2}$ (mmy^{-1})	R_p
Co-Fe $_{1/3/10}$	86.97	13.03	-509.4	13.8	15.0	2413
Co-Fe $_{1/4/10}$	84.74	15.26	-625.4	22.5	22.4	1789
Co-Fe $_{2/3/10}$	82.65	17.35	-597.5	19.4	21.1	1854
Co-Fe $_{2/4/10}$	80.49	19.51	-608.5	17.5	18.2	2099

This procedure of coating involving three different sets of Cyclic Cathode Current Densities (CCCDs) offers a means to optimize the composition of individual layers for the best configuration with the highest corrosion resistance. The corrosion data presented in Table 8.3 reveal that all multilayer Co-Fe alloy coatings exhibit lower Corrosion Rates (CR) compared to their monolayer counterparts deposited from the same bath. Moreover, among the various sets of CCCDs tested, the configuration with CCCDs at 1.0 and 3.0 A/dm^2 demonstrates the least CR. This finding suggests that the layers in the Co-Fe $_{1.0/3.0/10}$ configuration have the most optimal composition, resulting in the coating with the highest corrosion resistance. Consequently, 1.0 and 3.0 A/dm^2 have been selected as the optimal CCCDs for further layering.

8.3.2.2 Optimization of number of layers

It is a well-known fact that many properties, including corrosion resistance, can be enhanced by increasing interfacial structures through a multilayer technique. To fully leverage this approach, Co-Fe alloy coatings were electrodeposited, considering 1.0 and 3.0 A/dm^2 as the optimized Cyclic Cathode Current Densities (CCCDs) of the bath. In other words, multilayer Co-Fe alloy coatings were developed by periodically pulsing the current between 1.0 and 3.0 A/dm^2 to form coatings with the desired number of layers. Accordingly, multilayer Co-Fe alloy coatings with 10, 60, 120, 300, and 600 layers were developed, and their corrosion behaviors were evaluated. The chosen number of layers (or the thickness of each layer) was selected to

examine the effect of increasing the number of layers on corrosion resistance, within the limitations of the power source used in this study.

8.3.2.3 Corrosion study

Electrochemical AC and DC methods were used to study the corrosion behavior of multilayer Co-Fe alloy coatings and their experimental results are reported below.

i) EIS study

The Electrochemical Impedance Spectroscopy (EIS) technique serves as a potent tool for determining the electrical properties of materials and understanding the kinetics involved in the charge transfer process at the electrode–electrolyte interface (Raveendran and Hegde 2021). In a standard EIS experiment, the complex electrical impedance (Z) of a sample is measured across a broad frequency range, typically spanning from kilohertz to millihertz (Park et al. 2019). The Nyquist plots of multilayer Co-Fe alloy coatings with varying numbers of layers are presented in Figure 8.10. The electrochemical impedance response depicted in the Nyquist plots clearly demonstrates that the polarization resistance (R_p) values progressively increase with the number of layers up to 120 layers, after which they start decreasing. The diminishing diameter of the capacitive loop associated with Co-Fe $_{1.0/3.0/300}$ signifies a reduction in the corrosion protection of the multilayer Co-Fe alloy coating as the number of layers increases. This observation emphasizes that while an increase in layering enhances corrosion resistance up to a certain point, excessive layering can lead to a decline in corrosion protection for multilayer coatings.

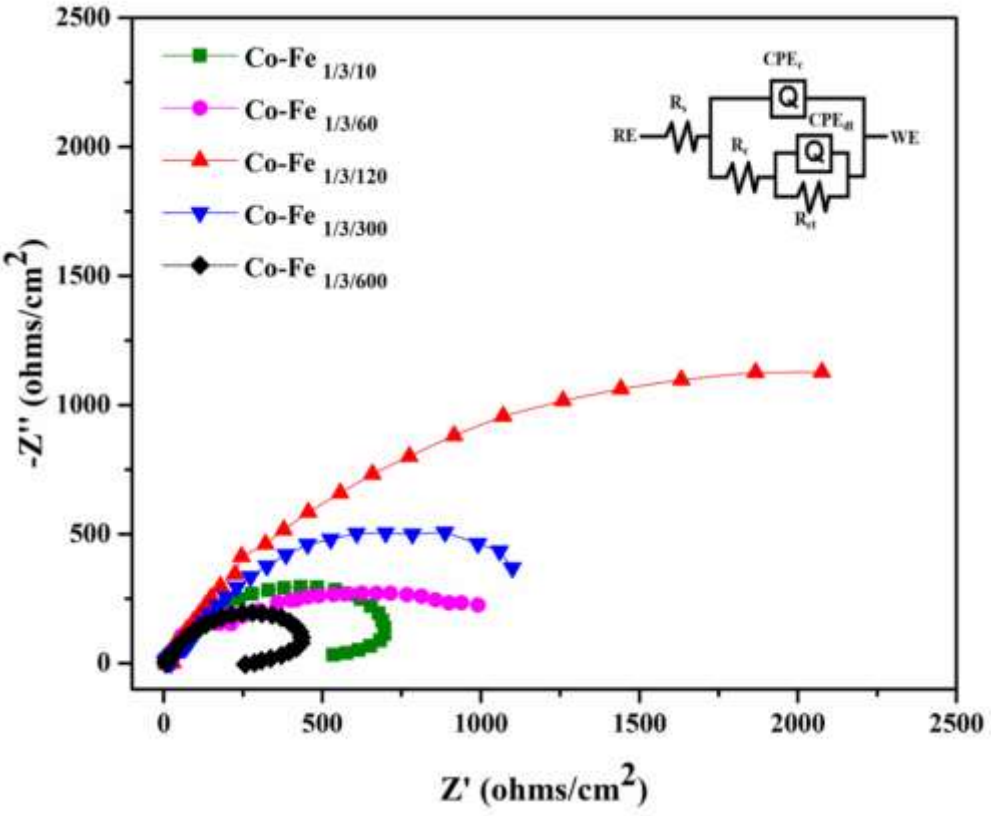

Figure 8.10 *- Nyquist plots of multilayer Co-Fe $_{1.0/3.0}$ alloy coatings having different number of layers deposited from optimized bath. Decrease in the value of charge transfer resistance (R_{ct}) may be seen as the layering is done beyond 120 layers*

The Nyquist plots' shapes suggest that the coatings of all configurations follow the same corrosion protection mechanism. The Co-Fe $_{1.0/3.0/120}$ configuration, with a large capacitive loop and high charge transfer resistance (R_{ct}) or polarization resistance, indicates that it is the most corrosion-resistant among all the examined coatings. The solution resistance (R_s) remained almost constant, as depicted in Figure 8.10. This consistency is attributed to the use of the same bath chemistry and cell configurations in the corrosion study. The R_p values show that the corrosion protection effectiveness of Co-Fe $_{1.0/3.0}$ coatings progressively increases with the number of layers up to120 layers, and then decreases

EIS data analysis typically involves fitting the data to an equivalent electric circuit (EEC) model. An equivalent circuit model is a combination of resistances, capacitances, and/or inductances, along with a few specialized electrochemical elements such as Warburg diffusion elements and constant phase elements. This combination aims to replicate the response of the electrochemical system when subjected to the same excitation signal (Jones DA, 2016). Hence,

an EEC is modelled to study the electrochemical behavior of the interface of Co-Fe $_{1.0/3.0/120}$ coating (optimal) in the test solution environment and is shown in the inset of Figure 8.10. Hence, from circuit elements corresponding to Co-Fe $_{1.0/3.0/120}$ coating, it may be seen that its improved corrosion resistance is due to the presence of its increased charge transfer resistance (R_{ct}).

Bode's plot is an alternative representation of the impedance in terms of the frequency represented directly along the X-axis. There are two types of Bode's diagram, called magnitude plot (log $|Z|$ *vs* log f) and phase angle plot (phase angle (θ) vs log f), describing the frequency dependencies of the $|Z|$ and phase, respectively. A Bode's plot is normally depicted logarithmically over the measured frequency range because the same number of points is collected at each decade. Accordingly, Bode's magnitude and phase angle plot of Co-Fe $_{1.0}$ and multilayer Co-Fe $_{1.0/3.0/120}$ coatings are drawn, and are shown in Figure 8.11. The highest value of log |Z| recorded by Co-Fe $_{1.0/3.0/120}$ alloy coatings at lower limit of the frequency (Figure 8.11 a) testimonies the fact that it is the most corrosion resistant compared to its monolayer alloy coatings. It is evidenced further by Bode's phase angle (θ) plot shown in Figure 8.11(b). It may be noted that Co-Fe $_{1.0/3.0/120}$ coating is more capacitive in nature (with highest negative phase angle value) compared to its monolayer counterpart. Thus, Bode's both magnitude and phase angle plot reveals that Co-Fe $_{1.0/3.0/120}$ coating is much more corrosion resistant than its monolayer counterpart.

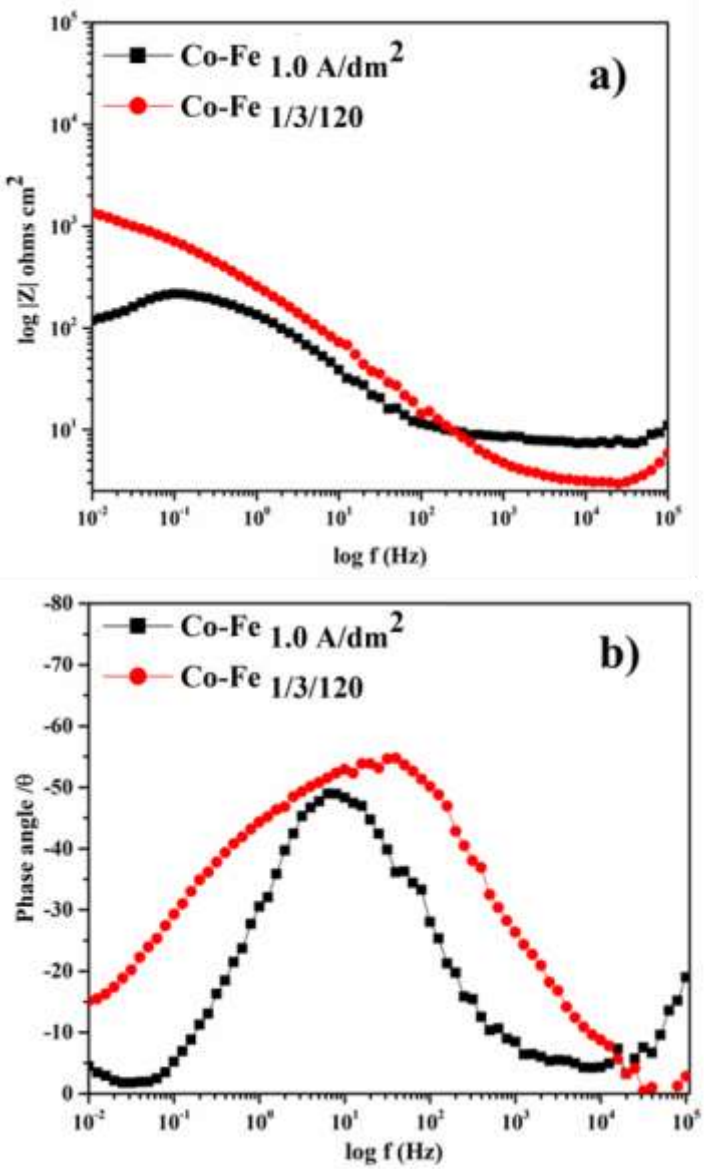

Figure 8.11- *Bode's plots of Co-Fe $_{1.0}$ and Co-Fe $_{1.0/3.0/120}$ alloy coatings deposited from the same bath for same duration: a) Magnitude plots, and b) phase angle plots*

ii) Potentiodynamic polarization study

The potentiodynamic polarization behavior of multilayer Co-Fe alloy coatings, with varying numbers of layers, was investigated and depicted in Figure 8.12. Corrosion rates (CRs) were determined using Tafel's extrapolation method, and the corrosion data for different multilayer configurations are presented in Table 8.5. For comparison, the CRs of monolayer Co-Fe deposited at 1.0 A/dm^2 are also provided in Table 8.5. The electrochemical corrosion data, obtained through Tafel's extrapolation method, supports the conclusion that the anticorrosion

performance of multilayer Co-Fe alloy coatings improves with an increasing number of layers, up to 120 layers. However, beyond 120 layers, there is a decline in anticorrosion performance. The configuration Co-Fe $_{1.0/3.0/120}$ exhibits the least CR, indicating that it represents the optimal coating configuration for superior corrosion resistance. The total thickness of the Co-Fe $_{1.0/3.0/120}$ multilayer alloy coating is approximately 6 μm, with an estimated average thickness of individual layers in the range of 50 nm. This suggests that the enhanced anticorrosion performance is attributed to the presence of alternate layers with different compositions in the nanometer thickness range. It's noteworthy that the observed increase in CR at a high degree of layering (300 layers corresponding to Co-Fe $_{1.0/3.0/120}$ coating) may be linked to layer diffusion effects. In simpler terms, at higher degrees of layering, multilayer coatings tend to behave more like monolayers. Therefore, the optimal anticorrosion performance is achieved with a balanced layering configuration, and excessive layering may lead to a decrease in performance due to layer diffusion effects (Yogesha et al. 2011) (Raveendran and Hegde 2021) (Shetty and Chitharanjan Hegde 2017).

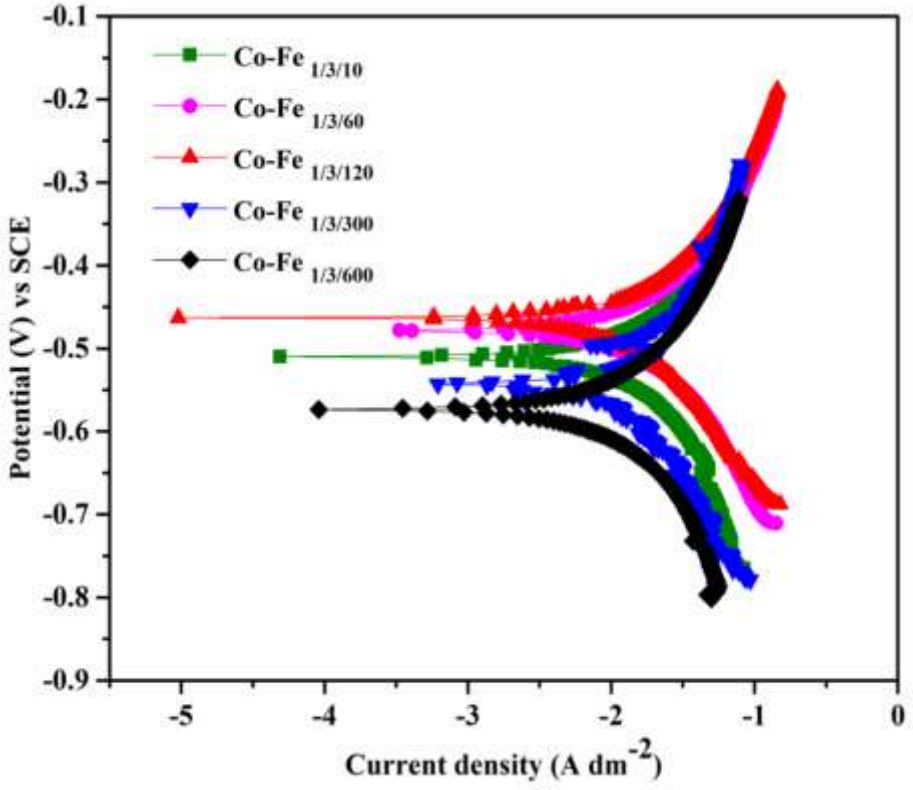

Figure 8.12 - *Tafel's plots of multilayer Co-Fe $_{1.0/3.0}$ alloy coatings having different number of layers deposited from optimized bath*

Table 8.4 - Corrosion data of multilayer Co-Fe alloy coatings having different number of layers deposited from the optimized bath.

Coating configuration	- E_{corr} (mV vs. SCE)	i_{corr} ($\mu A\ cm^{-2}$)	CR $\times 10^{-2}$ (mmy^{-1})	R_p	χ^2 (10^{-3})
Co-Fe $_{1/3/10}$	-510.3	13.8	15.0	2412	4.89
Co-Fe $_{1/3/60}$	- 451.6	14.1	10.3	3568	4.12
Co-Fe $_{1/3/120}$	- 463.9	4.5	4.9	6040	3.38
Co-Fe $_{1/3/300}$	-539.2	10.3	11.2	5396	5.64
Co-Fe $_{1/3/600}$	-544.7	14.4	15.7	2038	4.92
Co-Fe $_{1.0\ A/dm^2}$	-406.6	14.4	15.6	1735	5.16

Hence, it may be summarized that the anticorrosion performance of multilayer alloy coatings tends to increase with the number of layers. However, when the layers are excessively thinned (by increasing the number of layers), the anticorrosion performance may decrease due to the diffusion of layers. The optimal number of layers for achieving the best anticorrosion performance is a function of the bath, depending on the specific chemistry involved in it. It suggests that there is an optimal limit between layering and thickness that needs to be considered for achieving optimal corrosion resistance.

8.4 Comparison of corrosion behavior of monolayer and multilayer Co-Fe alloy coatings

The anticorrosion behavior of monolayer Co-Fe and multilayer Co-Fe alloy coatings (deposited under optimal conditions) through impedance and Tafel's methods are shown in Figure 8.13. It may be noted from both impedance and Tafel's behaviors that monolayer Co-Fe alloy coatings, deposited at 1.0 A/dm^2 and 3.0 A/dm^2 are more corrosive than Co-Fe $_{1.0/3.0/120}$ alloy coating. It is supported by the change of i_{corr} value and E_{corr} values (in Tafel's plot), and charge transfer resistance (R_{ct}) value in the case of impedance plot. The Nyquist plots shown in Figure 8.13(a) testimonies that Co-Fe $_{1.0/3.0/120}$ alloy coating has far better corrosion stability compared to both monolayer Co-Fe $_{1.0\ A/dm^2}$ and Co-Fe $_{3.0\ A/dm^2}$ alloy coating. The actual CR's

corresponding to monolayer Co-Fe $_{1.0\ A/dm^2}$ and Co-Fe $_{3.0\ A/dm^2}$ and multilayer Co-Fe $_{1.0/3.0/120}$ alloy coating, under optimal conditions are given in Table 8.4.

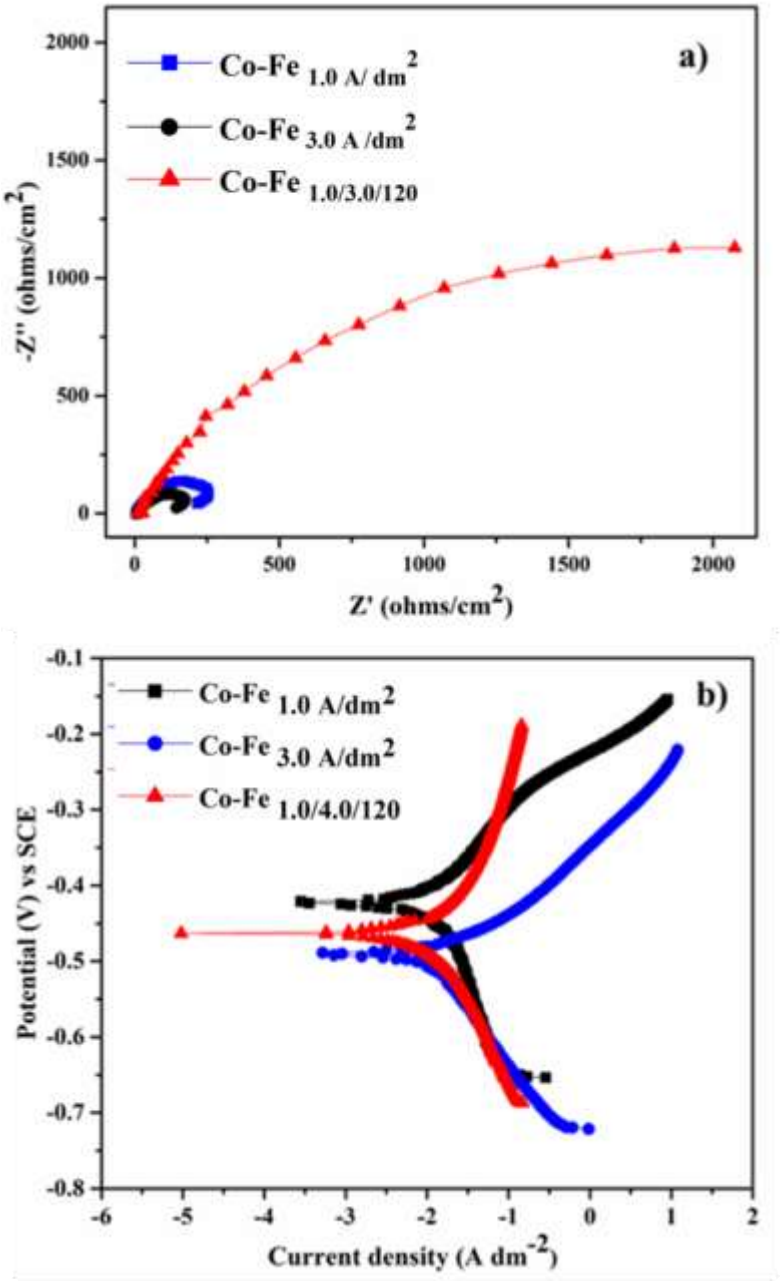

Figure 8.13 *- Comparison of anticorrosion behavior of multilayer Co-Fe $_{1.0/3.0/120}$ alloy coating with those of monolayer Co-Fe $_{1.0\ A/dm^2}$ and Co-Fe $_{3.0\ A/dm^2}$ alloy coating through: (a) Nyquist plots and (b) Tafel's plots*

8.5 Mechanism of corrosion

The corrosion protection mechanism for multilayer Co-Fe alloy coatings, as compared to its monolayer counterpart, is elucidated through a visual representation in Figure 8.14. The electrodeposited Co-Fe alloy coatings exhibit varying degrees of homogeneity based on the type of current pulses applied. In the case of the monolayer Co-Fe alloy coating, denoted as Co-Fe $_{1.0}$, where the coating is uniform or non-structured, corrosion progresses unhindered, allowing the electrolyte (corrosion medium) to rapidly reach the substrate, as depicted in Figure 8.14 (a). However, with the multilayer coating developed under optimal conditions, represented as Co-Fe $_{1.0/3.0/120}$, the presence of well-defined boundaries between layers becomes crucial. This characteristic enables the electrolyte to disperse both laterally and vertically, as illustrated in Figure 8.14 (b). The distinct layers in the multilayer coating contribute to enhanced corrosion protection by slowing down the penetration of the electrolyte, providing a more effective barrier against corrosion compared to the homogeneous monolayer coating**.**

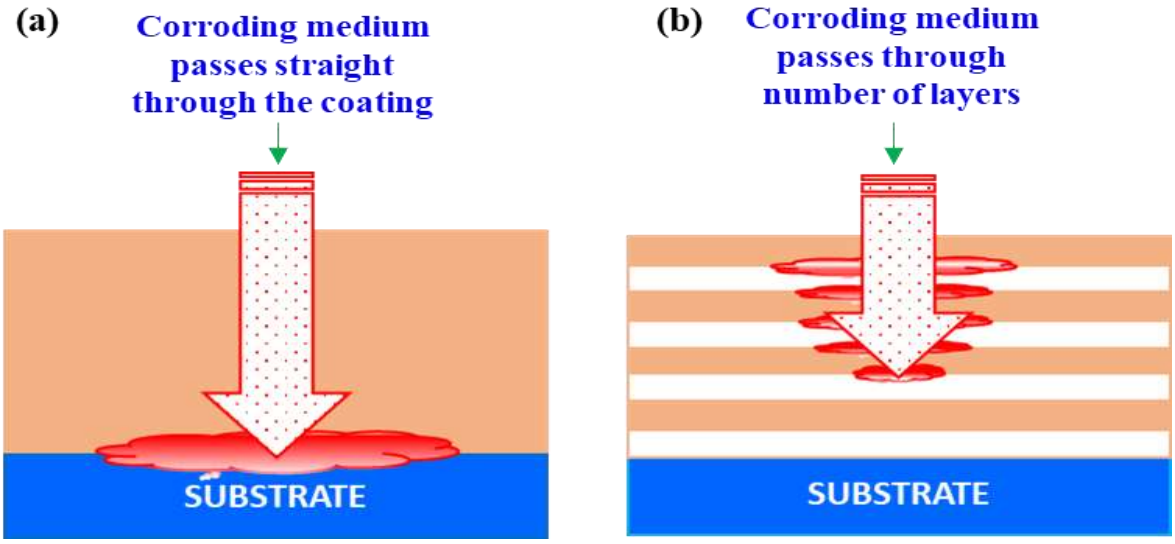

Figure 8.14 *- Representative diagram showing the mechanism of corrosion in Co-Fe alloy coatings, deposited under different conditions: (a) direct attract of the substrate in monolayer coating, (b) delayed corrosion due to layered structure of coating*

The multilayer structure exhibits a notable advantage in corrosion resistance compared to monolayer coatings. In Figure 8.14 (b), the illustration demonstrates that the lower layer of the multilayer structure comes in contact with the electrolyte only after the destruction of the

top layers. The corrosion process spreads gradually over the interface, layer by layer, and the substrate gets exposed to the corrosion medium only after the destruction of all layers. This characteristic results in a slower corrosion process compared to monolayer coatings. The increased anticorrosion performance of the multilayer coating with the number of layers, up to a certain limit, is attributed to the growing number of interfaces formed due to layering. Therefore, it can be concluded from Figure 8.14 (b) that the time required for the electrolyte to reach the substrate by penetrating through the multilayer coating is much greater than that through the monolayer coating. This delayed penetration contributes to enhanced corrosion resistance in the multilayer structure.

8.6 Conclusions

In the pursuit of a new bath for development of Co-Fe alloy coatings of high corrosion resistance, a new electrolytic bath has been proposed. Deposition conditions for development of monolayer Co-Fe alloy coatings showing highest corrosion resistance has been optimized. The anticorrosion behavior of monolayer Co-Fe alloy coating has been further improved by composition modulated multilayer approach from the same bath using square current pulses. The experimental results of investigation have evidenced the following facts:

1. The corrosion protection efficiency of monolayer Co-Fe alloy coatings have improved further by composition modulated multilayer (CMM) approach by proper selection of cyclic cathode current densities (CCCD's).
2. Multilayer Co-Fe alloy coatings have been developed by periodic modulation of current density, during the process of deposition. The composition of alternate layers can be controlled by proper modulation of current density (pulse amplitude) and duration of pulse (time), respectively.
3. The improved corrosion performance of multilayer Co-Fe alloy coatings were attributed to the increased number of interfaces, affected due to formation of layers of alloys having low and high Fe content, due to pulsed current density during deposition.
4. Under optimal condition, multilayer Co-Fe alloy coating, having Co-Fe $_{1.0/3.0/120}$ configuration is approximately three times more corrosion resistant than its monolayer coating, deposited from the same bath for same duration.

5. The corrosion stability of multilayer Co-Fe alloy coatings was found to be increased with degree of layering up to one level; and then decreased due to diffusion of layers.
6. Early attainment of homogeneity of multilayer Co-Fe alloy coating, with only 120 layers may be attributed by the limitation of small compositional change with current density.
7. Increase of CR of multilayer Co-Fe coating at higher degree of layering (after 120 layers) is due the diffusion of layers, as no significant compositional change of individual layers are likely to happen due to rapid change of current pulse.

SUMMARY AND CONCLUSIONS

This chapter summarizes the experimental results of investigation on electrodeposition and characterization of three binary alloy baths of nickel and cobalt, namely Ni-Ti, Co-P and Co-Fe for improved corrosion protection and electro-catalytic activity, through different methods of electroplating. Optimal bath compositions and operating variables required for development of alloy coatings of good performance, for the intended purpose are proposed. The corrosion protection efficiency, or electro-catalytic activity, or both of monolayer, multilayer and magneto-electrodeposition (MED) approach are compared. The electro-catalytic activity of Ni-Ti and Co-P alloy coatings for water electrolysis of HER and OER were compared, with their Ag-nanoparticles embedded composite coatings. Improved corrosion resistance and electro-catalytic efficiency of alloy coatings, developed through modern methods of deposition was analyzed in the light of induced type co-deposition followed in baths. The experimental results are compared with a note for future work, at the end.

9.1 THESIS LAYOUT

Electroplating stands as a crucial technology, focusing on coating cost-effective and readily available base materials with layers of various metals/alloys that possess superior properties, thereby expanding their utility to applications that would otherwise be economically impractical. The field of alloy plating is evolving both incrementally and dramatically, propelled by the extensive range of potential alloy combinations and their practical applications. Considering the progress in the electrodeposition of binary/ternary alloy coatings of Fe-group metals (Ni, Co, and Fe), few binary alloy baths of Ni and Co with Ti and P have been tried to explore. In this direction, three new Ni and Co based alloy baths, namely Ni-Ti, Co-P and Co-Fe have been formulated to develop their alloy coatings of good corrosion resistance and electro-catalytic efficiency. Optimization of bath compositions, and operating variables have been done using Hull cell method. The current densities have been optimized for development of their alloy coatings showing best performance against corrosion and good electro-catalytic activity of electro-splitting of water (as cathode and anode material for HER

and OER). The corrosion resistance of their conventional monolayer alloy coatings, developed using direct current (DC) were tried to improve further through modern methods of electroplating, namely magneto-electrodeposition (MED) and composition modulated multilayer (CMM), or simply *multilayer* method. The flow chart of research work embodied in the titled thesis is presented in Figure 9.1.

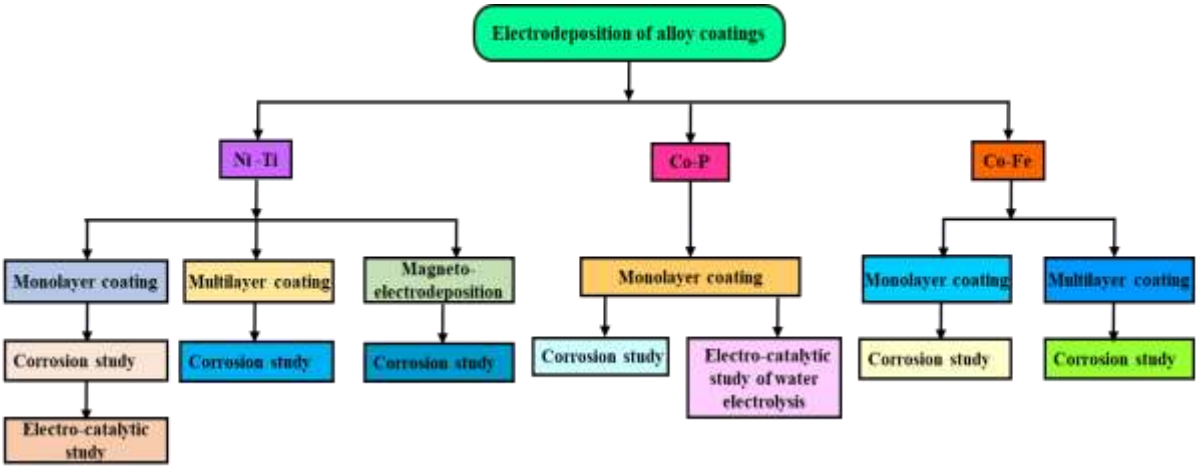

***Figure 9.1**- Flow chart of the research work presented in the thesis*

9.2 EXPERIMENTAL FRAMEWORK

9.2.1 Optimization of Ni-Ti, Co-P and Co-Fe alloy baths

Three electrolytic baths of binary alloys Ni-Ti, Co-P and Co-Fe have been proposed. The bath composition and operating variables required for development of their monolayer alloy coatings have been formulated. The optimal conditions necessary to obtain bright, uniform and good quality Ni-Ti, Co-P and Co-Fe alloy coatings on mild steel (MS) substrate have been formulated by standard Hull cell method (Kanani 2004). The bath composition and deposition parameters of three baths, required for development of their bright, uniform and metallic coatings is given in Table 9.1.

9.2.2 Electrodeposition of conventional monolayer alloy coatings

After formulation of three baths, namely Ni-Ti, Co-P and Co-Fe, their monolayer (conventional or homogeneous) alloy coatings have been developed using direct current (DC), or constant current. Then, knowing the fact that current density plays an important role on the composition and performance of alloy coatings they have developed at different current densities.

Table 9.1- Bath compositions and deposition parameters for Ni-Ti, Co-P and Co-Fe baths arrived by standard Hull cell method

Bath Constituents (g L^{-1})	Ni-Ti bath	Co-P bath	Co-Fe bath
Nickel sulphate	49.8	-	-
Titanium oxy sulpahte ($TiOSO_4$)	39.9	-	-
Cobalt chloride hexahydrate	-	13.2	-
Sodium hypophosphate ($NaPO_2H_2$)	-	22.5	-
Cobalt sulphate tetrahydrate	-	-	152
Ferrous sulphate	-	-	16
Trisodium citrate dihydrate	16.5		104.5
Potassium sodium tartarate	-	30	-
Ammonium chloride	-	49.5	8.0
Glycerol (mL/L)	3.3	-	-
Glycine	-	4.4	1.0
Deposition parameters			
Bath pH	4.0	8.5	3.5
Current density range	1.0- 4.0 Adm^{-2}	1.0- 4.0 Adm^{-2}	1.0-4.0 Adm^{-2}
Temperature		303K	
Anode		Graphite bar	
Cathode (substrate)		Mild steel or copper sheet/rod	
Deposition time		600 s	

Accordingly, monolayer alloy coatings of Ni-Ti, Co-P and Co-Fe alloy was carried out at different current densities, and optimal current density for deposition of their coatings, showing best performance against corrosion was identified.

Then, the corrosion behavior of these monolayer alloy coatings were further tried to improve by modern methods of electrodeposition, namely composition modulated multilayer (CMM) and magneto-electrodeposition (MED) methods. In addition, the electro-catalytic activity of Ni-Ti and Co-P alloy coatings were studied tested few alloy coatings were studied by depositing them on the tip of copper rod (1.0 cm^2 area). The scheme of the experimental work carried out for improving corrosion behavior of monolayer alloy coatings by other approaches is shown in Figure 9.2.

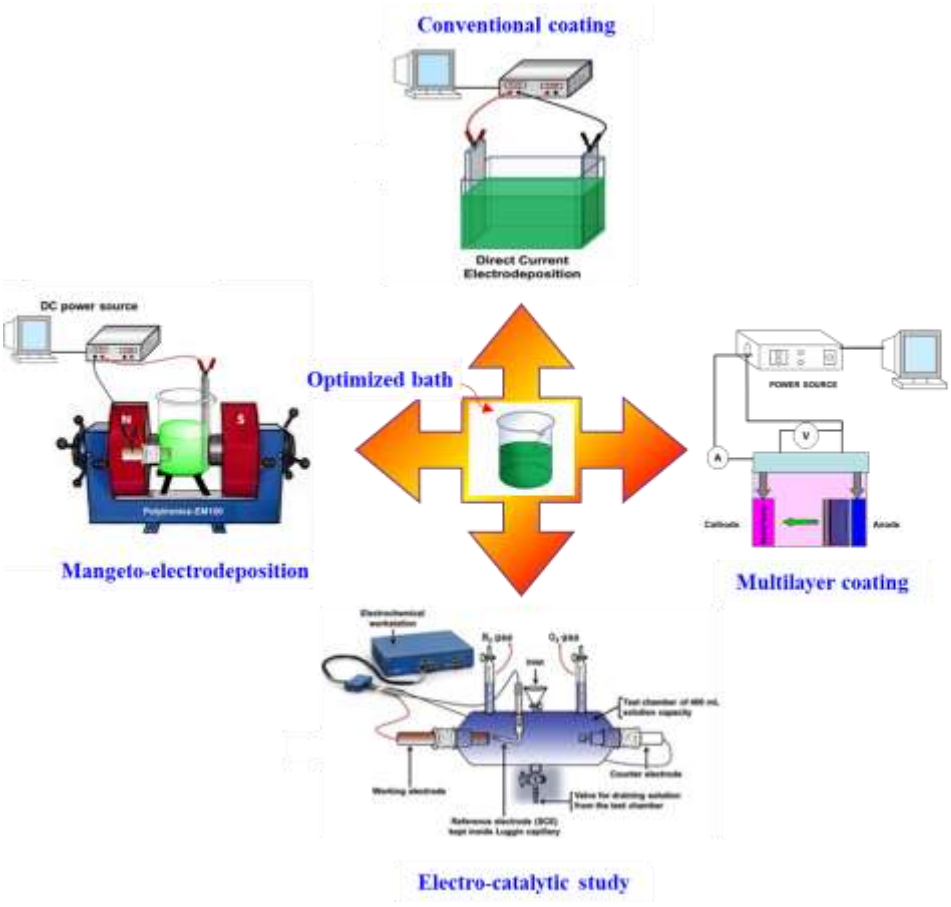

Figure. 9.2- Scheme showing different methods of electrodeposition to achieve better performances of alloy coatings for both corrosion and electro-catalytic activity using same optimal bath

9.2. 3 Development of Multilayer Ni-Ti and Co-Fe coatings

The corrosion protection efficiency of monolayer Ni-Ti and Co-Fe alloy system was tried to enhance by multilayer approach. Multilayer Ni-Ti and Co-Fe alloy coatings of different

configurations, having alternatively different alloy composition and thickness were developed by setting up the power source to switch between two cathode current density values. This approach was found to increase the corrosion resistance only up to a certain number of layers, and thereafter no improvement in its corrosion resistance was found.

9.2.4 Magneto-electrodeposition of Ni-Ti alloy coatings

The benefit of magneto-electrodeposition was tried to explore to improve the corrosion resistance property of conventional monolayer alloy coatings. Here, magnetic field (*B*) effect was induced parallel to the process of deposition. The MED Ni-Ti alloy coatings was developed by superimposing magnetic field *B*, simultaneously to the process of deposition by keeping the current density as constant (optimal). The magneto-electrodeposited (MED) Ni-Ti alloy coating was carried out at different intensities of *B*, applied both parallel and perpendicular to the direction of flow of ions in the bath.

9.3 SIGNIFICANT FINDINGS

9.3.1 Corrosion study of electrodeposited alloy coatings

The experimental results embodied in thesis are around the corrosion protection efficiency of three binary alloy coatings from Ni/Co-based baths, namely Ni-Ti, Co-P and Co-Fe. All depositions were accomplished for same duration of 10 min, and their corrosion protection efficiency have been studied in 3.5% NaCl medium, for comparison purpose. The current density at which conventional monolayer Ni-Ti, Co-P and Co-Fe coatings showed highest corrosion protection was considered as the optimal current density. Taking that optimal current density, as the deposition current density, corrosion protection efficiency of monolayer Ni-Ti, Co-P and Co-Fe alloy coatings were tried to improve by composition modulated multilayer, or simply multilayer coating technique. Multilayer coating of different configurations (having different number of layers, with alternatively different alloy composition) were developed by setting up the power source to switch between two cathode current density values. Hence, an optimal configuration was identified for best performance of Ni-Ti and Co-Fe alloy coating, against corrosion. A comparative account of bath pH, current density, coating configuration and corrosion rates of Ni-Ti, Co-P and Co-Fe alloy coatings are summarized in Table 9.2

Table 9.2- Comparative account of corrosion rates (CR's) of Ni-Ti, Co-P and Co-Fe alloy coatings developed from their optimal baths through different electrodeposition techniques (for duration of 10 minutes)

Alloy coating	Ni-Ti	Multi-layer Ni-Ti	MED Ni-Ti	Co-P	Co-Fe	Multi-layer Co-Fe
Bath pH	4.0			8.5	3.5	
Coating configuration	4.0 Adm^{-2}	Ni-Ti $_{2/4/120}$	MED⊥ Ni-Ti $_{0.3T}$	-	1.0 Adm^{-2}	Co-Fe $_{1/3/120}$
i_{corr} ($\mu A\ cm^{-2}$)	13.8	2.5	2.1	28.9	14.4	4.5
$CR\times10^{-2}(mmy^{-1})$ *(in 3.5% NaCl)*	14.0	2.62	2.56	34.9	15.6	4.9

Similarly, it may be seen that MED Ni-Ti with coating configuration MED ⊥ Ni-Ti $_{0.3T}$ and CMM-ED Ni-Ti and Co-Fe alloy coatings with Ni-Ti $_{2.0/4.0/120}$ and Co-Fe $_{1.0/3.0/120}$ configuration was found to be 7 times and 4 times more corrosion resistant than their respective conventional monolayer counterparts.

To summarize, with objective of developing a better corrosion resistant Co/Ni based alloy coatings from three baths, namely Ni-Ti, Co-P and Co-Fe using different modern methods of electrodeposition, like magneto-electrodeposition and multilayer method, a good degree of success was achieved. The corrosion performance of all coatings, deposited for same duration (600 s) were evaluated in common corrosion medium. It was concluded that corrosion performance of monolayer coatings of both alloys can be improved to many folds better by both multilayer and MED approaches, as evidenced by their CR values. Thus from corrosion study, it was found that CR's of monolayer Co/Ni-based alloy coatings (developed by conventional method using DC) can be decreased to many folds of their magnitude by following modern methods of electrodeposition, namely magneto-electrodeposition (MED)

and multilayer methods. It is evident from the plot of CR vs. different alloy coatings, shown in Figure 9.3.

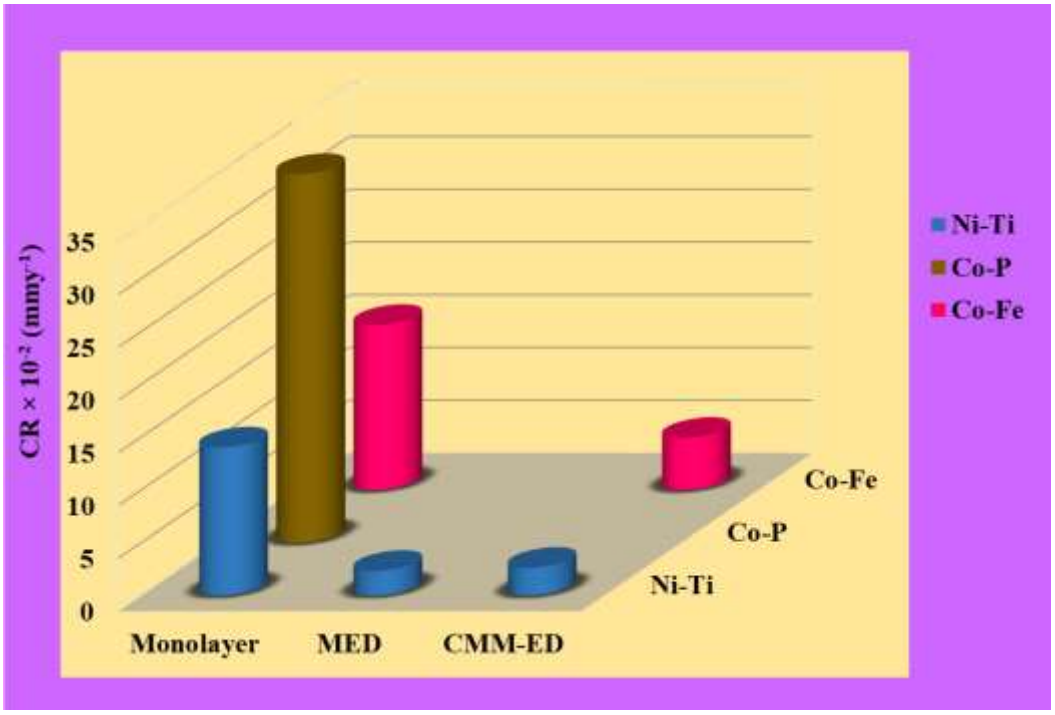

Figure. 9.3- *Histogram showing the CR's of monolayer Ni-Ti, Co-P, Co-Fe, MED Ni-Ti and multilayered Co-Fe, Ni-Ti alloy coatings studied in 3.5% NaCl medium (all at optimal condition)*

9.3.2 Electro-catalytic performance of alloy coatings

Electro-catalytic study of electrodeposited Ni-Ti and Co-P alloy, and their composite coatings developed from the proposed optimal baths were studied. The electro-catalytic efficiency of alloy coatings were studied for electro-splitting of water, by using them as cathode (for HER) and anode (for OER) in 1.0 M KOH medium. Electro-catalytic potential, in terms of both HER and OER were quantitatively assessed by measuring the amount of H_2 and O_2 evolved by the downward displacement of electrolyte from the graduated burette fitted to the custom-made alkaline water electrolyser. CV and CP methods were used to evaluate the electro-catalytic parameters and stability of the electrode material (electrodeposited alloy coatings), respectively. The experimental conditions used for electro-catalytic study of different coatings are shown in Table 9.3. Binary alloys, namely Ni-Ti and Co-P alloy coatings deposited at different current densities and were tested for their electro-catalytic efficiency. The effect of

metal contents on the electro-catalytic performances, in terms of HER and OER, have been studied. It was observed that the alloy coatings with higher wt. % of Ni in the deposit (obtained at higher current density) showed better activity for HER, compared to OER. Further, the effect of addition of Ag-nanoparticles into Ni-Ti and Co-P baths studied. They have been added at different concentrations, and optimal concentration for best electro-catalytic activity has been proposed.

Table 9.3- Experimental conditions employed for the electro-catalytic study of Ni-Ti, Co-P, Ni-Ti-Ag and Co-P-Ag composite coatings

Operating parameters	*Working conditions*
Working electrode	Ni-Ti, Co-P, Ni-Ti-Ag and Co-P-Ag
Reference electrode	Saturated calomel electrode
Counter electrode	Platinized platinum
Medium	1.0 M KOH
Potential range for CV(HER)	0.0 to -1.6V
Potential range for CV(OER)	0.0 to 0.75V
Scan rate for CV study	0.05 V s^{-1}
Time chosen HER and OER study	300 s
Applied constant current for CP analysis during HER activity	-300 mA
Applied constant current for CP analysis during OER activity	+300 mA
Duration of CP study	1800 s

The electro-catalytic activity of Ni-Ti and Co-P alloy and their composite coatings were evaluated for alkaline water splitting applications, by taking 1.0 M KOH as the electrolyte, and alloy coatings as electrodes. *i.e*. as cathode for HER and anode for OER. Electro-catalytic efficiency for hydrogen evolution reaction (HER) and oxygen evolution reaction (OER) were studied by cyclic voltammetry (CV) and chronopotentiometry (CP) techniques. The

experimental results of electro-catalytic study, such as peak current density of both HER and OER (i_{pc} and i_{pa}) and the volume of H_2 and O_2 liberated during electrolysis is summarized in Table 10.4. The electro-catalytic performance of monolayer alloy/composite coatings, like Ni-Ti, Co-P, Ni-Ti-Ag and Co-P-Ag have been studied and their relative performances has been shown diagrammatically in Figure. 9.4.

Table 9.4 - Volume of H_2 and O_2 evolved, as a measure of their electro-catalytic activity on the surface of different alloy coatings during alkaline water electrolysis

Coating configuration	Optimal c.d. for HER (A/dm^2)	Volume of H_2 evolved in 300 s (cm^3)	Optimal c.d for OER (A/dm^2)	Volume of O_2 evolved in 300 s (cm^3)
Ni-Ti	4.0	11.9	1.0	6.0
Co-P	1.0	10.8	4.0	5.8
Ni-Ti-Ag	4.0	13.6	-	-
Co-P-Ag	1.0	12.2	-	-

The experimental findings from the investigation indicate that the corrosion protection effectiveness of monolayer Ni-Ti alloy coatings can be enhanced up to five times its original magnitude through the use of the MED and CMM-ED approaches. It is noteworthy that, among the three binary alloy coatings examined, the electrodeposition of Ni-Ti and Co-P alloy coatings is categorized as an induced type of co-deposition (Eliaz and Gileadi 2008). The induced type of co-deposition is characterized by the fact that plating variables, such as current density, have little or no effect on the composition of alloy coatings. Therefore, in the present study, it is observed that the composition, and consequently, the corrosion and electro-catalytic behaviors of Ni-Ti and Co-P alloy coatings exhibit minimal dependence on variations in current density.

Hence, under this limitation of induced type of co-deposition inherent of optimal Ni-Ti and Co-P baths, the corrosion protection of their monolayer alloy coatings could able to improve to only small extent by taking the advent of multilayer and magneto-electrodeposition

techniques. Electro-catalytic study revealed that binary alloy coatings for both HER and OER were found to be changed slightly with current density (Tables 6.1 and 6.2, and 7.5, 7.6). Thus, small improvement in the corrosion and electro-catalytic behavior (in terms of volume of both H_2 and O_2 gas evolved) of Ni-Ti and Co-P alloy coatings with current density may be attributed to the small change of their composition with current density, inherent of induced type co-deposition.

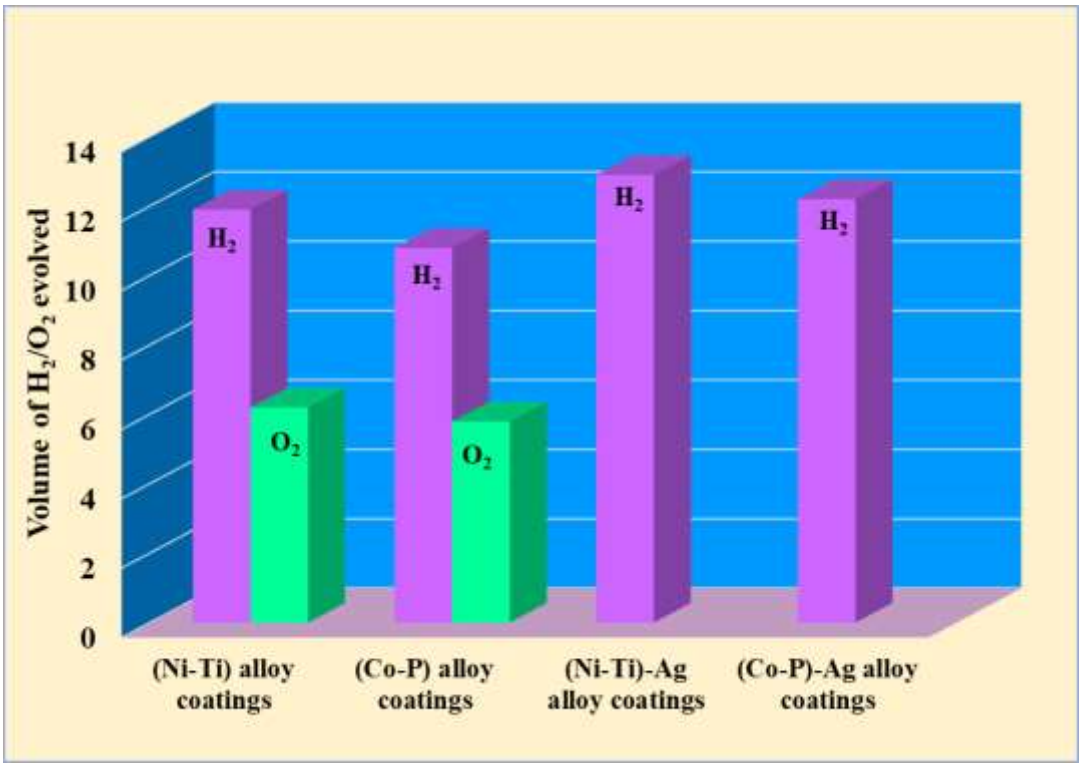

Figure. 9.4*-Relative electro-catalytic performance of conventionally electrodeposited Ni-Ti, Co-P, Ni-Ti-Ag and Co-P-Ag composite coatings obtained at their optimal coating configurations*

From the overall experimental investigation, it was observed that electrodeposited Ni-Ti alloy coatings are electrocatalytically more active towards both HER and OER compared to Co-P alloy coatings. Addition of Ag nanoparticles into Co-P alloy system enhanced its electro-catalytic activity towards HER, to bring its electro-catalytic activity on par with that of Ni-Ti alloy coatings.

9.4 CONCLUSIONS

Based on the experimental results of investigation carried out on electrodeposition of Ni-Ti, Co-P and Co-Fe alloy coatings from newly optimized baths through different methods of electrodeposition, and in the pursuit of achieving electrodeposits of higher efficiency of corrosion protection and better electro-catalytic efficiency for water electro-splitting, the following conclusions are drawn:

1. The proposed baths, namely of Ni-Ti, Co-P and Co-Fe alloy were found to develop bright, smooth and uniform coatings of better corrosion resistance, and good electro-catalytic activity.
2. The corrosion protection efficiency and electro-catalytic activity of monolayer alloy coatings from the proposed baths have been increased drastically through multilayer and magneto-electrodeposition (MED) techniques.
3. The developed Ni-Ti and Co-P alloy baths were found to follow induced type of co-deposition, whereas Co-Fe followed anomalous type of co-deposition, respectively over the current density range studied.
4. The corrosion performance of conventional monolayer electrodeposited Ni-Ti alloy coatings was improved about 7 times better through MED technique, by superimposing magnetic field (*B*), parallel and perpendicular during deposition.
5. The corrosion resistance property of monolayer Ni-Ti and Co-Fe alloy coating developed using citrate bath was increased substantially about 7 times and 4 times with composition modulated multilayer electrodeposition technique.
6. Electrochemical corrosion study demonstrated that the multilayer Co-Fe and Ni-Ti alloy coatings with 120 layers, represented as Ni-Ti $_{2.0/4.0/120}$ and Co-Fe $_{1.0/3.0/120}$ showed the least CR (2.6×10^{-2} mm y^{-1}) and (4.9×10^{-2} mm y^{-1}) compared to its monolayer counterpart, developed from same bath for same duration.
7. From the electro-catalytic study of Ni-Ti and Co-P alloy coatings for alkaline water splitting (1.0 M KOH) of HER and OER revealed that their electro-catalytic activity has strong dependency with their deposition current density determined composition, confirmed through cyclic voltammetry (CV) and chronopotentiometry (CP) study.

8. Addition of Ag nanoparticles into Ni-Ti and Co-P alloy matrix was found to increase its electro-catalytic activity of HER in alkaline water electrolysis, and is attributed to increased reactive sites for evolution of H_2.
9. The experimental results of different electrodeposited Ni-Ti and Co-P alloy, and their composite coatings showed that their corrosion stability and electro-catalytic efficiency bears a strong dependency on their properties
10. Thus, small improvement in both corrosion and electro-catalytic behavior (in terms of volume of both H_2 and O_2 gas evolved) of Ni-Ti and Co-P alloy coatings with current density may be attributed to induced type co-deposition.

*****

9.5 SCOPE FOR FUTURE WORK

- To study pulse electrodeposition of Ni-Ti, Co-P and Co-Fe alloys by varying the pulse frequency and duty cycle, and to examine their effect on their electrochemical properties.
- To study the electrodeposition of Ni-Ti-Fe, Co-P-Fe ternary alloy coatings, and to compare their corrosion and electro-catalytic behavior with that of their binary counter parts.
- To study the effect of ultrasound on the process of electrodeposition of above alloy coatings, and to optimize the deposition conditions of their monolayer and multilayer alloy coatings for peak performance against corrosion
- To examine the effect of two dimensional chalcogenides and metal organic frameworks in electro-codeposited Ni-Ti, Co-P and Co-Fe alloy coatings, and their electro-catalytic activity as bi-functional electrode in water electrolysis.

REFERENCES

Al-Bat'hi, S. A. M. (2015). "Electrodeposition of Nanostructure Materials." *Electroplating of Nanostructures*, M. Aliofkhazraei, ed., Rijeka: IntechOpen.

Amin, M. A., El-Bagoury, N., Saracoglu, M., and Ramadan, M. (2014). "Electrochemical and Corrosion Behavior of cast Re-containing Inconel 718 Alloys in Sulphuric Acid Solutions and the Effect of Cl-." *International Journal of Electrochemical Science*, 9(9), 5352–5374.

Anwar, S., Zhang, Y., and Khan, F. (2018). "Electrochemical behaviour and analysis of Zn and Zn–Ni alloy anti-corrosive coatings deposited from citrate baths." *RSC Adv.*, 8(51), 28861–28873.

Armyanov, S. (2000). "Crystallographic structure and magnetic properties of electrodeposited cobalt and cobalt alloys." *Electrochimica Acta*, 45(20), 3323–3335.

Aydoğmuş, T., Al-Zangana, N. J. F., and Kelen, F. (2020). "Processing of β-type biomedical ti74nb26 alloy by combination of hot pressing and high temperature sintering." *Konya Journal of Engineering Sciences*, 8(2), 269–281.

Bakhit, B., Akbari, A., Nasirpouri, F., and Hosseini, M. G. (2014). "Corrosion resistance of Ni–Co alloy and Ni–Co/SiC nanocomposite coatings electrodeposited by sediment codeposition technique." *Applied Surface Science*, 307, 351–359.

Barnett, S. M., Goldberg, K. I., and Mayer, J. M. (2012). "A soluble copper–bipyridine water-oxidation electrocatalyst." *Nature Chem*, 4(6), 498–502.

Bhat, R. S., Manjunatha, K. B., Prasanna Shankara, R., Venkatakrishna, K., and Hegde, A. Chitharanjan. (2020). "Electrochemical studies on the corrosion resistance of Zn–Ni–Co coating from acid chloride bath." *Appl. Phys. A*, 126(10), 772.

Bhat, R. S., Manjunatha, K. B., and Shetty, S. K. (2022). "Surface Features and Electrochemical Properties of Corrosion Resistant Ni–Ti Coatings." *Prot Met Phys Chem Surf*, 58(5), 1071–1076.

Braz Fernandes, F. M., Mahesh, K. K., Martins, R. M. S., Silva, R. J. C., Baehtz, C., and Von Borany, J. (2013). "Simultaneous probing of phase transformations in Ni-Ti thin film shape memory alloy by synchrotron radiation-based X-ray diffraction and electrical resistivity." *Materials Characterization*, 76, 35–38.

Brenner, A. (1963a). *Electrodeposition of alloys: principles and practice*. New York London: Academic Press.

Brenner, A. (1963b). "Electrodeposition of Alloys: PRINCIPLES and PRACTICE." *Electrodeposition of Alloys*, I, ii.

Brenner, A. (1963c). "Introduction to Induced Codeposition of Alloys Containing Tungsten, Molybdenum, Germanium, or Phosphorus." *Electrodeposition of Alloys*, Elsevier, 345–346.

Bull, S. J., and Jones, A. M. (1996). "Multilayer coatings for improved performance." *Surface and Coatings Technology*, 78(1–3), 173–184.

Bund, A., Koehler, S., Kuehnlein, H. H., and Plieth, W. (2003). "Magnetic field effects in electrochemical reactions." *Electrochimica Acta*, 49(1), 147–152.

Cavallotti, P. L., Vicenzo, A., Bestetti, M., and Franz, S. (2003). "Microelectrodeposition of cobalt and cobalt alloys for magnetic layers." *Surface and Coatings Technology*, 169–170, 76–80.

Chawa, G., Wilcox, G. D., and Gabe, D. R. (1998). "Compositionally Modulated Zinc Alloy Coatings For Corrosion Protection." *Transactions of the IMF*, 76(3), 117–120.

Cohen, U., Koch, F. B., and Sard, R. (1983). "Electroplating of Cyclic Multilayered Alloy (CMA) Coatings." *J. Electrochem. Soc.*, 130(10), 1987–1995.

Cullity, B. D. (1978). *Elements of x-ray diffraction*. Addison-Wesley series in metallurgy and materials, Reading, Mass: Addison-Wesley Pub. Co.

Eaton, P., and West, P. (2010). *Atomic Force Microscopy*. Oxford University Press.

Elias, L., Bhat, K. U., and Hegde, A. C. (2016). "Development of nanolaminated multilayer Ni–P alloy coatings for better corrosion protection." *RSC Adv.*, 6(40), 34005–34013.

Elias, L., and Hegde, A. C. (2016). "Synthesis and characterization of Ni-P-Ag composite coating as efficient electrocatalyst for alkaline hydrogen evolution reaction." *Electrochimica Acta*, 219, 377–385.

Eliaz, N., and Gileadi, E. (2008). "Induced Codeposition of Alloys of Tungsten, Molybdenum and Rhenium with Transition Metals." *Modern Aspects of Electrochemistry*, Modern Aspects of Electrochemistry, C. G. Vayenas, R. E. White, and M. E. Gamboa-Aldeco, eds., New York, NY: Springer New York, 191–301.

Fahidy, T. Z. (1983a). “Magnetoelectrolysis.” *Journal of applied electrochemistry*, 13(5), 553–563.

Fahidy, T. Z. (1983b). “Magnetoelectrolysis.” *J Appl Electrochem*, 13(5), 553–563.

Fahidy, T. Z. (2001). “Characteristics of surfaces produced via magnetoelectrolytic deposition.” *Progress in Surface Science*, 68(4–6), 155–188.

Fan, C., Piron, D. L., Sleb, A., and Paradis, P. (1994). “Study of Electrodeposited Nickel-Molybdenum, Nickel-Tungsten, Cobalt-Molybdenum, and Cobalt-Tungsten as Hydrogen Electrodes in Alkaline Water Electrolysis.” *J. Electrochem. Soc.*, 141(2), 382–387.

Frieze, A. S., Sard, R., and Weil, R. (1968). “Some Properties of Electroless Cobalt.” *J. Electrochem. Soc.*, 115(6), 586.

Ganesh, V., Vijayaraghavan, D., and Lakshminarayanan, V. (2005). “Fine grain growth of nickel electrodeposit: effect of applied magnetic field during deposition.” *Applied Surface Science*, 240(1–4), 286–295.

Girão, A. V., Caputo, G., and Ferro, M. C. (2017). “Application of Scanning Electron Microscopy–Energy Dispersive X-Ray Spectroscopy (SEM-EDS).” *Comprehensive Analytical Chemistry*, Elsevier, 153–168.

Gonsalves, C. N., and Hegde, A. C. (2021). “Development of corrosion-resistant Ni–Mo coatings from low-concentration bath: effect of magnetoconvection.” *Materials Science and Technology*, 37(14), 1187–1198.

Haseeb, A. S. M. A., Celis, J. P., and Roos, J. R. (1994). “Dual-Bath Electrodeposition of Cu/Ni Compositionally Modulated Multilayers.” *J. Electrochem. Soc.*, 141(1), 230–237.

Hegde, C., and Rao, V. R. (2014). “Effect of additives and operating parameters on deposit characters of Ni-Cd alloy.” *JEPT - Journal for Electrochemistry and Plating Technology*.

Hono, K., and Laughlin, D. E. (1989). “Evidence of phosphorous segregation in grain boundaries in electroless-plated Co-P thin film.” *Journal of Magnetism and Magnetic Materials*, 80(2–3), L137–L141.

Jakšić, J. M., Vojnović, M. V., and Krstajić, N. V. (2000). “Kinetic analysis of hydrogen evolution at Ni–Mo alloy electrodes.” *Electrochimica Acta*, 45(25–26), 4151–4158.

Jha, B. K., and Aina, B. (2016). “Role of induced magnetic field on MHD natural convection flow in vertical microchannel formed by two electrically non-conducting infinite vertical parallel plates.” *Alexandria Engineering Journal*, 55(3), 2087–2097.

Kanani, N. (2006). *Electroplating: basic principles, processes and practice*. Oxford: Elsevier Advanced Technology.

Kosta, I., Vicenzo, A., Müller, C., and Sarret, M. (2012). “Mixed amorphous-nanocrystalline cobalt phosphorous by pulse plating.” *Surface and Coatings Technology*, 207, 443–449.

Koza, J. A., Mogi, I., Tschulik, K., Uhlemann, M., Mickel, C., Gebert, A., and Schultz, L. (2010). “Electrocrystallisation of metallic films under the influence of an external homogeneous magnetic field—Early stages of the layer growth.” *Electrochimica Acta*, 55(22), 6533–6541.

Koza, J. A., Mühlenhoff, S., Żabiński, P., Nikrityuk, P. A., Eckert, K., Uhlemann, M., Gebert, A., Weier, T., Schultz, L., and Odenbach, S. (2011). “Hydrogen evolution under the influence of a magnetic field.” *Electrochimica Acta*, 56(6), 2665–2675.

Koza, J. A., Uhlemann, M., Gebert, A., and Schultz, L. (2008). “The effect of magnetic fields on the electrodeposition of CoFe alloys.” *Electrochimica Acta*, 53(16), 5344–5353.

Krause, A., Koza, J., Ispas, A., Uhlemann, M., Gebert, A., and Bund, A. (2007). “Magnetic field induced micro-convective phenomena inside the diffusion layer during the electrodeposition of Co, Ni and Cu.” *Electrochimica Acta*, 52(22), 6338–6345.

Krishnan, K. S. R., Srinivasan, K., and Mohan, S. (2002). “Electrodeposition of Compositionally Modulated Alloys—An Overview.” *Transactions of the IMF*, 80(2), 46–48.

La Niece, S., and Craddock, P. T. (Eds.). (1993). *Metal plating and patination: cultural, technical, and historical developments*. Oxford ; Boston: Butterworth-Heinemann.

Leisner, P., Nielsen, C. B., Tang, P. T., Dörge, T. C., and Møller, P. (1996a). “Methods for electrodepositing composition-modulated alloys.” *Journal of materials processing technology*, 58(1), 39–44.

Leisner, P., Nielsen, C. B., Tang, P. T., Dörge, T. C., and Møller, P. (1996b). “Methods for electrodepositing composition-modulated alloys.” *Journal of Materials Processing Technology*, 58(1), 39–44.

Li, R., Hou, Y., Dong, Q., Su, P., Ju, P., and Liang, J. (2018). “Wear and corrosion resistance of Co–P coatings: the effects of current modes.” *RSC Adv.*, 8(2), 895–903.

Lima, A. S., Salles, M. O., Ferreira, T. L., Paixão, T. R. L. C., and Bertotti, M. (2012). “Scanning electrochemical microscopy investigation of nitrate reduction at activated copper cathodes in acidic medium.” *Electrochimica Acta*, 78, 446–451.

Lingane, P. J., and Peters, D. G. (1971). “Chronopotentiometry.” *C R C Critical Reviews in Analytical Chemistry*, 1(4), 587–634.

Liu, Y., Li, H., and Li, Z. (2013). “EIS Investigation and Structural Characterization of Different Hot-Dipped Zinc-Based Coatings in 3.5% NaCl Solution.” *International Journal of Electrochemical Science*, 8(6), 7753–7767.

Luo, Q., Peng, M., Sun, X., Luo, Y., and Asiri, A. M. (2016). “Efficient electrochemical water splitting catalyzed by electrodeposited NiFe nanosheets film.” *International Journal of Hydrogen Energy*, 41(21), 8785–8792.

Pagliaro, M. (2009). “Catalysis for Sustainable Energy Production. Edited by Pierluigi Barbaro and Claudio Bianchini.” *Angew. Chem. Int. Ed.*, 48(49), 9220–9220.

Parthasaradhy, N. V. (1989). *Practical electroplating handbook*. Englewood Cliffs, N.J: Prentice Hall.

Paunovic, M., and Schlesinger, M. (2006). *Fundamentals of Electrochemical Deposition: Paunovic/Fundamentals of Electrochemical Deposition, Second Edition*. Hoboken, NJ, USA: John Wiley & Sons, Inc.

Pavithra, G. P., and Chitharanjan Hegde, A. (2013). “Production of layered coatings of Fe-Ni alloy for enhanced corrosion protection.” *Surf. Engin. Appl.Electrochem.*, 49(3), 261–266.

Platatorres, M., Torreshuerta, A., Dominguezcrespo, M., Arceestrada, E., and Ramirezrodriguez, C. (2007). “Electrochemical performance of crystalline Ni–Co–Mo–Fe electrodes obtained by mechanical alloying on the oxygen evolution reaction.” *International Journal of Hydrogen Energy*, 32(17), 4142–4152.

Pletcher, D. (1984). “Electrocatalysis: present and future.” *J Appl Electrochem*, 14(4), 403–415.

Pu, Z., Wei, S., Chen, Z., and Mu, S. (2016). “Flexible molybdenum phosphide nanosheet array electrodes for hydrogen evolution reaction in a wide pH range.” *Applied Catalysis B: Environmental*, 196, 193–198.

Ragsdale, S. R., Grant, K. M., and White, H. S. (1998). “Electrochemically generated magnetic forces. Enhanced transport of a paramagnetic redox species in large, nonuniform magnetic fields.” *Journal of the American Chemical Society*, 120(51), 13461–13468.

Reddy, S., Du, R., Kang, L., Mao, N., and Zhang, J. (2016). “Three dimensional CNTs aerogel/MoS x as an electrocatalyst for hydrogen evolution reaction.” *Applied Catalysis B: Environmental*, 194, 16–21.

Rosalbino, F., Delsante, S., Borzone, G., and Angelini, E. (2008). “Electrocatalytic behaviour of Co–Ni–R (R=Rare earth metal) crystalline alloys as electrode materials for hydrogen evolution reaction in alkaline medium.” *International Journal of Hydrogen Energy*, 33(22), 6696–6703.

Safavi, M. S., and Walsh, F. C. (2021). “Electrodeposited Co-P alloy and composite coatings: A review of progress towards replacement of conventional hard chromium deposits.” *Surface and Coatings Technology*, 422, 127564.

San, N. O., Nazır, H., and Dönmez, G. (2012). “Evaluation of microbiologically influenced corrosion inhibition on Ni–Co alloy coatings by Aeromonas salmonicida and Clavibacter michiganensis.” *Corrosion Science*, 65, 113–118.

Santos, D. M. F., Sequeira, C. A. C., and Figueiredo, J. L. (2013). “Hydrogen production by alkaline water electrolysis.” *Quím. Nova*, 36(8), 1176–1193.

Sapountzi, F. M., Gracia, J. M., Weststrate, C. J. (Kees-J., Fredriksson, H. O. A., and Niemantsverdriet, J. W. (Hans). (2017). “Electrocatalysts for the generation of hydrogen, oxygen and synthesis gas.” *Progress in Energy and Combustion Science*, 58, 1–35.

Shervedani, R. K., and Lasia, A. (1997). “Studies of the Hydrogen Evolution Reaction on Ni-P Electrodes.” *J. Electrochem. Soc.*, 144(2), 511–519.

Sun, C., Wang, Y., Su, Q., Guo, Z., and Shi, L. (2016). “The Tribological Property and Microstructure of Ni-Ti Coating Prepared by Electrodeposition and Heat Treatment.” *Advances in Materials Science and Engineering*, 2016, 1–6.

Swaminathan, J., and Meiyazhagan, A. (2020). “Characterization of Electrocatalyst.” *Methods for Electrocatalysis*, Inamuddin, R. Boddula, and A. M. Asiri, eds., Cham: Springer International Publishing, 425–451.

Swathirajan, S. (1986). “Potentiodynamic and Galvanostatic Stripping Methods for Characterization of Alloy Electrodeposition Process and Product.” *J. Electrochem. Soc.*, 133(4), 671–680.

Thangaraj, V., Eliaz, N., and Hegde, A. C. (2009). “Corrosion behavior of composition modulated multilayer Zn–Co electrodeposits produced using a single-bath technique.” *J Appl Electrochem*, 39(3), 339–345.

Toker, S. M., Canadinc, D., Maier, H. J., and Birer, O. (2014). “Evaluation of passive oxide layer formation–biocompatibility relationship in NiTi shape memory alloys: Geometry and body location dependency.” *Materials Science and Engineering: C*, 36, 118–129.

Trasatti, S., and Doubova, L. M. (1995). “Crystal-face specificity of electrical double-layer parameters at metal/solution interfaces.” *Faraday Trans.*, 91(19), 3311.

Turner, J. A. (2004). “Sustainable Hydrogen Production.” *Science*, 305(5686), 972–974.

Venkatakrishna, K., and Chitharanjan Hegde, A. (2010). “Electrolytic preparation of cyclic multilayer Zn–Ni alloy coating using switching cathode current densities.” *J Appl Electrochem*, 40(11), 2051–2059.

Vicenzo, A., and Cavallotti, P. L. (2004). “Growth modes of electrodeposited cobalt.” *Electrochimica Acta*, 49(24), 4079–4089.

Wang, M., Guo, D., and Li, H. (2005). “High activity of novel Pd/TiO2 nanotube catalysts for methanol electro-oxidation.” *Journal of Solid State Chemistry*, 178(6), 1996–2000.

Waskaas, M., and Kharkats, Y. I. (1999). “Magnetoconvection Phenomena: A Mechanism for Influence of Magnetic Fields on Electrochemical Processes.” *J. Phys. Chem. B*, 103(23), 4876–4883.

Wendt, H. (1994). “Preparation, morphology and effective electrocatalytic activity of gas evolving and gas consuming electrodes.” *Electrochimica Acta*, 39(11–12), 1749–1756.

Wilcox, G. D., and Gabe, D. R. (1993). “Electrodeposited zinc alloy coatings.” *Corrosion Science*, 35(5–8), 1251–1258.

Wu, J., Peng, Z., and Yang, H. (2010). “Supportless oxygen reduction electrocatalysts of CoCuPt hollow nanoparticles.” *Phil. Trans. R. Soc. A.*, 368(1927), 4261–4274.

Yogesha, S., Bhat, R. S., Venkatakrishna, K., Pavithra, G. P., Ullal, Y., and Hegde, A. C. (2011). “Development of Nano-structured Zn-Ni Multilayers and their Corrosion Behaviors.” *Synthesis and Reactivity in Inorganic, Metal-Organic, and Nano-Metal Chemistry*, 41(1), 65–71.

You, B., and Sun, Y. (2018). “Innovative Strategies for Electrocatalytic Water Splitting.” *Acc. Chem. Res.*, 51(7), 1571–1580.

Yuan, X.-Z., Song, C., Wang, H., and Zhang, J. (2010). *Electrochemical Impedance Spectroscopy in PEM Fuel Cells*. London: Springer London.

LIST OF PAPERS PUBLISHED AND COMUNICATED

1. **Harshini Sai G** and A. Chitharanjan Hegde* "Electrochemical deposition and characterization of Co-P alloy coatings for better corrosion protection". published in Journal of Electrochemical society of India, Vol: (70) 1&2 Jan - April 2021 8-16.

2. **Harshini Sai G and** A. Chitharanjan Hegde*** "**Electrochemical deposition and characterization of NiTi alloy coatings for better corrosion protection". published in Canadian metallurgical quarterly Journal.

3. **Harshini Sai G and** A. Chitharanjan Hegde***** Development of composition modulated multilayer (NiTi) alloy coatings for improved corrosion protection of mild steel published in the Journal of Protection of Metals and Physical Chemistry of Surfaces).

4. **Harshini Sai G and** A. Chitharanjan Hegde*** "**Improvisation of corrosion performance of Ni-Ti alloy coating through magneto electrodeposition". (Manuscript under review in the Journal of Bulletin of Materials Science).

5. **Harshini Sai G** and A. Chitharanjan Hegde* Development of nanolaminated Co-Fe alloy coatings for better corrosion protection of mild steel (Manuscript under preparation)

PAPERS PRESENTED AND ATTENDED IN THE CONFERENCES

1. Participated and presented a paper titled **Electrochemical deposition and characterization of Co-P alloy coatings for better corrosion protection** in ***National Symposium on Electrochemical Science and Technology [NSEST-2021]*** on 24-25 June 2022 organized by the Electrochemical Society of India and Department of Inorganic and Physical Chemistry, IISC, Bengaluru.
2. Participated in Two Day ***International Conference on Recent Trends in Applied Sciences [ICRTAS-2022]*** conducted by Srinivas Institute of Technology, Mangalore on August 3rd and 4th 2022.
3. Participated and presented a paper titled **Development of nanolaminated Co-Fe alloy coatings for better corrosion protection of mild steel** in ***International Conference***

on Corrosion and Coatings (i3C) on December 07th and 8th 2022 organized by IIM Jamshedpur, India in association with Tata Steel, CSIR-NML & NIT Jamshedpur.

4. Participated and presented a paper titled **Effect of addition of MWCNT on corrosion behavior of Co-P alloy coatings** in National Conference on ***Advances in Analytical techniques for materials and Bio-medical application (AATMABIMAN-2022)*** held during 15-16 December 2022 at Rani Chennamma University, Belagavi.
5. Participated in the International e-Symposium on ***Materials Development and Scale-up for Membrane separation, Sensing, Energy and Biological Applications (MDS-MSEB)*** held during 24-25th January-2023 (Virtual Mode) Organized by SRM Institute of Technology, Chennai.
6. Participated and presented a paper titled **Development of nanolaminated multilayer NiTi alloy coatings for better corrosion protection** in 34th Annual General Meeting of ***MRSI and the 5th Indian Materials Conclave*** December 12-15 organized by School of Material Science and Technology Indian Institute of Technology (BHU), Varanasi.

BIODATA

PERSONAL INFORMATION:

Name : HARSHINI SAI G.

Father's name : P.C.L. RAMANA

Gender : Female

Nationality : Indian

Date of Birth : 02-11-1996

Permanent Address : Door No: 14-484/11,
Back side to Marrimanu Street,
Kuppam.
Chittoor District – 517425,
Andhra Pradesh.

Contact No : +917780284255

Email- id : g.harshinisai@gmail.com

EDUCATIONAL QUALIFICATION:

COURSE	NAME OF THE INSTITUTION	YEAR OF PASSING	CGPA/ PERCENTAGE
M.Sc. Chemistry	SASTRA University, Thanjavur, T.N	2019	7.5
B.Sc.	Sree Vidhyanikethan Degree College, Tirupati, A.P	2017	86%
HSE	Narayana Junior College, Nellore, A.P	2014	91.1%
SSC	Adarsh English Medium High School, Kuppam, A.P.	2012	9.2

PROJECT COMPLETED:

M.Sc. Project on "Development of α-Mno_2 as a bifunctional catalyst for electrically rechargeable Zinc air batteries" under Dr. S. Devaraj, SASTRA University, Thanjavur (2019).

AREA OF RESEARCH: Electroplating

Research Skills:

- Skillful in developing alloy coatings using advanced methods of electrodeposition like magneto- electrodeposition and multilayer electrodeposition., Electrocatalytic study of different alloys.
- Hands-on experience in using electrochemical workstations VERSASTAT-3, Biologic SP 150 and Gill AC.
- Proficient in material characterization techniques like Electrochemical Impedance Spectroscopy, Potentiodynamic polarization technique, Cyclic Voltammetry, Chronopotentiometry, Potentiostatic and Galvanostatic methods, XRD, Scanning Electron Microscopy and AFM
- Assisted students in completing **MS and Summer Internship projects**.

Skills	:	Origin, MS Office, EC Lab 2.1, VersaStudio 3.0, Xpert Highscore, ZsimpWin, Gwyddion, Preparing Scientific reports, Abstracts, Power Point Presentations

LIST OF PUBLICATIONS:

1. **Harshini Sai G and A. Chitharanjan Hegde* "**Electrochemical deposition and characterization of Co-P alloy coatings for better corrosion protection" published in Journal of Electrochemical society of India Vol: (70) 1&2 Jan. & April 2021 8-16
2. **Harshini Sai G and A. Chitharanjan Hegde* "**Electrochemical deposition and characterization of NiTi alloy coatings for better corrosion protection" published in Canadian metallurgical quarterly Journal.

3. **Harshini Sai G and A. Chitharanjan Hegde* "**Development of composition modulated (NiTi) alloy coatings for better corrosion protection on mid steel" published in Protection of Metals and Physical Chemistry of Surfaces Journal.

CONFERENCES ATTENDED:

1. Participated and presented a paper titled **Electrochemical deposition and characterization of Co-P alloy coatings for better corrosion protection** in ***National Symposium on Electrochemical Science and Technology [NSEST-2021]*** on 24-25 June 2022 organized by the Electrochemical Society of India and Department of Inorganic and Physical Chemistry, IISC, Bengaluru.
2. Participated in Two Day ***International Conference on Recent Trends in Applied Sciences [ICRTAS-2022]*** conducted by Srinivas Institute of Technology, Mangalore on August 3rd and 4th 2022.
3. Participated and presented a paper titled **Development of nanolaminated Co-Fe alloy coatings for better corrosion protection of mild steel** in ***International Conference on Corrosion and Coatings (i3C)*** on December 07th and 8th 2022 organized by IIM Jamshedpur, India in association with Tata Steel, CSIR-NML & NIT Jamshedpur.
4. Participated and presented a paper titled **Effect of addition of MWCNT on corrosion behavior of Co-P alloy coatings** in National Conference on ***Advances in Analytical techniques for materials and Bio-medical application (AATMABIMAN-2022)*** held during 15-16 December 2022 at Rani Chennamma University, Belagavi.
5. Participated in the International e-Symposium on ***Materials Development and Scale-up for Membrane separation, Sensing, Energy and Biological Applications (MDS-MSEB)*** held during 24-25th January-2023 (Virtual Mode) Organized by SRM Institute of Technology, Chennai.
6. Participated and presented a paper titled **Development of nanolaminated multilayer NiTi alloy coatings for better corrosion protection** in 34th Annual General Meeting of ***MRSI and the 5th Indian Materials Conclave*** December 12-15 organized by School of Material Science and Technology Indian Institute of Technology (BHU), Varanasi.